FINAL REPORT

ON

DOSE ESTIMATION

FOR THREE VICTIMS OF JCO ACCIDENT

Editor: Kenzo Fujimoto

April 2002

National Institute of Radiological Sciences

Printed in Japan

NOTE

This is the English version final report of the Dose Estimation Working Group for Three Victims that was established at the National Institute of Radiological Sciences just after the accident to estimate the doses of the three JCO workers who were severely exposed to radiation by the criticality accident. The Japanese version was published on February 2002 (NA02a). Within a few days after the accident, the Working Group provided the estimated dose, required for the treatment of the three severely exposed workers, and then published the results of the group activities in various formats, such as the interim report NIRS-M-138 (NA00) on February 29, 2000. All the 1,000 copies of the Interim Report were distributed and are now in wide use. The issue of the interim report did not mark the end of the activities of the Working Group: the Group has continued its studies to obtain as much knowledge as possible from the disaster. These studies include 1) dose measurements of samples provided in the latter stage, 2) computational simulation analyses to derive more precise dose distribution within the human body, and 3) investigation of depth dose distribution in the body using Transient Experiment Critical Facility in JAERI (TRACY). This report details the dose estimation experiments carried out by the Group, including the measurements and analyses conducted after the interim report was published. This report supersedes the entire content of the interim report and covers the dose estimation of the three workers who were severely exposed during the JCO criticality accident.

The data in this report is presented for academic purposes with the consent of the three severely exposed workers and/or their families. We would like to express our deep condolences to their families who lost their loved one due to the accident.

The members of the Dose Estimation Working Group and the names of persons who participated in the dose estimation studies are listed below. A number of individuals other than these persons assisted the dose estimation for the JCO criticality accident. We would like to thank them for their cooperation.

Member of Dose Estimation Working Group for Three Victims（The divisions and sections are for fiscal 1999, when the criticality accident occurred.）

Chairperson: Kiyomitsu Kawachi (Deputy Director-General)
Vice Chairperson: Kenzo Fujimoto (Director of Human Radiation Environment Division)
Acting Vice Chairperson: Yoshikazu Nishimura (Section Head of Biokinetics and Internal Dose Assessment, Human Radiation Environment Division)

Member
  Planning and Coordination Office
    Tsuneya Matsumoto, Yutaka Hishiyama, Yukio Kamakura
  Technology and Safety Division
    Shizuo Monma, Hajime Sato, Yasutaka Kurata, Noriyuku Yoshida
  Education and Scientific Service Division
    Hisamasa Joshima, Yoshiyuki Shirakawa
  Radiation Research Division
    Takeshi Hiraoka, Takehiro Tomitani, Sadao Shibata, Yutaka Noda
  Radiobiology and Biodosimetry
    Isamu Hayata
  Radiotoxicology and Protection Division
    Michikuni Shimo, Akira Koizumi, Nobuhito Ishigure
  Human Radiation Environment Division
    Yoshikazu Nishimura, Masae Yukawa, Kunio Shiraishi, Katsumi Kurotaki, Hidenori Yonehara
  Radiation Health Division
    Hirohiko Tsujii, Makoto Akashi, Gen Suzuki
  Environmental and Toxicological Sciences Research Group
    Yuji Nakamura, Yasuyuki Muramatsu, Hiroshi Takeda, Kiriko Miyamoto, Satoshi Yoshida
  International Space Radiation Laboratory
    Kazunobu Fujitaka, Koichi Ando, Hiroshi Yamaguchi
  Accelerator Physics and Engineering Division
    Fuminori Soga
  Advisors: Tetsuo Iwakura, Toshiyuki Nakajima, Yoshikazu Kumamoto (Senior Research Counselor)

List of the names involved in the dose estimation (The divisions and sections are for fiscal 1999, when the criticality accident occurred. The divisions and sections of those persons who participated after the accident are as at the time that they began their participation.)

Initial Response
Yutaka Noda (Radiation Research Division),
Akira Koizumi (Radiotoxicology and Protection Division),
Shizuo Monma, Yasutaka Kurata, Kengo Soga, Noriyuki Yoshida, Mitsuhiro Kuchiki, Akinori Sasaki, Yoshiki Horikoshi, Norihiro Miyashiro, Shinji Sato, Yasuhiro Morikawa, Shingo Koeda (Technology and Safety Division)

Dose Estimation by Blood Components
Makoto Akashi, Gen Suzuki, Sakae Tanosaki, Toshiyasu Hirama, Kenichi Nakagawa, Norikazu Kuroiwa, Hirohiko Tsujii (Radiation Health Division)

Chromosome Analyses
Isamu Hayata, Masako Minamihisamatsu, Reiko Kanda, Akira Furukawa (Radiobiology and Biodosimetry Division),
Collaborator: Masao Sasaki (Radiation Biology Center, Kyoto University)

Gamma Ray Spectrometry
Yutaka Noda (Radiation Research Division),
Yasuyuki Muramatu, Keiko Tagami, Tadaaki Ban-nai, Shigeo Uchida (Environmental and Toxicological Sciences Research Group),
Hidenori Yonehara, Yoshikazu Nishimura, Masae Yukawa, Shinji Tokonami (Human Radiation Environment Division),
Akira Koizumi (Radiotoxicology and Protection Division)

Measurement of Stable Elements (Na, K, P, Br, S , Ca)
Satoshi Yoshida, Yasuyuki Muramatu (Environmental and Toxicological Sciences Research Group),
Yoshito Watanabe, Shinzo Kimura (Human Radiation Environment Division)

Measurement of ^{32}P
Masae Yukawa, Yoshikazu Nishimura, Yoshito Watanabe, Hee-Sun Kim, Shinzo Kimura (Human Radiation Environment Division),
Hiroshi Takeda, Kiriko Miyamoto, Shouichi Fuma (Environmental and Toxicological Sciences Research Group)

Imaging Plate
Shinzo Kimura (Human Radiation Environment Division),
Hisamasa Joshima (Education and Scientific Service Division)

ESR Measurement of Teeth
Kunio Shiraishi, Hidenori Yonehara, Masaki Matsumoto (Human Radiation Environment Division),
Collaborator: Tadakura Miyazawa, Midori Iwasaki (Ouu University)

Dose Calculation
Nobuhito Ishigure (Radiotoxicology and Protection Division)

Computational Simulation
Nobuhito Ishigure (Radiotoxicology and Protection Division),
Kiyomitsu Kawachi (Deputy Director-General),
Collaborator: Yasuhiro Yamaguchi, Akira Endo (JAERI)

Dose Measurement using TRACY
Takeshi Hiraoka, Akifumi Fukumura, Kaname Omata (Radiation Research Division),
Kiyomitsu Kawachi (Deputy Director-General),
Naruhiro Matsufuji (Accelerator Physics and Engineering Division),
Nobuhito Ishigure (Radiotoxicology and Protection Division),
Collaborator: Akio Oono, Hiroki Sono (JAERI)

Whole Body Counter
Tetsuo Ishikawa (Human Radiation Environment Division),
Yoshihisa Kokuzawa (Technology and Safety Division)

Logbook Keeping
Akira Koizumi (Radiotoxicology and Protection Division),
Yutaka Noda (Radiation Research Division),
Kenzo Fujimoto, Masae Yukawa (Human Radiation Environment Division)

Management of Privacy of Victims
Makoto Akashi (Radiation Health Division)

Technical Assistance for Measurements
Mutsumi Tanaka, Shinnosuke Yamasaki, Fuyuki Kouno, Noriko Kuroda, Kazuhiko Yamamoto

Editorial Assistance
Naoko Isoda (Environmental Radiation Protection Research Group)

ABSTRACT

On September 30, 1999, at about 10:35 in the morning, a criticality accident occurred in a uranium conversion test plant at JCO in Tokai-mura. Three workers who were purifying uranium were severely exposed to radiation. The National Institute of Radiological Sciences (NIRS), which is a Tertiary Radiological Emergency Facility, agreed to admit the workers, established a Countermeasure Headquarters and a Dose Estimation Working Group for Three Victims and started preparing to receive the workers. The procedures implemented by the entire National Institute of Radiological Sciences concerning this accident are summarized in the "The report of the criticality accident in a uranium conversion test plant in Tokai-mura" NIRS-M-154 (NA02b). The present report describes the response of the Dose Estimation Working Group.

To inform readers on the principal methodology that were used to estimate the dose, the key details directly related to dose estimation are all covered in Chapter II, "Dose Assessment," after the brief introduction of accident in Chapter I, "Review of the Accident." The secondary details of methods and measurement data are covered in Chapter III, "Measurement and Analysis of Biological Materials." Chapter IV discusses the various problems encountered during the dose estimation process. The initial actions and chemical analyses are described in the Appendices.

For the criticality accident in the JCO, the radiation dose was estimated using three main methods: lymphocyte counting, chromosome analysis, and measurements of the specific activity of ^{24}Na in blood samples. At the time of publication of the Interim Report by the Dose Estimation Working Group for Three Victims (NA00), the doses of the three workers were estimated by these three methods to be 1-4.5, 6-10, and 16-20+ GyEq. At the latter stage more precise analyses estimated doses of 1-5, 6-8, and 16-23 GyEq by lymphocyte counting; doses of 2.8-3.2, 6.9-10, and 16-30+ GyEq by chromosome analyses; and doses of 0.81, 2.9, and 5.4 Gy with respect to neutrons and 1.5, 4.1 and 9.9 Gy with respect to gamma radiation by means of ^{24}Na specific activity measurements. These values fall within the estimations in the Interim Report but are more precise. Of these estimated doses, the methods based on counting the numbers of lymphocytes in the peripheral blood or which examined chromosomal abnormalities could not distinguish the dose contribution of neutrons from that of gamma rays; these doses were estimated by comparing the previous results based on gamma ray effects. Therefore, we could not use radiation dose units such as Gy or Sv but used another unit: GyEq. On the other hand, the method used to estimate the doses from the specific activity of ^{24}Na in the blood can only derive doses attributable to neutrons. Therefore, the doses of gamma rays had to be estimated using other methods, such as investigating the readings from radiation monitors during the accident and performing computational simulations. At the initial stage, the total dose was estimated in GyEq units using an RBE of 1.7 and the dose estimated by the specific activity of ^{24}Na in the blood. However, after further investigation, we concluded that the best method for expressing dose estimations was to express them in units of Gy for each component, neutron and gamma rays. For the temporary evaluation of health effects on the entire body and comparison with the results derived from other dose estimation methods, we judged it was necessary to assume an appropriate RBE and derive the sum of the neutron and gamma ray doses. For these purposes, the doses of the three workers estimated from the specific activity of ^{24}Na in the blood and using a RBE of 1.7 were 2.9, 9.0, and 19 GyEq, respectively for the three workers.

Taking these inaccuracies into account, we compared the results of these dose estimation methods and derived overall doses to be 2-3, 6-9 and 16-25 GyEq for the three workers. The ranges do not reflect the uneven dose distribution in the bodies; rather, they show the ranges of estimation by various methods.

CONTENTS

I. REVIEW OF THE ACCIDENT

On September 30, at about 10:35 in the morning, a criticality accident occurred at the uranium conversion test plant of JCO Co. Ltd. in Tokai-mura, Ibaraki Prefecture, Japan. The accident occurred while two workers were pouring uranyl nitrate into a precipitation tank. The two workers (Mr. A and Mr. B) and another worker who was in the next room (Mr. C) realized that an abnormality had occurred and withdrew to a decontamination room, which was located near the entrance of the control area. Mr. C attempted to use a telephone within the control area to alert people to the accident, but it did not function. While Mr. C was trying to use the phone, Mr. A fainted in the decontamination room, and Mr. B was taking care of him. Other workers hurried to the room in response to the area monitor alarm. They removed the three workers to outside of the control area, telephoned the Tokai Village Fire Department, and requested that an ambulance be sent at 10:45 (GE99a, FU99, FU00a,b,c).

The three workers were transferred to the National Mito Hospital by ambulance, which arrived within minutes. The workers received First Aid treatment at the hospital. It was then decided, since they showed severe symptoms, to transfer them to the National Institute of Radiological Sciences (NIRS) that is designated as the tertiary Radiological Emergency Facility by the Japanese government. NIRS set up a Countermeasure Headquarters immediately after being informed of the accident. Its first meeting was held at 14:30 on the same day and the operational condition of the equipment was examined and prepared for admitting the workers. At 14:16, the three workers and a physician from the National Mito Hospital left the Mito City heliport aboard a disaster prevention helicopter supplied by Ibaraki Prefecture, and arrived at Toke heliport, Chiba City, at 14:45. Members of the Division of Technology and Safety in NIRS were waiting at Toke heliport. The workers were transferred by ambulance to the Medical Care Building for Radiation Emergency of NIRS, arriving at 15:25. Mr. A and Mr. B were taken into the building on stretchers, and Mr. C, who was less severely affected, walked in by himself. At NIRS, the members of the Division of Technology and Safety checked and confirmed that the helicopter, the ambulances, and ambulance staff were not contaminated with radioactive materials. The degrees of contamination of the three workers were examined. While the medical team treated the workers, specialists in physical and biological dosimetry began estimating the doses that the workers had received. Since none of the workers was wearing a dosimeter at the time of the accident, it was imperative to estimate the dose urgently using indirect methods. The Dose Estimation Working Group for Three Victims was formed under the leadership of Dr. K. Kawachi (Deputy Director-General) to systematically estimate the doses.

To ensure appropriate treatment of workers exposed to radiation, it is essential to find out immediately the degree of external and internal contamination, exposure dose, the types of radiation and the configuration of exposure pattern (uniform exposure, non-uniform exposure or local exposure). The priority, particularly in individuals who may have been exposed to high levels of radiation, is first to carry out life-saving treatment, and then to check for external and internal contamination by radioactive materials and to remove the contamination if any is present.

The three workers taken into NIRS were not wearing dosimeters at the time of the accident, and NIRS did not receive any precise information about the accident itself or any other data. However, the institute began treating the workers immediately on their arrival at the hospital since two of the three workers showed severe symptoms. During the treatment, the staff of the Division of Technology and Safety examined the radiation level around their bodies and measured the radioactivity in their nose smear samples, vomit samples and their clothes. Based on their measurements the Working Group confirmed that the workers had not been externally or internally contaminated by radioactive materials. The activity of ^{24}Na was detected in the vomit samples, showing that the accident had been a criticality incident. The data showed that there were no contaminants to be removed from their body surfaces and that no chelating agents were required to remove internal contamination. The medical staff thus concentrated on the treatment of the workers as being exposed only externally to gamma rays and neutrons. The initial response of the Institute is described in detail in Appendix A. It was then necessary to determine the doses, the type of radiation, and the configuration of the exposure pattern. Physical and biological dosimetry was carried out on the blood, clothes, belongings, hair, and urine of the workers. The following chapter describes the measurements and analyses performed to estimate the doses.

II. DOSE ASSESSMENT

Introduction

This Chapter II describes the facts that are directly related to the present dose assessment. The methods of biological dosimetry are described in Sections A, B and C, and physical dosimetry methods are given in Sections D, E and F. A summary of the dose estimation derived by these assessment methods is given in Section G. Chapter III includes 1) data that did not directly contribute to the present dose estimation but was helpful in gaining an understanding of the uneven dose distribution and in deriving dose estimation by ^{24}Na measurements and 2) data that may be useful in any future dose assessments.

II.A. Dose estimation of whole-body exposure from prodromal symptoms (AK01)

Acute radiation syndrome has four stages by the symptoms that appear after radiation exposure (see Table II.A.1). The stage immediately after exposure or within several hours of the exposure, when nausea, vomiting, and fever (prodromes) appear, is called the prodromal period. The IAEA Safety Reports Series No. 2 (IA98) shows the relationship between the prodromes of acute radiation syndrome and gamma ray doses, which was determined by studying victims exposed to gamma rays in the past and analyzing their prodrome appearances and radiation doses (see Table II.A.2 and 3). In the rest of this section, the dose is expressed as an equivalent dose to gamma rays (GyEq). According to the previous experience shown in Table II.A.2, Mr. A showed a body temperature of 38.5 ℃ on the day of the accident, suggesting an exposure to at least 6 GyEq. Vomiting within ten minutes of the exposure, and diarrhea within one hour, led to a dose estimation of over 8 GyEq. Previous reports of accidents have shown that unconsciousness was likely to appear for an exposure to over 50 GyEq. Mr. A lost consciousness for 10-20 seconds. Vomiting at about one hour after the exposure and no diarrhea suggested that Mr. B was exposed to 4 to 6 GyEq. Mr. C did not show prodromes, except for slight nausea when he was in the helicopter transporting him to hospital, suggesting an exposure to up to 4 GyEq.

Table II.A.1 Stages of acute radiation syndrome

Exposure			Time	
	Prodromal period	Latent period	Critical or manifestation period	Recovery (Death)
	Anorexia Nausea Vomiting Diarrhea	No symptom	Infection Bleeding Dehydration Shock	

Table II.A.2 Latent phase of acute radiation symptom

Dose	1 – 2 GyEq	2 – 4 GyEq	4 – 6 GyEq	6 – 8 GyEq	> 8 GyEq
Latent period (days)	21 - 35	18 - 28	8 - 18	7 or less	0
Principal symptoms	Fatigue Weakness	Fever Infection Bleeding Epilation Fatigue	High fever Infection Bleeding Epilation	High fever Diarrhea Vertigo	High fever Diarrhea Epilation Consciousness
Lethality(%)*	0	0 - 50	20 - 70	50 - 100	100

Cited from the IAEA Safety Reports Series No. 2 (IA98) and modified.
*The percentages are approximate values when no treatment is conducted.　Mortality varies depending on the conditions of exposure or treatments.

Table II.A.3 Prodromal phase of acute radiation syndrome

Doses	1-2 GyEq	2-4 GyEq	4-6 GyEq	6-8 GyEq	>8 GyEq
Vomiting					
(Onset)	after 2 h	1-2 h	within 1 h	within 30 min	within 10 min
(%)	10-50	70-90	100	100	100
Diarrhea			moderate	severe	severe
(Onset)	-	-	3-8 h	1-3 h	<1 h
(%)	-	-	<10	>10	100
Headache	slight	mild	moderate	severe	severe
(Onset)	-	-	4-24 h	3-4 h	1-2 h
(%)	-	-	50	80	80-90
Consciousness	unaffected	unaffected	unaffected	may be altered	unconsciousness
(%)	-	-	-	-	100
					(>50 Gy)
Body temperature	normal	increased	fever	high fever	high fever
(Onset)	-	1-3 h	1-2 h	<1 h	<1 h
(%)	-	10-80	80-100	100	100

Cited from the IAEA Safety Reports Series No. 2 (IA98) and modified. The doses are mainly gamma ray doses at the time of exposure.

II.B. Dose estimation from the reduction curves of blood cells and lymphocytes (AK01)

The Appendix of ANNEX G "Early effects in man of high doses of radiation" of 1988 UNSCEAR Report (UN88, BA95) describes a method for estimating doses using the reduction curves of lymphocytes, neutrophils, and platelets after the exposure to gamma rays of the 0 to 10 GyEq range (see Fig. II.B.1). Lymphocytes are one of the most sensitive to radiation and show sharp drops in numbers, which are proportional to the dose of exposure. On the other hand, lymphocytes are known to decrease with the application of adrenocortical steroids during medical care or with excess stress. Neutrophils and platelets are ephemeral in the peripheral blood, and thus reflect the reduction of hematopoietic stem cells in the bone marrow. The time variation of neutrophils, lymphocytes and platelets of Mr. A, B and C are shown in Fig. II.B.2, Fig. II.B.3 and Fig. II.B.4, respectively.

	a	b
Day 0	5.65	34.37
Day 1	2.44	17.45
Day 2	1.39	9.97
Day 3	1.04	7.26
Day 4	0.88	5.66
Day 5	0.83	4.81
Day 6	0.81	4.41

Dose = a - b log (No. Lymph)
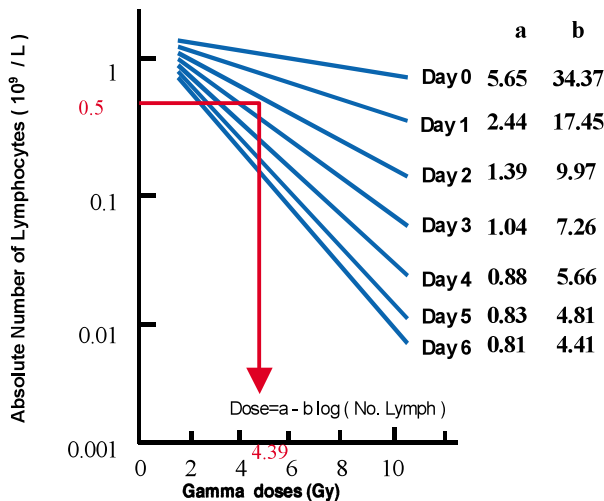
Fig.II.B.1 Dose estimation by number of lymphocytes (UN88)

As shown in Fig. II.B.2, it was possible to count the number of peripheral lymphocytes of Mr. A on the day of the accident and up to the third day. However, we could not estimate the dose from the graph of his lymphocyte number (Fig. II.B.1) and therefore estimated the value by using an estimation equation. The dose estimated was over 10 GyEq (16 – 23 GyEq). Neutrophils showed a transient rise after the exposure, then a linear drop in a log-log plot, and reached 0 on the seventh day after the accident as shown in Fig. II.B.2. Platelets also showed a linear log-log drop after the exposure, and he needed platelet transfusion from the seventh day. The reduction curves of neutrophils and platelets are equal to an estimation of over 10 GyEq, which is a dose that kills most of the hematopoietic stem cells.
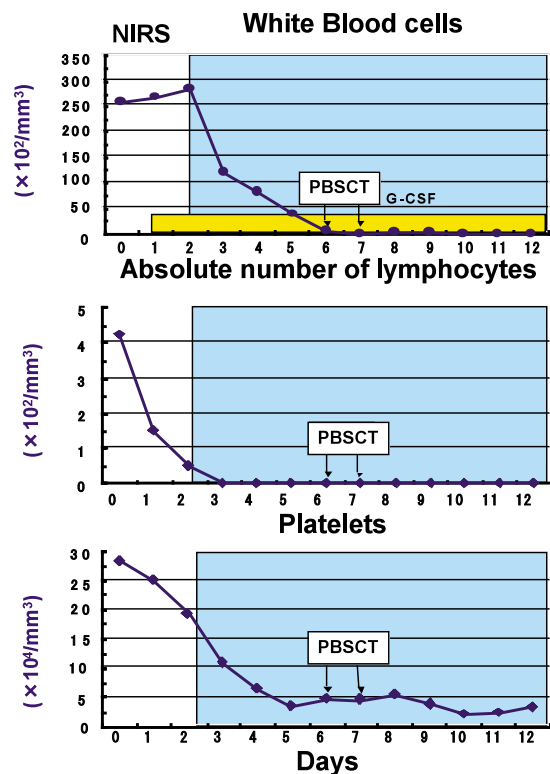
Fig.II.B.2 Time variation of blood components of Mr. A
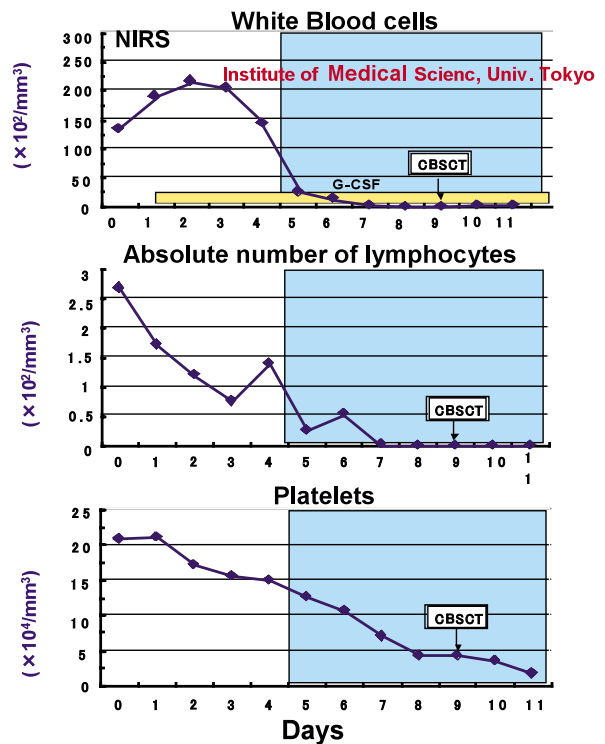
Fig.II.B.3 Time variation of blood components of Mr. B
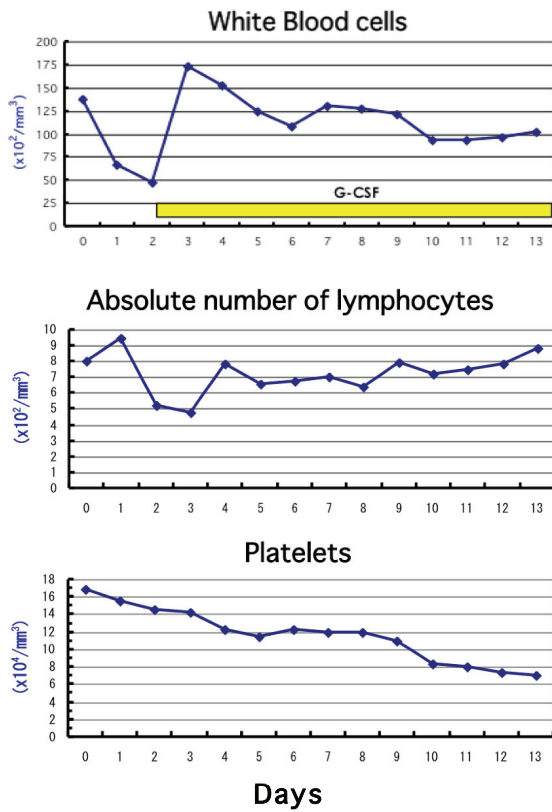
Fig.II.B.4 Time variation of blood components of Mr. C

It was possible to count the number of lymphocytes of Mr. B up to the eighth day (see Fig. II.B.3). The numbers of lymphocytes counted on the first to third days suggested an exposure to over 10 Gy Eq, but the lymphocyte counted on the fourth to seventh days indicated an estimated exposure to 6 – 8 GyEq. Platelets showed a linear drop after the fifth day, and the inclination led to an estimation of 6 GyEq.

For Mr. C, the lymphocyte count suggested an exposed dose of approximately 1 – 5 GyEq (see Fig. II.B.4). Since there was a certain distance between Mr. C and the criticality source, he was likely exposed uniformly to radiation. During his stay in hospital, epilation was observed at the head. The numbers of leukocytes and platelets reached a nadir three weeks after the accident, and transfusions of platelets were necessary. This clinical course suggests an exposure to about 3 GyEq.

II.C. Dose estimation by chromosome analysis (HA01a,b)

II.C.a. Sample preparation and analysis

Dose estimation by chromosome analysis is performed using peripheral lymphocytes. In the standard method, the blood for the analysis is taken from exposed persons more than 24 hours after exposure, when the circulating and extravascular pools are fully mixed in the body. For the present case, however, because of the observed rapid drop in lymphocyte numbers, we decided to collect blood at 9, 23 and 48 hours after the accident.

Already at 9 hours after the accident, the proportion of lymphocytes in relation to total white blood cells had fallen to the extremely low values of 1.9 % in Mr. A, 2.1 % in Mr. B and 15 % in Mr. C. Normal values are 25-48%. For Mr. A and Mr. B, it appeared to be impossible to collect a sufficient number of lymphocytes to make chromosome preparations using the conventional method, since most of the lymphocytes would probably have been lost during the culturing and harvesting processes. Even if it were possible to make chromosome slides, it would be difficult or impossible to analyze them because the frequency of metaphase would be extremely low due to mitotic delay caused by high-dose radiation.

To overcome these difficulties, we used two new techniques which we had developed as part of the Science and Technology Agency's Nuclear Crossover Research Project: a high yield chromosome preparation method (HA92) and easy biodosimetry for high-dose radiation exposure using drug-induced, prematurely condensed ring chromosomes (PCC-R) (KA99). The former method was developed to prepare chromosome samples suitable for analysis with automatic devices. This method concentrates the lymphocytes, increases the recovery rate of the sedimentary cells by centrifugation, and markedly raises the frequency of analyzable cells. The latter method was developed for detecting chromosome aberrations in interphase nuclei instead of metaphase chromosomes. After exposure to high-dose X or gamma rays (over 10 Gy), few cells are able to enter mitosis when cultured and so are harvested at metaphase, having been arrested by a mitotic inhibitor such as colcemid. On the other hand, okadaic acid effectively induces prematurely condensed chromosomes even in lymphocytes exposed to 20 Gy. Since this PCC-R method uses only ring chromosomes as an indicator of dose, it enables a rough but much faster dose estimation than the conventional method of scoring dicentrics (multicentric chromosomes within centromeres are counted as n-1 dicentric chromosomes), ring chromosomes and fragments. PCC-R analysis is a practical method for biodosimetry, especially for high-dose estimations.

Chromosome preparation and observation for the present dose estimation was performed according to the method described below:

(1) Lymphocytes were separated from 8 ml of peripheral blood and mixed with 12 ml of a culture medium consisting of 9.6 ml of RPMI 1640 solution, 2.4 ml of calf serum, 0.72 mg of kanamycin and 0.24 ml of PHA, and then divided into two centrifuge tubes for tissue culture.

(2) One tube was processed for PCC-R scoring, and the other was used for conventional analysis. Both were cultured for 48 hours at 37 °C. The former was treated with 500 nM okadaic acid for the last hour of culture. The latter was supplemented with 0.3 μg of colcemid at the start of the culture.

(3) The lymphocytes were treated and fixed using a high-yield harvesting method. Air-dried slides were densely stained with Giemsa's solution.

(4) Chromosome aberrations were scored under a microscope. All the cells carrying aberrations were photographed.

II.C.b. Dose estimation and the calculation formula

Dose estimation using the PCC-R method was made by comparing the observed data with the experimentally obtained values for PCC-R dose response after exposure to 200 keV X-rays (Fig. II.C.1). The estimation based on the dicentrics and rings in Mr. C was made according to the standard method outlined in IAEA Technical Report Series No. 260 (IA86), based on an equation for calculating ^{60}Co gamma rays: $Y = (2.31 \pm 0.88) \times 10^{-2}D + (6.33 \pm 0.25) \times 10^{-2}D^2$ (M. S. Sasaki, unpublished). The radiation doses of Mr. A and Mr. B were higher than the dose that can be estimated with this formula, which is only suitable for doses up to 6 Gy. Therefore, estimates were made by a direct comparison of the observed frequencies with those obtained in a study of 1.9 MeV X-rays (quality factor = 1) by Norman and Sasaki (NO66) (Fig. II.C.2).
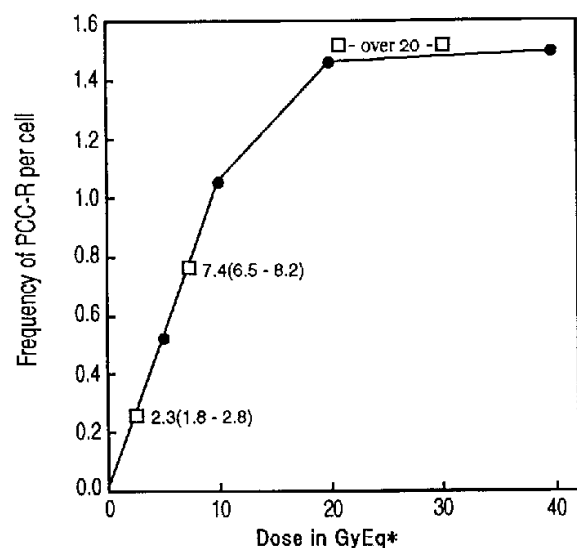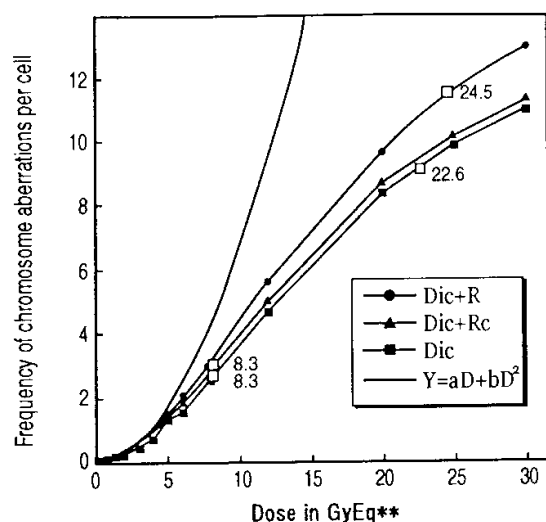

Fig. II.C.1 Dose-response curve of PCC-R

Fig. II.C.2 Dose-response curves of dicentrics and ring chromosomes, and the estimated doses of Mr. A and Mr. B

II.C.c. Results

c.1. Dose estimation by PCC-R analysis

It is essential to estimate the dose as quickly as possible in cases involving exposure to high doses of radiation. Therefore, we first examined the frequencies of PCC-R in the samples obtained 9 hours after the accident, by which we could quickly, though crudely, estimate the radiation dose. The PCC-R analysis for estimating the doses of the three workers took approximately one hour. The results are listed in Table II.C.1.

Table II.C.1 Results of dose estimation by PCC-R
Analysis using samples obtained 9 hours after the accident

Mr. A	75 PCC-R/50 cells	>20 GyEq*
Mr. B	38 PCC-R/50 cells	7.8 GyEq*
Mr. C	13 PCC-R/50 cells	2.6 GyEq*

Note: Doses (GyEq*) were estimated by using the dose-response curve of PCC-R obtained in experiments conducted at the National Institute of Radiological Sciences.

c.2. Dose estimation by analysis of dicentrics and ring chromosomes

Since this was the world's first attempt to estimate exposed dose by analyzing PCC-R, we needed to promptly check the results shown in Table II.C.1 by comparing them with doses estimated using the conventional method of scoring dicentrics and ring chromosomes (Dic + Rc). However, the scoring of Dic + Rc in Mr. A and Mr. B was extremely difficult or impossible in the short term due to their very low mitotic index (1/100 to 1/1000 of the normal value) and the complicated morphology of aberrant chromosomes. Therefore, first, analysis of Dic + Rc to check the PCC-R results was performed only for Mr. C. The analysis of 50 cells of Mr. C took approximately 1 hour. The estimated value was 2.4-3.2 GyEq***, fairly consistent with the result of the PCC-R analysis.

The doses estimated by PCC-R analysis for the three workers and the result for Mr. C obtained by the conventional method were reported at the meeting held to plan clinical treatment, held at 10:25 am on October 3, three days after the accident.

Thereafter, we concentrated on the analysis of Dic + Rc, which gives a more precise estimation of dose than does by PCC-R analysis. We started with Mr. B, but the analysis took a long time since dividing cells were scarce and several complicated aberrant chromosomes were observed per cell. While conducting this difficult analysis, we simultaneously had to prepare chromosome slides from the 23- and 48-hour samples of the three workers and had to plan a chromosome analysis for the residents of Tokai-mura, who had been, or were suspected of being, exposed to low doses of radiation. Therefore, at the meeting to plan clinical treatment held on the morning of October 7, we were able to report the results for only 13 cells in the 9-hour sample of Mr. B. The dose estimated from the results for these 13 cells was higher than 6 GyEq, which was also consistent with the result of the PCC-R analysis for this worker.

Between October 7 and 13, we were able to finish the analysis of 15 cells from the 9-hour sample of Mr. A, 40 cells from the 9-hour sample of Mr. B, and 100 cells from the 23-hour sample of Mr. C. In the sample from Mr. A, it was not rare to find a chromosome with several centromeres, and it was not always possible to identify all 46 centromeres in each cell. Additionally, it was not possible to distinguish between ring chromosomes with (Rc) and without (Ra) a centromere. An overall count of ring chromosomes (R) was therefore made for Mr. A. The number of dicentrics (Dic) was scored conservatively, which would give a lower estimated dose for Mr. A than the dose actually received. The estimated dose was 24.5 GyEq using the analysis of Dic+R for Mr. A. On the 13th day after the accident, this time-consuming but precise estimation of dose by conventional metaphase analysis as shown in Table II.C.2 confirmed that all the values for the three workers obtained by PCC-R analysis were reliable.

Table II.C.2 Estimated dose by conventional analysis up to October 13, 1999

Samples obtained 9 hours after the accident		
Mr. A	158 Dic+R/15 cells	24.5 (13.1->30)GyEq**
Mr. B	160 Dic+Rc/53 cells	8.3 (6.3-10.5) GyEq**
Mr. C	28 Dic+Rc/50 cells	2.8 (2.4-3.2) GyEq***
Sample obtained 23 hours after the accident		
Mr. C	64 Dic+Rc /100 cells	3.0 (2.7-3.3) GyEq***

Note: The doses (GyEq**) were estimated by direct comparison of the observed frequencies with those obtained in a study using 1.9 MeV X-rays by Normal and Sasaki (NO66). Dose (GyEq***) estimation was made using a calculation of dose-response for ^{60}Co gamma rays: Y = $(2.31 \pm 0.88) \times 10^{-2}D + (6.33 \pm 0.25) \times 10^{-2}D^2$.

c.3. Final results of the estimated dose

After concentrated effort, we succeeded in analyzing all the 9-, 23- and 48-hour samples from the three workers using the conventional metaphase method. In addition, to increase the reliability of these results, we analyzed 50 more cells per sample in the PCC-R preparations. The results are shown in Table II.C.3 and Figs. II.C.1 and II.C.2 (HA01b). From all these analyses of the doses to three workers, A, B and C were estimated to be 24.5 (16.0->30), 8.3(6.9-10.0), 3.0 (2.8-3.2) GyEq, respectively.

Table II.C.3 Frequencies of chromosome aberrations in lymphocytes and estimated doses in the three workers after the accident

Worker	Indicator	9-hour	23-hour	48-hour	Total	Estimated dose
A	PCC-R	150/100	-	-	150/100	>20 GyEq*
	Dic	445/50	197/20	73/8	715/78	22.6 (15.0->30) GyEq**
	Dic+R	563/50	250/20	90/8	903/78	24.5 (16.0->30) GyEq**
B	PCC-R	77/100	-	-	77/100	7.4 (6.5-8.2) GyEq*
	Dic	199/75	127/50	153/50	479/175	8.3 (6.9-9.8) GyEq**
	Dic+Rc	224/75	147/50	166/50	537/175	8.3 (6.9-10.0) GyEq**
C	PCC-R	24/100	-	-	24/100	2.3 (1.8-2.8) GyEq*
	Dic+Rc	63/100	64/100	64/100	191/300	3.0 (2.8-3.2)GyEq***

Table II.C.4 Response measures taken for chromosome analysis of the three victims of the criticality accident in Tokai-mura

September 30, 1999	
10:35	A criticality accident occurred at Tokai-mura
15:25	Three victims were transferred from Mito to the National Institute of Radiological Sciences by helicopter and ambulance.
16:00	The media and agents for culture were freshly prepared.
19:30	Blood samples, 9 ml each, were collected. The lymphocyte separation was started (at 9 hours after the accident).
20:30	The first culture was started.

October 1, 1999	
9:30	The blood samples for the second chromosome analysis were collected (at 23 hours after the accident).
10:30	The second culture was started.

October 2, 1999	
10:30	The blood samples for the third chromosome analysis were collected (at 48 hours after the accident).
11:30	The third culture was started.
19: 30	Okadaic acid was added to the three tubes of the first culture.
20:30	The harvesting of the first culture was started.
21:30	The harvesting of the first culture was completed. The fixed cells were kept in a freezer.
23:30	Air-dried slides were prepared, stained with Giemsa's solution, and embedded.

October 3, 1999
1:00	Microscopic observation was started.
2:00	The PCC-R analyses for the three workers were completed, and doses were estimated (at 53.5 hours after blood sampling, or 62.5 hours after the accident).
3:00	Chromosome slides for the Dic+R analysis were prepared again since they were found to be fixed insufficiently.
5:30	The Dic+R analysis for Mr. C was completed, and dose was estimated (at 57 hours after blood sampling, or 66 hours after the accident).
9:30	Okadaic acid was added to the three tubes of the second culture.
10:25	The estimated doses were reported at the meeting to plan clinical treatment. They were based on the results of the PCC-R analysis for the three workers, and those of the Dic+R analysis for Mr. C.
10:30	The harvesting of the second culture was started.
11:30	The harvesting of the second culture was completed. The fixed cells were kept in a freezer.

October 4, 1999
10: 30	Okadaic acid was added to the three tubes of the third culture.
11:30	The harvesting of the third culture was started.
12:30	The harvesting of the third culture was completed. The fixed cells were kept in a freezer.

October 13, 1999
10:30	The Dic + Ring analyses confirmed the doses estimated in three workers by PCC-R to be accurate. The doses of the three workers were reported at the meeting to plan clinical treatment.

Acknowledgments

II.D. Dose assessment based on ^{24}Na measurements

Introduction

During this criticality accident, neutrons were released in large quantities and activated various surrounding materials. The quantification of activation products in stainless steel objects, as well as measurements of the residual radioactivity in the precipitation tank, was used to estimate the total number of fissions. The human body is also subject to activation, and various radionuclides were produced in the bodies of the workers. Of the various radionuclides produced, ^{24}Na is usually generated in the largest quantity and is the easiest to detect. We therefore used measurements of ^{24}Na content as a physical dosimetry strategy. This Section D of Chapter II describes the data related to measurements of ^{24}Na blood levels, which were directly used for dose estimation. The data on other neutron activated radioanuclides, which were used as backup data, is included in Chapter III.

II.D.a. Blood

a.1. Gamma ray spectrometry (^{24}Na measurements) (MU01a)

This Section D.a describes the methods we used to measure the gamma ray nuclides in the blood samples of the three workers and the results of the measurements focusing on ^{24}Na.

Samples and analytical methods

Blood samples were collected on September 30, immediately after the three JCO workers arrived at NIRS, as well as on the next day (October 1), and were subjected to gamma ray spectrometry. The blood samples were transferred from syringes to containers for measurement in styrene U8 cylindrical containers, 45 mm in inner diameter at the bottom. Small amounts of heparin were added to prevent blood coagulation. The gamma rays were measured using three germanium semiconductor detectors. The volume of the blood samples collected on October 1 was 20 ml for each person. On September 30, blood samples were collected immediately after the workers arrived at NIRS and were used for various tests. The blood that remained in the syringes (6.4 ml, 11.9 ml, and 7.6 ml for workers A, B, and C, respectively) was also subjected to gamma ray spectrometry. These samples showed partial coagulation, since almost 20 hours had passed since being taken. They were redissolved by addition of 2 ml of Solvable (Packard Bioscience).

To ensure the reliability of the measurement values and to derive accurate analytical results, gamma ray spectrometry was conducted by three different groups. The gamma rays were measured using three germanium semiconductor detectors at the Radiation Research Division (Measurement Room at the Medical Care Building for Radiation Emergencies in the Third Research Building), the Human Radiation Environment Division (Second Low Level Radiation Measurement Laboratory at the First Research Building), the Environmental and Toxicological Sciences Research Group (Environmental Radiation Measurement Laboratory in the Third Research Building), and were mutually compared. The semiconductor detectors at the Measurement Room of the Medical Care Building for Radiation Emergencies, Second Low level Radiation Measurement Laboratory, and Environmental Radiation Measurement Laboratory are named here G1, G2, and G3, respectively, and their type number and performances are listed in Table II.D.1.

Table II.D.1 Semiconductor detectors used to measure gamma rays

Detector	Place of installation (Division in charge of measurement)	Manufacturer of the detector, type number	Relative efficiency (%)	Energy resolution FWHM at 1.33 MeV (keV)
G1	Measurement Room of the Medical Care Building for Radiation Emergencies (Radiation Research Division)	Ortec (US), GMX-20190-P	23	1.95
G2	Second Low Level Radiation Measurement Laboratory in the First Research Building (Human Radiation Environment Division)	Canberra (US), model GC1318	14.8	1.8
G3	Environmental Radiation Measurement Laboratory in the Third Research Building (Environmental and Toxicological Sciences Research Group)	Ortec (US), model 137CP2-2	25	1.8

The three detectors were mutually calibrated by preparing a 20 ml standard sample (Amersham, IsotrackQCY48) in a container (U8) of the same shape as that used for the blood samples.

The number of the sample, the date of sampling, the time that the measurement started, and the duration of the measurement are listed in Table II.D.2 for gamma ray spectrometry of the blood samples.

Table II.D.2 Starting time and duration of the measurement

Sample	Time at which the sample was obtained (time after the accident)	Measurement 1 Starting time of measurement, detector, duration	Measurement 2 Starting time of measurement, detector, duration	Measurement 3 Starting time of measurement, detector, duration	Measurement 4 Starting time of measurement, detector, duration	Measurement 5 Starting time of measurement, detector, duration
A-1	Sep.30 15:40 (5.1 hours)	Oct.1 21:49 G2, 3000 sec	Oct.8 18:14 G3, 80000 sec			
B-1	Sep.30 15:40 (5.1 hours)	Oct.2 20:12 G2, 3000 sec				
C-1	Sep.30 15:40 (5.1 hours)	Oct.1 20:28 G2, 3000 sec				
A-2	Oct.1 12:27 (25.9 hours)	Oct.1 13:33 G2, 3000 sec	Oct.1 14:49 G1, 3000 sec	Oct.2 8:48 G1, 6000 sec	Oct.7 18:00 G3, 20000 sec	
B-2	Oct.1 13:38 (27.0 hours)	Oct.1 14:29 G2, 3000 sec	Oct.1 16:47 G1, 4000 sec	Oct.2 12:20 G1, 2000 sec	Oct.2 16:46 G1, 6000 sec	Oct.6 15:44 G3, 30000 sec
C-2	Oct.1 14:25 (27.8 hours)	Oct.1 19:22 G2, 3000 sec	Oct.2 10:31 G1, 6000 sec	Oct.7 1:18 G3, 20000 sec		

Results of the measurements

The gamma ray spectra of the blood samples of workers A, B, and C, which were determined at the Medical Care Building for Radiation Emergencies, are given in Appendix A. The peaks used for quantification analyses of ^{24}Na were 1,368.6 keV and 2,754.0 keV. The results of the analyses by the Radiation Research Division, Human Radiation Environment Division, and Environmental and Toxicological Sciences Research Group are summarized in Tables II.D.3, II.D.4, and II.D.5, respectively. The ^{24}Na measurements in the Table were converted to radioactive concentrations at the time of the criticality accident (September 30, 10:35). We used 14.96 hours as the physical half-life. To correct the Na loss through urination and other biological processes with the elapse of time, a biological half-life of 10 days, which is used by the ICRP Publ. 30 (IC80) was used.

Table II.D.3 Measurements by the Radiation Research Division

Sample	Sample obtained at:	Starting time of measurement	^{24}Na concentration Bq ml^{-1} At the time of sampling	^{24}Na concentration Bq ml^{-1} At the time of the accident*
A-2	Oct.1 12:27	Oct.1 14:49 Oct.2 8:48 (measured twice)	47.1 ± 0.6**	168 ± 2**
B-2	Oct.1 13:38	Oct.1 16:47 Oct.2 12:20 Oct.2 16:46 (measured three times)	23.8 ± 0.6**	90.0 ± 2.3**
C-2	Oct.1 14:25	Oct.2 10:31	5.91 ± 0.29	23.0 ± 1.1

* The biological half-life was also taken into account in the estimation.
** Average of two or three measurements

Table II.D.4 Measurements by the Human Radiation Environment Division

Sample	Sample obtained at:	Starting time of measurement	^{24}Na concentration Bq ml^{-1} At the time of sampling	^{24}Na concentration Bq ml^{-1} At the time of the accident*
A-2	Oct.1 12:27	Oct.1 13:33	49.2 ± 0.6	176 ± 2
B-2	Oct.1 13:38	Oct.1 14:29	24.3 ± 0.32	91.8 ± 1.2
C-2	Oct.1 14:25	Oct.1 19:22	5.85 ± 0.14	23.0 ± 0.5
A-1	Sep.30 15:40	Oct.1 21:49	130 ± 2	167 ± 3
B-1	Sep.30 15:40	Oct.2 20:12	85.6 ± 2.0	110 ± 3
C-1	Sep.30 15:40	Oct.1 20:28	20.0 ± 0.6	25.7 ± 0.9

* The biological half-life was also taken into account in the estimation.

Table II.D.5 Measurements by the Environmental and Toxicological Sciences Research Group

Sample	Sample obtained at:	Starting time of measurement	^{24}Na concentration Bq ml^{-1}	
			At the time of sampling	At the time of the accident*
A-2	Oct.1 12:27	Oct.7 18:00	45.6 ± 4.1	163 ± 15
B-2	Oct.1 13:38	Oct.6 15:44	24.5 ± 1.2	92.6 ± 4.6
C-2	Oct.1 14:25	Oct.7 1:18	5.7 ± 0.8	23.0 ± 3.1

* The biological half-life was also considered in the estimation.

Estimation of ^{24}Na radioactive concentration at the criticality accident

As shown in Tables II.D.3 to II.D.5, the ^{24}Na measurements in the blood samples in the three groups were close to each other. The mean ^{24}Na radioactive concentrations at the time of blood sampling were derived from these values. The mean values are:

Mr. A (Blood sampling: October 1, 12:27)
$\qquad$ 47.3 ± 1.4 Bq ml^{-1}
Mr. B (Blood sampling: October 1, 13:38)
$\qquad$ 24.2 ± 0.5 Bq ml^{-1}
Mr. C (Blood sampling: October 1, 14:25)
$\qquad$ 5.82 ± 0.28 Bq ml^{-1}

From these mean values, we estimated the radioactive concentrations of ^{24}Na at the criticality accident (September 30, 10:35) using a physical half-life of 14.96 hours and a biological half-life of 10 days as used by ICRP Publ. 30.

Mr. A $\qquad$ 169 ± 5 $\quad$ Bq ml^{-1}
Mr. B $\qquad$ 91.6 ± 1.7 $\quad$ Bq ml^{-1}
Mr. C $\qquad$ 22.9 ± 1.1 $\quad$ Bq ml^{-1}

Here, the data of the samples obtained on October 1 were mainly used (the mean of the measurements using the three detectors). The data of the samples obtained on September 30 were used only as reference. On September 30, the blood was sampled from the workers for medical tests and the blood that remained in the syringes was collected and used for ^{24}Na measurements. The blood samples taken on September 30 were small in volume and partially coagulated, and the ^{24}Na concentration was measured using only one detector (G2). The samples therefore were used only as a rough estimate of ^{24}Na. Just for reference, we give a comparison of the blood samples on September 30 and October 1. The ^{24}Na concentration (after correcting for the physical and biological half lives) in the blood sample obtained on September 30 was 20% higher than the sample obtained on October 1 for Mr. B and approximately 12% higher for Mr. C. However, Mr. A showed a slightly lower value for the September 30 sample than that taken on October 1. Although the results varied, the overall tendency was lower ^{24}Na concentrations in the samples collected on October 1 than those sampled on September 30.

a.2. Measurement of stable Na

To estimate the doses based on the ^{24}Na that was generated by neutron activation, the specific activity should be determined after quantifying the stable sodium (^{23}Na) present. Therefore, we completely decomposed the blood samples with acid, and analyzed the concentration of stable sodium using inductively coupled plasma atomic emission spectrometry (ICP-AES). The samples used for the analyses were the samples collected on September 30 and October 1 from the three workers. Solvable was added to the samples of September 30 after sampling. Therefore, we also analyzed Solvable and investigated its effects on the concentrations of the elements.

Samples and analytical methods

Using a micropipette, we placed 100 µl of the blood from each sample into a Teflon vessel. Since the blood samples obtained on September 30 were coagulating, we conducted sampling by weighing approximately 100 mg. We added 2 ml of 68% nitric acid, tightly sealed the vessel, and heated and decomposed the samples for 1 hour in a microwave oven. After the decomposition process, we heated the samples on a hotplate installed within a clean draft, and dried the samples, which we then dissolved in 1 ml of 68% nitric acid and dried once again. The residues were transferred to 20 ml polyethylene vials using 0.5 ml of 27% nitric acid. The samples were adjusted to 20 ml by measuring their weight, and were used as the mother samples for analysis (nitric acid concentration: 0.68%, ratio of dilution to the original blood: 200 times). The samples were further diluted 2,000 or 10,000-fold compared with the original blood before analysis (nitric acid concentration: 0.68%). To correct for fluctuations in sensitivity during measurement, yttrium was added to the sample and standard solution as the internal standard to make a concentration of 2 µg ml^{-1} of solution. The measurements were conducted using ICP-AES (Seiko, SPS-7700). The wavelength and cumulative time used for the analysis were 588.995 nm and 3 seconds, respectively. The calibration curves were drawn by using the multi-element standard solution (SPEX-XSTC-21), which was diluted to 0.1, 0.3, 1.0, 3.0, 10, and 30 µg/ml^{-1}. We sampled 100 µl of Solvable, and decomposed and analyzed it in the same way as the blood samples. Each sample was decomposed and analyzed twice (three times for some samples) to investigate the deviation in the analytical results. Sodium is a very common element in the environment and may enter from the environment during the sample preparation and analysis. Therefore, the operation was conducted within a clean room, and a clean

draft was used during the decomposition and dilution operations. Highly purified nitric acid (Tamapure, AA-100) was used. Pure water was prepared using MilliQ SP TOC. The vessels and vials for the samples were washed in advance with nitric acid and pure water. (We used a slightly modified version of the analytical method described by Yoshida and Muramatsu (YO97) for the ICP-AES analyses.)

Results of the analyses

The results of the analyses are summarized in Table II.D.6. The sodium concentration in the blood samples obtained on October 1 was 2,050 µg ml^{-1} for Mr. A, 2,110

µg ml^{-1} for Mr. B, and 1,860 µg ml^{-1} for Mr. C. According to ICRP Publ. 23 (IC75), the total amount of sodium in the blood of a standard human is 10 g and the total volume of blood is 5,200 ml (Tables 105 and 108 in ICRP Publ. 23). Therefore, the average concentration of stable sodium in the blood is

$$10 \text{ g} / 5{,}200 \text{ ml} = 1{,}900 \text{ µg ml}^{-1}.$$

Our analytical values were very similar to this value. The sodium concentrations in the blood samples obtained on September 30 were high, and it is clearly necessary to take into account the sodium contained in Solvable, which was added to the blood samples after sampling.

Table II.D.6 Analytical results of stable sodium in blood

Sample	Worker	Date of sampling	Unit	Sample code	Concentration	Mean	Standard deviation
Blood	A	Oct. 1	(µg ml^{-1})	BL-Oh-01-a BL-Oh-01-b	2080 2020	2050	42
		Sept. 30*	(µg^{-1})**	BL-Oh-30-d BL-Oh-30-e	3610 3410	3510	140
	B	Oct. 1	(µg ml^{-1})	BL-Sh-01-a BL-Sh-01-b	2120 2100	2110	14
		Sep. 30*	(µg g^{-1})**	BL-Sh-30-c BL-Sh-30-d	2950 3030	2990	57
	C	Oct. 1	(µg ml^{-1})	BL-YK-01-a BL-YK-01-b	1840 1880	1860	28
		Sep. 30*	(µg g^{-1})**	BL-YK-30-a BL-YK-30-b BL-YK-30-c	3590 3450 3050	3250	280
Solvable			(µg ml^{-1})	Sol-a Sol-b	9300 9430	9370	92

*The blood samples that were obtained on September 30 contained added Solvable, which influenced the Na concentration.
**Since the samples were coagulating, the volumes of the samples were determined by weight.

a.3. Specific activity

The amount of radionuclides produced by the exposure of neutrons is determined by the concentration of target stable elements and the density of neutron fluence (flux density). Specific activities were determined from the radioactivity of activated biological samples and the analytical data for their stable elements, which are described above. In other words, the specific activity (a) was derived by dividing the activity concentration (A) by the concentration of stable sodium (m), ($a = $ A/m). By deriving the specific activities in the biological samples of the three workers, we were able to calculate the quantity of neutrons they had received during the accident (the neutron fluence) and thence estimate the doses. The methodology for estimating the dose by measuring ^{24}Na in the blood is provided in several reports (IA82, IA01, FE93). Blood is easy to sample, and, since it circulates throughout the body, is effective in estimating the average whole body dose.

We calculated the specific activities from the ^{24}Na radioactive concentrations and the concentrations of stable sodium in the blood samples of the three workers

(MU01b). The results are listed in Table II.D.7. The values of these samples were especially important for dose estimation of the workers, which is described in the next section (II.D.a.4).

From the derived specific activity values, we were able to estimate the total amount of ^{24}Na generated in the bodies of the three workers at the time of the criticality accident. For each worker, the total amount of ^{24}Na was derived by multiplying the specific activity value, the weight of the worker, and the amount of sodium per kilogram weight (1.43 g of Na per kilogram), which was derived from the total amount of sodium (100 g) in ICRP's standard man [Publ. 30 (IC80)], weighing 70 kg. The workers had stated their weights to be 73-74 kg for Mr. A, 65 kg for Mr. B, and 68 kg for Mr. C. These values are likely to be very similar to their weights at the time of the criticality accident. Since two values of 73 kg and 74 kg were recorded for Mr. A, we used the mean of these values, 73.5 kg, for calculation. The total amounts of ^{24}Na in the bodies of workers A, B, and C are listed in the last column of Table II.D.7, and were 8.7, 4.0, and 1.2 MBq, respectively.

Table II.D.7 Amounts of ^{24}Na and stable Na in the blood samples of the three workers and specific activities

Worker	^{24}Na concentration (Bq ml^{-1} or Bq g^{-1})	^{24}Na concentration after the correction with biological half-life (Bq ml^{-1} or Bq g^{-1})	Concentration of stable Na (mg ml^{-1} or mg g^{-1})	Specific Activity (Bq ^{24}Na) (g Na)$^{-1}$	Total amount of ^{24}Na in the body (MBq)*
A	157 ± 4.6	169	2.05	8.24 E+04	8.7
B	84.7 ± 1.6	91.6	2.11	4.34 E+04	4.0
C	21.1 ± 1.0	22.9	1.86	1.23 E+04	1.2

Notes: Radioactivity concentrations were converted to the time of the criticality accident (10:35 September 30, 1999).
The correction between the accident time and the time that the samples were obtained was conducted assuming a biological half-life of sodium of 10 days (ICRP-30 (IC80)).
Specific activity was defined as ^{24}Na concentration divided by the concentration of stable sodium.
* The total amounts of ^{24}Na (Bq) were calculated from the weights of workers A (73.5 kg), B (65 kg), and C (68 kg) and their specific activity values. The amount of stable sodium per kilogram of weight was assumed to be 1.43 g per kilogram (IC80).

a.4. Dose estimation based on the measurement of ^{24}Na in blood

Introduction

The human body contains various nuclides that are prone to activation by thermal neutrons, such as sodium (^{23}Na), phosphorus (^{31}P), potassium (^{39}K and ^{41}K), and calcium (^{44}Ca). Of these nuclides, ^{24}Na is commonly used to estimate doses during criticality accidents since it is generated from ^{23}Na in large quantities, is distributed throughout the body, has a half-life of 14.96 days and emits high energy gamma rays, which are easy to detect.

We also analyzed the radioactivity of ^{24}Na in the blood of the three workers who were heavily exposed to radiation to estimate the doses.

The method we used for estimating neutron doses is fundamentally the same as the method described in a report published by the Oak Ridge National Laboratory (FE93) and IAEA Manual (IA82). We used the latest data for various parameters that were needed for the estimation, such as neutron energy spectrum, percentage of neutrons captured by the human body, and the conversion coefficient of absorbed dose per unit fluence for each tissue. The process of computation is shown in Fig. II.D.1(a) and Fig. II.1(b).
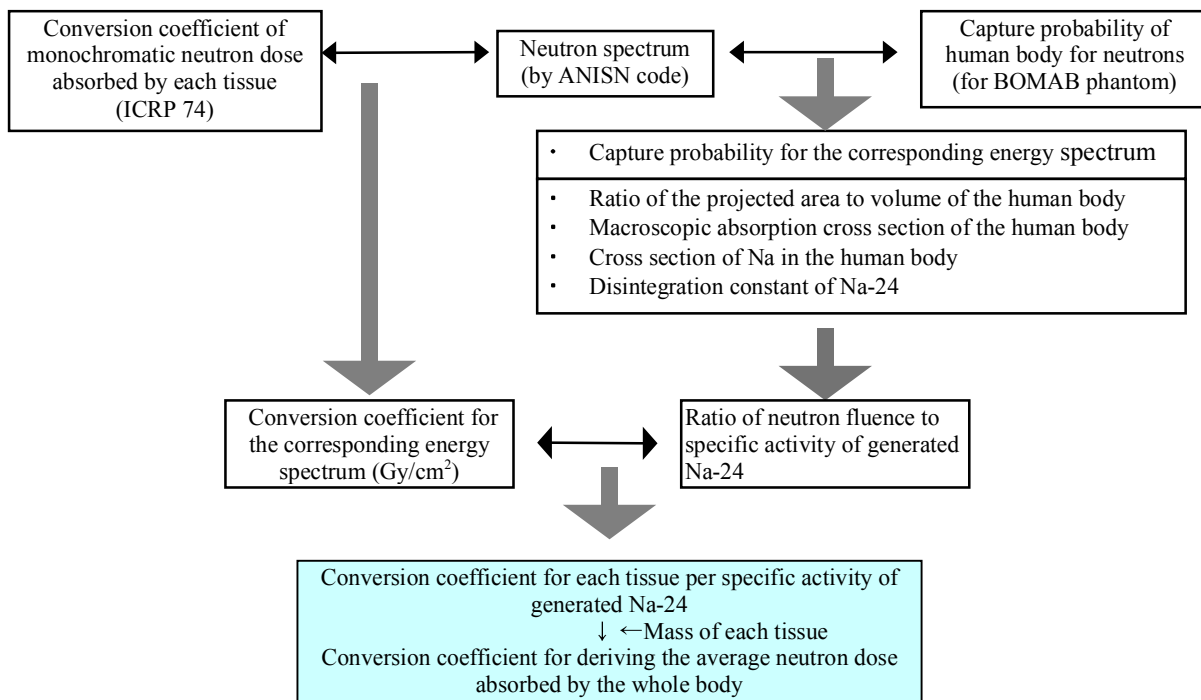
Fig. II.D.1 (a) Process of computing the conversion coefficient for neutron dose
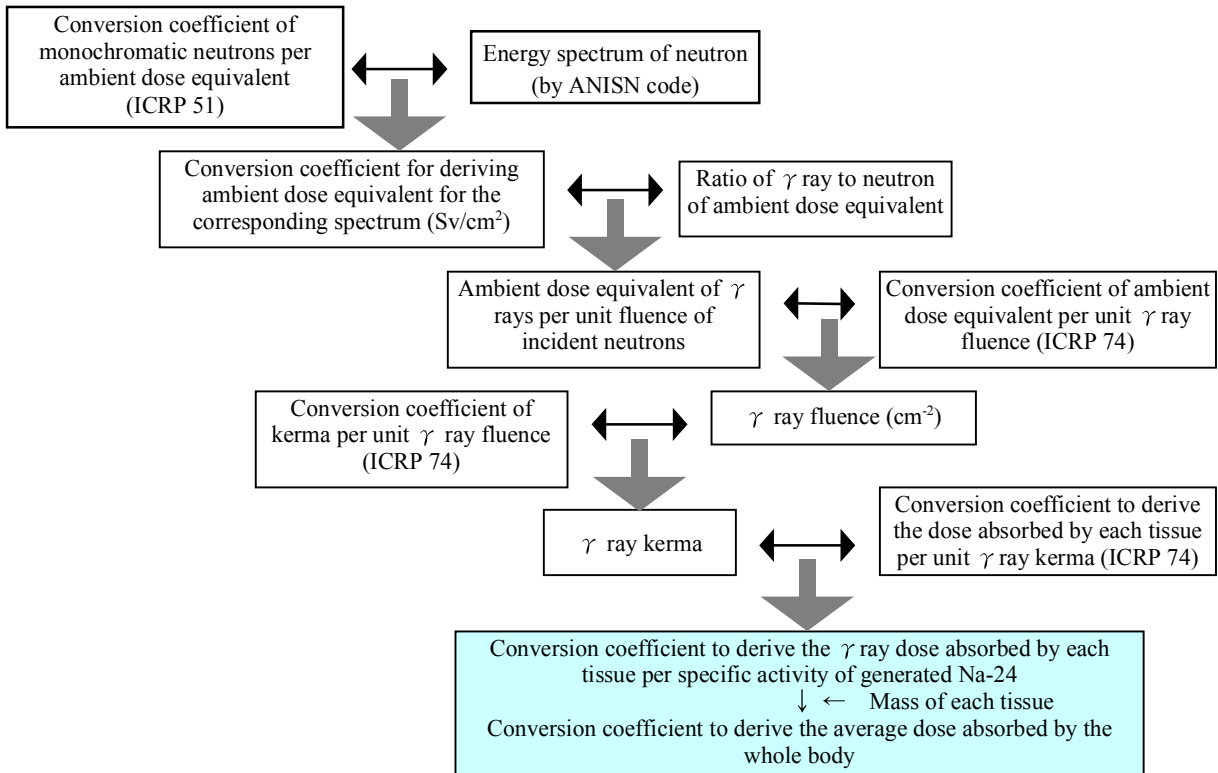
```
┌─────────────────────────┐              ┌─────────────────────────┐
│ Conversion coefficient of│             │ Energy spectrum of neutron│
│ monochromatic neutrons per│    ↔        │  (by ANISN code)        │
│ ambient dose equivalent  │             │                         │
│   (ICRP 51)             │             └─────────────────────────┘
└─────────────────────────┘
              ┌─────────────────────────┐         ┌─────────────────────────┐
              │ Conversion coefficient for deriving│   ↔  │ Ratio of γ ray to neutron│
              │ ambient dose equivalent for the │        │ of ambient dose equivalent│
              │ corresponding spectrum (Sv/cm²) │        └─────────────────────────┘
              └─────────────────────────┘
                    ┌─────────────────────────┐     ┌─────────────────────────┐
                    │ Ambient dose equivalent of γ│  ↔ │ Conversion coefficient of ambient│
                    │ rays per unit fluence of │      │ dose equivalent per unit γ ray│
                    │ incident neutrons       │      │ fluence (ICRP 74)       │
                    └─────────────────────────┘      └─────────────────────────┘
        ┌─────────────────────────┐        ┌─────────────────────────┐
        │ Conversion coefficient of│   ↔    │ γ ray fluence (cm⁻²)   │
        │ kerma per unit γ ray fluence│     └─────────────────────────┘
        │   (ICRP 74)             │
        └─────────────────────────┘
                    ┌─────────────────────────┐      ┌─────────────────────────┐
                    │   γ ray kerma          │  ↔   │ Conversion coefficient to derive│
                    │                         │      │ the dose absorbed by each tissue│
                    └─────────────────────────┘      │ per unit γ ray kerma (ICRP 74)│
                                                     └─────────────────────────┘
```

Conversion coefficient to derive the γ ray dose absorbed by each tissue per specific activity of generated Na-24
↓ ← Mass of each tissue
Conversion coefficient to derive the average dose absorbed by the whole body

Fig. II.D.1 (b) Process of computing the conversion coefficient for gamma ray dose

a.4.1) Estimation of average whole-body neutron dose

(1) Irradiation geometry

The method described in the Oak Ridge National Laboratory and IAEA technical reports assumes that neutrons uniformly enter from the front of a standing person. We also assumed this irradiation geometry.

The job that the workers were doing at the time of the accident suggests that they were likely to have been exposed from the front. However, Mr. B was bending over while pouring uranium nitrate solution into the precipitation tank. Since Mr. A and Mr. B were very close to the precipitation tank when they were exposed to radiation, they were likely to have been exposed non-uniformly. However, we concluded that the aforementioned assumptions were acceptable as a first approximation and used this geometry to estimate the doses since the dose assessment required in an emergency had to be performed quickly.

(2) Neutron energy spectrum

Data on a spherical system computed by ANISN codes, provided by the Japan Nuclear Cycle Development Institute, were used as the energy spectra of neutrons. According to this data, the energy spectrum varies slightly depending on the distance of the target from the solution. Since 1) it was impossible to identify precisely the positions of the three workers at the time of exposure, 2) the distance of a person to the solution varies according to body part, and 3) the data by ANISN is one-dimensional

and cannot express the direction dependency of the spectra, it was not significant to use different spectra for each worker. This analysis used the spectrum at 60 cm from the center of the criticality solution, where Mr. A was likely to be exposed, for all three workers. The energy spectrum used in the calculation is shown in Fig. II.D.2.
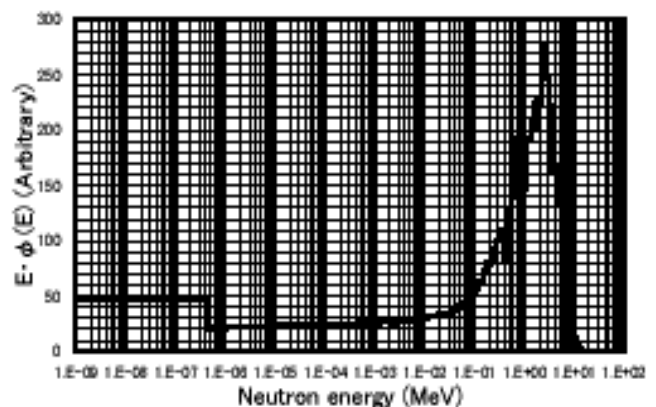

Fig. II.D.2 Energy spectrum of neutrons used for calculation

(3) Dose of monochromatic neutrons absorbed by each tissue

The absorbed doses per unit fluence $D_i(E)$ (pGy cm^2) of each tissue i with respect to monochromatic neutrons were obtained from ICRP Publication 74 (IC96). Its data comprise a summary of the latest simulation analyses using MIRD phantom and others, and are decided to be

the most reliable of available conversion coefficients at present. It should be noted that the dose of secondary gamma rays generated in the workers' bodies by the incident neutrons is included in the conversion coefficient. The $D_i(E)$ values are shown in Fig. II.D.3 for the main tissues.
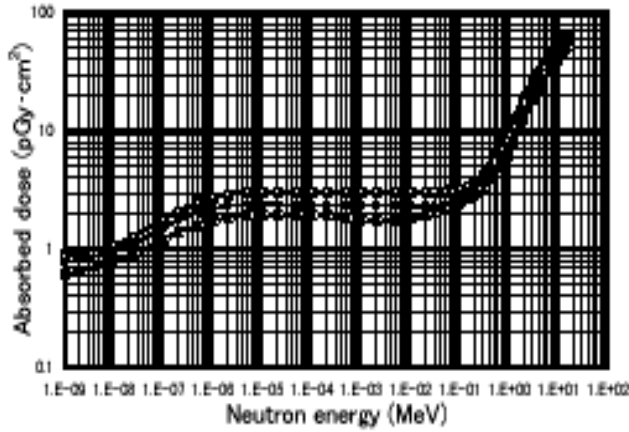
Fig. II.D.3 Dose absorbed by each tissue per unit neutron fluence (IC96)

□: Colon, ●: Lung, ✻: Bone marrow

(4) Dose absorbed by each tissue

The absorbed dose per unit fluence D_I (pGy cm^2) of tissue i with respect to the aforementioned energy spectrum $\phi(E)$ was determined using the following equation:

$$D_i = \frac{\int D_i(E) \cdot \phi(E) dE}{\int \phi(E) \, dE} \quad (1)$$

The conversion coefficient of the whole body dose was derived by averaging the dose for each tissue weighted by the mass of the individual tissue.

The conversion coefficients that we derived for the main organs and the whole body are shown in the following Table.

Bone marrow	6.96 (pGy cm^2)
Colon	9.42 (pGy cm^2)
Lung	9.97 (pGy cm^2)
Whole body	9.57 (pGy cm^2)

(5) Estimation of neutron fluence using the measurements of ^{24}Na in the blood

The specific activity a of ^{24}Na generated per unit weight of stable sodium can be approximately expressed using the following equation (FE93, IA82):

$$a = \frac{\lambda}{(V\rho)} \times (S\Phi) \times \left\{ \frac{(\sigma\rho N_{av}/W)}{\Sigma_T} \right\} \times \xi \quad (2)$$

where

- a : specific activity; activity of ^{24}Na produced per 1 gram of ^{23}Na (Bq^{24}Na / g ^{23}Na),
- λ : disintegration constant of ^{24}Na (1.28E-5 s^{-1}),
- V : volume of the body; here, the value of the BOMAB phantom was used (68,280 cm^3) (CR81),
- ρ : Na concentration in the body (g cm^{-3}),
- S : projected area of the body; here, the value of the front vertical projection (5,690 cm^2) of the BOMAB phantom was used (CR81),
- Φ : fluence of incident neutrons (cm^{-2}),
- σ : microscopic absorption cross section of ^{23}Na for thermal neutrons (0.534b) (FE93),
- N_{av} : Avogadro number (6.02E23),
- W : atomic weight of sodium (23),
- Σ_T : macroscopic capture cross section of the human body for thermal neutrons (0.02339 cm^{-1}) (HU59), and
- ξ : capture probability of human body for the corresponding energy spectrum; here, the value that was calculated by Cross et al. for the BOMAB phantom filled with diluted salt water was used (CR81), and the difference in hydrogen content between water and human tissue was corrected (IA82).

The fluence of neutrons that irradiated the body was calculated from specific activity a (Bq ^{24}Na / g^{23} Na) using the following equation:

$$\Phi = 6.9 \times 10^6 \times a \ (\text{cm}^{-2}) \quad (3)$$

(6) Conversion coefficients of neutron dose with respect to the specific activity of ^{24}Na

The conversion coefficient for the whole-body dose with respect to the specific activity of ^{24}Na was determined by multiplying the conversion coefficient of the absorbed dose per unit fluence that was calculated for the whole body and Equation (3).

The whole-body dose D_n was determined using the specific activity a and the following equation:

$$D_n = 6.6 \times 10^{-5} \times a \ (\text{Gy}) \quad (4)$$

We compared the conversion coefficients of neutron doses that we determined with the values shown in various references (see Table II.D.8).

Table II.D.8 Comparison of neutron dose conversion coefficients in various references

Reference	Sarov (IA01)	ORNL(FE93)	Maruyama (MA68)	IPSN (RA99)	This study
Gy/(Bq/g)	1.02×10^{-4}	1.45×10^{-4}	2.09×10^{-4}	6.8×10^{-5}	6.6×10^{-5}

For the criticality accident at Sarov, the whole-body neutron dose was estimated from the ^{24}Na concentration in the blood (IA01). The conversion coefficient was 0.0509 Gy (Bq ml^{-1})$^{-1}$. This value was multiplied by the sodium concentration in the blood of the ICRP reference man 0.002 g ml^{-1} (IC75) to derive the conversion coefficient for the neutron dose. The conversion coefficient was approximately 1.5 times larger than our coefficient value. This difference is probably caused by the difference in neutron spectrum, which is in turn attributable to differences in the materials and structure of the critical assembly.

The ORNL report (FE93) states the conversion coefficients for neutron dose for critical assemblies of various materials and structures. The value in the Table is a coefficient relating to the critical assembly solutions and is the average for a 10 cm and 30 cm radius. The doses in the ORNL report are not the mean values but the maximum values, and so the coefficient is much larger than the value derived in this study.

The conversion coefficient derived by Maruyama (MA68) is approximately three times larger than our value. This is attributable to the differences in spectra and the various parameters used. The main reason is that Maruyama used the first collision dose, not the mean whole-body dose.

On October 28 and 29, 1999, NIRS invited nine specialists in radiation disorder treatments and dose estimations from abroad. A participant from IPSN (Institute for Protection and Nuclear Safety), France orally

presented the value in the Table as the conversion coefficient for the neutron dose that his group had estimated for the Tokai accident. This value was very close to the value that we estimated.

(7) Measurement of ^{24}Na and stable sodium concentrations in the blood

Blood samples of 20 cm^3 were collected from each of the three workers on the day after the accident. The ^{24}Na and stable sodium concentrations in the blood samples were measured. The ^{24}Na concentrations were measured with Ge semiconductor detectors, and crosschecked by the three groups. Measurements of sodium isotopes were performed using ICP-AES. The data was used to derive the specific activity of ^{24}Na. The details of these measurements are described in this report in Chapter II, Section D.a.1 to D.a.3.

The activity of ^{24}Na at the time of exposure was determined using a physical half-life of 14.96 hours and a biological half-life of 10 days (IC80). Since the three workers received intravenous administration before the blood samples were taken, this may have accelerated the excretion of ^{24}Na or diluted the specific activity of ^{24}Na in the blood. The evaluation of these effects is discussed in Chapter IV, Section B.

(8) Estimation of the average whole-body neutron dose

The neutron doses estimated using the methods described above are summarized in Table II.D.9.

Table II.D.9 Estimated neutron doses

Worker	Specific activity (during the accident)	Average whole-body absorbed dose
A	8.24 x 10^4 Bq g^{-1}	5.4 Gy
B	4.34 x 10^4 Bq g^{-1}	2.9 Gy
C	1.23 x 10^4 Bq g^{-1}	0.81 Gy

a.4.2) Estimation of the average whole-body gamma ray dose

(1) Introduction

To estimate the gamma ray dose near the precipitation tank, the criticality should be analyzed precisely using models that accurately reproduce the criticality precipitation tank that caused the accident as well as its periphery. NIRS conducted precise analyses in cooperation with the Japan Atomic Energy Research Institute (JAERI). The results of the analyses are described in Section E of this chapter. This Section D.a.4 describes methods for estimating gamma ray doses based on the data we acquired immediately after the accident. The finally estimated gamma ray doses are not the values described in this section but were derived using the ratio of neutrons to gamma rays, which was obtained by precise analyses. (See Section G of Chapter II.)

(2) Estimation based on environmental dose monitoring

The environmental dose was monitored near the JCO at about 20:45 on September 30 by JAERI. The data were used to estimate the average whole-body gamma ray doses of the workers through the following procedure.

①Ratio of neutrons to gamma rays per ambient dose equivalent

According to the monitoring results, the neutron to gamma ray ratio of the ambient dose equivalent was about 9:1. This ratio was used to estimate the gamma ray doses of the three exposed workers.

②Conversion of ambient dose equivalent to absorbed doses

ICRP Publication 51 lists the conversion coefficients for estimating the ambient dose equivalent from monochromatic neutrons per unit fluence (IC87). Using these coefficients and the neutron energy spectra shown in Fig. II.D.2, we derived the conversion coefficient for the ambient dose equivalent per unit neutron fluence. The

ambient dose equivalent with respect to neutrons absorbed by each worker was calculated by multiplying the conversion coefficient and the neutron fluence estimated from ^{24}Na. One-ninth of this value was used as the ambient dose equivalent of gamma rays.

The absorbed dose was calculated from the ambient dose equivalent of gamma rays using the following procedure.

(i) The ICRP Publication 51 shows the conversion coefficient for ambient dose equivalent per unit gamma ray fluence (IC87). The gamma ray fluence was derived by dividing the ambient dose equivalent of gamma rays by this coefficient.

(ii) The gamma ray kerma was derived by multiplying this gamma ray fluence and the kerma conversion coefficient per unit gamma ray fluence given in ICRP Publ. 74 (IC96).

(iii) The absorbed dose of each tissue was derived by multiplying the gamma ray kerma and the absorbed dose conversion coefficient per unit gamma ray kerma in Publ. 74. The absorbed dose for the whole body was calculated by computing the weighted average of the doses using the weight of each tissue.

From the above investigation, we derived the following equation for calculating gamma ray dose D_γ:

$$D_\gamma = 1.03 \times 10^{-4} \times a \quad \text{Gy} \tag{5}$$

(3) Estimation based on the IAEA Technical Report

The IAEA Technical Report Series No. 211 (IA82) shows a plot for reading off the estimated gamma ray kerma / neutron kerma ratio from the ratio of the number of hydrogen nuclei to the number of ^{235}U nuclei or from criticality solution volume. We estimated the averaged gamma ray dose for whole body using this plot following the procedure described in the rest of this Section D.a.4.

①Ratio of gamma ray kerma to neutron kerma

The plot of the ratio of gamma ray kerma to neutron kerma, which is cited from the IAEA technical report, is shown in Fig. II.D.4.

The volume of the criticality solution was assumed to be about 40 liters (GE99a). The volume of cooling water was estimated to be 20 liters from the design drawing of the precipitation tank. The gamma ray kerma to neutron kerma ratio was read for the total volume of 60 liters from Fig. II.D.4, and came to 2.4.

The ratio of the number of hydrogen nuclei to the number of ^{235}U nuclei was calculated from the concentrations of uranium and ^{235}U enrichment in the uranyl nitrate solution, and came to 550. The gamma ray kerma to neutron kerma ratio was read from Fig. II.D.4 for the atomic nuclei ratio of 550, and came to 1.8.

We used a ratio of 2.1, which is the average of 2.4 and 1.8, since we had no evidence by which to judge the reliability of these values.
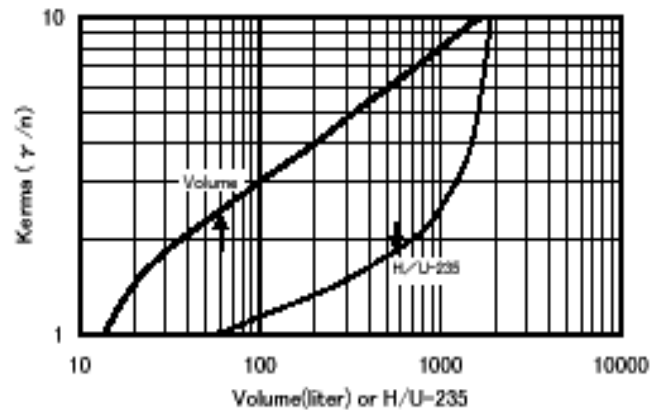

Fig. II.D.4 Gamma ray kerma to neutron kerma ratio (IA82)

②Calculation of dose absorbed from kerma ratio

The ICRU Report 46 (IC92) lists neutron kerma factors for unit monochromatic neutron fluence of various energy levels. From these kerma factors and the energy spectrum shown in Fig. II.D.2, we calculated the neutron kerma per unit monochromatic neutron fluence. By multiplying this value by 2.1, we determined the kerma of each tissue to gamma rays.

The dose absorbed by each tissue was then calculated from the kerma of the tissue to gamma rays according to the following procedure:

(i) The kerma ratio between the air and tissue was derived using the mass energy absorption coefficients of gamma rays to soft tissues and the air, which are listed in ICRU Report 44 (IC89a). The air kerma was derived by multiplying the kerma ratio by the kerma of the tissue to gamma rays.

(ii) The dose absorbed by the tissue was determined by multiplying the air kerma by the dose conversion coefficient per unit kerma, which is given in ICRP Publ. 74 (IC96). The dose absorbed by the whole body was then derived by calculating the weighted average using the weights of the tissues.

From the above investigation, we derived the following equation for calculating gamma-ray dose:

$$D_\gamma = 1.59 \times 10^{-4} \times a \quad \text{Gy} \tag{6}$$

(4) Estimated gamma ray doses

The gamma ray doses estimated by the aforementioned methods are summarized in Table II.D.10 together with neutron dose estimations.

18

Table II.D.10 Estimated average neutron and gamma ray doses absorbed by whole bodies

Worker	Neutrons (Gy)	Gamma rays (Gy)	
		Estimated from monitored data	Estimated from IAEA 211
A	5.4	8.5	13
B	2.9	4.5	6.9
C	0.81	1.3	2.0

a.4.3) Estimation of doses for each organ

Of the three workers, Mr. C was most likely to have received relatively uniform irradiation from the front. We estimated the absorbed doses of Mr. C for each organ and tissue using the methods described above. The results are listed in Table II.D.11.

Table II.D.11 Absorbed dose at each organ and tissue (Mr. C)

Organ or tissue	Neutrons (Gy)	Gamma rays (Gy)	
		From monitored data	From IAEA 211
Gonads	1.5	1.5	2.4
Bone marrow	0.59	1.1	1.8
Colon	0.79	1.3	2.1
Lung	0.84	1.3	2.1
Stomach	1.1	1.4	2.2
Bladder	1.1	1.4	2.2
Liver	0.94	1.4	2.1
Esophagus	1.1	1.2	1.8
Thyroid gland	1.3	1.6	2.5
Skin (whole body)	0.97	1.3	2.1
Bone surface	0.62	1.2	1.9
Other tissues	0.78	1.3	1.9

The values in the table show that both the absorbed doses and the dose contribution ratios of neutron to gamma rays varied considerably according to organ or tissue.

a.4.4) Conclusion

This Section D.a.4 describes methods for estimating doses from the specific activity of ^{24}Na in the blood and the estimated results for the three workers. The neutron dose was estimated to be 5.4 Gy for Mr. A, 2.9 Gy for Mr. B, and 0.81 Gy for Mr. C. The gamma ray doses were assessed using the monitoring data and the IAEA Technical Report Series No. 211 (IA82), and were 8.5 and 13 Gy for Mr. A, 4.5 and 6.9 Gy for Mr. B, and 1.3 and 2.0 Gy for Mr. C, respectively. The gamma ray dose was further investigated using the analyses described in Section E of Chapter II. The final values are given in Section G of Chapter II.

The characteristics of the exposure in this accident were 1) simultaneous exposure to neutrons and gamma rays, which have different effects on the human body, and 2) non-uniform dose distribution. These were likely to affect the clinical progress of the workers. However, the information that could be acquired from the conventional dose estimation methods applied to the present criticality accident was restricted to average whole-body doses and to total doses due to neutrons and gamma rays.

Precise dose estimation required further investigation of other aspects including clinical courses, radiation field near the precipitation tank, radiation transportation simulation that accurately reproduces the postures of the workers, and actual measurements of doses using experimental criticality devices. As part of those purposes, we conducted joint studies with the Japan Atomic Energy Research Institute. The results are described in detail in Section E and F of this chapter.

II.D.b. Whole body counter

b.1. Estimation of ^{24}Na activity in the body

b.1.1) Introduction

A typical 70-kg human body contains about 100 g sodium (^{23}Na). When the human body is exposed to neutrons, the (n, γ) process in ^{23}Na gives rise to ^{24}Na which emits 1,369 keV and 2,754 keV gamma rays. These gamma rays can be detected using a whole-body counter. One of the severely exposed workers, Mr. C, was measured with a whole-body counter at NIRS. The dose was estimated based on the whole-body measurement of ^{24}Na.

b.1.2) Whole-body count of Mr. C

The whole body count of Mr. C was carried out in the following way.
(1) Date of measurement
The measurement started at 14:29 on October 2, 1999, 51 hours and 54 minutes after Mr. C had been exposed.
(2) Description of whole-body counter
The walls of a shielded room consist of 200 mm-thick steel sheet lined with 3 mm of lead and 3 mm of Lucite. The internal dimensions are 2.6 m x 1.7 m x 1.85 m. Two NaI(Tl) detectors (8 inches diameter x 4 inches) were located above and below the bed. The distance from the bed to the upper detector was 36 cm and that to the lower detector was 14 cm. The bed was made of acrylic resin board, about 7 mm in thickness.
(3) Measurement protocol
The geometry for whole-body counting is illustrated in Fig. II.D.5. The two detectors scanned Mr. C from head to toe at a speed of 10 cm min^{-1}. The counting time was 987 s (live time).
(4) Description of subject
Mr. C put on clean overalls before the measurement. His body height was 164.5 cm and body weight was 67.8 kg.
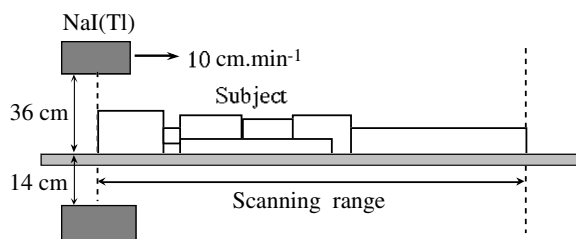
Fig. II.D.5 Measurement geometry for whole-body counting

b.1.3) Calibration

(1) Phantoms
Calibration phantoms equipped with the whole-body counter were two block-type phantoms of the adult size; one was filled with ^{137}Cs solution, and the other was filled with ^{40}K solution. Using these phantoms, the whole-body counter was calibrated for two energies, i.e., 662 keV and 1,461 keV. The calibration phantoms were measured on the same day that Mr. C was measured.

(2) Estimation of calibration coefficient
Calibration coefficients were calculated using the following equation:

$$E_i = S_i / (T\, A_i\, I_i)$$

E_i : Calibration coefficient (cps / photon),
i : Gamma ray energy (MeV) (i = 0.66, 1.369, 1.461)
S_i : Photo-peak area T = Counting time (s),
A_i : Activity in the phantom (Bq) and
I_i : Gamma ray emission rate.

The following values were used for T, A_i, and I_i:
T = 1943 s, $A_{0.662}$ = 1359 Bq, $A_{1.461}$ = 18477 Bq, $I_{0.662}$ = 0.851, and $I_{1.461}$ = 0.107.

There are several methods for calculating photo-peak area S. Two different methods shown in Section b.4 were used in the present study. Calibration coefficients calculated using Method (1) were $E_{0.662}$ = 6.071 x 10^{-3} cps/photon, and $E_{1.461}$ = 5.370 x 10^{-3} cps/photon. Those calculated with Method (2) were $E_{0.662}$ = 6.043 x 10^{-3} cps/photon, and $E_{1.461}$ = 5.206 x 10^{-3} cps/photon.

(3) Dependence of calibration coefficient on gamma ray energy
The calibration coefficient depends on gamma ray energy. The calibration coefficients were, however, measured for only two energies: 662 keV and 1,461 keV. Thus, an interpolation was made from the two measured points to estimate a calibration coefficient for 1,369 keV. To determine an appropriate function for interpolating, the dependence of the calibration coefficient on gamma ray energy was investigated using four point sources. Fig. II.D.6 shows the relationship between the calibration coefficient and gamma ray energy.
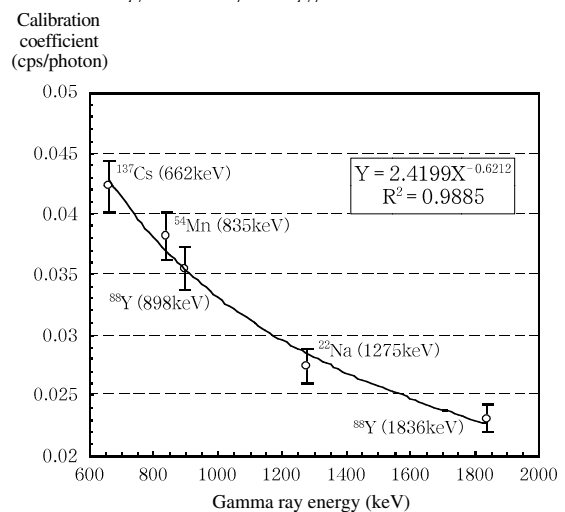
Fig. II.D.6 Dependence of calibration coefficient on gamma ray energy (point sources)

As shown in Fig. II.D.6, the calibration coefficient can be related with gamma ray energy by a power function ($Y = aX^b$). Although this relationship was obtained by measurement of point sources, it was assumed that a power function ($Y = aX^b$) could be fitted for the relationship for phantoms.

(4) Calibration coefficient for ^{24}Na

To estimate a calibration coefficient for ^{24}Na, a power function to relate gamma ray energy and the calibration coefficient was determined from the two measurement values, i.e., the calibration coefficients of the ^{137}Cs and ^{40}K phantoms. Variables a and b for a power function $Y = aX^b$ (X: gamma ray energy in keV, Y: calibration coefficient in cps/photon) were determined from two data sets (X, Y).

The following values of (a, b) were derived using two different methods for photo-peak analysis (shown in Section b.4.): (a, b) = (0.016614, -0.15499) for Method (1), and (a, b) = (0.020536, -0.18834) for Method (2). From these values, the calibration coefficients for the 1,369 keV peak were calculated at 0.005405 cps/photon (Method (1)) and 0.005270 cps/photon (Method (2)).

b.1.4) Estimation of ^{24}Na activity (at the time of measurement)

(1) Estimation of 1,369 keV photo-peak area

A gamma ray spectrum for Mr. C is shown in Fig. II.D.7. Two photo-peaks for ^{24}Na are clearly observed. The 1,369 keV photo-peak area for this spectrum was calculated using two different methods, as shown in Section b.4. The photo-peak area $S_{1.369}$ estimated using Method (1) was 367,440. The activity of ^{24}Na at the time of measurement was estimated at 68,880 Bq using the calibration coefficient of $E_{1.369}$ = 0.005405 cps/photon and a gamma ray emission rate of 1.00 (1,369 keV for ^{24}Na).

The photo-peak area $S_{1.369}$ estimated with Method (2) was 362,920. The activity of ^{24}Na at the time of measurement was estimated at 69,770 Bq using the calibration coefficient of $E_{1.369}$ = 0.005270 cps/photon and a gamma ray emission rate of 1.00 (1,369 keV for ^{24}Na).
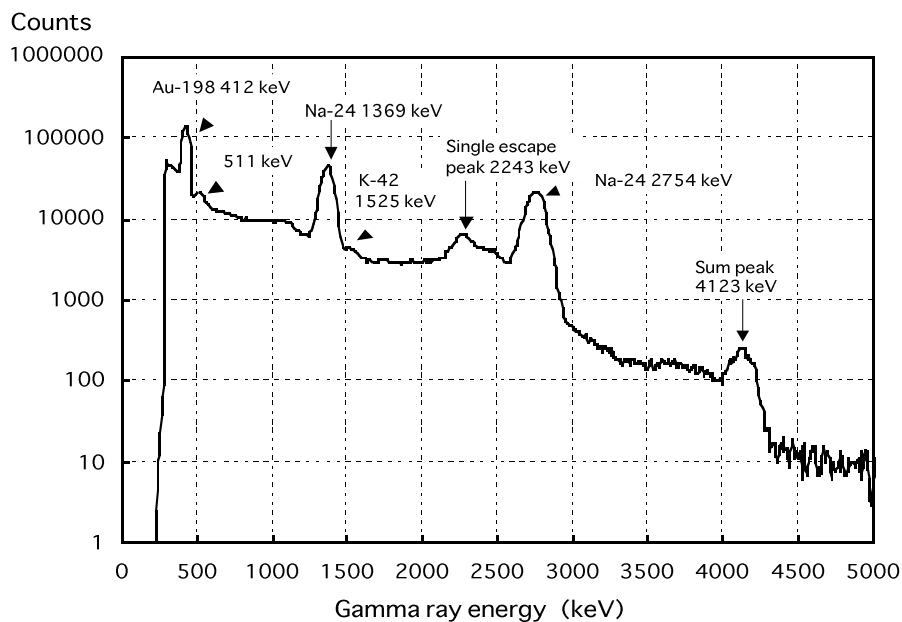

Fig. II.D.7 Gamma ray spectrum of Mr. C

(2) Effects of sum-peak and ^{40}K peak on the 1,369 keV peak

The estimation of the 1,369 keV photo-peak area can be influenced by the sum-peak (i.e. 4,123 keV = 1,369 keV + 2,754 keV) and the ^{40}K peak resulting from potassium present in the body. The effects of these factors on the 1,369 keV peak were discussed in the following way.

The ^{40}K photo-peak (1,461 keV) resulting from body potassium overlapped with the 1,369 keV photo-peak. The overlap causes an overestimation of the 1,369 keV photo-peak area. The ^{40}K photo-peak area overlapped with the 1,369 keV peak area was estimated on the basis of spectra for normal subjects (about 30 males) who have been measured periodically using the whole-body counter at NIRS. The overlapping area was estimated within a range of 2,000-3,000, which was below 1% of the 1,369 keV peak area.

If no correction is made, the presence of the 4,123 keV sum-peak causes an underestimation of the 1,369 keV peak area. Spectrum analysis showed the underestimation resulting from the sum-peak to be approximately 9,600. The value was, however, about 2.6 % of the 1,369 keV peak area. In addition, the degree of underestimation due to the sum-peak was compensated for by the overestimation resulting from the ^{40}K peak. Consequently, the effects of the sum-peak and the ^{40}K photo-peak on the 1,369 keV photo-peak area were about 2%, a value small enough to be neglected.

(3) Estimation of ^{24}Na activity

The activity of ^{24}Na was estimated at 68,880 Bq using Method (1) and 69,770 Bq using Method (2), showing only a small difference of about 1% between the two values. In the following calculation, the average of these two estimated values (69,300 Bq) was used as the activity of ^{24}Na at the time of measurement.

b.2. Estimation of specific activity at the time of exposure

b.2.1) Decay correction

To estimate the ^{24}Na activity at the time of exposure (10:35, September 30, 1999), decay corrections were made using a physical half-life of 14.959 h (FI96) and a biological half-life of 10 d (IC75). The activity at the time of exposure was calculated at 896,200 Bq.

The biological half-life for Mr. C may not have been precisely 10 d. When using a biological half-life of 7 d, the activity at the time of exposure was calculated at 955,700 Bq, 7 % higher than 896,200 Bq. Assuming a biological half-life of 5 d, the activity was calculated at 1,041,400 Bq, which was 16 % larger than 896,200 Bq.

b.2.2) Estimation of specific activity

According to the ICRP Reference Man (IC75), the human body contains about 1.4 g sodium per kg of body weight. The total body sodium for Mr. C was calculated as 94.9 g by multiplying 1.4 g by his body weight (67.8 kg). The specific activity (^{24}Na (Bq) / ^{23}Na (g)) at the time of exposure was calculated at 9,440 Bq/g by dividing the activity of ^{24}Na (896,200 Bq) by total body sodium (94.9 g).

Some references report different sodium contents to that of the above value. According to the reference (SE90), the sodium content per one-kilogram body weight was within the range of 0.92 – 1.61 g; the total body sodium for Mr. C (body weight: 67.8 kg) resulted in a range of 62.4 – 109.2 g. The specific activity was, therefore, estimated at being within a range of 8,210 – 14,360 Bq g^{-1}. Kennedy et al. (KE83) carried out an experiment on neutron activation of 18 males whose ages were from 40 to 70 y. They estimated total body sodium to be within a range of 74.8 – 99.4 g (average: 83.7 g). Using this range of total body sodium, the specific activity resulted in a range of 9,020 – 11,980 Bq g^{-1}.

These references indicate that total body sodium varies among individuals. It should be noted that the total body sodium value used in the calculation influences the estimation of the specific activity.

b.3 Dose estimation

Maruyama et al. estimated a conversion coefficient that relates specific activity with neutron dose (MA68). There was an urgent need for dose estimation immediately after the accident. The conversion coefficient (0.2092 mGy per specific activity) estimated by Maruyama et al. was used under these emergency conditions. The neutron dose was estimated at 2.0 Gy using the above conversion coefficient and the specific activity of 9,440 Bq/g.

The dose conversion coefficient for neutrons was updated after re-examination to be 0.066 mGy per specific activity (see Chapter II Section D). While the computational simulation for dose reconstruction suggested that the ratio of gamma ray dose to neutron dose is 1.83 (see Chapter II, Section E). Using the revised values and the specific activity of 9,440 Bq g^{-1} based on the ICRP Reference Man, the doses to Mr. C were estimated at 0.62 Gy from neutrons and 1.1 Gy from gamma rays. These doses corresponded to 2.2 GyEq, assuming the RBE of neutrons to be 1.7 (see Chapter II, Section G and Chapter IV, Section F).

b.4. Methods of photo-peak analysis

1. Method (A)

The photo-peak area S is calculated as shown in Fig. II.D.8 by the correction coefficient C_1; the value of C_1 is given according to the ratio of m (2m: width of peak area) to FWHM (Full Width at Half Maximum) (NO80). The width of peak area was taken so that m/FWHM had a value of 1.3 – 1.4.
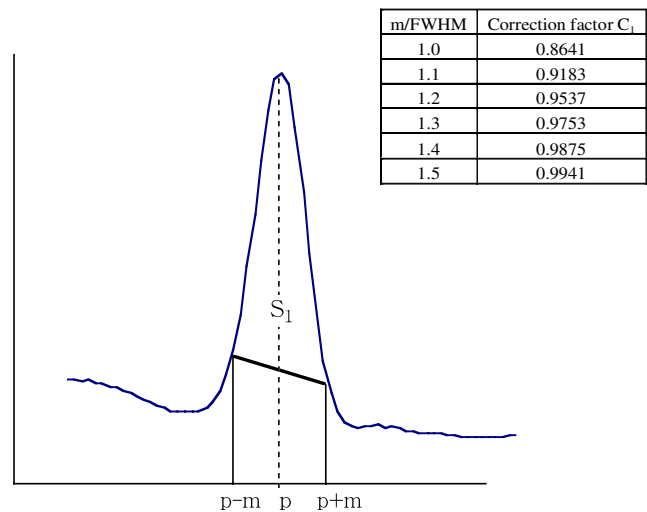
m/FWHM	Correction factor C_1
1.0	0.8641
1.1	0.9183
1.2	0.9537
1.3	0.9753
1.4	0.9875
1.5	0.9941

Fig. II.D.8 Method of photo-peak analysis (A)

The photo-peak area for each peak was calculated in the following way.

(1) ^{137}Cs phantom (662 keV peak)
    m/FWHM : 1.39 (m: 8, FWHM for the 662 keV peak: 5.74)
    C_1 : 0.9863 (interpolated from the values shown in Fig. II.D.8)
    S_1 : 13,460
    $S_{0.662}$: 13,460/0.9863 = 13,646

(2) ^{40}K phantom (1,461 keV peak)
    m/FWHM : 1.30 (m: 12, FWHM for the 1,461 keV peak: 9.24)

C_1 : 0.9753
S_1 : 20,120
$S_{1.461}$: 20,120/0.9753 = 20,630

(3) Mr. C (1,369 keV peak)
 m/FWHM : 1.37 (m:12, FWHM for the 1,369 keV peak: 8.76)
 C_1 : 0.9838
 S_1 : 361,488
 $S_{1.369}$: 367,440

2. Method (B)

The photo-peak area S is calculated as shown in Fig. II.D.9 by the correction coefficient C_2; the value of C_2 is given according to the ratio of m (2m: width of peak area) to FWHM (N080). The width of peak area was taken so that m/FWHM had a value of 1.3 – 1.4.

(1) ^{137}Cs phantom (662 keV peak)
 m/FWHM : 1.39 (m:8, FWHM for the 662 keV peak: 5.74)
 C_2 : 0.9989 (interpolated from the values in Fig. II.D.9)
 S_2 : 13,568
 $S_{0.662}$: 13,568/0.99989 = 13,583

(2) ^{40}K phantom (1,461 keV peak)
 m/FWHM : 1.30 (m:12, FWHM for the 1,461 keV peak: 9.24)
 C_2 : 0.9978

S_2 : 19,953
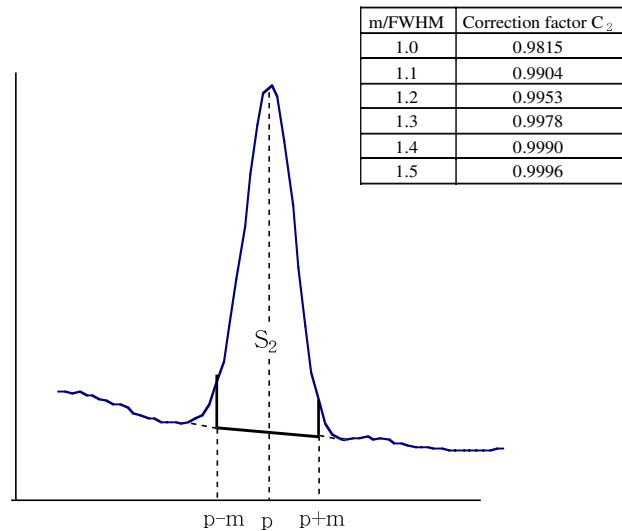$S_{1.461}$: 19,953/0.9978 = 19,996

(3) Mr. C (1,369 keV peak)
 m/FWHM : 1.37 (m: 12, FWHM for the 1,369 keV peak: 8.76)
 C_2 : 0.9986
 S_2 : 362,416
 $S_{1.369}$: 362,416/0.9986 = 362,920

m/FWHM	Correction factor C_2
1.0	0.9815
1.1	0.9904
1.2	0.9953
1.3	0.9978
1.4	0.9990
1.5	0.9996

Fig. II.D.9 Method for photo-peak analysis (B)

23

II.E. Dose reconstruction by computational simulation （IS01a, b, EN01）

Introduction

The characteristics of the exposure during this accident were: 1) the workers were simultaneously exposed to neutrons and gamma rays with different effects and attenuation coefficients within the human body, and 2) the two workers who were pouring the uranium solution were non-uniformly exposed. These factors were likely to affect the clinical symptoms of the workers. However, the methods described so far provide estimates for average whole-body doses and are not useful for estimating the relative contributions of neutrons and gamma rays.

In a joint study with the Japan Atomic Energy Research Institute, we estimated the doses absorbed by each part of the skin or body, for neutrons and gamma rays separately, using the Monte Carlo simulation method, which reproduced the positions and postures of workers and the process of radiation transportation.

II.E.a. Methods

This method estimates the dose absorbed by each part of the skin or body by positioning numerical phantoms that reproduce the position and postures of Mr. A and Mr. B near the precipitation tank, and simulating the criticality reaction and the process of radiation transportation.

a.1. Computer codes and parameters

Radiation transportation in and near the precipitation tank was calculated using the MCNP-4B (BR97) continuous energy Monte Carlo code. The codes were also used to calculate the neutron fluences per unit area of skin. On the other hand, to determine the dose distribution within the workers' bodies, we used Monte Carlo code MCNPX (WA99). For the cross section library of neutrons, FSXLIB-J3R3 (KO94) was used, which is based on a data library that has already been verified in Japan, JENDL-3.2 (NA95). The data from a cross section library of MCPLIB02 (HU96) was used to determine the transportation of photons. The average neutron doses absorbed by the skin and the whole body were derived by multiplying the neutron fluences, which were determined using the above codes, by the kerma factors listed in ICRU Report 46 (IC92).

a.2. Numerical phantoms

As a numerical phantom, we used a humanoid phantom with movable arms and legs, which was developed at the Japan Atomic Energy Research Institute (YA92). This numerical phantom is MIRD-5 type numerical phantom (SN69) but has arms and legs that are independently moveable, with spherical joints at the shoulders, elbows, and hips, and which were able to reproduce the postures of the workers at the time of the accident. The body tissues consisted of soft tissue, lung tissue, and bone tissue. The phantom is 170 cm high and 74 kg in weight, similar to the body sizes of Mr. A and Mr. B.

a.3. Numerical models of the precipitation tank and its periphery

Based on design drawings of the precipitation tank, we modeled the tank into which uranium solution was being poured and the cooling water jacket. The sections above the upper cap, angles for fixing the precipitation tank, and the tip of the agitator were simplified.

a.4. Estimation of exposure scenario

An analysis of this accident using kinetic codes (GE00) suggests that when the nuclear fission reaction occurred, it emitted a sharp pulse and then gradually faded, following a repeating damped oscillation at a cycle of approximately 10 seconds. According to interviews with the three workers, Mr. A and Mr. B detected the abnormality as a flash of blue light that was emitted when criticality occurred. They then quickly retreated from the site. This suggested that exposure to neutrons and gamma rays that were generated during the first pulse, was dominant. Mr. A and Mr. B were estimated to be exposed to these radiations while pouring uranium solution into the precipitation tank.

a.4.1) Fission number of the first pulse

From neutron monitoring data at the Naka Institute of the Japan Atomic Energy Research Institute, the discrete value during the first second, which corresponds to the first pulse, was estimated to account for ($2.6 \pm 0.6\%$) of the total value during the entire period of criticality (GE99b). The total number of fissions, from the analyses of the uranium solution in the precipitation tank, was estimated to be (2.49 ± 0.14) x 10^{18} (GE00). From these values, the number of fissions during the first pulse was estimated to be (6.5 ± 1.9) x 10^{16}.

The analysis using a kinetic code derived 5 x 10^{16} as the number of fissions during the first pulse (GE00), which is slightly smaller but similar to the above value when errors are taken into account. For the computational simulation, we used 6.5 x 10^{16}, the value estimated from the measurements.

a.4.2) Estimation of posture

Based on interviews with Mr. B, who was pouring the uranium solution, and Mr. C, who was relatively slightly affected, we attempted to reconstruct the conditions using a mock-up facility built inside JCO's conversion test building and persons who were the same height as the workers. A photograph of the mockup is shown in Fig. II.E.1. We estimated positions and postures that did not contradict the contents of the interview or make it difficult to pour the solution into the precipitation tank, and measured the distances of the two persons from the precipitation tank and the angles of their body, legs, and arms.

As described in Section E of Chapter III of this report, the specific activities were measured for ^{32}P and ^{45}Ca within the bone samples of the two workers. We also computed the specific activities of ^{32}P and ^{45}Ca in the bones and compared the values with the measurements to determine the angles of the body to the precipitation tank.

Fig. II.E.1 Reconstruction of the event in the mock-up facility

II.E.b. Results and discussion

b.1. Computed neutron and gamma ray spectra

Fig. II.E.2 shows the spectrum of neutrons that were leaking from the surface of the precipitation tank. There is no significant difference in spectrum shape between the upper and side surfaces of the precipitation tank.
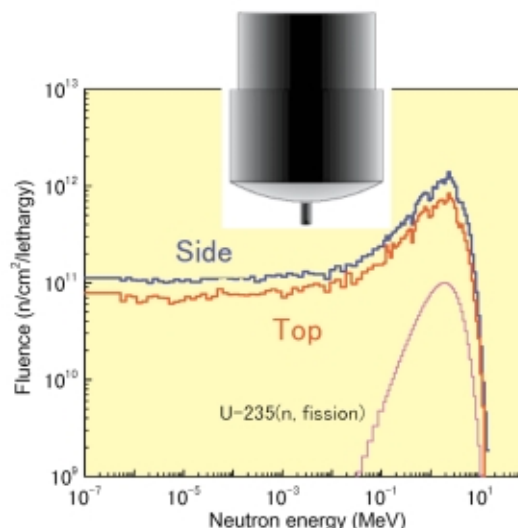

Fig. II.E.2 Leaking neutron spectrum

Fig. II.E.3 shows the gamma ray spectrum. The spectrum draws smooth curves with peaks near 0.3 MeV. Since the spectrum does not show a peak for captured gamma rays at 2.2 MeV, most of the gamma rays were likely to have been generated by nuclear fission itself. For gamma rays, there is no significant difference in the shape of spectrum between the upper and side surfaces of the precipitation tank.
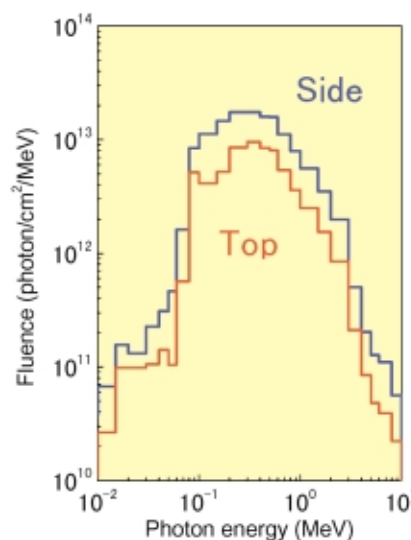

Fig. II.E.3 Leaking gamma ray spectrum

b.2. Estimated positions and postures of the workers during exposure

Fig. II.E.4 shows a computer graphic image showing the estimated positions and postures of the workers during exposure. The injury map at the skin of Mr. A (YA01) shows that the right side of the body was more seriously injured than the left, suggesting that his

25

right side was nearer to the precipitation tank. In other words, Mr. A was likely to have been standing at an angle to the precipitation tank with his right shoulder leaning forward. We compared the measured and calculated specific activities of ^{32}P and ^{45}Ca in the bones, and estimated the angles of the body parts of Mr. A as described in the rest of this section. The bone samples that were used for this purpose were the anterior intestinal spur and the seventh precordial costa, which were near to the precipitation tank and which gave data for both the right and left sides. The measured and calculated values are listed in Table II.E.1. The details of the measurements are described in Section E of Chapter III of this report.

The ratios of the specific activities in the right and left anterior intestinal spurs agreed between the measured and computed values when θ = about 15° for both ^{32}P and ^{45}Ca. On the other hand, the right to left ratios of the measured and calculated values for the seventh precordial costa agreed when θ was about 35°. From these results, we estimated the angle θ of the body of Mr. A to the precipitation tank to have been in the range of 15° to 35°. We used 25°, the average of 15° and 35°, for our computational simulation analysis.
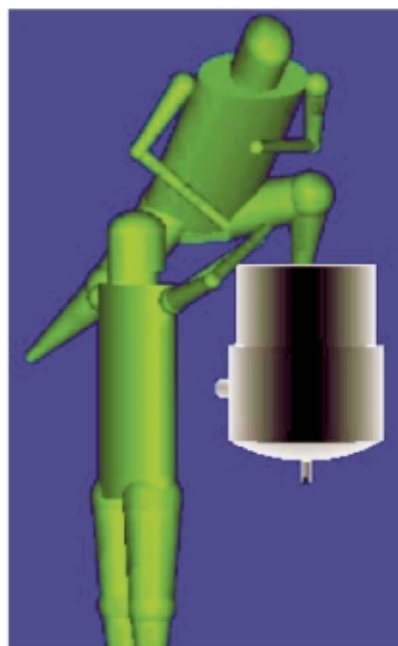

Fig. II.E.4 Estimated positions of the workers during exposure

Table II.E.1(a) Specific activity of ^{32}P in the anterior intestinal spur of Mr. A (Bq mg^{-1})

Measured values		Computed values					
		θ = 20°		θ = 30°		θ = 40°	
Left	Right	Left	Right	Left	Right	Left	Right
1.37	2.35	1.4	3.0	1.1	3.4	0.7	3.7
1.72 (right / left)		2.1		3.1		5.3	

Table II.E.1(b) Specific activity of ^{45}Ca in the anterior intestinal spur of Mr. A (Bq g^{-1})

Measured values		Computed values					
		θ = 20°		θ = 30°		θ = 40°	
Left	Right	Left	Right	Left	Right	Left	Right
9.63	16.31	10.2	22.3	8.1	26.0	5.5	27.6
1.69 (right / left)		2.2		3.2		5.1	

Table II.E.1(c) Specific activity of ^{45}Ca in the seventh precordial costa of Mr. A (Bq g^{-1})

Measured values		Computed values					
		θ = 20°		θ = 30°		θ = 40°	
Left	Right	Left	Right	Left	Right	Left	Right
7.28	18.21	10.6	19.1	8.3	19.2	6.4	20.0
2.50 (right / left)		1.8		2.3		3.1	

b.3. Spatial dose distribution near the precipitation tank

Before the doses of the workers were calculated, the neutron flux, gamma ray flux and their energy spectra near the precipitation tank were calculated using the computational simulation method. The resultant radiation field was used to calculate the tissue-absorbed doses of microscopic volume elements by using the kerma factor with respect to neutrons and the mass energy absorption coefficient with respect to gamma rays (IC92), and to estimate the dose distribution in the space around the precipitation tank. The results of these calculations are shown in Fig. II.E.5. The Y axis represents the absorbed dose per 1 x 10^{17} nuclear fission. Our analysis revealed the following.

1) Fig. II.E.5 shows that the absorbed gamma ray dose, if expressed in units of Gy, is slightly higher (18% - 35%) than the neutron dose at a height of 115 cm (near

the surface of the body) at all distances from the precipitation tank for the range we calculated.

2) Fig. II.E.5 shows that the dose varied markedly depending on the distance from the precipitation tank.
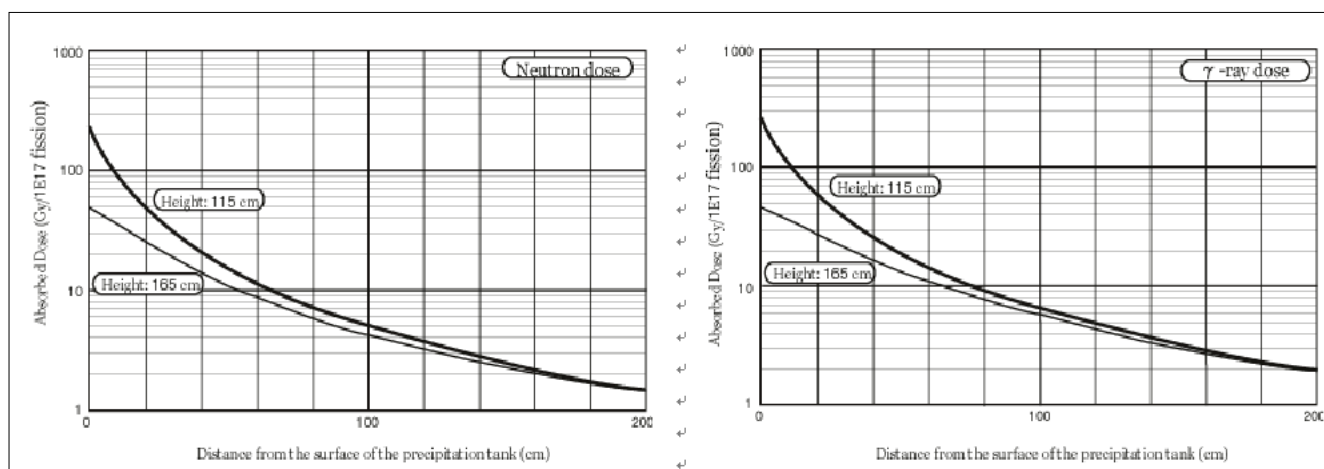
For example, the dose at a distance 10 cm from the tank was double that at 20 cm from the tank. Also, for vertical distance, the dose at 115 cm in height and 10 cm away from the tank was about 2.5 times greater than the dose at a height of 165 cm, which is the height of the face.

Fig. II.E.5 Dose distribution near the precipitation tank

b.4. Average whole body dose

Table II.E.2 lists the average dose absorbed by the whole body and the specific activity of ^{24}Na for Mr. A and Mr. B, which were determined by the computational simulation. The kerma factor of the bones varied depending on the body parts (IC92). In this computational simulation, we assumed that the bones were principally composed of cortical bone and red bone marrow, used their kerma factors to calculate the doses absorbed by the bones, and adopted their mean values as the average absorbed dose.

The Table also shows the results of the dose assessment based on the ^{24}Na measurements in the blood, which is described in Section D of Chapter II. The computational simulation separately estimated the charged particle component and the secondary gamma ray component, which were generated within the phantom, as the doses attributable to neutrons entered the phantom. On the other hand, the dose estimation described in Section D of Chapter II used the neutron conversion coefficients listed in ICRP Publ. 74 (IC96). These neutron conversion coefficients include the absorbed dose of the secondary gamma rays, which are generated by neutrons entered the human body. Therefore, the dose caused by the gamma rays generated in the human body after neutron irradiation is included in the neutron dose. By adding the absorbed dose of gamma rays that was generated within the workers' bodies to the neutron dose, the results of our computational simulation show that the gamma ray dose was 1.83 times larger than the neutron dose in Mr. A and was 1.43 times larger in Mr. B.

We then calculated the ratios of the doses estimated from the computational simulation to the doses based on the ^{24}Na measurements and listed in Table II.E.3. The

values of the computational simulation are larger than those obtained by ^{24}Na measurement for all neutron doses, gamma ray doses, and specific activities of ^{24}Na.

In the computational simulation both the absorbed doses and specific activities of ^{24}Na were proportional to the number of nuclear fissions during the first pulse. The estimated fission number contains an uncertainty of approximately 30%. Moreover, the results of the computational simulation were sensitive to the distance between the phantom and the precipitation tank. For example, we assumed for simulation purposes that the distance from the surface of the precipitation tank to the central axis of the phantom of Mr. A was 55 cm. If the distance had been 10 cm greater, at 65 cm, the absorbed doses would have been reduced by approximately 20% for both neutrons and gamma rays. On the other hand, the specific activity measurements of ^{24}Na were probably affected by the intravenous administration, which may have accelerated the excretion of ^{24}Na and/or diluted the specific activity, as described in Section D.a.4 of Chapter II. The results of the specific activity measurements, which are listed in Table II.E.2, were derived by assuming a biological half-life of 10 days. If the biological half-life were shortened to 5 days (IC80), the values would increase by 8%. As described in Section B.b of Chapter IV, the results of a simulation analysis using a compartment model suggest the possibility that the specific activity measurements were 20% lower than the actual values at the time of the criticality accident due to the acceleration of excretion and dilution by the intravenous administration. The values estimated by these computational simulations and ^{24}Na specific activity measurements are likely to resemble each other more closely when the uncertainty of the methods is fully taken into consideration.

Table II.E.2 Average dose absorbed by whole body and specific activity of ^{24}Na

Worker	Method	Charged particle component attributable to incident neutrons	Secondary gamma ray component attributable to incident neutrons	Gamma ray generated at the precipitation tank	Specific activity of ^{24}Na (10^4 Bq g^{-1})
A	Simulation	6.76	1.43	15.01	11.57
A	^{24}Na measurement in the blood	5.4		8.5, 13	8.24
B	Simulation	3.99	0.89	6.97	6.80
B	^{24}Na measurement in the blood	2.9		4.5, 6.9	4.34

Table II.E.3 Ratios of estimated values: (simulation) / (^{24}Na measurements in blood)

Worker	Charged particle and secondary gamma ray components attributable to incident neutrons	Gamma ray generated at the precipitation tank	Specific activity of ^{24}Na
A	1.5	1.2～1.8	1.40
B	1.7	1.0～1.5	1.57

b.5. Absorbed dose conversion coefficient per unit specific activity

The absorbed dose conversion coefficients per unit specific activity of ^{24}Na must be known to quickly assess doses. Table II.E.4 lists conversion coefficients derived by the computational simulation and the methods described in Section D of Chapter II.

The conversion coefficients of neutron doses were similar for the computational simulation and the method described in Section D of Chapter II. The gamma ray dose of Mr. A was an intermediate value between those derived using monitored data and the data in the IAEA technical report. The gamma ray dose of Mr. B was similar to the value derived from monitored data. The results of this computation simulation analysis support the validity of the dose assessment method based on ^{24}Na measurements in the blood, which is described in Section D of Chapter II.

Table II.E.4 Absorbed dose conversion coefficient per unit specific activity

Worker	Method	Neutrons[1]	Gamma rays[2]	
A	Computational simulation	7.08×10^{-5} (6.6×10^{-5})[3]	1.30×10^{-4} (1.2×10^{-4})[3]	
A	^{24}Na measurement in the blood	6.6×10^{-5}	1.03×10^{-4} from monitored data	1.59×10^{-4} from IAEA 211 data
B	Computational simulation	7.18×10^{-5} (6.9×10^{-5})[3]	1.03×10^{-4} (9.8×10^{-5})[3]	
B	^{24}Na measurement in the blood	6.6×10^{-5}	1.03×10^{-4} from monitored data	1.59×10^{-4} from IAEA 211 data

1) The sum of the doses of the charged particle component and the secondary gamma ray component attributable to the neutron influx to the human body.
2) Dose attributable to the gamma rays that were generated in the precipitation tank.
3) Values in parentheses denote estimates made by taking into account the scattering effect of the surface of the concrete floor.
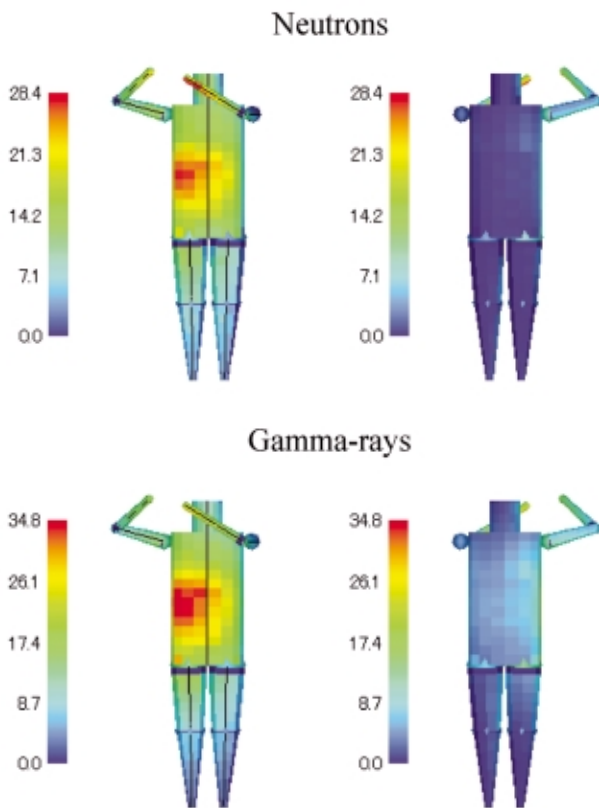
b.6. Dose distribution in the skin

Fig. II.E.6 shows the skin dose distribution of the phantom representing Mr. A (hereinafter referred to as "Phantom A"). The phantom was divided into sections 5 cm in length along the vertical axis, into 16 parts around the circumference for the body and the head and into 8 for the legs and arms. The dose values shown in the Figure are normalized with the ^{24}Na specific activity measurements. In other words, the values were derived by multiplying the doses determined by the computation

and the ratio of ^{24}Na specific activity (measured value / calculated value). In the Figure, the dose of secondary gamma rays, which was attributable to the neutron into the human body, is included in the gamma ray dose, and the neutron dose is only for the charged particle component.

For the computational simulation, we assumed that Mr. A was exposed while standing 25 degrees aslant to the precipitation tank with the right side of the body nearer to the tank than his left side. The simulation analysis showed the maximum absorbed doses to be at

the right side of the abdomen: 27 Gy for neutrons and 35 Gy for gamma rays. These values are over 5 times greater than the average whole body doses for neutrons and almost 3 times greater for gamma rays. On the skin of the chest and abdomen, its dose decreases with the distance from the right abdomen, showing that the worker was very unevenly exposed. The computed dose distribution corresponds to the seriousness of the skin injury on the chest and abdomen of the worker. The particularly high doses on the chest and abdomen may have affected the interpretation of chromosome analyses. The results of this computational simulation analysis provide data that enables discussion of this possibility and other issues.

Neutrons

Gamma-rays

Fig. II.E.6 Skin dose distribution in Phantom A

The distribution of absorbed dose in the skin around the body of Phantom A and the dose contribution of neutrons are shown in Fig. II.E.7. The neutron dose on the back was notably low due to absorption by the tissues. The minimum value on the back was 0.6 Gy, which is just 2% of the maximum value. The drop in gamma ray dose were not as marked as that for the neutron dose, and the minimum value was 7 Gy, which is 20% of the maximum. Due to this large difference in attenuation between neutrons and gamma rays, the contribution of neutron dose was 44% on the surface of the chest and abdomen but was less than 10% on the back. The result of the computation that the dose on the back is lower than the doses on the chest and abdomen

agrees with the clinical diagnosis that dermal injury on the back of Mr. A was relatively slight.
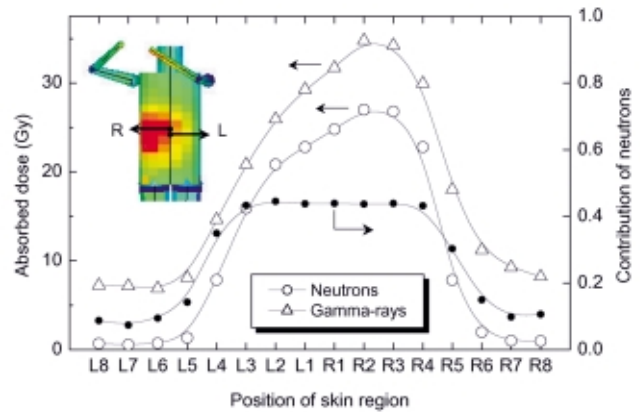
Fig. II.E.7 Distribution of skin-absorbed dose around the body of Phantom A and the contribution of neutron dose

As shown in Fig. II.E.6, the doses were similar on the right and left hands of Phantom A. Since pouring uranium solution is dangerous and had to be performed carefully, it is natural to assume that he was supporting the funnel with both hands. As described in Section E of Chapter III, the specific activities of ^{32}P and ^{45}Ca in the bone of the forefinger were almost the same for the right and left hands. The results of the simulation analysis agreed with the results of the radiochemical analyses of bone samples. On the other hand, the left branchium was less seriously injured than the right branchium, and the computational results did not agree with this diagnosis. In the simulation test that attempted to reproduce the operation using the mock-up facility, it was easy to estimate the position of the right hand, which was supporting the funnel. However, there are many possibilities for the position of the left hand, and therefore the result of the simulation analysis for the left hand is likely to be less reliable than the data for the other body parts.

The skin dose distribution of the phantom representing Mr. B (hereinafter referred to as "Phantom B") is shown in Fig. II.E.8. The skin-absorbed doses of Phantom B were the largest along the center axis of the body near the boundary between the chest and abdomen, and reached 8.4 Gy for neutrons and 8.3 Gy for gamma rays. The maximum dose to the thigh was almost the same as that to the trunk. The simulation showed that Mr. B received a lower dose than Mr. A to the skin, and was relatively uniformly exposed on the chest and abdomen. These exposure characteristics agree with the clinical diagnosis of less serious skin injury than Mr. A. Fig. II.E.9 shows the skin-absorbed dose distribution around the body of Phantom B and the contribution of the neutron dose. As with Phantom A, Phantom B shows a marked attenuation of neutron dose on the back.
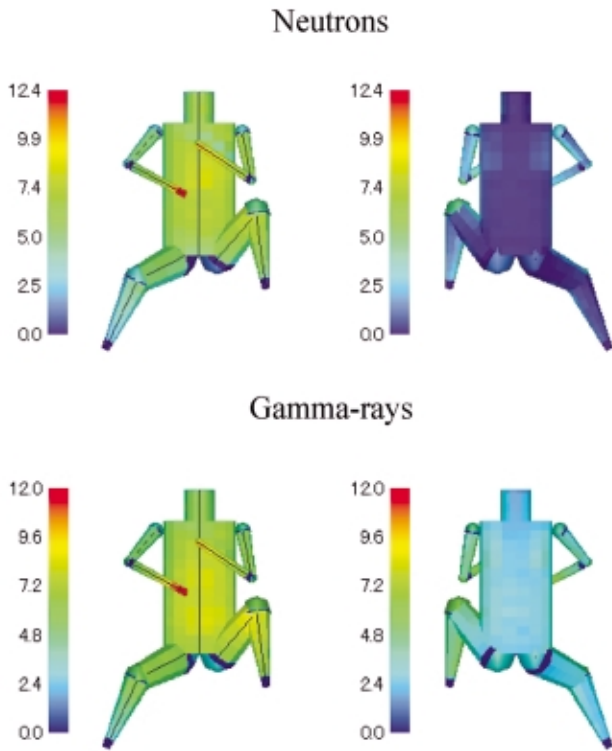
29

Neutrons

Gamma-rays

Fig. II.E.8 Skin dose distribution of Phantom B

The doses shown in the Figure are normalized to measurements of ^{24}Na specific activity, as in the figures for skin dose distribution. Reflecting exposure from the right front, the Figure shows high depth doses on the right side of the body. Neutrons rapidly attenuated inside the body due to energy loss by elastic scattering with hydrogen nuclei. The Figure shows deep penetration of neutrons into the part that corresponds to the lungs, reflecting the low density of the lungs. Compared to neutrons, gamma rays kept relatively high levels of dose in deep sections of the body, making the effects of gamma rays more prevalent in deeper body sections.
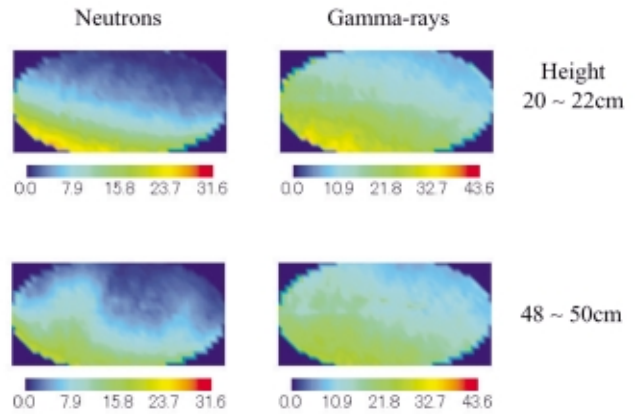

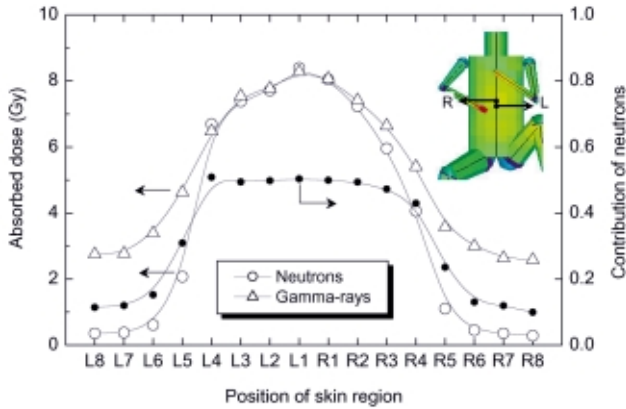**Fig. II.E.10 Depth dose distribution in Phantom A**

Fig. II.E.9 Distribution of skin-absorbed dose around the body of Phantom B and the contribution of neutron dose

b.7. Depth dose distribution

Fig. II.E.10 shows the depth dose distribution of Phantom A on cross sections of the body. The lower side of the section is the abdominal region, and the upper side is the back. The height values on the right of the Figure are the distance from the crotch. The cross sections at 20 to 22 cm (where the middle part of the intestine is included) and 48 to 50 cm (where the middle parts of the lungs are included) are shown, which are likely to be important in terms of comparison with clinical diagnoses.
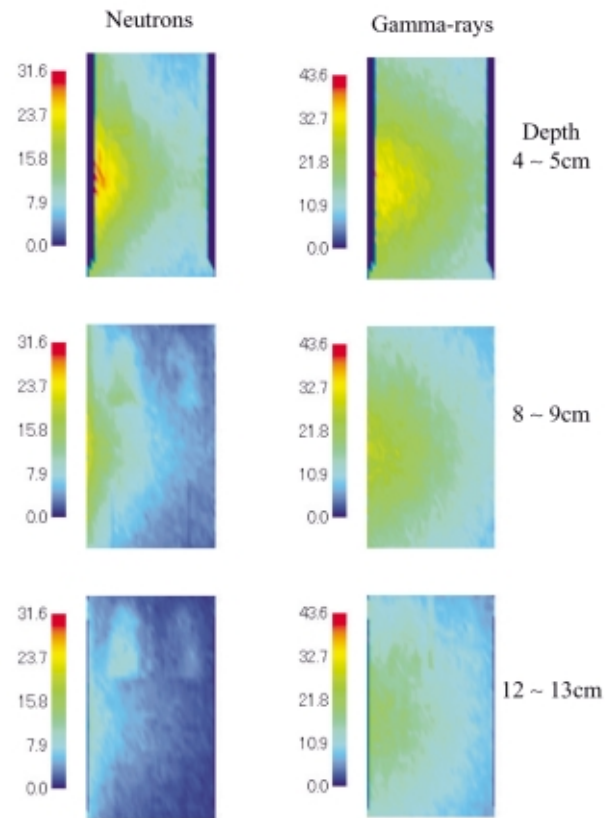

Fig. II.E.11 Dose attenuation in longitudinal cross sections of the body of Phantom A

Fig. II.E.11 shows the dose distribution in longitudinal cross sections of the body of Phantom A. The lower side of the sections is the crotch, and the upper side is the neck. The depth shown on the right of the Figure is the depth from the front to the back. We show the abdominal part of the gastrointestinal tract with cross sections 4 to 5 cm in depth, the central part with sections 8 to 9 cm in depth, and the back part in sections 12 to 13 cm. The depth doses are high on the right side, confirming exposure from the right front.
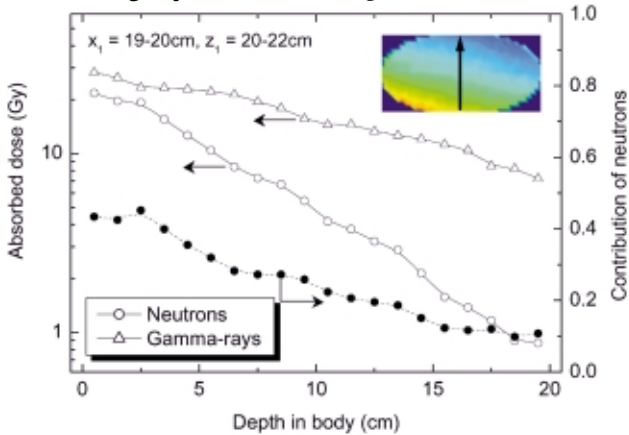

Fig. II.E.12 Dose attenuation in Phantom A

Fig. II.E.12 plots the doses at different depths in the body of Phantom A from the front to the back. The distribution is for a height of 20 to 22 cm from the crotch, where the middle part of the intestine is included. The neutron dose attenuated almost exponentially. The apparent attenuation coefficient was calculated to be 0.17 cm^{-1}. The attenuation of gamma rays was not as steep as seen for the neutrons. Therefore, neutrons accounted for close to 40% of the total dose at a depth of 3 cm, but fell to 30% at 6 cm, 25% at 10 cm, and less than 10% on the back, where the gamma ray dose accounted for the highest proportion. The dose at the depth of 4 cm to 12 cm, where most of the intestine is likely to be present, was 14 to 4 Gy for neutrons and 23 to 14 Gy for gamma rays. Simple addition shows a total dose of 37 to 18 Gy for the intestine. According to our knowledge of the effects of high-dose exposure on the human body, such high levels of exposure should cause immediate and serious injuries to the gastrointestinal tract. However, the injuries appeared much later.
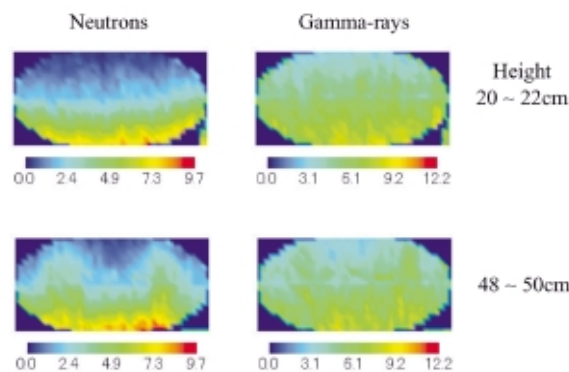
Fig. II.E.13 Dose attenuation in Phantom B

At a height of 48 to 50 cm, which crosses the right lung, the dose at the depths of 3 to 17 cm, where most of the lung is likely to be present, was 16 to 4 Gy for neutrons and 23 to 14 Gy for gamma rays. Simple addition gives a total dose of 39 to 18 Gy.

The dose distributions in the latitudinal and longitudinal cross sections of the body of Phantom B are shown in Figs. II.E.13 and II.E.14, respectively. The attenuation of dose with depth from the front to the back in the body of Phantom B is shown in Fig. II.E.15.

Fig. II.E.14 Dose attenuation in longitudinal cross sections of the body of Phantom B

Fig. II.E.15 Dose attenuation in the body of Phantom B

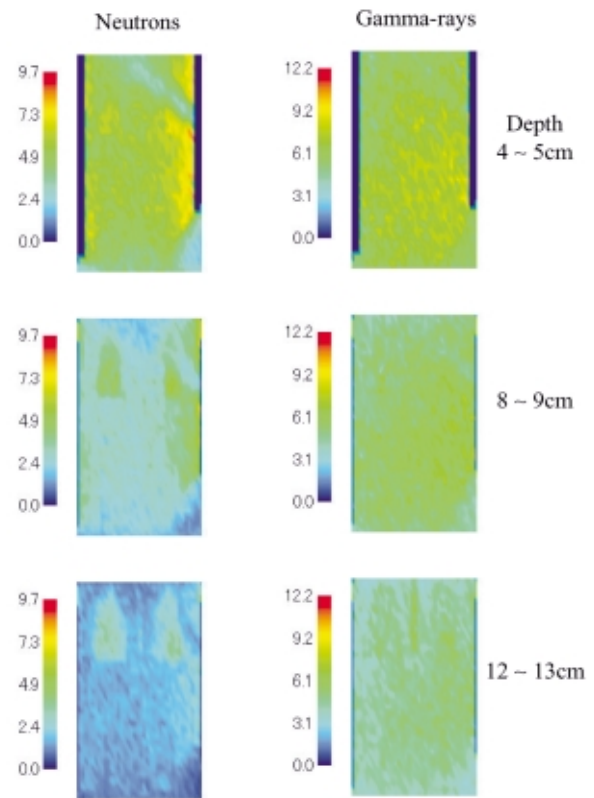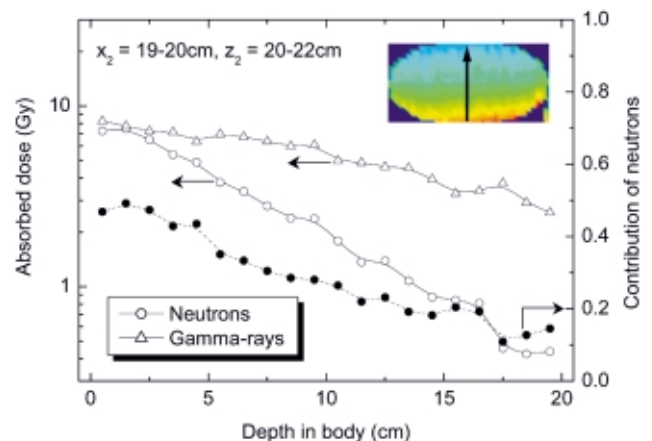The dose at depths of 4 to 12 cm was 5 to 1 Gy for neutrons and 7 to 5 Gy for gamma rays. Simple addition shows a total dose of 12 to 6 Gy. On the other hand, although not plotted on a graph, at a height of 48 to 50 cm, which crosses the right lung, the dose at the depths of 3 to 17 cm, which was mostly occupied by the lung, was 7 to 2 Gy for neutrons and 8 to 4 Gy for gamma rays. Simple addition gives a total dose of 15 to 6 Gy.

II.E.c. Conclusions

For a scientific understanding of the effects of high dose exposure and to develop its medical treatment methods, the absorbed neutron and gamma ray doses must be assessed for each part of the skin and deeper parts of the body. In a joint study with the Japan Atomic Energy Research Institute (JAERI), we conducted Monte Carlo simulation analyses on radiation transportation by reproducing the positions and postures of the workers at the time of the accident to identify the neutron to gamma ray ratio of the absorbed doses, the absorbed dose distribution on the skin, and the internal dose attenuation. Various problems concerning dose assessment are discussed in Chapter IV using the results of the computational simulation analyses.

The computational simulation method used in the analyses by modeling the positions and postures of the workers is a novel approach, and is expected to develop into a new methodology for precise dose assessment at criticality accidents.

The contents of this Section E are based on the results obtained in a joint study project between NIRS and JAERI, entitled "Dose reconstruction for workers heavily exposed during the criticality accident at Tokai-mura" (EN01).

II.F. Depth dose distribution estimation using TRACY

Introduction

The Nuclear Fuel Cycle Safety Engineering Research Facility at JAERI has a transient experiment critical facility (TRACY) that uses uranyl nitrate as fuel, as did the precipitation tank of JCO that caused the criticality accident. A phantom filled with water was positioned in the TRACY reactor chamber. The dose distribution was then measured inside the phantom using cavity chambers while operating the reactor at low power. We quantitatively analyzed the attenuation of neutron and gamma ray doses inside the phantom.

II.F.a. Experimental methods

A schematic diagram of the device is shown in Fig. II.F.1.

The core of TRACY is a cylinder 50 cm in outer diameter. It has a cylindrical cavity 7.6 cm in diameter for inserting a safety rod. The reactor is operated by filling the tank with approximately 110 liters of 9.98% uranyl nitrate solution. There is no cooling water jacket. On the other hand, the uranyl nitrate solution that was poured into the precipitation tank of JCO was at a concentration of 18.8%, and reached criticality with approximately 40 l of the solution.
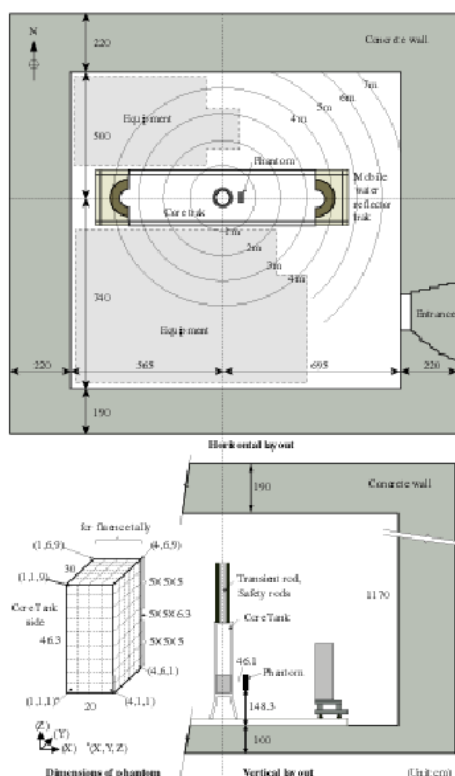

Fig. II.F.1 Schematic diagram of the experimental device

The phantom used was an elliptical cylinder 30 cm wide, 20 cm thick and 50 cm high, made of 5 mm-thick acrylic resin. The phantom was filled with tap water and positioned 46.1 cm from the surface of the core tank.

The dose was measured by inserting a pair of cavity chambers of different neutron sensitivity into the phantom, and scanning the inside of the phantom using a three-dimensional driving apparatus. The power fluctuation of TRACY was corrected by positioning a monitor cavity chamber on the front surface of the phantom and monitoring the fluctuation in power during the measurement. The sensitivity of the cavity chambers to neutrons and gamma rays was derived by calculating the weighted mean of the energy spectra obtained by computational simulation.

II.F.b. Experimental results

Our measurements of the dose distribution toward the deeper parts of the phantom along the central axis are shown in Fig. II.F.2. The doses along the horizontal direction crossing the central axis and along the height direction were almost uniform and were not affected by position, suggesting that the irradiation was uniform.

As Fig. II.F.2 shows, the neutron dose attenuated exponentially with depth. The apparent attenuation coefficient is 0.204 cm^{-1}. The attenuation of the gamma rays was less marked than for neutrons and caused a build-up of doses. The extrapolated gamma-ray dose was double the neutron dose at a depth of 0 cm, or at the surface of the phantom, but was 10 times greater at a depth of 100 mm. According to the results of the computational simulation (see Chapter II, Section E.b.3), the neutron and gamma ray doses were not significantly different at the surface of the tissues. TRACY, which contained approximately 3 times the volume of the solution in the JCO precipitation tank, was likely to cause larger attenuation of neutrons, produce more captured gamma rays, and therefore show high gamma-ray doses than the JCO precipitation tank.
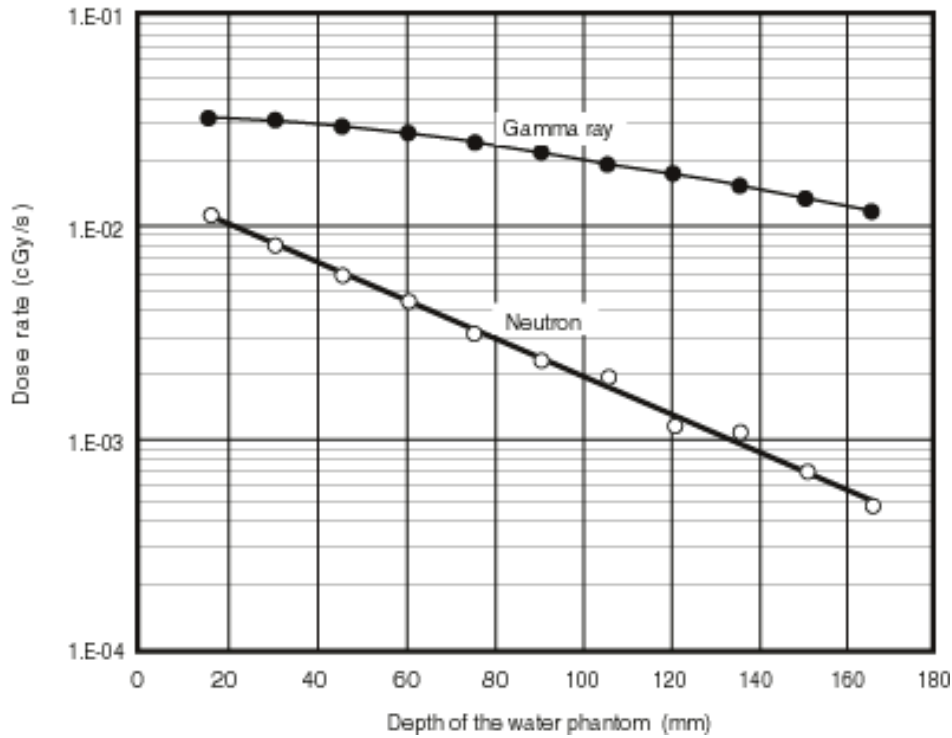
Fig. II.F.2 Measurements of depth dose in the phantom

II.F.c. Conclusion

We measured the dose distributions of neutrons and gamma rays, which were emitted from a critical facility (TRACY), in a water-filled phantom. Since the structure and composition of TRACY are different from the JCO precipitation tank that caused the criticality accident, our experiment using TRACY was not a complete reconstruction of the accident. However, measurements of dose distributions of fission neutrons are scarce, and we hope that our results will be useful as experimental data to verify the validity of various computational simulation methods.

The study described in Section F of Chapter II was conducted under a joint study contract entitled "Dose reconstruction for workers heavily exposed during the criticality accident at Tokai-mura," which was signed by NIRS and JAERI on February 1, 2000.

II.G. Summary of dose estimation

Table II.G.1 summarizes the methods and their estimated doses described in Chapter II. The first line shows "Initially estimated doses," which were urgently evaluated within several days after the admission of three workers to NIRS in order to predict the development of their symptoms and determine their medical treatment strategies. The values were primarily determined by measuring the activity concentration of ^{24}Na in the blood and by using Sarov's conversion coefficient (IA01). The values in the second line in the Table are those quoted in the final report of the Criticality Accident Investigation Committee, which was established within the government to identify the causes of the accident, based on the dose estimation presented by NIRS in the Committee in December 1999 (GE99a). Lines ① to ⑤ present the final dose values estimated using each method, the brief explanations are described in this Section G. The currently estimated doses shown at the bottom of the Table were derived based on all the results of these dose reconstruction analyses.

Table II.G.1 Estimated doses (biologically equivalent gamma ray dose: GyEq)

Method	Worker		
	A	B	C
Initially estimated doses	18	10	2.5
Report of the Criticality Accident Investigation Committee (December 24, 1999)	16〜20 or over 20	6〜10	1〜4.5
① Prodromes	over 8	4〜6 or over 6	less than 4
② Blood components (mainly lymphocyte counts)	16〜23	6〜8	1〜5
③ Chromosome analysis	16〜 over 30	6.9〜10	2.8〜3.2
④ Specific activity of ^{24}Na in the blood (neutrons and gamma rays: Gy)	(5.4, 9.9)	(2.9, 4.1)	(0.81, 1.5)
④ Total dose (assuming RBE = 1.7)	19	9.0	2.9
⑤ Human counter (neutrons and gamma rays: Gy)	-	-	(0.62, 1.1)
Currently estimated doses	16〜25	6〜9	2〜3

The most rapid but rough estimation of dose can be conducted by the prodromes when a person is heavily exposed to radiation. The doses of the workers of this accident were also estimated from their prodromes, such as fever, vomiting, and diarrhea. The doses were over 8 GyEq for Mr. A, 4 to 6 or over 6 GyEq for Mr. B, and less than 4 GyEq for Mr. C based on the former experiences of accidents. However, dose estimation based on prodromes just gives us a rough estimation, which must be supported by other dose estimation methods.

Dose reconstruction was also attempted using the reduction curves of lymphocytes, neutrophils, and platelets, which are sensitive to radiation, in the peripheral blood. Lymphocyte counts led to estimates of 16 to 23 GyEq for Mr. A, 6 to 8 GyEq for Mr. B, and 1 to 5 GyEq for Mr. C. The dose of Mr. C was more precisely determined later from his clinical progress to be approximately 3 GyEq. This dose estimation method takes more than two days, since it is based on reduction in blood components.

Chromosome analysis is attracting a lot of attention these days as a useful technique for dose estimation. However, it requires a lot of time and labor. Sampling of blood is usually initiated 24 hours after the exposure to make sure that the blood has becomes uniformly distributed throughout the body. The blood samples are then cultured for 48 hours, and abnormal chromosomes are counted. Therefore, at least 3 days are required after exposure to estimate the dose. For this criticality accident, blood samples were collected 9 hours after the accident as an emergency case. Blood samples were also obtained 23 hours and 48 hours after the accident to improve the precision of dose estimation by multiple samples. While Table II.G.1 shows the dose ranges estimated by the method, the most certain values were 25 GyEq for Mr. A, 8.3 GyEq for Mr. B, and 3.0 GyEq for Mr. C.

Of the dose estimation methods used for this criticality accident, the one using the specific activity of ^{24}Na in the blood is one of the most reliable methods. Based on the concentration measurements of ^{24}Na with Ge detectors and stable Na with ICP-AES the neutron doses were estimated to be 5.4, 2.9 and 0.81 Gy, respectively for the three workers. Their statistical uncertainty could be deduced by the propagation of errors using the data in Section D.a.1 and Section D.a.2 of Chapter II to be 4, 2 and 5 % for workers A, B and C, respectively. While they might have a systematic error and be underestimated by approximately 20% due to the dilution of Na by intravenous administration, as discussed in Section B of Chapter IV.

This method, however, derives only neutron doses. Therefore, as described in Section E of Chapter II, computational simulation analyses were conducted to calculate the ratios between the neutron and gamma ray

doses of Mr. A and Mr. B. The ratios for Mr. A and Mr. B are 1.83 and 1.43, respectively. The gamma ray doses of the workers were then estimated by multiplying their neutron doses by the gamma ray-to-neutron ratios. The gamma dose of Mr. C, whose dose ratio was not computationally analyzed, was estimated using the results of the computational simulation of Mr. A, who showed the larger dose ratio (gamma ray / neutron) of the two, to prevent underestimation (see Section D of Chapter IV). The computational simulation analyses also calculated the specific activity of ^{24}Na that was generated within the phantoms. The neuron dose conversion factors per unit specific activity (Gy/(Bq/g)) found from these calculation closely agreed with the values used for dose estimation based on the specific activity measurements of ^{24}Na in the blood, described in Section D.a.4 of Chapter II.

According to this method, the neutron and gamma ray doses were 5.4 and 9.9 Gy for Mr. A, 2.9 and 4.1 Gy for Mr. B, and 0.81 and 1.5 Gy for Mr. C, respectively. Since the doses estimated from prodromes, lymphocyte counts, and chromosome analysis cannot be separately expressed for neutrons and gamma rays but as their total effect on the human body, the values estimated from ^{24}Na specific activity measurements in the blood were converted into units of GyEq using RBE = 1.7, which has been derived from $LD_{50/7}$ intestinal death of a mouse after irradiation with 13 MeV neutrons (KO01). The GyEq doses of workers A, B, and C were 19, 9.0, and 2.9 GyEq, respectively. These values, however, may be underestimated by approximately 20% due to the dilution of Na by intravenous administration.

A human counter estimated the amount of ^{24}Na in the whole body. The dose was calculated from the measurement, as in the dose estimation method based on the ^{24}Na measurements in the blood. However, unlike the blood sample method, the human counter cannot actually determine the amount of stable sodium in the whole body, so the result may contain an error that is attributable to the estimate of specific activity value used in the calculation.

Therefore, the human counter method is less precise than the Ge measurements of ^{24}Na in blood samples. For this criticality accident, the human counter method was applicable to only Mr. C. Using the same conversion factor as in ^{24}Na measurements in the blood, the neutron dose was estimated to be 0.62 Gy, and the gamma ray dose was 1.1 Gy.

The absorbed doses (Gy) of neutrons and gamma rays need to be summed to assess the biological effects since the workers were exposed to both neutrons and gamma rays in this accident. Usually, the total dose is determined by assuming an RBE to high LET neutrons. However, as described in Section F of Chapter IV, this RBE cannot be unequivocally determined and is very difficult to select the right value. Moreover, we attempted to derive a vaguely defined dose in the form of a general average dose to the whole body and not a dose for a specific biological effect.

On the other hand, prodrome analysis revealed the effects of radiation on the skin and digestive organs. The lymphocyte count method studied the effects on the whole body based on the radiation sensitivity of lymphocytes, and chromosome analysis was used to analyze the effects on the whole body based on the radiation sensitivity of chromosomes.

Taking these inaccuracies into account, we compared the results of these dose estimation methods and derived overall doses, which are shown in the last line of the Table. These values are one type average dose for the whole body. The ranges do not reflect the uneven dose distribution in the bodies; rather, they show the ranges of estimation by various methods. These values are largely effective in estimating and assessing the overall prognosis of the workers.

To predict more in detail the manifestation and seriousness of the injuries of the organs, the doses to individual organs or tissues must be estimated. Particularly in cases of uneven exposure, as in this criticality accident, the neutron dose and gamma ray dose must be separately determined in Gy units for each organ or tissue.

III. MEASUREMENT AND ANALYSIS OF BIOLOGICAL MATERIALS

Introduction

Three workers were heavily exposed to radiation in the criticality accident, resulting in several kinds of nuclide, such as ^{24}Na, being produced in their bodies. Quantification of the activation products in the bodies enabled estimation of exposure doses. In the previous chapter (II.D "Dose assessment based on ^{24}Na measurements"), the method of estimating dose using ^{24}Na concentration in the blood was discussed and the estimates obtained were presented. This chapter summarizes data obtained during measurement of concentrations of nuclides other than ^{24}Na in blood, including several other samples (MU01a,b). These data, although not directly used for that particular dose estimation, serve as a basis for providing information on exposure patterns, reveal uneven dose distribution, back up the ^{24}Na measurement results and suggest new techniques for evaluating doses. Among gamma-emitting nuclides other than ^{24}Na, concentrations of ^{42}K (half-life: 12.36 hours) and ^{82}Br (35.30 hours) were quantitatively determined, and data were obtained from samples such as blood, urine, and vomit. These nuclides were produced by (n, γ) reaction with thermal neutrons. As for beta-emitting nuclides, concentrations of ^{32}P (14.26 days) were determined. ^{32}P is produced by (n, γ) reaction in ^{31}P (stable phosphorus), contained abundantly in blood, as well as (n, p) reaction in the ^{32}S (stable sulfur), present in high quantities in human hair. Values for ^{32}P, produced by ^{32}S activation, are important for evaluation of fast neutrons. Not only the samples, such as blood, hair, urine and vomit, obtained from the three exposed workers immediately after the accident, but also the bone samples donated by Mr. A and Mr. B's families after their deaths were subjected to ^{32}Pa and ^{45}Ca (164 days) analysis. The data obtained contributed to discussion of exposure dose distribution in the body. Tooth samples were analyzed using electron spin resonance (ESR).

To evaluate the products of radionuclides, it is essential to obtain accurate data on concentrations of target stable elements. Such data make it possible to obtain the specific activity (i.e. the ratio of concentration of radionuclides to that of stable elements) and to estimate neutron fluence and exposure doses. Thus, concentrations of stable elements contained in blood, hair, urine, vomit and so on were also measured.

III.A. Blood

III.A.a. Gamma ray spectrometry (Measurement of nuclides other than ^{24}Na)

Samples and measurement methods

Sampling of blood specimens and measurements were performed as described in II.D.a.1.

Measurement results

The measurement results of ^{42}K (1,524 keV) and ^{82}Br (776.5 keV) which were produced by neutrons as well as those described in II.D.a.1 are shown in the following Table III.A.1(a), Table III.A.1(b) and Table III.A.1(c). The measurements performed by the Environmental and Toxicological Sciences Research Group showed the values of ^{42}K to have fallen below the detection limit, since the values were determined seven days after the accident. The measurements performed by the Radiation Research Division and the Human Radiation Environment Division revealed the photopeak of ^{82}Br to be below the detection limit because measurements were started at an early stage, they were subject to interference by the Compton components of ^{24}Na. For a comparison among the samples, refer to Chapter IV, Section A (Comparison of Specific Activities).

Table III.A.1(a) Measurements by Radiation Research Division

Sample	Sample obtained at:	Time measurement started	^{24}Na concentration Bq ml^{-1}		^{42}K concentration Bq ml^{-1} (At the time of sampling)
			At the time of sampling	At the time of the accident*	
A-2	Oct. 1 12:27	Oct. 1 14:49 Oct. 2 8:48 (Two measurements)	47.1 ± 0.6**	168 ± 2**	5.1 ± 0.9**
B-2	Oct. 1 13:38	Oct. 1 16:47 Oct. 2 12:20 Oct. 2 16:46 (Three measurements)	23.8 ± 0.6**	90.0 ± 2.3**	2.2 ± 0.6**
C-2	Oct. 1 14:25	Oct. 2 10:31	5.91 ± 0.29	23.0 ± 1.1	0.2 ± 0.2

* The biological half-life was also used in the estimation.
** Average of two or three measurements.

Table III.A.1(b) Measurements by the Human Radiation Environment Division

Sample	Sample obtained at:	Time measurement started	^{24}Na Concentration Bq ml^{-1}		^{42}K concentration Bq ml^{-1} (At the time of sampling)
			At the time of sampling	At the time of the accident*	
A-2	Oct. 1 12:27	Oct. 1 13:33	49.2 ± 0.6	176 ± 2	6.61 ± 0.53
B-2	Oct. 1 13:38	Oct. 1 14:29	24.3 ± 0.32	91.8 ± 1.2	2.58 ± 0.35
C-2	Oct. 1 14:25	Oct. 1 19:22	5.85 ± 0.14	23.0 ± 0.5	N.D.
A-1	Sep. 30 15:40	Oct. 1 21:49	130 ± 2	167 ± 3	22.3 ± 2.7
B-1	Sep. 30 15:40	Oct. 2 20:12	85.6 ± 2.0	110 ± 3	N.D.
C-1	Sep. 30 15:40	Oct. 1 20:28	20.0 ± 0.6	25.7 ± 0.9	N.D.

* The biological half-life was also used in the estimation.
N.D.: Not detectable

Table III.A.1(c) Measurement results by the Environmental and Toxicological Sciences Research Group

Sample	Sample obtained at:	Time measurement started	^{24}Na concentration Bq ml^{-1}		^{42}K concentration Bq ml^{-1} (At the time of sampling)
			At the time of sampling	At the time of the accident*	
A-2	Oct. 1 12:27	Oct. 7 18:00	45.6 ± 4.1	163 ± 15	0.15 ± 0.047
B-2	Oct. 1 13:38	Oct. 6 15:44	24.5 ± 1.2	92.6 ± 4.6	0.083 ± 0.021
C-2	Oct. 1 14:25	Oct. 7 1:18	5.7 ± 0.8	23.0 ± 3.1	N.D.

* The biological half-life was also used in the estimation.
N.D.: Not detectable

III.A.b. Measurement of stable elements (Na, K, P, and Br)

For dose evaluation using ^{24}Na produced by neutron activation, part of the blood was completely decomposed with acid, and stable sodium was analyzed by inductively coupled plasma atomic emission spectrometry (ICP-AES). At the same time, stable isotopes, ^{39}K, ^{31}P, ^{79}Br and ^{81}Br, which are regarded as useful for dose evaluation using neutron activation were analyzed. Samples were obtained from the three exposed workers on September 30 and October 1. Solvable was added to the September 30 samples after collection. Therefore, solvable was also analyzed to examine how it affected the presence of each of these elements.

Samples and analytical methods

The sample preparation and analysis methods for blood were as described in II.D.a.2. The measurements were carried out using ICP-AES (Seiko Instruments, SPS-7700), at the following wavelengths (nm) and integration times:

	Wavelength	Integration time (s)
Na :	588.995	3
K :	766.490	8
P :	214.914	10

The analysis of bromine can be summarized as follows: The sample (50-100 µl) was weighed into a ceramic boat and vanadium pentoxide powder to act as an oxidizer and a melter added to it. It was then placed in a quartz combustion tube (inside diameter: 22 mm; length: 50 cm) and heated at 1,000 ˚C under oxygen flow. The volatilized bromine was trapped in a dilute solution of tetramethylammonium hydroxide (TMAH). The trapped solution, correctly diluted, was analyzed using high-frequency inductively coupled plasma mass spectrography (ICP-MS). (For further details, refer to Schnetger & Muramatsu (SC96) and Muramatsu & Yoshida (MU99)).

Results of the analyses

The results obtained by the analyses described above are summarized in Table III.A.2. The Na concentrations in blood on October 1 were 2,050, 2,110 and 1,860 µg ml^{-1} for Mr. A, Mr. B and Mr. C, respectively. All the blood samples collected on September 30 had a higher Na concentration, indicating that the sodium contained in Solvable, added to the blood samples, needed to be taken into consideration. The potassium and phosphorus content in Solvable, however, is so low that their effects can be disregarded. There was only minor variation among individuals with respect to potassium and phosphorus blood concentrations: for the October 1 blood samples, potassium was 1,390-1,500 µg ml^{-1} and phosphorus was 320-360 µg ml^{-1}. These values agree approximately with those in the ICRP reference model. The values for stable elements obtained here are important in determining specific activities, as described later.

Table III.A.2 Results of stable elements (Na, K, P, and Br)

Sample	Worker	Date of sampling	Unit	Code of sample		Na	K	P	Br
Blood	A	Oct. 1	(μ g ml^{-1})	BL-Oh-01-a		2,080	1,440	360	4.4
				BL-Oh-01-b		2,020	1,430	350	4.0
					Mean	**2,050**	**1,440**	**360**	**4.2**
					S.D.	42	7	7	0.3
Blood	B	Oct. 1	(μ g ml^{-1})	BL-Sh-01-a		2,120	1,410	300	4.8
				BL-Sh-01-b		2,100	1,370	340	5.2
					Mean	**2,100**	**1,390**	**320**	**5.0**
					S.D	14	28	28	0.3
Blood	C	Oct. 1	(μ g ml^{-1})	BL-Yk-01-a		1,840	1,490	350	3.8
				BL-Yk-01-b		1,880	1,500	330	4.2
					Mean	**1,860**	**1,500**	**340**	**4.0**
					S.D.	28	7	14	0.2
Blood*	A	Sep. 30	(μ g g^{-1})**	BL-Oh-30-d		3,610	1570	400	35.0
				BL-Oh-30-e		3,410	1,490	380	37.3
					Mean	**3,510**	**1,530**	**390**	**36.1**
					S.D.	140	57	14	1.6
Blood*	B	Sep. 30	(μ g g^{-1})**	BL-Sh-30-c		2,950	1,320	260	24.3
				BL-Sh-30-d		3,030	1,370	280	26.0
					Mean	**2,990**	**1,350**	**270**	**25.1**
					S.D.	57	35	14	1.3
Blood*	C	Sep. 30	(μ g g^{-1})**	BL-Yk-30-a		3,590	1,700	360	32.1
				BL-Yk-30-b		3,450	1,570	380	34.4
				BL-Yk-30-c		3,050	1,460	350	
					Mean	**3,250**	**1,520**	**370**	**33.2**
					S.D.	280	78	21	1.7
Solvable	C	Oct. 1	(μ g ml^{-1})	Sol-a		9,300	18	<5	145.3
				Sol-b		9,430	23	<5	
					Mean	**9,370**	**21**	**<5**	
					S.D.	92	4		

* Solvable added
** Since the samples were coagulating, the volume of the samples was determined by weighing.
S.D.: Standard deviation
Note: The September 30 blood sample values should be discussed in consideration of the Na contained in Solvable.

III.A.c. Measurement of ^{32}P in blood

^{32}P contained in the blood of the exposed workers, collected on October 1, was measured using a low background beta ray spectrometer.

The blood samples were prepared by freeze-drying those used for ^{24}Na measurement. They were then powdered and placed onto a stainless steel sample plate in a uniform layer.

The energy calibration curve and counting efficiency used were the same as those used in the measurement of ^{32}P in hair (refer to III.B.c). Table A.3 shows the three workers' ^{32}P concentrations at the time of the accident. Although there is a difference in exposure dose, there is practically no difference between the ^{32}P concentrations of Mr. A and Mr. B. ^{32}P is produced by ^{32}S (n, p) ^{32}P and ^{31}P

(n, γ) ^{32}P reactions. Table III.A.2 shows that the P concentrations in the blood of Mr. A and Mr. B are 360 µg ml^{-1} and 320 µg ml^{-1}, respectively. Unfortunately, the S concentrations in blood were not determined quantitatively. ICRP Publ. 23 (IC75) states that the S and P contents of a reference man are 10 g and 1.9 g, respectively. The cross section of S to fast neutrons rises at 2 MeV, reaching 0.1 b at around 3 MeV. The cross section of P to thermal neutrons is 0.19 b. Meanwhile, the neutron fluence to the body can be determined by Fig. II.E.2 in Section E, Chapter II: fast neutrons and thermal neutrons have roughly the same fluence. These facts, however, do not explain why the ^{32}P concentrations of Mr. A and Mr. B are practically at the same level, as shown in Table III. A.3.

Table III.A.3 ^{32}P concentrations in blood at the time of the accident (Bq ml^{-1})

Collection date	Amount	Mr. A	Mr. B	Mr. C
Oct. 1, 1999	20 ml	2.36	2.35	1.59

III.B. Hair

Like blood, hair can contain neutron activation products. Quantitative determination of their nuclides provides information on exposure doses and dose distributions of each area of the body of the three exposed workers. Measurement of ^{32}P contained in their hair is expected to provide information on fast neutron components. In addition, U isotopes were measured and the hair contamination pattern was examined. Samples and measurement items are outlined below.

Date and time of sample collection:
Mr. A: Head hair – Oct. 15, 1999
Mr. A: Pubic hair – Oct. 4, 1999
Mr. B: Head hair and pubic hair – Oct. 4, 1999
Mr. C: Head hair – Oct. 15, 1999
(Note: Apart from the above, a small amount was collected on October 1 for qualitative analysis.)

Measurement items:
Measurement of ^{24}Na and other nuclides, using a Ge detector
Measurement of stable Na, P, S, K and Br using ICP-AES and U isotopes, using ICP-MS
Measurement of ^{32}P using a low beta-ray background spectrometer
Measurement of ^{32}P using a liquid scintillation counter

III.B.a. Gamma ray spectrometry

Gamma nuclides produced in the hair by reaction with neutrons were measured using a Ge detector. Identifying the radionuclides and their concentrations contained in hair serves not only to detect activation products produced by neutrons but also to obtain information on external contamination caused by the uranium fission products released during the accident.

a.1. Samples and measurement methods

Hair samples were collected as described above. They were cut into small pieces using scissors, and then placed in a measurement vessel (U8 vessel or 20 ml thin vial) for weighing. Gamma-emitting nuclides were measured with a Ge detector using the same analysis method as for the blood as described above.

a.2. Results

First, for contamination monitoring, small quantity of the hair samples were measured using the Ge detector, and qualitatively identified nuclides were detected (initially, only approximately 0.1 g was provided for the hair sample). ^{24}Na, an activation product, was detected in the hair samples of Mr. A and Mr. B. ^{91}Sr, ^{91m}Y and ^{140}Ba were also detected from the sample taken from Mr. C, who had been exposed to the smallest dose (Fig. III.B.1). It is thought that these nuclides are not activation products generated inside the hair, but are daughter nuclides of radioactive rare gases produced by nuclear fission, which were released from the uranium solution into the atmosphere. These daughter nuclides may have become attached to the victims' hair via the air of the workroom during the accident. Mr. A and Mr. B were working very close to the precipitation tank, while Mr. C was at a distance; however, the ^{91}Sr and ^{140}Ba content of both Mr. A and Mr. B's hair was far lower than for Mr. C. This is probably because Mr. A and Mr. B were wearing their helmets and left the workroom immediately after the accident, resulting in less exposure to external contamination. On the other hand, Mr. C, although wearing a helmet when the accident occurred, returned later to the accident site without his helmet. It is presumed that Mr. C's hair absorbed the daughter nuclides produced by radioactive rare gases at that time. In addition, since daughter nuclide production from a radioactive rare gas takes time, it is assumed that the workroom air contained a higher amount of ^{91}Sr and ^{140}Ba some time after the accident than immediately after it occurred.

Table III.B.1 shows the results on the concentrations of ^{24}Na and ^{82}Br in hair (dry weight concentrations at 80 °C). The amount of hair sampled from Mr. A was a very small 0.3 g, entailing greater errors in ^{24}Na measurements and making it impossible to detect ^{82}Br, while that from Mr. B was sufficient to enable ^{82}Br detection. The ^{24}Na concentration (converted to the time of the accident) in hair samples from Mr. A and Mr. B was 130 Bq g^{-1} and 17 Bq g^{-1}, respectively; that is, the concentration found in Mr. A's hair is eight times higher than Mr. B's. This is a significant difference, considering that the ^{24}Na content in blood from Mr. A was nearly twice that in the blood from Mr. B. This may be explained by the results of the stable sodium analysis described later. The stable sodium concentration in hair from Mr. A was approximately four times higher than that in hair from Mr. B, resulting in greater ^{24}Na production in Mr. A's hair. Also, the high stable sodium concentration detected in Mr. A's hair may have been affected by sweat adhering to the surface of the hair; thus it can be considered that Mr. A's ^{24}Na includes components that adhered to the surface of the hair, mixed with sweat, after ^{24}Na production in the body.
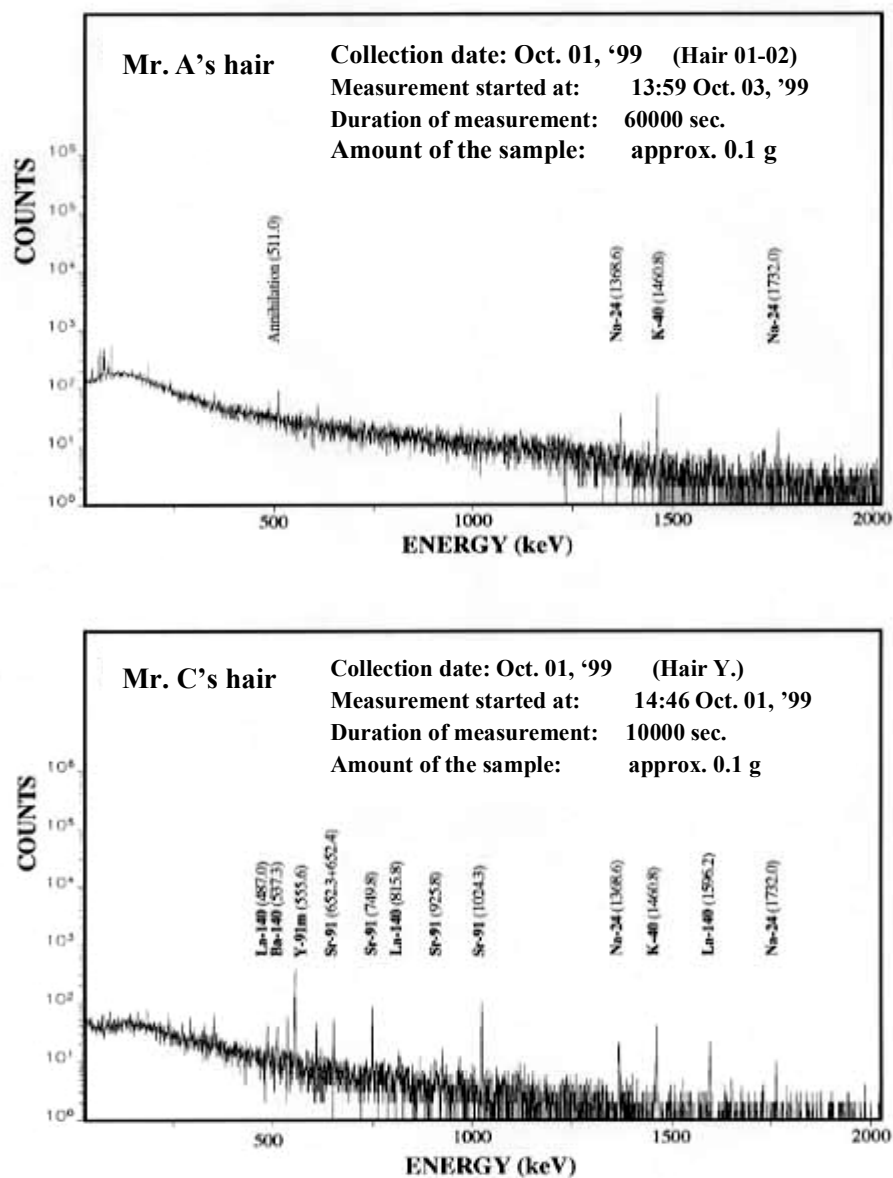
40

Fig. III. B.1 Gamma ray spectrum of hair

Table III.B.1 ²⁴Na and ⁸²Br concentrations in hair (at the time of the accident)

Sample	Worker	Code of the sample	Date of sampling	^{24}Na (Bq g^{-1}) At the time of the accident (Sep.30 1999, 10:35 a.m.)		^{82}Br (Bq g^{-1}) At the time of the accident (Sep.30 1999, 10:35 a.m.)	
				Concentration	Standard deviation	Concentration	Standard deviation
Hair	A	HA-Oh-Sc-a	Oct. 1	130	20	N.D.	
Hair	B	HA-Sh-Sc-a	Oct. 4	17	0.95	0.14	0.021

N.D.: Not detectable

Note: These values were obtained under unmodified conditions and without air-drying.

III.B.b. Measurement of stable elements (Na, K, P, Br and S) and U isotopes

Dose evaluation using ^{32}P, produced by ^{31}P (n, γ) reaction or ^{32}S (n, p) reaction associated with neutron activation, requires quantification of ^{31}P (stable phosphorus) and ^{32}S (stable sulfur). Acid was used to completely decompose part of the hair, and the stable phosphorus and sulfur contained in it were analyzed. Stable sodium, stable potassium and stable bromine were also analyzed to obtain the specific activities of ^{24}Na, ^{42}K and ^{82}Br. Uranium concentrations and isotopic ratios (^{235}U/^{238}U) were also measured to check the hair for surface uranium contamination.

b.1. Samples and analysis method

Samples were obtained from the head hair of the three exposed workers. For some of them, the right side of the head was analyzed separately from the left. To verify the validity of our analysis method, two kinds of human hair powder reference material for comparison (HH-5 and HH-13, the National Institute for Environmental Studies) were also analyzed. The recommended values were compared with our measured values.

The hair was cut into pieces with scissors, and dried at 80 ˚C until no further weight loss was observed; 35-350 mg of this dried material was weighed out and placed in a Teflon decomposition vessel. Before hermetically sealing the vessel, 68% nitric acid solution was added. The contents of the sealed vessel were then thermally decomposed in a microwave oven. Decomposed samples were handled in the same way as the previously described blood samples. The measurement was carried out using ICP-AES (Seiko Instruments, SPS-7700), with the same wavelength, integration time, number of times of repetition of the analysis and preparation of a standard solution as those for the previously described blood measurements.

Bromine was analyzed using a similar method to that employed for handling the blood samples. Approximately 50 μg of hair sample was weighed into a ceramic boat, thermally decomposed within a quartz tube, and then quantified using ICP-MS.

Uranium was analyzed using a solution made by decomposing the hair samples with nitric acid (the same solution as used for the ICP-AES analysis), after which its concentration was measured using ICP-MS. The ratio of ^{235}U to ^{238}U was also measured by ICP-MS.

b.2. Analytical results

Table III.B.2 summarizes the results obtained, except for those for sulfur shown in Table III.B.4, which will be described later. The analyzed results of human hair powder reference material for comparison agreed approximately with the recommended values. As for HH-5, the recommended value for phosphorus is 165 μg g^{-1}, while our measured value was 153 μg g^{-1}, producing an error of 7%. No recommended value for phosphorus is available for HH-13. The errors in sodium and potassium fell within 8% for both HH-5 and HH-13.

The phosphorus concentrations in the hair of the three workers ranged from 58 – 297 μg g^{-1}, the sodium from 40 – 2,040 μg g^{-1}, and the potassium from 109 – 470 μg g^{-1}. Clearly, Mr. A's hair had a higher concentration than the other two or an ICRP Publ. 23 (IC75) reference man. Since Mr. A was perspiring profusely when brought to NIRS, it is possible that the sweat adhering to the surface of his hair caused the high sodium concentration.

Table III.B.3 shows the uranium concentrations and the ^{235}U/^{238}U ratios of the hair samples. The three workers were handling enriched uranium (^{235}U enriched to 18.8%). If their hair was contaminated with this enriched uranium, it is possible that the uranium concentration in hair would be high, with a high ^{235}U/^{238}U ratio. The measured values for uranium concentrations ranged from 0.8 ppm to 13 ppm. Little information is available on average uranium concentrations in human hair. Thus, the uranium contained in the human hair powder reference material (HH-5), created by the National Institute for Environmental Studies (NIES), was also analyzed, giving a uranium concentration of 0.03 ppm. Compared with this value, the three workers' concentrations are extremely high, the highest being seen in Mr. C's sample. Meanwhile, the workers' ^{235}U/^{238}U ratios ranged from 0.052 to 0.11: higher than the normal ratio (0.00725) present in nature. These facts demonstrate that the three exposed workers had all been affected by enriched uranium in some way. The head hair samples from Mr. A were collected in three different areas, with uranium concentrations and ^{235}U/^{238}U rations varying widely. The head hair sample from Mr. B had the lowest uranium concentration and the highest ^{235}U/^{238}U ratio (0.110) of the three workers.

On the assumption that all the excess uranium in workers' hair samples, compared with the value seen in the human hair powder reference material (HH-5) are from contamination by 18.8% enriched uranium (^{235}U/^{238}U ratio: 0.22), it follows that theoretical ^{235}U/^{238}U ratios of the three workers should be 0.21-0.22. The actual ^{235}U/^{238}U ratios measured were markedly lower than those theoretical values. From these results, it is thought that the three workers' hair was only slightly directly influenced by uranium during the accident, and that the high levels of uranium detected in their hair resulted from handling uranium before the accident (e.g. uranium for the light water nuclear reactor).

Table III.B.2 Analytical results of stable elements (Na, K, P and Br) in hair

Sample	Worker	Date of sampling	Unit*	Code of sample	Na	K	P	Br
Head hair**	A	Oct.1	(μg (g-dry)$^{-1}$)	HA-Oh-Sc-a	2,040	470	132	8.9
				HA-Oh-Sc-b				9.3
				Mean				**9.1**
				S.D.				0.3
Head hair	B	Oct.4	(μg (g-dry)$^{-1}$)	HA-Sh-Sc-a	465	106	146	10.3
				HA-Sh-Sc-b	457	112	146	9.5
				Mean	**461**	**109**	**146**	**9.9**
				S.D	5	4	0	0.6
Head hair (right side)	A	Oct.4	(μg (g-dry)$^{-1}$)	HA-Oh-R-a	1,800	141	246	
				HA-Oh-R-b	1,770	144	270	
				Mean	**1,790**	**143**	**258**	
				S.D.	21	2	17	
Head hair (left side)	A	Oct.4	(μg (g-dry)$^{-1}$)	HA-Oh-L-a	1,730	144	313	
				HA-Oh-L-b	1,600	140	281	
				Mean	**1,670**	**142**	**297**	
				S.D.	92	3	23	
Head hair (right side)	C	Oct.4	(μg (g-dry)$^{-1}$)	HA-Yk-R-a	16	149	54	
				HA-Yk-R-b	65	155	63	
				Mean	**40**	**152**	**58**	
				S.D.	35	5	6	
Human hair powder reference material for comparison (HH-5)								
			(μg (g-dry)$^{-1}$)	HH-5	27.5	34.8	153	
				HH-5b	28.7	35.8	153	
				Mean	**28**	**35**	**153**	
				S.D.	1	1	0	
				Recommended value	26	34	165	
				Measured value / Recommended value	1.08	1.04	0.93	
Human hair powder reference material for comparison (HH-13)								
			(μg (g-dry)$^{-1}$)	HH-13	62.8	67.7	161	
				HH-13b	65.2	72.0	160	
				Mean	**64**	**70**	**161**	
				S.D.	2	3	1	
				Recommended value	61			
				Measured value / Recommended value	1.05			

* Calculated on the weight basis of having been dried at 80 ˚C until reaching a constant mass.
　　(dry/wet ratio: HA-Oh-Sc = 0.9013, HA-Sh-Sc = 0.9192)
** Too small an amount; measured once only
S.D.: Standard deviation

Table III.B.3 Uranium concentration and uranium isotope ratio (^{235}U/^{238}U) in hair

Hair sample		Total number of	^{238}U		^{235}U/^{238}U	
	Sample number	samples	ppm（average）	R.S.D. (%)	Ratio	R.S.D. (%)
	HA-Oh-L	2	0.92	0.3	0.0616	0.6
Mr. A	HA-Oh-R	2	1.49	0. 9	0.0742	0. 8
	HA-Oh-Sc	1	3.06		0.0835	
Mr. B	HA-Sh-Sc	2	0.81	4.2	0.110	0.4
Mr. C	HA-YK-R	2	13.2	3.5	0.0518	0.3
Human hair powder reference material（for comparison） NIES-HH-5		2	0.03	2.8	0.0074	2.2
Standard rocks（for comparison） JB-1（YO96）		3	1.66	4.2	0.0073	0.2

R.S.D.: Relative standard deviation

III.B.c. Measurement of ^{32}P contained in hair

Human hair contains a great deal of sulfur. Measurement of ^{32}P radioactivity produced in hair as a result of ^{32}S (n, p) ^{32}P reaction with fast neutrons enables estimation of fast neutron dose. In 1997, when a criticality accident occurred at the Russian Federation Nuclear Center, Sarov, Russia, fast neutron dose estimation was carried out for several parts of body surface by measuring ^{32}P contained in the hair of an exposed person (IA01). We followed this example when collecting hair samples, which we attempted to use to estimate exposure dose. ^{32}P was measured using a low background beta ray spectrometer (Fuji Electric Co., Pico-beta), liquid scintillation counting and radiochemical analysis (Refer to Appendix B for radiochemical analysis).

c.1. Measurement using low background beta ray spectrometer

c.1.1) Sample preparation

The samples for the low background beta ray spectrometer were prepared using the following method. The head and pubic hair was cut into pieces with ophthalmic scissors, and 40 – 1,000 mg were placed onto a stainless steel sample plate (25 mm in diameter and 6 mm in depth) in a uniform layer. To obtain a sample for stable element measurement, part of the head hair (approximately 100 mg), to which nitric acid had been added, was wet-ashed using the microwave decomposition system.

c.1.2) Calibration curve and counting efficiency

Energy calibration for beta ray measurement was performed using ^{32}P, ^{35}S and ^{45}Ca standard solutions obtained from the National Institute of Science and Technology (NIST) in USA.
As of March 15, 2000, the guaranteed radioactivity concentration of each of the three solutions was 5.998 kBq g^{-1} (± 1.6%), 6.438 kBq g^{-1} (± 2.6%), and 6.020 kBq g^{-1} (± 2.5%), respectively.

A 250 mg contamination-free hair sample was weighed out and placed onto the sample plate of the low background beta ray spectrometer. A small amount of shampoo solution was dropped into the plate before addition of ^{32}P standard solution. This was dried with an infrared lamp to prepare a standard radiation source for determination of measurement efficiency. When a range of 240-1,711 keV (maximum energy) was set for ^{32}P, a measurement efficiency of 15.6% was obtained. The measurement data for ^{32}P was converted (physical half-life: 14.26 days) from the date of the measurement to the date of the accident (September 30, 1999).

c.2. Measurement using a liquid scintillation counter

To gain a rapid measure of the radioactivity level in the hair, ^{32}P was measured using a liquid scintillation counter (TA01).

An approximately 100 mg hair sample was dissolved in tissue solubilizer (Soluene-350, Packard), and decolorized with a small amount of hydrogen peroxide solution. After decolorization, the residual hydrogen peroxide solution was removed from the sample by heating in a temperature-controlled bath at 55 ˚C for 30 minutes, and then a scintillator (Hionic-fluor, Packard) was added to prepare the sample for liquid scintillation counting.

Meanwhile, 20, 40, 60, 80, 100, 200 and 300 mg contamination-free hair samples were weighed, all of which were conditioned using a solubilizer and a decolorizer. ^{32}P solution containing a known amount of radioactivity was then added to each sample to prepare quenching reference samples. Measurement efficiency was obtained from these reference materials, and a calibration curve for quench correction was made. Counting was carried out in two channels: Channel A (5-1,700 keV) and Channel B (50-1,700 keV); Channel B counts were adopted as reporting values in consideration of the results of the follow-up experiment on radioactivity decay described in III.D.c.2.2) "Follow-up experiment of radioactivity decay".
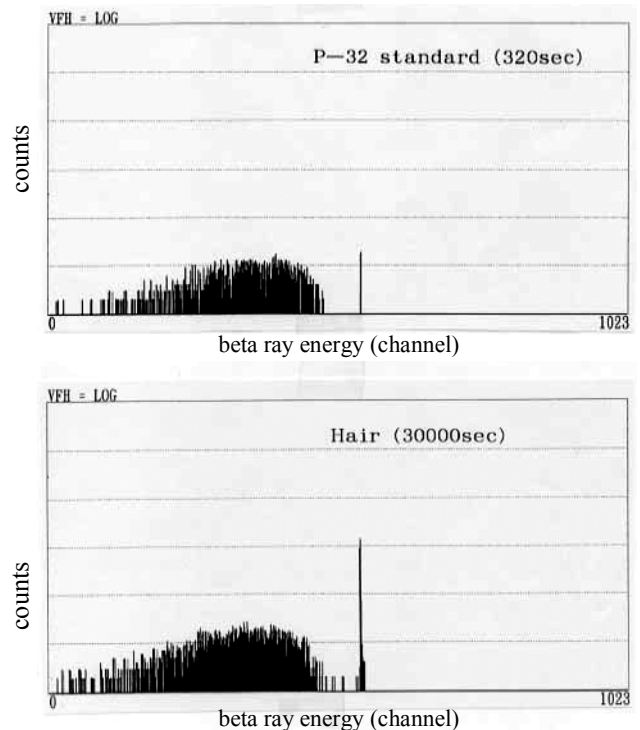
Note: The peaks in the higher energy range in the spectrum are created by cosmic rays.

Fig. III.B.2 Beta ray spectrum of hair

Table III.B.4 Results of ^{32}P and stable element concentration in hair

Sample	^{32}P (Bq g^{-1}) Pico-beta	^{32}P (Bq g^{-1}) LSC	P (μg g^{-1} · dry)*	S (μg g^{-1} · dry)
Mr. A Right head hair	3.9	5.6	258	43,850
Mr. A Left head hair	4.5	4.6	297	
Mr. A Pubic hair	19.8	28.6		
Mr. B Head hair	2.3	6.5	146	37,800
Mr. B Pubic hair	8.8	10.1		
Mr. C Head hair	N.A.	N.A.	58	49,650

* Refer to Table III.B.2
Pico-beta: Low background beta ray spectrometer
LSC: Liquid scintillation counter
N.A.: Decay products of radioactive rare gases (Kr, Xe) caused serious contamination; it was impossible to determine beta ray from ^{32}P only.

c.3. Results with a low background beta ray spectrometry and a liquid scintillation counting

Fig. III.B.2 shows the beta ray spectrum of hair and Table III.B.4 shows the measurement results. Table III.B.4 includes P and S concentrations measured using ICP-AES.

c.4. Radiochemical analysis of ^{32}P in hair

To back up measurements with the low background beta ray spectrometer and the liquid scintillation counter performed in NIRS, we asked the Japan Chemical Analysis Center (JCAC) to carry out radiochemical analysis of our samples for the purpose of isolation of phosphorus. The operation at the Center was performed using the following method: Part of the hair, approximately 3 g, was burned under pressurized oxygen, and ^{32}P was separated as ammonium magnesium phosphate precipitates. These precipitates were mounted on the sample plate of the low background beta ray spectrometer. Ammonium magnesium phosphate precipitates were also obtained from a ^{32}P standard solution to use as a calibration source in order to correct the difference in geometric shape of the hair sample. For further information on the radiochemical analysis procedure and radioactivity measurement results with a low background gas flow counter, see Appendix B "Chemical Analysis".

c.5. Discussion

Measurement of ^{32}P was performed with a low background beta ray spectrometer as well as liquid scintillation counter and backed up with the radiochemical analysis by JCAC. Liquid scintillation method was effective in rapidly determining radioactivity levels, due to its measurement efficiency of nearly 100% and simplicity of handling samples. However, it was found that the counter was apt to give measurements higher than those obtained with the low background beta ray spectrometer, as indicated in Table III.B.4. This is probably because the counting included beta-emitters other than ^{32}P. ^{32}P measurement by radiochemical isolation, described in Appendix B, was the most desirable method, since it is capable of measuring unmixed phosphorus. Nevertheless, the method requires relatively large amount of sample and proficient techniques in addition to the time consuming job. Therefore, we submit part of our samples to JCAC for the radiochemical analysis to verify the low background beta ray spectrometer measurements. Results of measurements by radiochemical separation were slightly lower than those obtained with the low background beta ray spectrometer. The possible reason for this discrepancy could be either the existence of contaminated nuclides in the energy range of the low background beta ray spectrometer or incomplete recovery of ^{32}P in radiochemical isolation. Our analysis of the beta ray spectra of the low background beta ray spectrometer has confirmed that there is very little risk of any contaminated nuclides being present over the whole energy range. It is not clear why our results disagree with those obtained by radiochemical analysis performed by JCAC. Further discussion is provided in Appendix B.

III.C. Fast neutron fluence estimation based on ^{32}P measurement in hair

Fig. III.C.1 shows cross-sectional data for a nuclear reaction, ^{32}S(n,p)^{32}P. This information was obtained from the JENDL-3.2 Library of Nuclear Data Center in JAERI. The Figure demonstrates that this nuclear reaction is produced with fast neutrons having effectively 2 MeV or greater.

As indicated in Fig. II.D.3 in Chapter II, Section D, the absorbed dose of fast neutrons per unit fluence is extremely large. Thus, estimation of fast neutron fluence is important in dose estimation. Here, estimation of fast neutron fluence in the haired area of each exposed worker has been performed using the previously described measurement results of ^{32}P and P in hair. In addition, the number of nuclear fissions in the first pulse of the critical initial burst has been estimated from estimated neutron fluence and irradiation distance.
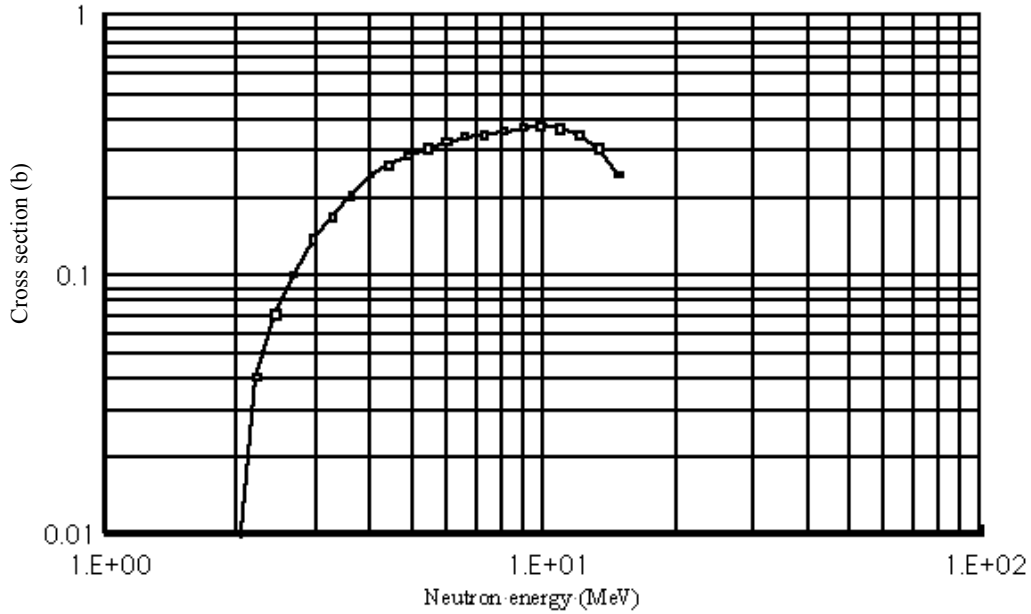

Fig. III.C.1 Cross section of the nuclear reaction ^{32}S(n, p)^{32}P

III.C.a. Relation between ^{32}P radioactivity produced and neutron fluence in the haired area

Radioactivity produced in hair samples can be calculated using Equation (1):

$$A = \lambda \cdot N_{s \to p} = \frac{\lambda \cdot \sin\theta \cdot \Phi \cdot M \cdot \varepsilon \cdot N_{av} \cdot f \int \sigma(E) \cdot \phi(E) \cdot dE}{W \cdot \int \phi(E) \cdot dE} \quad (1)$$

Where

A : ^{32}P radioactivity (Bq) produced in hair samples,

$N_{S \to P}$: the number of nuclear transformation (^{32}S→ ^{32}P) in the samples,

λ : the decay constant (5.626E-7 s^{-1}),

θ : the angle of incidence to the sample surface,

Φ : fast neutron fluence (cm^{-2}),

$\sigma(E)$: microcosmic cross section (cm^2),

M : sample weight (g),

ε : Salfur content per 1 g of sample,

N_{av} : the Avogadro constant (6.02E23),

f : ^{32}S natural abundance (0.95) and

W : atomic weight of sulfur (32).

Therefore, radioactivity per 1 g of sample a (Bq g^{-1}) can be calculated using Equation (2):

$$a = A/M = \frac{1.01 \times 10^{16} \cdot \sin\theta \cdot \Phi \cdot \varepsilon \cdot \int \sigma(E) \cdot \phi(E) dE}{\int \phi(E) dE} \quad (2)$$

The integration part of this equation has been calculated from neutron energy spectra used in the dose calculation based on ^{24}Na in blood and the cross section data obtained from the JENDL Library, resulting in Equation (3) for 2 MeV or greater:

$$\frac{\int_{2MeV}^{\infty} \sigma(E) \cdot \phi(E) dE}{\int_{2MeV}^{\infty} \phi(E) dE} = 1.75 \times 10^{-25} \quad (3)$$

In conclusion, 2 MeV or greater fast neutron fluence can be calculated using ^{32}P radioactivity and sulfur content, using Equation (4):

$$\Phi = 5.66 \times 10_8 \cdot \varepsilon \cdot \sin\theta \quad \text{cm}^{-2} \quad (4)$$

III.C.b. Incident angle of neutrons to the surface of samples

Here we make the assumption that the three workers were exposed to radiation only at the spot where they were working at the time of the accident. Although it can be assumed that neutrons were produced from the whole solution, their spatial distribution has not been identified. Thus, we will assume that they were emitted from one point in the solution, with the height of the center of the solution from the floor being 115 cm from the installation height of the precipitation tank.

As described in Chapter II, Section E, the working operations were reproduced in the mock-up facility of the conversion testing facility at JCO using NIRS staff of nearly the same height as the workers in order to identify the position of each worker at the time of the accident.

Mr. A: It is assumed that the irradiation distance on the surface of his trunk was 55 cm from the center of the solution. On the assumption that the head hair samples were collected from the area 10 cm back from the face and 170 cm higher from the floor, the estimate for the irradiation distance of his hair can be calculated as SQR$\{(55+10)^2+(170-115)^2\}$ = 85 cm. Since the hair was collected from the right and left sides of the head, the angle of incidence to the hair is estimated to be equal to or slightly greater than that to the face. Thus the correction factor is estimated to be approximately arcsin θ = (55+10)/85 = 0.76, which corresponds to an angle of incidence of 49.5 degrees. On the assumption that the pubic hair samples were collected from the position at 85 cm above the floor, the estimate for the irradiation distance of Mr. A's pubic hair can be calculated to be SQR$\{55^2+(115-85)^2\}$ = 63 cm. It is presumed that since the pubic hair is pressed to the skin by underwear, its angle of incidence is almost equal to that to the body close to the pubic hair. Thus the correction factor is estimated to be approximately sinθ = 55/63 = 0.87, which corresponds to an angle of incidence of 60.5 degrees.

Mr. B: From the reproduction of the operations in the mock-up facility, it was assumed that neutrons entered from a direction almost perpendicular to the face and the trunk. On the assumption that the pubic hair is pressed to the skin, neutrons entered his pubic hair at normal incidence. Thus the correction factor for the angle of incidence θ was taken here to be 1. As for his hair samples, since it was impossible to identify from which area they were collected, random incidence was assumed. In this case, the correction coefficient can be calculated as follows:

$$\frac{\int_0^{\pi/2} \cos\theta \cdot \sin\theta\, d\theta}{\int_0^{\pi/2} \sin\theta\, d\theta} = 0.5$$

III.C.c. Estimates for fast neutron fluence

Table III.C.1 shows the estimation results of fast neutron fluence based on the hair analysis results.

Table III.C.1   2 MeV or greater fast neutron fluences in each haired area

Sample	Specific activity obtained with Pico-beta	S content	Fluence
Mr. A:			
Right head hair	3.9 Bq g^{-1}	0.04385 g g^{-1}	6.6E10 cm^{-2}
Left head hair	4.5 Bq g^{-1}	*	7.6E10 cm^{-2}
Pubic hair	19.8 Bq g^{-1}	*	2.9E11 cm^{-2}
Mr. B:			
Head hair	2.3 Bq g^{-1}	0.03780 g g^{-1}	6.8E10 cm^{-2}
Pubic hair	8.8 Bq g^{-1}	**	1.3E11 cm^{-2}

*   The value for the right head hair was used as the S content. (Refer to Table III.B.4)
**   The value for the hair was used as the S content.
Pico-beta: Low background beta ray spectrometer

As for Mr. A, the fast neutron fluence in the head hair area was approximately one fourth that in the pubic hair area, and for Mr. B, nearly half. These differences cannot be interpreted only in terms of differences in irradiation distance of each area. For instance, for Mr. A, the ratio between the squares of each irradiation distance can be obtained: $63^2/85^2$ = 0.55. Also, as for Mr. B, it is presumed that there is little difference between the irradiation distances of the head hair area and the pubic hair area. The possible reason for the fluence in the head hair area being lower may be absorption of neutrons due to the helmet and the tissue of the head itself.

III.C.d. Estimation of the number of fissions in the first-pulse

The number of first pulse fissions in the initial burst was estimated using the fast neutron fluences previously estimated.

The number of fissions N can be calculated as a function of neutron fluence, using Equation (5):

$$N = \frac{\Phi_{ALL} \times 4\pi R^2}{n \cdot \varsigma} \tag{5}$$

where:

Φ_{ALL} : incident neutron fluence (cm^{-2}) in the whole energy region,

R : irradiation distance (cm),

n : the number of neutron emissions per fission and

ζ : neutron escape probability from the precipitation tank.

Here, 1.02 is used as the value for $n \cdot \zeta$. It has been derived collaterally from the analysis process of the stainless steel net performed by JAERI (Attachment 5 of Reference 1, issued by the Government Accident Countermeasure Headquarters of the Science and Technology Agency, November 4, 1999)

In conclusion, the number of fissions can be calculated based on neutron fluence and irradiation distance using Equation (6):

$$N = 12.3 \Phi_{ALL} \times R^2 \tag{6}$$

2 MeV or greater fast neutron fluence is calculated at 21% of the fluence of the whole energy region from the neutron spectrum shown in Fig. II.D.2, Chapter II, Section D. As a result, the number of fissions can be calculated using fast neutron fluence by Equation (7):

$$N = 58.7 \Phi \times R^2 \tag{7}$$

The estimate for the fast neutron fluence in the head hair area has been affected by the helmet and the tissue of the head, as previously described, leaving major uncertainties. Thus it was decided that the estimate for the pubic hair area should be used for estimation of the number of fissions. The reproducing of the working procedures carried out in the mock-up facility provided estimates for the irradiation distance in the pubic hair area of each worker: 63 cm for Mr. A and 78 cm for Mr. B. As a result, the number of fissions in the first pulse can be estimated as shown in Table III. C.2.

Table III.C.2 Estimates for the number of fissions in the first pulse

Sample	Irradiation distance	Fast neutron fluence	Number of fissions
Mr. A: Pubic hair	63 cm	2.9 E11 cm^{-2}	6.8 E16
Mr. B: Pubic hair	78 cm	1.3 E11 cm^{-2}	4.6 E16

The number of fissions in the first pulse has been evaluated to be $(6.5 \pm 1.9) \times 10^{16}$ from the neutron monitoring data at the Naka Institute of JAERI, as described in Chapter II, Section E. Meanwhile, analyses using kinetic code derived 5×10^{16} as the number of fissions during the first pulse (GE00). The estimates that we have obtained here based on the measurement results of ^{32}P in hair agree relatively well with these values.

III.D. Urine and vomit

It is thought that urine and vomit, since they are also likely to contain activation products produced in the body, can be used for dose evaluation, particularly as they are less invasion samples. This Section D discusses urine and vomit in consideration of their potential for dose evaluation.

III.D.a. Gamma ray spectrometry

a.1. Samples and measurement methods

The samples subjected to this analysis were mainly mixtures of urine collected between September 30, when the three exposed workers arrived at NIRS, and October 1, 6:00 a.m. (These samples were labeled with collection dates "September 30 - October 1"). As for Mr. B, a sample which is recorded as being taken on September 30 was kept and also subjected   (It is not known at what time on September 30 it was collected. It appears to have been collected until the late evening.). Vomit samples were kept after being collected from Mr. A and Mr. B on the way to or right after their arrival at NIRS, and were subjected to analysis for radionuclides and stable elements. There were three vomit samples. One was Mr. A's and the other two Mr. B's. They took the form of translucent liquid, probably gastric juices without any solid material, since the workers had vomited several times soon after the accident.
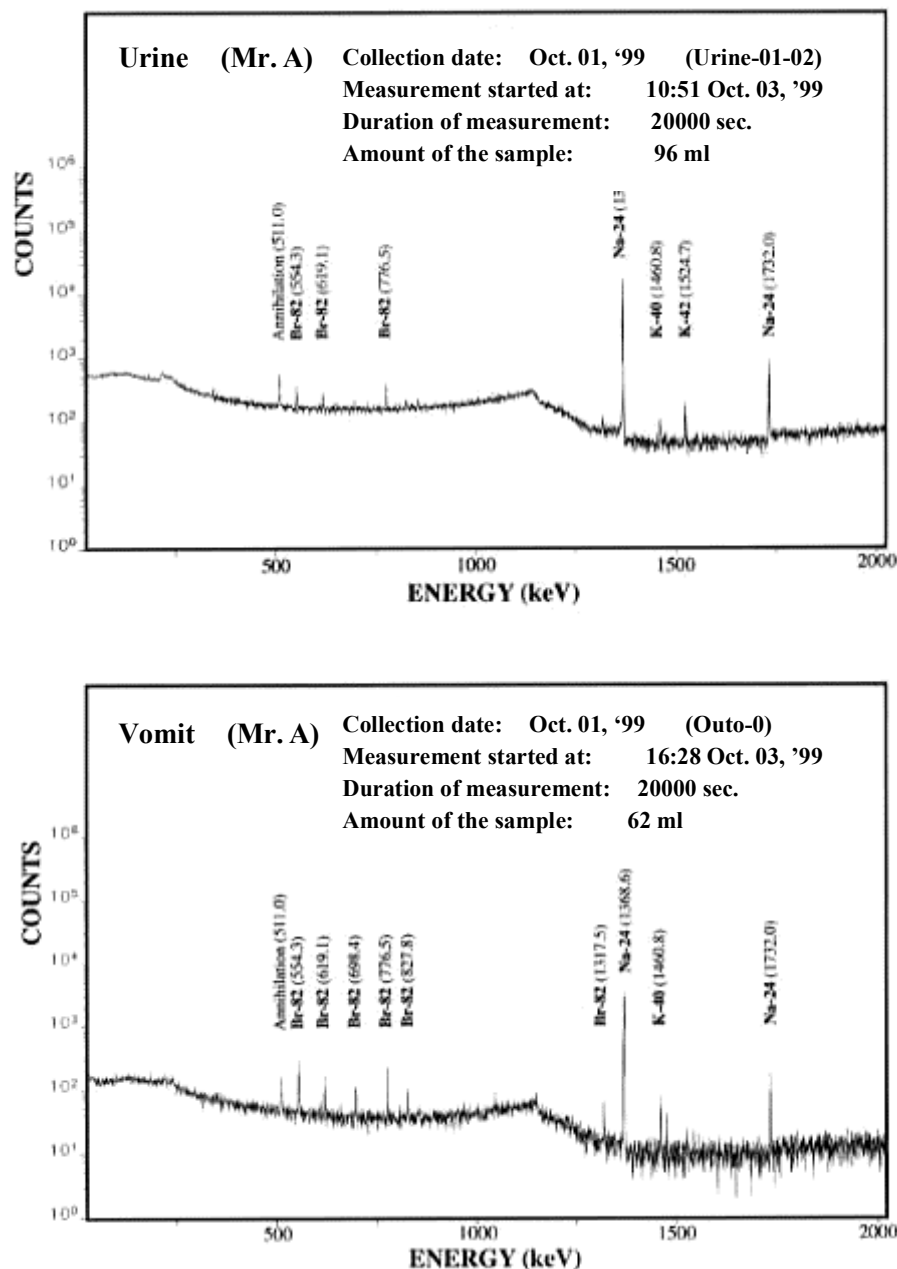

Fig. III.D.1 Gamma ray spectra of urine and vomit

a.2. Results

Measurement results of gamma-emitting nuclides contained in urine samples are shown in the upper rows of Table III.D.1 and their gamma ray spectra in the upper row of Fig. III.D.1. ^{24}Na, ^{82}Br and ^{42}K were detected from all the samples. Among ^{24}Na concentrations of the "September 30-October 1" samples, Mr. B's was the highest at 178 Bq ml^{-1}, Mr. A's was the next highest at 121 Bq ml^{-1}, and Mr. C's was the lowest at 40 Bq ml^{-1}. These individual variations are different from those in the blood sample results (In the blood, Mr. A's concentration was the highest, followed by Mr. B's). The results for stable elements, as described later, showed Mr. A's stable sodium concentration in urine to be very low: less than half that of Mr. B' or Mr. C's. This may have also led to the low ^{24}Na amounts produced in Mr. A's urine. As for ^{42}K and ^{82}Br, Mr. A's concentration was higher than Mr. B's, demonstrating the same pattern as that for ^{24}Na concentration in blood. Furthermore, in the ratios of ^{24}Na

to stable sodium in urine (i.e. specific activity), as described later, the three workers' values show nearly the same pattern of the specific activity in the blood (For specific activities, refer to Chapter IV, Section A).

Measurement using urine samples provides higher detection sensitivity than those using materials such as blood. This is because urine samples can be obtained in larger volumes of 100 ml or more.

The measurement results of gamma-emitting nuclides contained in vomit samples are shown in the lower rows of Table III.D.1 and their energy spectra in the lower row of Fig. III.D.1. In the measurements of Mr. B's liquid-like sample, values for ^{24}Na and ^{82}Br were higher than those seen in the other two samples. This is because the other two samples were obtained by extraction from paper towels: They had been saturated with vomit, which was rinsed out into water; this water was then measured. The lower concentrations are due to their dilution in this water. It was decided, therefore, that for the two types of samples from Mr. B, only liquid-like samples should be used for discussion of specific activity, as described later.

Table III.D.1 ^{24}Na, ^{42}K and ^{82}Br concentrations in urine and vomit (Corrected to the time of the accident)

Sample	Worker	Sample code	Collection date	^{24}Na (Bq ml^{-1} or Bq g^{-1})		^{42}K (Bq ml^{-1} or Bq g^{-1})		^{82}Br (Bq ml^{-1} or Bq g^{-1})	
				Concentration	S.D.	Concentration	S.D.	Concentration	S.D.
Urine	B	UR-Sh30-a	Sep. 30	165	0.40	8.53	0.65	0.150	0.015
Urine	A	UR-Oh01-a	Sep.30-Oct.1 morning	121	0.50	12.5	0.99	0.115	0.012
Urine	B	UR-Sh01-a	Sep.30-Oct.1 morning	178	0.47	7.60	0.78	0.0793	0.015
Urine	C	UR-Yk01-a	Sep.30-Oct.1 morning	40.2	0.25	2.30	0.45	0.0294	0.0074
Vomit*	A	OT-Oh-B-a	Sep. 30	42.3	0.39	2.95	0.81	0.189	0.011
Vomit**	B	OT-Sh-W-a	Sep. 30	25.7	0.57	N.D.		N.D.	
Vomit**	B	OT-Sh-L-a	Sep. 30	98.7	1.3	N.D.		0.359	0.032

N.D.: Not detectable
*   Extracted from paper towels
** In liquid condition

III.D.b. Measurement of stable elements (Na, P, K and Br)

Dose evaluation using radionuclides produced by neutron activation requires quantification of related stable elements. Urine and vomit samples were completely decomposed with acid, and the stable sodium, potassium, phosphorus and bromine contained in them were analyzed.

b.1. Samples and analysis method

The urine and vomit samples subjected to stable element analysis were the same as those used for gamma-emitting nuclide measurements. A 1-ml urine/vomit sample was fractionated into a Teflon decomposition vessel with a micropipette; 2 ml of 68% nitric acid was added to it before subjecting it to thermal decomposition in a microwave oven for one hour. Subsequent preparation of other sample solutions was performed in the same way as for the previously described blood samples. The

measurement was carried out using ICP-AES (Seiko Instruments, SPS-7700), with the same wavelength, integration time, number of times of repetition of the analysis and preparation of a standard solution as those used for the previously described blood measurements. Bromine was analyzed employing a similar method to that used in handling the blood samples: A urine or vomit sample was thermally decomposed within a quartz tube, absorbed in a trapping solution, and then quantified using ICP-MS.

b.2. Results

Table III.D.2 shows the results obtained by the analysis of the urine samples for stable elements. The sodium concentration in September 30 urine from Mr. B was 3,120 µg ml^{-1}. The sodium concentration in the October 1 urine samples from Mr. A, B and C was 1,390 µg ml^{-1}, 3,590 µg ml^{-1} and 2,940 µg ml^{-1}, respectively. All these values are lower than 4,310 µg ml^{-1}, the sodium concentration of an IPRC reference man (IC75). Notably,

Mr. A's value was only one-third of the average. The markedly lower concentrations of sodium in their urine could have been due to other factors such as changes in metabolism caused by irradiation or the large volumes of intravenous drips administered for treatment purposes; both may have affected the urine concentrations in the workers. Their potassium concentrations ranged from 900 µg ml^{-1} to 1,120 µg ml^{-1}, and phosphorus from 17 µg ml^{-1} to 334 µg ml^{-1}, all of which are lower than those of an ICRP reference man. The reasons for this are not clear.

Table III.D.2 also shows the results obtained from analysis of the vomit samples for stable elements. Mr. B's liquid vomit sample was compared with his blood sample. It was found that the sodium concentration in the vomit was slightly lower and ^{24}Na concentration slightly higher than those in the blood. The potassium and phosphorus concentrations obtained from this analysis were too low to be detected. Mr. B's liquid vomit sample contained a higher concentration of stable elements than the other two workers'. The reason for this could have been that the other two samples were obtained by extraction from paper towels into water, decreasing their concentration.

Table III.D.2 Analytical results of stable elements (Na, K, P and Br) in urine and vomit

Sample	Worker	Date of sampling	Unit	Code of sample		Na	K	P	Br
Urine	B	Sep. 30	(µg ml^{-1})	UR-Sh-30-a		3,110	1,120	11	6
				UR-Sh-30-b		3,120	1,110	10	6
					Mean	**3,120**	**1,120**	**10**	**6**
					S.D.	7	7	1	0
Urine	A	Sep.30–Oct.1 morning	(µg ml^{-1})	UR-Oh01-a		1,370	901	27	3
				UR-Oh01-b		1,400	899	29	2
					Mean	**1,390**	**900**	**28**	**2**
					S.D.	21	2	2	0
Urine	B	Sep.30–Oct.1 morning	(µg ml^{-1})	UR-Sh01-a		3,550	1,090	16	3
				UR-Sh01-b		3,620	1,100	18	3
					Mean	**3,590**	**1,100**	**17**	**3**
					S.D.	49	7	1	0
Urine	C	Sep.30–Oct.1 morning	(µg ml^{-1})	UR-Yk01-a		2,880	1,000	307	5
				UR-Yk01-b		3,000	1,040	361	5
					Mean	**2,940**	**1,020**	**334**	**5**
					S.D.	85	28	38	0
Vomit*	A	Sep. 30	(µg ml^{-1})	OT-Oh-B-a		448	<80	<100	4
				BL-Oh-B-b		467	<80	<100	4
					Mean	**458**	**<80**	**<100**	**4**
					S.D.	13			0
Vomit*	B	Sep. 30	(µg ml^{-1})	OT-Sh-W-a		406	<80	<100	4
				OT-Sh-W-b		428	<80	<100	4
					Mean	**417**	**<80**	**<100**	**4**
					S.D.	16			0
Vomit**	C	Sep. 30	(µg ml^{-1})	OT-Sh-L-a		1,790	250	<100	15
				OT-Sh-L-b		1,640	198	<100	14
					Mean	**1,720**	**224**	**<100**	**15**
					S.D.	106	37		1

* Extracted from a paper towel
** Gastric juice-like yellow substance

III.D.c. ^{32}P measurement in urine

The three exposed workers were hospitalized at NIRS, the University of Tokyo Hospital and the Institute of Medical Science of the University of Tokyo. Urine was collected every day during their stay. The urine was subjected to radioactivity analysis, which detected ^{32}P. It is assumed that phosphorus in the body had been activated and transformed to ^{32}P. ^{32}P analysis appears to be a means of dose evaluation potentially useful in criticality accidents. For this reason, the ^{32}P in the urine of the three workers was measured (NI02).

c.1. Measurement with a low background beta ray spectrometer

c.1.1) Sample collection and preparation

Among the 24-hour urine samples collected from the three workers, the volumes of some samples were not known. On the day of transfer and the day following transfer from NIRS to the University of Tokyo Hospital and the Institute of Medical Science, no urine was collected.

50 ml was sampled from each 24-hour collection, placed in a plastic vessel (diameter: 50 mm; height: 60 mm) for freeze-drying. Part of the freeze-dried urine

(approximately 200 - 2,000 mg) was weighed out onto a stainless steel sample plate (diameter: 25 mm; depth: 6 mm) to form a uniform layer. This dried urine, covered with a thin piece of paper, was subject to low background beta ray spectrometry.

c.1.2) Calibration curve and measurement efficiency

To obtain a calibration source, urine was collected from a healthy adult, freeze-dried and kept in a desiccators. 0.1, 0.5, 1.0, 1.5 and 2.0 g of the dried urine powder were weighed out and put in individual sample plates, each of which was uniformly saturated with 100 µl of a ^{32}P standard solution and then re-dried in a desiccators. This was used as the calibration source for calibrating counting efficiency. When the ^{32}P energy range was set to 40 – 1,627 keV, the measurement efficiency for samples varied according to the thickness, for reasons of beta ray self-absorption, but stabilized in a range between 7% and 19%.

c.2. Measurements using a liquid scintillation counter

c.2.1) Sample preparation and measurement conditions

1 ml of distilled water was added to the freeze-dried urine samples (200-2,000 mg), and then a tissue solubilizer Soluene-350 (1-2 ml) and hydrogen peroxide solution (0.4 – 0.8 ml) were added.

Next, the residual hydrogen peroxide solution was removed from the sample by heating in a temperature-controlled bath at 55 ˚C for 30 minutes, after which a scintillator (Hionic-fluor) added. The sample to be subjected to liquid scintillation was prepared and a calibration curve for quench correction was made with a contamination-free urine sample from a healthy adult and a ^{32}P solution containing a known level of radioactivity. Counting was carried out using two channels: Channel A (5-1,700 keV) and Channel B (50-1,700 keV); Channel B counts were adopted as reporting values in consideration of the results of the follow-up experiment on radioactivity decay as described below.

c.2.2) Follow-up experiment of radioactivity decay

It was possible that the hair and urine samples contained contaminated radionuclides other than ^{32}P. To perform this assay, decay half-lives of potentially present mixed radionuclides were compared with the ^{32}P decay half-life by carrying out time-series measurements in two energy ranges: Channel A (5-1,700 keV) and Channel B (50-1,700 keV). The decay rates of radioactivity measured in Channel A were slower than that of ^{32}P, suggesting that other radionuclides, with a longer decay half-life than ^{32}P, were present. Decay half-lives in Channel B, however, agreed approximately with the decay half-life of ^{32}P. Thus it was demonstrated that liquid scintillation counting enables measurements excluding radioactivity other than that emitted by ^{32}P by limitation of the energy range during measurement. For this reason, Channel B measurements were adopted in this study.

c.3. Results of ^{32}P in urine from a low background beta ray spectrometer and a liquid scintillation counter

Fig. III.D.2 shows the beta ray spectra of a ^{32}P reference sample. Table III.D.3 shows the measurement results of radioactivity in urine with a low background beta ray spectrometer; Table III.D.4 shows those obtained using a liquid scintillation counter. A comparison of the radioactivity levels extrapolated back to the time of the accident show the values of the low background beta ray spectrometer to agree roughly with those obtained using the liquid scintillation counter, demonstrating the validity of our measurement results. Furthermore, Fig. III.D.3 shows changes with time in ^{32}P-radioactivity detected in 24-hour urine samples. In this Figure, the curve obtained from the phosphorus retention function described by Jackson and Dolphin (JA66) has been superimposed. The data appears to consist of the 0.5, 2 and 19-day components of the biological half-life of phosphorus as described in ICRP Publ. 30.
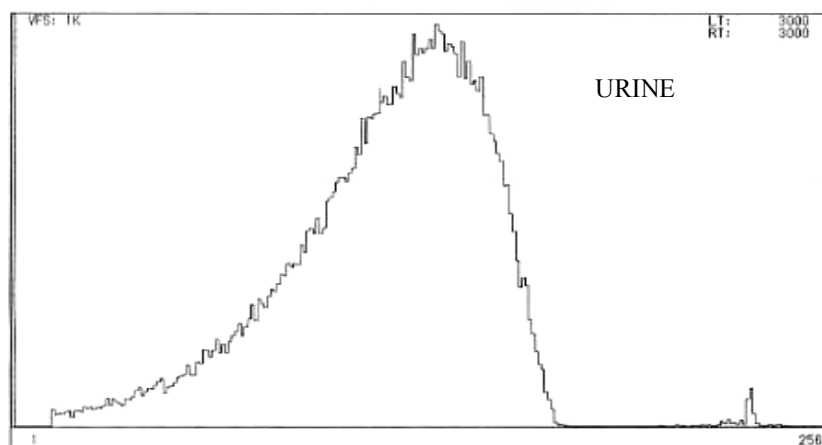

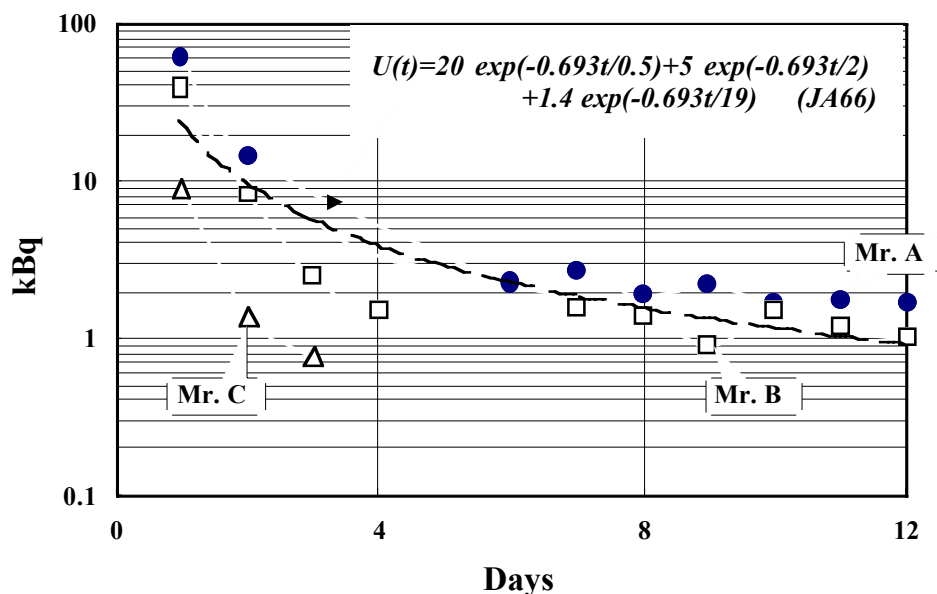**Fig. III.D.2 Beta ray spectrum of urine**

$$U(t)=20 \ exp(-0.693t/0.5)+5 \ exp(-0.693t/2)$$
$$+1.4 \ exp(-0.693t/19) \quad (JA66)$$

Fig. III.D.3 ^{32}P radioactivity detected in 24-hour urine (Bq/day; corrected to the time of the accident)

Table III.D.3 Results of ^{32}P in urine using beta ray spectrometer

Worker	Collection date	Dried urine amount used for measurement	Totlal urine volume for a day	Radioactivity concentration of total urine for a day (at the time of the accident)	Total radioactivity of total urine for a day (at the time of the accident)	Counting error in radioactivity of total urine for a day (at the time of the accident)
	Oct. 1999	(g)	(ml)	(Bq ml^{-1})	(Bq)	($\pm$Bq)
A	1	0.443	3,000	20.2	60,500	713
	2	0.714	2,143	6.9	14,789	202
	6	0.191	2,680	0.9	2,294	52
	7	0.162	3,040	0.9	2,708	59
	8	0.256	2,460	0.8	1,875	36
	9	0.204	1,760	1.3	2,212	49
	10	0.796	2,040	0.8	1,660	25
	11	0.413	2,830	0.6	1,838	32
	12	0.457	2,680	0.6	1,674	29
B	1	0.242	3,220	12.2	39,157	466
	2	0.986	3,448	2.4	8,174	130
	3	0.486	2,430	1.0	2,479	50
	4	0.184	3,448	0.4	1,495	30
	7	0.449	4,760	0.3	1,553	34
	8	0.213	3,170	0.4	1,383	30
	9	1.003	2,240	0.4	891	12
	10	0.395	3,480	0.4	1,502	28
	11	0.464	4,400	0.3	1,216	22
	12	0.657	4,600	0.2	1,034	17
C	1	0.494	2,730	3.4	9,258	135
	2	0.907	1,900	0.7	1,352	23
	3	0.575	2,000	0.4	769	13

53

Table III.D.4 Results of ^{32}P in urine using liquid scintillation counter

Worker	Collection date Oct. 1999	Dried urine amount used for measurement (g)	Radioactivity concentration in dried urine collection (Bq g^{-1})	Dry weight ratio (dry %)	Total urine volume for a day (ml)	Radioactivity concentration of total urine volume for a day (at the time of the accident) (Bq ml^{-1})	Total Radioactivity of turine volume for a day (at the time of the accident) (Bq)
A	1	0.206	270.8	1.4	3,000	23.43	70,276
	2	0.576	23.3	4.5	2,143	6.63	14,210
	6	0.789	4.3	4.2	2,680	1.13	3,026
	7	0.878	3.6	4.2	3,040	0.96	2,904
	8	1.703	2.7	4.7	2,460	0.78	1,915
	9	1.967	2.6	5.6	1,760	0.91	1,598
	10	1.563	3.1	4.2	2,040	0.81	1,660
	11	1.710	2.3	3.9	2,830	0.57	1,621
	12	2.183	1.9	4.2	2,680	0.49	1,325
B	1	0.741	82.9	2.3	3,220	12.04	38,771
	2	0.686	12.3	3.4	3,448	2.64	9,101
	3	0.602	7.3	2.3	2,430	1.05	2,547
	4	1.042	2.8	2.6	3,448	0.45	1,538
	7	0.893	1.7	3.6	4,760	0.39	1,857
	8	0.665	1.5	4.2	3,170	0.40	1,278
	9	1.503	1.2	3.8	2,240	0.29	659
	10	1.699	1.1	4.1	3,480	0.29	1,007
	11	1.455	1.2	3.3	4,400	0.24	1,041
	12	1.092	1.2	2.9	4,600	0.22	1,025
C	1	0.581	22.8	2.5	2,730	3.58	9,768
	2	0.879	2.4	5.0	1,900	0.76	1,437
	3	0.892	2.1	2.8	2,000	0.37	738

c. 4. Discussion

In case of emergency, urine is extremely useful as a less invasive sample. In the Pajarito criticality accident that occurred in Los Alamos in 1946, eight persons were severely exposed to neutron and gamma ray irradiation, one of whom died nine days after the accident (HO48). In that event, both ^{24}Na in blood and ^{32}P produced in urine were determined. It was reported that ^{32}P concentrations in urine, estimated from stable phosphorus concentrations in serum, were lower than the theoretical value, demonstrating no dose dependency. After the Y-12 Plant-III criticality accident at Oak Ridge in 1958, in the light of the Pajarito experience, no study was made of ^{32}P concentrations in urine (HU59).

In our study, ^{32}P concentrations were measured after the short-lived nuclides had decayed. However, concerning the three exposed workers, the ratio among ^{32}P concentrations in urine corresponded closely with that in ^{24}Na concentrations in the blood (Table III.D.5). There may be several reasons why dose dependency was not observed in ^{32}P contained in urine in previous criticality accidents. For example, (1) the stable phosphorus concentration in serum, used to calculate the theoretical value, may have been incorrect (IC75, CO78) and (2) the

instruments of the time were likely to measure short-lived nuclides together with ^{32}P. More detailed examination is needed, taking into account the influence of short-lived nuclides. Nevertheless, we suggest that measurement of ^{32}P in urine in the event of a criticality accident is an extremely effective tool for estimating neutron exposure dose as the first approximation.

Furthermore, measurement results of ^{32}P in urine with the low background beta ray spectrometer and liquid scintillation counter roughly agreed. It seems that not many laboratories own a low background beta ray spectrometer. A liquid scintillation counter is, however, a common piece of equipment and does not require pre-treatment of samples, allowing it to serve as an effective means of simple and prompt neutron dose estimation.

Table III.D.5 Concentration of ^{32}P in urine on the first day after the accident, and relative concentration ratio for the workers

Worker	^{32}P in urine		^{24}Na in blood	
	Concentration (Bq ml^{-1})	Ratio	Concentration (Bq ml^{-1})	Ratio
A	20.2 ± 0.2	6.1	169 ± 5.0	7.4
B	12.2 ± 0.1	3.7	91.3 ± 1.7	4.0
C	3.3 ± 0.1	1	22.8 ± 1.1	1

III.E. Bone

Bone, composed primarily of hydroxyapatite, contains high concentrations of phosphorus and calcium. Radionuclides are produced in the body by neutron activation of stable isotopes of these elements. Clarification of distribution of radionuclides in each part of the body provides information on whole-body distribution of neutron dose. Whole-body distribution information reveals the locations of each part of the body relative to the precipitation tank, which acted as the neutron source at the time of exposure. This information can be fed into a computational simulation of radiation transport, which makes it possible to build a detailed picture of neutron and gamma ray dose in each organ of the body.

This Section E reports analyses of bone samples from the remains of the two workers who died from the effects of the accident. We carried out ^{32}P and ^{45}Ca measurement by beta ray spectrometry, together with measurements of gamma-emitting nuclides and an analysis of radioactivity distribution within bones using imaging plate technique.

III.E.a. Measurement of ^{32}P and ^{45}Ca using beta ray spectrometry (WA01, MI02).

a.1. Sample preparation and measurement method

After the death of the two heavily exposed workers, bone samples (approximately 1-13 g) were obtained from 14 sites in each body. The bones were ashed at 450 ˚C and pounded in an agate mortar. Approximately 0.2 g of nitric acid was added to this bone powder to digest completely in a microwave decomposition system. ^{32}P was radio-chemically separated as ammonium magnesium phosphate precipitate, and ^{45}Ca as calcium carbonate precipitate. Each precipitate, mounted on a piece of filter paper, was subjected to quantification of ^{32}P and ^{45}Ca with a low background beta ray spectrometer. Precipitates were formed from ^{32}P and ^{45}Ca standard solutions using a method similar to that employed for bone samples; these precipitates were used as the calibration source for measurement efficiency and beta ray self-absorption. The counting efficiency was approximately 18% for ^{32}P and 1% for ^{45}Ca. To obtain ^{32}P and ^{45}Ca specific activity, the precipitates after the beta ray measurement were dissolved again by addition of nitric acid and stable element concentrations of phosphorus and calcium were measured using an ICP-AES (Seiko Instrument Inc., SPS-7000A).
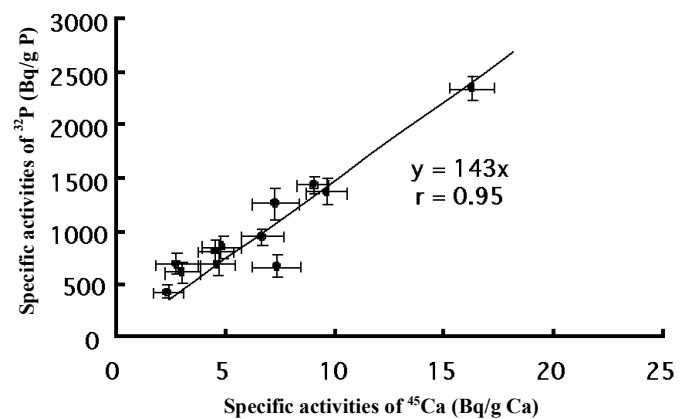

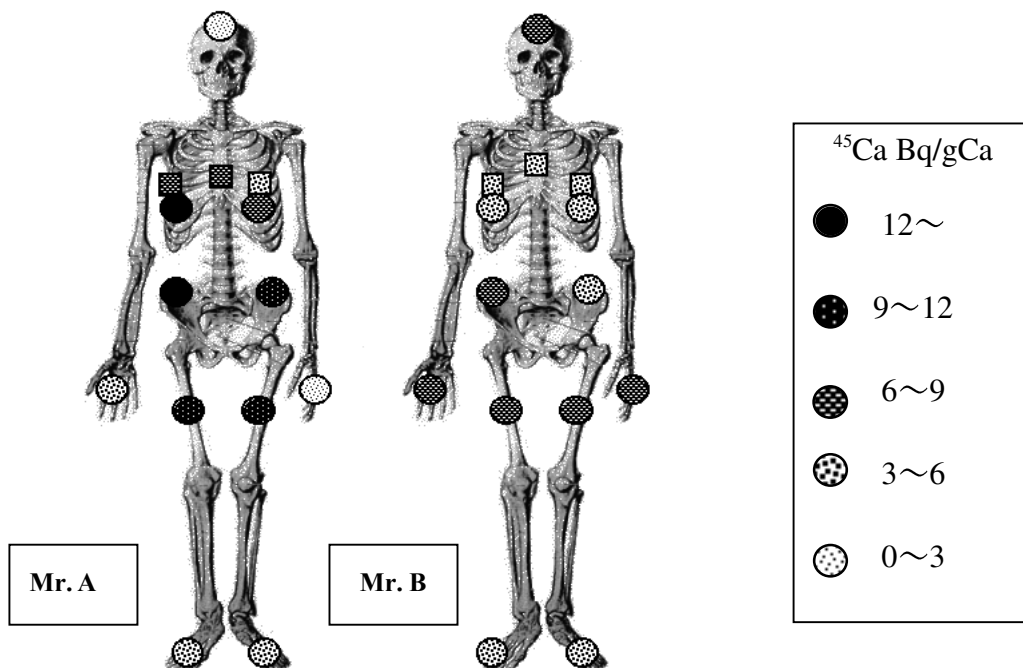**Fig. III.E.1 Correlation between ^{32}P and ^{45}Ca concentrations in bones**

Fig. III.E.2 Distribution of ^{45}Ca concentrations in bones

a.2. Results

^{32}P (half-life: 14.26 days) and ^{45}Ca (half-life: 163.8 days) were detected in the bone sample from Mr. A, who died 82 days after the accident, and ^{45}Ca only from Mr. B, who died 210 days after the exposure. There was a positive correlation between the specific activities of ^{32}P and ^{45}Ca in the bone samples from Mr. A (Fig. III.E.1), demonstrating that both these specific activities could be indicators of thermal neutron fluence in bones. Fig. III.E.2. shows the ^{45}Ca distribution in the whole body bones of Mr. A and Mr. B. As for Mr. A, higher specific activities are observed chiefly in the trunk bones and femur, with the highest in the right rib and the right iliac bone. For Mr. B, there is not such a large difference in the specific activity observed in bones with different body sites. Mr. B's trunk bones show lower specific activities than Mr. A's; Mr. B's frontal bone and the bones of the right and left fingers show relatively high specific activities. These observations suggest that Mr. A was exposed by neutrons mainly on the right center part of the body; Mr. B was exposed to high doses, particularly in the face and fingers. These data provide useful information on the workers' postures at the time of the accident and for exposure dose estimation.

III.E.b. Analysis of radioactive nuclides using gamma ray spectrometry

Although our focus was on analyzing bone samples for beta rays (^{45}Ca and ^{32}P), it was also necessary to examine whether or not gamma-emitting radionuclides produced by activation would be detected in bones. Therefore, non-destructive analysis using a Ge detector was also performed.

b.1. Sample preparation and measurement method

In ^{45}Ca and ^{32}P analysis, samples are subjected to a separation process involving decomposition by acid. Gamma ray measurement was therefore performed before the decomposition of samples, using a Ge detector (Ortec GMS-30185, FWHM: 1.8 keV), coupled to a multichannel analyzer (Seiko EG&G 7800). (During measurement, one channel was set to 0.5 keV so that measurement up to 2,000 keV was possible.)

First, as a pretest, only eight samples among the bone samples from Mr. A were subjected to measurement: the frontal bone, the anterior area of the seventh rib (right and left), the posterior area of the seventh rib (right and left), the right femur, and the anterior superior iliac spine (right and left), all of which were 1.1 g - 9.0 g by dry weight. They were placed in a plastic container having a similar size to that of a U-8 container, and measured in unmodified form for 40,000 seconds. Then the right femur (the center area) was measured again for approximately one million seconds since the bone was

two times heavier and was expected to have received a higher dose than the others.

b.2. Results

Each of the eight samples was measured for 40,000 seconds with a Ge detector. No significant gamma ray peaks attributable to the accident were detected such as ^{24}Na (half-life: 14.9 hours) and ^{42}K (half-life: 12.3 hours), which were observed in the blood, urine and other samples immediately after the accident; however, our measurements were performed on the 97th day after the accident; many nuclides were undetectable due to their having decayed.
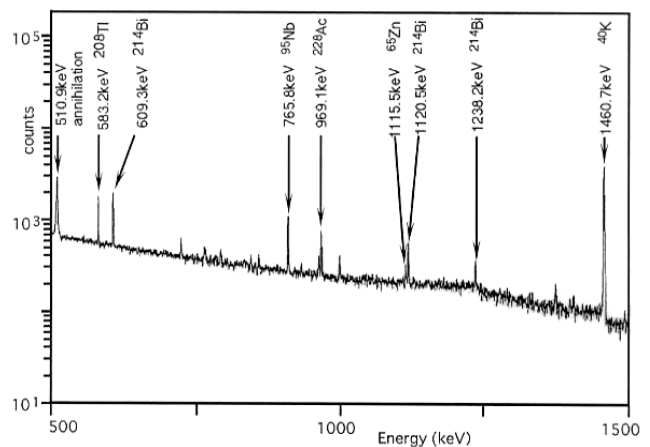

Fig. III.E.3 Gamma ray spectrum of the right femur

Mr. A's right femur (center) sample, expected to have been exposed to the highest dose, was measured for one million seconds. A peak was observed at around 1,115.5 keV, corresponding to the energy of ^{65}Zn (half-life: 244 days). Fig. III.E.3 shows a gamma ray spectrum of the femur sample. Peaks other than the ^{65}Zn peak resulted from background radiation, and no nuclides associated with neutron activation were detected. It is thought that the right femur (center), closer to the precipitation tank where the criticality accident occurred, were exposed to a large neutron fluence. Furthermore, it can be inferred that the sample, large enough in amount, was measured for a relatively long period of time, leading to detection of ^{65}Zn, which has relatively a long half-life. However, accurate quantification requires efficiency calibration that takes the shape of the bone into account. Also, to obtain neutron doses, it is necessary to analyze stable zinc (^{64}Zn, etc.) by further decomposition. Nevertheless, as previously described, our bone analysis was focused on beta ray measurement, and its treatment had a higher priority, so only qualitative analysis was performed for the gamma ray spectrometry. (Semi-quantitative determination demonstrated that ^{65}Zn concentrations were equal to or less than 0.02 Bq g^{-1} with respect to the dry weight of the bone.)

III.E.c. Confirmation of neutron activation of bone tissue using imaging plate

To investigate thermal neutron distribution in bone tissue, the right seventh rib of Mr. A, who died 82 days after the accident, was subjected to detection of ^{32}P and ^{45}Ca, produced by neutron activation, using an imaging plate (IP).

c.1. Measurement method

A segment (40 μm in thickness) was prepared from of Mr. A's right seventh rib and exposed to an imaging plate (IP) (Fuji Photo Film Co., Ltd., BAS-MS2025), for three days and then seven days. It was then analyzed using a RI Bio-Imaging Analyzer (Fuji Photo Film Co., Ltd., BAS-2000).

c.2. Results and discussion

Measurement was started on approximately the 100th day after the accident. A bone sample-like image could be observed against the background noise by the naked eye from the IP image that had been exposed for three days. However, no significant difference was found from the image analysis data using photostimulated luminescence intensity per unit area (PSL/S), compared with the background. IP's minimum detectable exposure is defined as the amount providing PSL/S = 0.4. In practice, however, it depends on the spatial frequency of patterns and images. In addition, it seems that factors such as the observer's findings, training and eyesight as well as viewing conditions are involved (MI01). Although exposure time was extended to seven days, aiming to increase the detection limit, increased background noise prevented us from confirming the shape of the bone sample. According to technical information provided by Fuji Photo Film, if a long-time exposure is carried out without using a Shield Box, the amount of fogging would reach more than one third of the measurement range in one week. Therefore, it seemed reasonable to assume that shape of the bone sample could not be confirmed because of possible fogging produced by cosmic radiation or gamma rays emitted by the walls of the storage area (FU93a, b).

To assume how ^{32}P, ^{45}Ca and ^{40}K, pre-existing natural radioactive nuclides, contributed to the IP image obtained from bone samples, stable Ca, P and K concentrations were measured using an inductively coupled plasma atomic emission spectrometer (IRIS, Nippon Jarrell-Ash Co., Ltd.). Part of Mr. A's right seventh rib, used for the analysis of activation products in bones, and right femur was subjected to this form of measurement. While stable K concentrations varied according to the collection site of bone tissues, they were two orders lower than those of Ca (376 mg g^{-1}) and P (172 mg g^{-1}), as shown in Table III.E.1. From these results, a reading was obtained for ^{40}K radioactivity per unit area of 6.7 x 10^{-7} Bq mm^{-2} (MI98) in the right seventh rib segment. According to Miyahara's report (MI98), the maximum detection sensitivity when using a Shield Box for the purpose of reducing background noise was 9.8 x 10^{-6} Bq mm^{-2} for ^{32}P (1.711 MeV) for the exposure time of four weeks and 7.7 x 10^{-5} Bq mm^{-2} for ^{14}C (0.156 MeV) with a time exposure of three months. The radioactivity level of ^{40}K (1,312 MeV) contained in our sample was one order lower than the maximum detection sensitivity of ^{32}P or ^{14}C, demonstrating that ^{40}K affected the IP only slightly. Another three-day exposure was performed from January 10 to 13, 2001, one full year after the initial measurement. The bone tissue could not be identified from the IP image with the naked eye. It was therefore shown that the IP image of the bone, confirmed on approximately the 100th day after the accident, resulted from ^{32}P and ^{45}Ca, with little effect of long-lived ^{40}K evidence.

In these measurements, analysis of ^{32}P and ^{45}Ca distribution in bones failed because of their low levels in the bone samples. However, it was verified that quantification of ^{32}P and ^{45}Ca was possible using techniques such as reduction of background. From the previously described measurements of Mr. A's right seventh rib, the specific activity in the bone segment per unit area on the 100th day after the accident was estimated using the low background beta spectrometer counts: approximately 3 x 10^{-5} Bq mm^{-2} for ^{32}P and 3 x 10^{-5} Bq mm^{-2} for ^{45}Ca. It was suggested that reduction of background noise, using a Shield Box, would have enabled adequate ^{32}P measurement, compared with the maximum detection sensitivity reported by Miyahara. Furthermore, in measurements using bone segments, the absolute abundance of P and Ca contained in the sample tends to reduce the measurement sensitivity. It is assumed that measurement sensitivity can be improved using the block contact technique to bring the IP into direct contact with the bone sample.

Table III.E.1 Ca, P and K concentrations in the right seventh rib and right femur of Mr. A

Element	Concentration in the (left) seventh rib (mg g^{-1})	Concentration in the (right) femur (mg g^{-1})
Ca	376	377
P	172	174
K	3.12	2.42

III.F. Bone marrow

Mr. A was transferred to the University of Tokyo's Faculty of Medicine, where he underwent bone marrow transplantation on October 6. Although it was confirmed that the new marrow had been accepted, chromosomal aberrations in Mr. A's blood were observed even after the transplantation. We received an inquiry from the doctors whether or not the bone(s)/bone marrow had become a radiation source. Part of Mr. A's bone marrow was sent to us, and was subjected to gamma ray and beta ray counting. The bone marrow was sampled at the University of Tokyo Hospital on October 16, and samples were sent to NIRS on November 12. The samples were subjected to gamma ray counting immediately after their receipt, followed by beta ray counting using the pre-treatment described below.

Samples

Bone marrow in breastbone: 1.0192 g
0.1 g was weighed out for liquid scintillation counting
The rest, 0.9348 g, was dried under an electric heater (final dry weight 0.0556 g)

Bone marrow in iliac bone: 1.9359 g
0.2 g was weighed out for liquid scintillation counting.
The rest, 1.6780 g, was dried under an electric heater (final dry weight 0.2252 g)

A qualitative analysis of gamma-emitting nuclides with a Ge detector revealed no radioactive nuclides produced by neutron activation.

Meanwhile, the dried bone samples, mounted onto a sample plate, were subjected to beta ray counting for 50,000 seconds using a low background beta ray spectrometer. A low level of ^{32}P was detected. The results indicated in term of ^{32}P activity and the counting errors are as follows. They have been converted to the time of the accident.

Bone marrow in breast bone: 0.012 ± 0.004 Bq (0.013 ± 0.004 Bq g^{-1})

Bone marrow in iliac bone: 0.053 ± 0.004 Bq (0.032 ± 0.003 Bq g^{-1})

The geometry of bone marrow samples did not agree completely with that of the standard samples. However, it is thought that the variation did not exceed the counting error, because the samples were too small (i.e. too thin) to have a high degree of self absorption. In beta ray counting with a liquid scintillation counter, no significant difference was observed from the background, partly because the volume of the samples was extremely small.

In conclusion, it can be inferred that the observed chromosomal aberrations were not attributable to radioactive nuclides in bone marrow for two reasons: (1) no gamma-emitting radionuclides were detected and (2) the level of the beta ray radioactivity was very low.

III.G. ESR measurement of teeth and nails

III.G.a. ESR measurement of the teeth of the heavily exposed workers

Introduction

Electronic spin resonance (ESR) dosimetry on tooth enamel started with re-evaluations of the A-bomb irradiation doses in Hiroshima and Nagasaki (OK85), and has included studies on the correlation between radiation dose recorded in tooth enamel and the frequency of chromosome aberrations in Hiroshima A-bomb survivors (NA98) and includes reports on basic application of this technique by Iwasaki et al. (IW93, IW95, IW98). Although ESR dosimetry using the teeth is an effective method, its application has limitations in that teeth sampling requires the tooth to be extracted, since the tooth enamel has to be separated from the dentine. The principle of ESR lies in the formation of carbonate ion radicals in tooth enamel (hydroxyapatite) by exposure. Since such radicals are stable, dosimetry can be achieved by measuring the quantity of radicals using ESR. This Section G discusses the ESR dosimetry process using teeth collected from the cadavers of two of the victims of the criticality accident at JCO.

a.1. Experimental

Sample preparation: Tooth samples for dosimetry were obtained from the cadavers of Mr. A and Mr. B: the upper right third molar from Mr. A, and the upper right first premolar and upper left second premolar from Mr. B. Enamel was separated from each of them using a diamond cutter after dividing each tooth in half: one half facing the cheek side of the mouth and the other facing the tongue side. The enamel was ground into particles ranging in size between 500 µm and 1,400 µm (IW93).

ESR measurement: The enamel sample within a certain particular size range was placed in an ESR sample tube (4 mm in diameter), and subjected to measurement at ambient temperature using a JEOL ESR system (JEOL-RE-1X), with microwave output power: 5 mW; modulation frequency: 100 kHz; field modulation width: 0.32 mT; scanning magnetic field: 328 ± 5 mT; scanning period: 16 min; and time constant: 0.1 sec. ESR intensity was obtained from the ratio between the signal caused by free radicals formed in tooth enamel and the manganese marker.

a.2. Results and discussion

The obtained enamel with uniform particle size weighed between 60 mg and 140 mg. Fig. III.G.1 shows an example of the ESR spectrum. Using the relative intensity of sample signal to the mean of the right and left of the manganese standard signals and from the comparison with the calibration curve of standard radiation samples using ^{60}Co gamma rays, absorbed doses, which corresponded to the amount of ^{60}Co gamma rays, were obtained: 11.8 ± 3.6 Gy and 12.0 ± 3.6 Gy for the buccal side and lingual side of Mr. A's upper right third molar, respectively; 11.3 ± 3.4 Gy and 10.8 ± 3.3 Gy for the buccal side and lingual side of Mr. B's upper right first premolar, respectively; and 11.7 ± 3.5 Gy and 11.4 ± 3.4 Gy for the buccal side and lingual side of Mr. B's upper left second premolar, respectively. The errors are due to variations among individuals.

As described in Chapter III, Section B.a and B.b, the estimated specific activities of ^{24}Na in hair at the time are 6.4×10^4 and 3.7×10^4 Bq g^{-1} for Mr. A and Mr. B, respectively. The average absorbed doses in the whole body, estimated using gamma rays, are 9.9 Gy for Mr. A and 4.1 Gy for Mr. B. Both parameters indicate a roughly twofold difference between the two workers (Refer to Chapter II, Section G). As for tooth enamel doses, it is concluded at the present stage that there is no difference between the two persons' exposure doses, irrespective of the location of the teeth, including whether from the buccal side and lingual side; otherwise, individual errors are involved. Strictly speaking, the dose estimates we obtained for tooth enamel were based on standard samples irradiated by ^{60}Co gamma rays. The criticality accident at JCO involved mixed irradiation of neutrons and gamma rays. In the future, therefore, we plan to examine free radical generation in tooth enamel exposed to neutrons.
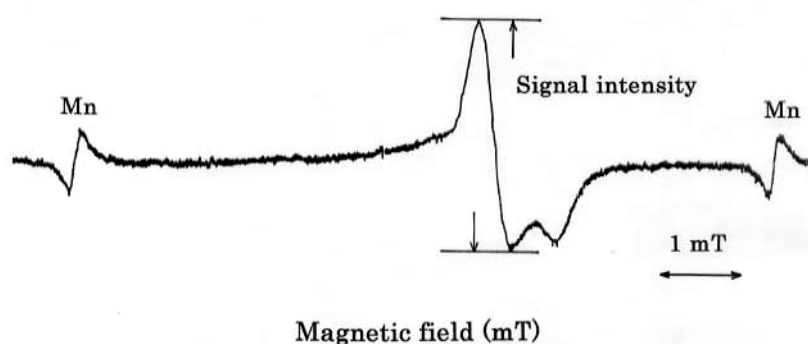

Fig. III.G.1 ESR spectra of Mr. A's molar (buccal side) enamel sample

III.G.b. ESR measurement of the nails of the highly irradiated workers

Introduction

In an emergency like the JCO criticality accident, electronic spin resonance (ESR) radiation exposure dosimetry is a helpful dosimetry technique, not only for the public but also for radiation workers. In particular, if a worker is not carrying a dosimeter, some materials in the vicinity of the place where the accident occurred can be useful to dose estimation for the workers (NA96, SH97). Also, one of the ESR applications for irradiated human body or tissues is tooth enamel (IW98).

The principle of ESR lies in the formation of radicals in the chemical substances by irradiation. Since some radicals are stable for extended periods, radiation dosimetry can be achieved by using ESR to measure the quantity of these radicals by using ESR. For example, in the Chernobyl accident, external exposure doses were estimated by measuring the quantity of free radicals formed in sugar left inside an evacuated house (NA94). In the JCO accident, though, no signals above the detection limit were detected from sugar collected inside or outside the JCO facilities (SH00).

After the JCO accident, fingernails were collected from the exposed workers. It has not been demonstrated in any other studies that nails are appropriate materials for ESR dosimetry. This Section G.b reports the observed results of ESR signal fading (changes in time) of nails from the two exposed workers.

b.1. Experimental

On the fourth day after the accident, clippings from the right and left little fingernails, 16 mg and 17 mg in weight, respectively, were collected from Mr. B. On the 62nd day (December 2), 214 mg of Mr. A's toenails were collected. The nails were rinsed in warm water and air-dried.

ESR Measurement: The bigger nails were cut into pieces small enough to be placed in the ESR sample tube (4 mm in diameter), and then subjected to measurement at room temperature using a JEOL ESR system (JEOL-RE-2X), with microwave output power: 3 mW; modulation frequency: 100 kHz; field modulation width: 1.25 mT; scanning magnetic field: 334 ± 15 mT; scanning period: 8 min; and time constant: 0.03 sec. The nail sample kept in the sample tube was left as it was, and its changes with elapse of time were traced for approximately three months. ESR relative intensity was obtained from the ratio between the radical signal formed in the nails and the signal due to the manganese standard.

b.2. Results and discussion

Fig. III.G.2 shows changes with time in the left fingernail sample. The relative intensity on the first day was 1.26, gradually decreasing to reach an approximately constant value of 0.42 on the 20th day. The initial intensity of the right fingernail sample was slightly lower than the left (i.e. 0.80). However, it reached a constant value of 0.40 after 20 days, as did the left sample. It is assumed that the difference in signal between right and left fingernails resulted from the difference in sample weight and quantity of free radicals present when the nails were cut.

Mr. A's toenails, collected on the 62nd day after exposure, showed almost the same pattern of change from 0.95 to 0.57 as Mr. B's fingernails. Since the toenails were larger, the possibility of direction dependency was examined. The toenail samples were measured several times at different insertion angles (0, 90, 120, 180, 240, and 270˚), and a relative intensity of 0.96 ± 0.04 (six measurements) with an error of approximately 4% was obtained. It was found that a direction dependency almost has not in toenail samples. The two persons' nails, collected on 62 days after the accident, showed almost the same fading curve. It is therefore assumed that the ESR intensity changes were due to deterioration of nail constituents (i.e. a radical decrease in constituent amino acid); they were not in relation to free radicals formed by radiation exposure.

Some reports claim that nails can act as a useful sample for radiation dosimetry, and some say that free radicals formed in nails disappear within approximately 5-10 minutes of exposure (NA82). We have not yet seen any satisfactory reports on nail dosimetry. Considering the JCO accident, it is necessary to clarify this problem in terms of ESR application as soon as possible.
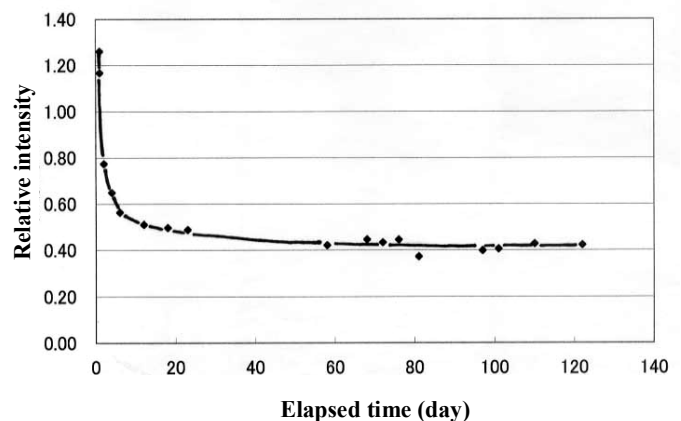

Fig. III.G.2 Changes with time in ESR intensity of nail samples

60

IV. DISCUSSION

Introduction

The dose assessment of the workers who were exposed at the criticality accident was not an easy task. There are many factors concerned and several ways for the dose assessment. Main problems with the dose assessment were described in Section G of Chapter II "Summary of dose estimation." In this chapter, these problems are discussed in more detail.

IV.A. Comparison of specific activities

In this Section A, we discuss the specific activity of ^{24}Na in blood, which was used for dose assessment in Chapter II, as well as that in other samples. Specific activities of isotopes such as ^{82}Br and ^{42}K in different samples are also mentioned.

IV.A.a. Specific activities of ^{24}Na

Measurements of specific activity of ^{24}Na in blood are summarized in Table II.D.7 in Section D.a.3 of Chapter II. The specific activity of ^{24}Na, including measurements in samples other than blood, such as urine, vomit (gastric juice), and hair, and related data are summarized in Table IV.A.1. Based on the half-life of ^{24}Na, these values were converted to the time of the accident. For the conversion the physical half-life as well as the biological half-life, the value for sodium of 10 days, which is noted in ICRP Publ. 30 (IC80), were taken into consideration.

The use of values for specific activity enables direct comparison of data from different samples, which could not be compared using only concentration of radioactivity. For example, values of ^{24}Na in the "September 30 to the morning of October 1" urine samples show 121 Bq ml^{-1} for Mr. A and 178 Bq ml^{-1} for Mr. B, indicating the value for Mr. B to be higher than that for Mr. A, the reverse of the individual difference observed in blood. However, concerning specific activity, targeted ^{23}Na (stable sodium) concentration is used as a denominator; therefore, the value shows 9.0 x 10^4 Bq ^{24}Na /g Na for Mr. A and 5.2 x 10^4 Bq ^{24}Na /g Na for Mr. B, showing the value for Mr. A to be higher, similar to his blood value.

The neutron exposure of the three workers can be compared using the specific activities of ^{24}Na. For example, if the blood value for Mr. A is assumed to be 1.0, that for Mr. B is 0.52 and Mr. C's is 0.15 (Table IV.A.1). A similar ratio was obtained from a comparison using the specific activity value of urine, indicating 0.57 for Mr. B and 0.16 for Mr. C. However, a comparison of different samples obtained from an identical worker, the specific activity values of ^{24}Na in vomit, urine, and blood fell in value in this order, and the value in hair is clearly low. Low specific activity in hair may be related to its greater distance from the neutron source (the uranium solution) than the center of the body; the incident angle of the neutrons; and masking by the helmet. Also, there are several reasons for blood showing a lower specific activity than urine and vomit, including non-uniform irradiation and non-uniform distribution of targeted stable sodium in the body. The dilution effect caused by stable sodium transferred into the blood through intravenous administration may be also important, and will be described in the following Section B.

Table IV.A.1 Amounts of ^{24}Na and stable Na in the samples and specific activities

Worker	Samples and date of sampling		^{24}Na concentration (Bq ml^{-1} or Bq g^{-1})	^{24}Na concentration corrected biological half-life (Bq ml^{-1} or Bq g^{-1})	Stable Na concentration (mg ml^{-1} or mg g^{-1})	Specific activity (Bq^{24}Na)(g Na)$^{-1}$	Intensity ratio in Mr. A (by sample)
A	Blood	10/1	157 ± 4.6	169	2.05	8.24E+04	1.00
	Urine	9/30 – 10/1 morning	121 ± 0.5	125	1.39	9.01E+04	1.00
	Vomit	9/30	42.3 ± 0.4	42.3	0.46	9.24E+04	1.00
	Hair 10/1		130 ± 20	130	2.04	6.36E+04	1.00
B	Blood	10/1	84.7 ± 1.6	91.6	2.11	4.34E+04	0.53
	Urine	9/30 – 10/1 morning	178 ± 0.5	185	3.58	5.15E+04	0.57
	Urine	9/30	165 ± 0.4	168	3.11	5.40E+04	0.60
	Vomit	9/30	98.7 ± 1.3	98.7	1.72	5.76E+04	0.62
	Hair	10/1	17.0 ± 1.0	17.0	0.46	3.69E+04	0.58
C	Blood	10/1	21.1 ± 1.0	22.9	1.86	1.23E+04	0.15
	Urine	9/30 – 10/1 morning	40.0 ± 0.3	41.4	2.94	1.41E+04	0.16

Note: Decay extrapolated back to the time of the accident.
As noted in ICRP-30, ten days was adopted as the biological half-life of sodium (IC80), and back-extrapolation was performed between the accident and sample collection.
Urine samples were composite samples and mean sampling time was assumed to be 6 p.m. on September 30 for the September 30 sample and 11 p.m. on September 30 for September 30 - October 1 morning sample.
Specific activity was defined as the value obtained by dividing ^{24}Na concentration by stable Na concentration.

IV.A.b. Specific activities of ^{82}Br

The relatively longer half-life of ^{82}Br enables the limits of detection to be lowered by measuring over a long period. Specific activities of ^{82}Br in blood, urine, vomit, and hair were determined using measurements of ^{82}Br and analysis of stable bromine. Although targeted ^{81}Br accounts for 49.3% of stable isotopes of bromine, the specific activity was calculated as the ratio of ^{82}Br to the total amount of bromine (elemental concentration) in this Section A. The results are summarized in Table IV.A.2. Decay correction was carried out to obtain the activity at the time of the accident using the biological half-life of 10 days that is noted in ICRP Publ. 30 (IC80) as the value for bromine.

Using the same procedure as ^{24}Na, the neutron exposures of the three workers were compared with the specific activities of ^{82}Br. If the specific activity for Mr. A is assumed to be 1.0, that in blood for Mr. B is 0.51 (the value for Mr. C was under the limit of detection), and that in urine for Mr. B and Mr. C is 0.49 and 0.13, respectively. These ratios are similar to those obtained for ^{24}Na and may reflect the fluence of neutrons to which they were exposed. Also, there is no significant difference in the specific activities among the blood, urine, and vomit of the three workers. In other words, the blood values were almost the same as or slightly lower than those of urine and vomit for ^{82}Br, although the blood values were relatively lower than those for urine and others for ^{24}Na. This may be due to a limited dilution effect caused by low concentration of stable bromine in the intravenous administration, leading to a slight decrease in the specific activity of bromine. The specific activity of ^{82}Br in hair, detected only in Mr. B, was apparently lower than that in blood, suggesting, among other factors, a relationship with distance from the neutron source.

Table IV.A.2 Amounts of ^{82}Br and stable Br in the samples and specific activities

Worker	Samples and date of sampling		^{82}Br concentration (Bq ml^{-1} or Bq g^{-1})	^{82}Br concentration corrected biological half-life (Bq ml^{-1} or Bq g^{-1})	Stable Na concentration (mg ml^{-1} or mg g^{-1})	Specific activity (Bq^{82}Br)(g ^{82}Br)$^{-1}$	Intensity ratio in Mr. A (by sample)
A	Blood	10/1	0.23 ± 0.06	0.25	4.2	5.9E+4	1.00
	Urine	9/30 – 10/1 morning	0.12 ± 0.01	0.12	2.4	5.2E+4	1.00
	Vomit	9/30	0.19 ± 0.01	0.19	3.7	5.1E+4	1.00
	Hair	10/1			9.1		
B	Blood	10/1	0.14 ± 0.03	0.15	5.0	3.0E+4	0.51
	Urine	9/30 – 10/1 morning	0.15 ± 0.02	0.16	5.7	2.7E+4	0.53
	Urine	9/30	0.079 ± 0.01	0.08	3.4	2.4E+4	0.46
	Vomit	9/30	0.36 ± 0.03	0.36	14.7	2.4E+4	0.48
	Hair	10/1	0.15 ± 0.04	0.15	9.9	1.5E+4	
C	Blood	10/1			4.0		
	Urine	9/30 – 10/1 morning	0.029 ± 0.007	0.030	4.7	6.5E+3	0.13

Note: The decay curve was extrapolated back to the time of the accident.
As noted in ICRP-30, 10 days was adopted as the biological half-life of bromine (IC80), and the decay curve was extrapolated back to the time of the accident.
Urine samples were composite samples and mean sampling time was assumed to be 6 p.m. on September 30 for the September 30 sample and 11 p.m. on September 30 for the September 30 - October 1 morning sample.
Specific activity was defined as the value obtained by dividing ^{82}Br concentration by stable Br concentration.

Table IV.A.3 Amounts of ^{42}K and stable K in the samples and specific activities

Worker	Samples and date of sampling		^{82}Br concentration (Bq ml^{-1} or Bq g^{-1})	^{82}Br concentration corrected biological half-life (Bq ml^{-1} or Bq g^{-1})	Stable Na concentration (mg ml^{-1} or mg g^{-1})	Specific activity (Bq^{82}Br)(g ^{82}Br)$^{-1}$	Intensity ratio in Mr. A (by sample)
A	Blood	10/1	21.7 ± 3.7	22.2	1.44	1.6E+04	1.00
	Urine	9/30 – 10/1 morning	12.5 ± 1.0	12.6	0.90	1.4E+04	1.00
	Vomit	9/30			<0.08		
	Hair	10/1			0.47		
B	Blood	10/1	10.0 ± 2.6	10.3	1.39	7.4E+03	0.48
	Urine	9/30 – 10/1 morning	8.5 ± 0.65	8.6	1.12	7.7E+03	0.55
	Urine	9/30	7.6 ± 0.78	7.7	1.10	7.0E+03	0.50
	Vomit	9/30			0.22		
	Hair	10/1			0.11		
C	Blood	10/1			1.49		
	Urine	9/30 – 10/1 morning	2.3 ± 0.45	2.3	1.02	2.3E+03	0.16

Note: The decay curve was extrapolated back to the time of the accident.
As noted in ICRP-30, thirty days was adopted as the biological half-life of potassium (IC80), and back-extrapolation was performed between the accident and sample collection.
Urine samples were composite samples and mean sampling time was assumed to be 6 p.m. on September 30 for the September 30 sample and 11 p.m. on September 30 for the September 30 - October 1 morning sample.
Specific activity was defined as the value obtained by dividing ^{42}K concentration by stable K concentration.

IV.A.c. Specific activities of ^{42}K

^{42}K, due to its short half-life of about 12 hours, was detected in very few samples. Specific activities of ^{42}K were determined using measurements of ^{42}K and analysis of stable potassium. Although targeted ^{41}K accounts for 6.73 wt% of stable isotopes of potassium, the specific activity was calculated as the ratio of ^{42}K to the total amount of potassium (elemental concentration) in this Section A. The results are summarized in Table IV.A.3. Decay correction was carried out to obtain the activity at the time of the accident using the biological half-life of 30 days that is reported in ICRP Publ. 30 (IC80) as the value for potassium.

If the specific activity for Mr. A is assumed to be 1.0, that in blood for Mr. B is 0.48 (the value for Mr. C was under the limit of detection), and that in urine for Mr. B and Mr. C is 0.50 and 0.16, respectively. These ratios are similar to those obtained for ^{24}Na and ^{82}Br. When the specific activities were compared between blood and urine, similar to ^{82}Br, the value in blood was almost the same or slightly higher than that in urine sampled on the same day.

IV.A.d. Estimation of neutron fluence (rough calculation)

Next, rough estimate of neutron fluence was made using these specific activities. If the number of target atoms was denoted as N, the induced radioactivity can be expressed in the following equation:

$$A = N \Phi \sigma \lambda \quad \text{or} \quad \Phi = A / (N \sigma \lambda) \quad (1)$$

where

A : radioactivity of induced isotope (Bq)

Φ : neutron fluence (cm^{-2})

σ : cross section of nuclear reaction for thermal neutron (cm^2):
^{23}Na: 0.534, ^{41}K: 1.46, ^{81}Br: 2.69 barn (1 barn: 1 x 10^{-24} cm^2)

λ : decay constant of the induced isotope (s^{-1}).

When known values, including the decay constant and cross section of nuclear reaction (using the value in the thermal neutron region temporarily) of each isotope were substituted in this Equation (1), neutron fluence (Φ)

can be obtained from the following equations using a value for the specific activity (a):

^{24}Na $\Phi = 5.6 \times 10^6$ a   (2)

^{42}K $\Phi = 1.9 \times 10^7$ a   (3)

^{82}Br $\Phi = 4.4 \times 10^7$ a   (4)

In these equations, the value in the thermal neutron region is used as the value of the cross section of the nuclear reaction on the assumption that the target is located at one point. The fluence was estimated from the blood specific activity values of Mr. A using the equations above ((2), (3), and (4)) and shown below:

Calculation from the specific activity of ^{24}Na:

$$\Phi = 4.6 \times 10^{11} \ (cm^{-2})$$

This value is 20% lower than that calculated taking into account the neutron spectrum (Equation (3) in Chapter II, Section D.a.4). However, this equation may be useful for a rapid estimation in an early stage after the accident.

Also, for the comparison, estimates of neutron fluence using the blood bromine and potassium data from Mr. A are shown as follows:

Calculation from the specific activity of ^{42}K:

$$\Phi = 6.8 \times 10^{11} \ (cm^{-2})$$

Calculation from the specific activity of ^{82}Br:

$$\Phi = 1.1 \times 10^{12} \ (cm^{-2})$$

These values are clearly higher than those obtained from sodium. In particular, fluence calculated from ^{82}Br is twice as high as that from ^{24}Na. The effect of resonance absorption appears to be the reason. In other words, because of greater effect of resonance absorption in the epithermal region of neutrons on activation of potassium and (especially) bromine, there will be a large discrepancy between this outcome and calculation from only thermal neutrons. Compared with this, there is little effect of resonance absorption on the dose assessment using ^{24}Na.

Although the evaluation above was carried out assuming that the target element is located at one point, sodium is in fact distributed widely throughout the body. Also, the quantity of activated product depends on neutron energy. (As for ^{24}Na, there is a description of more precise dose assessment based on the effect of neutrons in the body and the neutron energy spectrum in Section D of Chapter II. However, in that case, the basic data is also the specific activity of ^{24}Na as described in this Section A.)

IV.B. Influence of intravenous administration

After the criticality accident, dose assessment of the three seriously exposed workers was conducted based on the radiation measurements of ^{24}Na in blood samples the day after the accident. To estimate specific activity in the blood at the moment of the accident, pursuant to the ICRP model, 10 days was used as the biological half-life of ^{24}Na. However, intravenous administration was conducted for these three workers as an initial treatment immediately after their arrival at NIRS. Since this intravenous administration solution included stable sodium (referred to as Na), it was pointed out that there is a possibility of accelerated excretion of ^{24}Na or dilution effect of blood specific activity. As part of the error evaluation, this problem was approached using the following three procedures: a. evaluation of systemic Na gain after intravenous administration; b. simulation using a compartment model; and c. comparison of the specific activity of activated products in different biological samples. These three procedures will be described in the above order.

IV.B.a. Total increase of Na in body

In ICRP Publ. 23 (IC75), systemic exchangeable Na is stated to be 40 – 42 meq (milliequivalent) per 1 kg body weight. Based on a body weight of 73.5 kg for Mr. A, 65 kg for Mr. B, and 68 kg for Mr. C, systemic exchangeable Na is calculated to be 3,100 meq or 71 g, 2,700 meq or 62 g, and 2,700 meq or 62 g, respectively, for the three workers. Also, Na in the intravenous administration fluid, which was used to treat the three exposed workers, was estimated to be 823 meq, 938 meq, and 776 meq, respectively. For the maximum estimation of systemic Na gain after the intravenous administration, it was assumed that no Na in the intravenous administration fluid was excreted directly from the blood into the urine before it had spread throughout the body. The specific activity of ^{24}Na in systemic exchangeable Na was thus diluted as follows.

Mr. A   3,100/(3,100+823) = 0.79
Mr. B   2,700/(2,700+938) = 0.74
Mr. C   2,700/(2,700+776) = 0.78

In Section D.a.4 of Chapter II, ^{24}Na activity on occurrence of the accident was estimated on the assumption that the biological half-life of ^{24}Na is 10 days. In other words, due to metabolic processes, the specific activity of ^{24}Na was considered to decay as follows.

Mr. A   exp (-0.69315/10x1.078) = 0.928
Mr. B   exp (-0.69315/10x1.127) = 0.925
Mr. C   exp (-0.69315/10x1.201) = 0.920

The ratios of these values and dilution effects are indicated as follows:

Mr. A   0.79/0.928 = 0.85
Mr. B   0.74/0.925 = 0.80
Mr. C   0.78/0.920 = 0.85

It is suggested that the specific activities of ^{24}Na might be underestimated by 15-20% in Section D.a.4 of Chapter II.

On the other hand, according to ICRP Publ. 30 pt 2 (IC80), the biological half-life of ^{24}Na in the human body, which is greatly affected by the intake of stable Na, ranges between 5 days for Na intake of 30 g d^{-1} and 335 days for Na intake of 0.25 g d^{-1}. Na in the intravenous administration fluid used for these three workers was estimated to range between 770 and 940 meq, or 18 and 22 g. As described in Section E.b.4 of Chapter II, if the biological half-life is shortened to 5 days, the estimated amount of ^{24}Na generated at the time of the accident increases by about 8%, then the dose estimated in Section D.a.4 of Chapter II might be underestimated by 8%.

IV.B.b. Compartment model

A medical staff involved in treatment of these workers has provided us with data regarding intravenous administration as well as regarding urinary excretion. Based on this information, change in Na and ^{24}Na in blood over time was simulated using a compartment model.

b.1. Model

The plasma, tissue, and bladder were treated as compartments for exchangeable Na in the body. The model used for simulation is shown in Fig. IV.B.1. A small amount of Na in non-plasma components, which exists in cells, is assumed to be non-exchangeable.
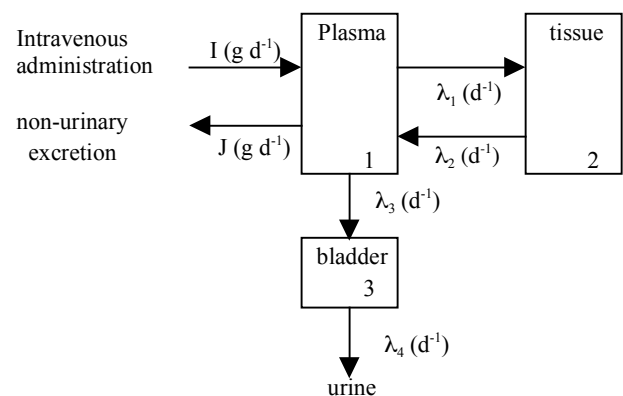

Fig. IV.B.1 Compartment model of exchangeable Na

b.2. Differential equation

Stable Na and ^{24}Na in each compartment in Fig. IV.B.1 are expressed as the following simultaneous differential equations.

Stable Na (A_i: Na content in compartment i)

plasma compartment :

$$dA_1/dt = I + \lambda_2 A_2 - \lambda_1 A_1 - \lambda_3 A_1 - J$$

tissue compartment :

$$dA_2/dt = \lambda_1 A_1 - \lambda_2 A_2$$

bladder compartment :

$$dA_3/dt = \lambda_3 A_1 - \lambda_4 A_3$$

Na in blood other than plasma:

$$dA_0/dt = 0$$

^{24}Na (B_i : activity of ^{24}Na in compartment i)

plasma compartment :

$$dB_1/dt = \lambda_2 B_2 - \lambda_1 B_1 - \lambda_3 B_1 - J \times (B_1/A_1) - \lambda_R B_1$$

tissue compartment :

$$dB_2/dt = \lambda_1 B_1 - \lambda_2 B_2 - \lambda_R B_2$$

bladder compartment :

$$dB_3/dt = \lambda_3 B_1 - \lambda_4 B_3 - \lambda_R B_3$$

^{24}Na in blood other than plasma:

$$dB_0/dt = - \lambda_R B_0$$

where, λ_R is decay constant.

b.3. Parameter values

The value for each parameter in the differential equations above was estimated or assumed as follows.

(1) Exchangeable Na in the body

In ICRP Publ. 23 (IC75), systemic exchangeable Na is noted to be 40 – 42 meq kg^{-1} and Na in plasma is noted to be 10 g. In other words, there is exchangeable Na between 54.4 g (= 0.040 eq kg^{-1} × 23 g eq^{-1} × 70 kg - 10 g) and 57.62 g (= 0.042 eq kg^{-1} × 23 g eq^{-1} × 70 kg - 10 g), or average 56 g, in tissue except for blood in ICRP reference man with 70 kg body weight. In this report, systemic exchangeable Na concentration, which was assumed to be 41 meq kg^{-1}, was multiplied by body weight of each worker to calculate systemic Na amount. Ratio of Na in plasma and tissue was assumed to be 10 (plasma): 56 (tissue) defined for the reference man.

Blood other than plasma include small amount of Na and the value is 0.57 g according to ICRP Publ.23. In this calculation, 0.057-fold (= 0.57/10) amount of Na and ^{24}Na in plasma was assumed to exist in blood components other than plasma in each worker.

(2) Na administration rate I (g d^{-1})

Each intravenous administration fluid had a different Na concentration. Therefore, the actual Na administration rate for each worker might have been different. Also, only total Na excretion was obtained during the intravenous administration period, but not the time course of urinary excretion of Na. Therefore, a simulation of complex changes in Na administration rate would not be meaningful. In this study, it was assumed that Na was infused at a fixed rate from immediately after the workers' arrival at NIRS until 2 p.m. on October 1, and that no intravenous administration was conducted before their arrival and after 2 p.m. on October 1. Na administration rate calculated from provided data is shown in Table IV.B.1.

Table IV.B.1 Na administration rate for each worker via intravenous administration fluid

Worker	Before arrival	Arrival: 2 p.m. (Oct. 1)	After 2 p.m (Oct. 1)
A	0	18.94 / 0.941 = 20.13 g d^{-1}	0
B	0	21.56 / 0.941 = 22.91 g d^{-1}	0
C	0	17.85 / 0.941 = 18.97 g d^{-1}	0

(3) Transfer rate from plasma to tissue λ_1 and from tissue to plasma λ_2

According to a report (SE90), 97% of exchangeable Na is present in the extracellular fluid as Na$^+$ ions. Therefore, Na in intravenous administration fluid injected into the blood will spread rapidly through the whole body via the circulatory system. The rate of transfer from plasma to tissue λ_1 is assumed to be 99.8 d^{-1} (half-life 10 min.), 33.3 d^{-1} (half-life 30 min.), and 11.1 d^{-1} (half-life 90 min.) as working hypothesis to carry on the calculation.

As described in (1) in this Section B, 10 and 56 g of Na exist in the plasma and tissue, respectively. λ_2 must be (plasma Na/tissue Na)-fold of λ_1, so that the consistency of ratio of Na in plasma and tissue is maintained. In the present calculation, λ_2 was then assumed to be 0.179-fold (= 10 / 56) of λ_1.

(4) Na excretion

For each worker, there is data on Na concentration in urine and urinary volume excreted immediate after arrival. Total Na in urine was calculated using these data. Non-urinary Na excretion is noted to be 1.1 g d^{-1} in ICRP Publ. 23. There is no evidence of increased sweating due to the intravenous administration; therefore, non-urinary Na excretion rate J (g d^{-1}) in Fig. IV.B.1, was assumed to be a constant value 1.1 g d^{-1}.

On the other hand, urinary Na excretion between immediately after the accident and arrival at NIRS is unknown. Urinary Na excretion per 24 hours is noted to be 3.3 g in the ICRP reference man in ICRP Publ. 23. Urinary Na excretion up to arrival at NIRS was estimated to be 0.66 g (3.3 g d^{-1} × 0.201 d), on the assumption that this amount of Na had been excreted at a fixed rate. The

calculated total urinary Na excretion from the time of the accident to 2 p.m. on October 1 is shown in Table IV.B.2.

Table IV.B.2 Na excretion until 2 p.m. on October 1

Worker	Before arrival		After arrival			
	Urinary Na excretion	Non-urinary Na excretion	Urinary excretion	Urinary Na concentration	Urinary Na excretion	Non-urinary Na excretion
A	0.66 g	0.22 g	4.00 ℓ	63 meq ℓ$^{-1}$	5.80 g	1.04 g
B	0.66 g	0.22 g	4.32 ℓ	171 meq ℓ$^{-1}$	16.99 g	1.04 g
C	0.66 g	0.22 g	3.73 ℓ	141 meq ℓ$^{-1}$	12.10 g	1.04 g

5) Transfer rate from plasma to bladder λ_3

By solving numerically the differential equations in Section b.2, the transfer rate from plasma to bladder λ_3 that leads the values of the Na excretion in Table IV.B.2 was obtained. The results are shown in Table IV.B.3

Table IV.B.3 Transfer rate from plasma to bladder λ_3

Worker	$\lambda_1 = 99.8$ d^{-1}	$\lambda_1 = 33.3$ d^{-1}	$\lambda_1 = 11.1$ d^{-1}
A	0.5315 d^{-1}	0.5239 d^{-1}	0.5042 d^{-1}
B	1.9556 d^{-1}	1.9468 d^{-1}	1.9427 d^{-1}
C	1.3157 d^{-1}	1.3079 d^{-1}	1.2877 d^{-1}

### (6) Urinary excretion rate λ_4

The ICRP biokinetic model shows urinary excretion rate from the bladder to be 12 d^{-1}. This rate can be applied to cases where urinary excretion is 1.4 l d^{-1}. As shown in Table IV.B.2, much more than 1.4 l of urine was actually discharged by all three workers. The urinary excretion rate was assumed to be proportional to the total volume of urinary excretion per day.

b.4. Results

(1) Time course of stable Na in blood

The effect of intravenous administration on stable Na in blood was calculated. Fig. IV.B.2 shows an example of 33.3 d^{-1} of the transfer rate from plasma to tissue λ_1; in other words, the result of 30 min. of half-life.

In Fig. IV.B.2, points showing discontinuity indicate initiation (left) and termination (right) time of the intravenous administration. Arrows indicate the time of blood collection. The intravenous administration increased the levels of blood stable Na in all three workers but with individual differences. The high rate of increase in Mr. A resulted from the rate of transfer into bladder λ_3, determined based on data indicating only a small amount of urinary Na excretion. On the other hand, a low increasing rate in Mr. B resulted from λ_3, determined based on data indicating a large amount of urinary Na excretion. These results suggest that the specific activity of ^{24}Na may have been diluted by the intravenous administration.
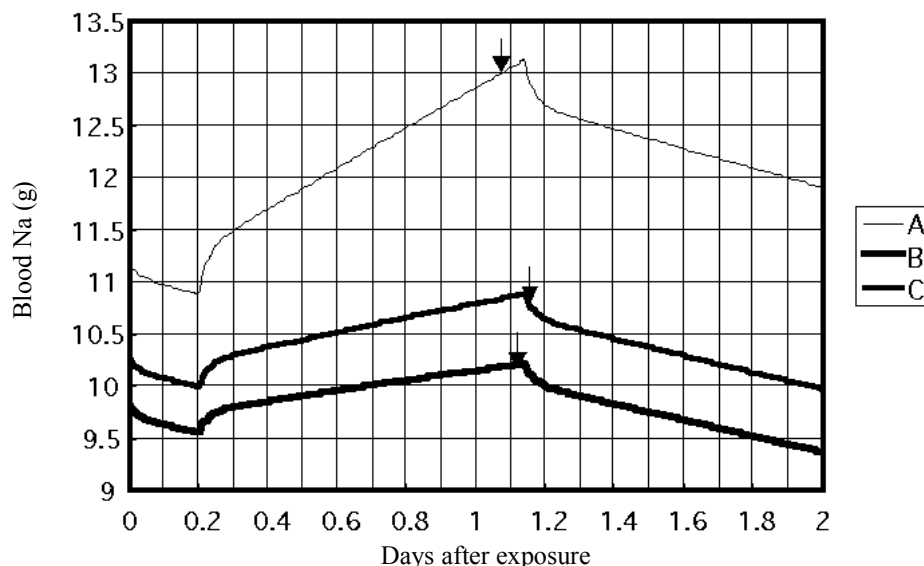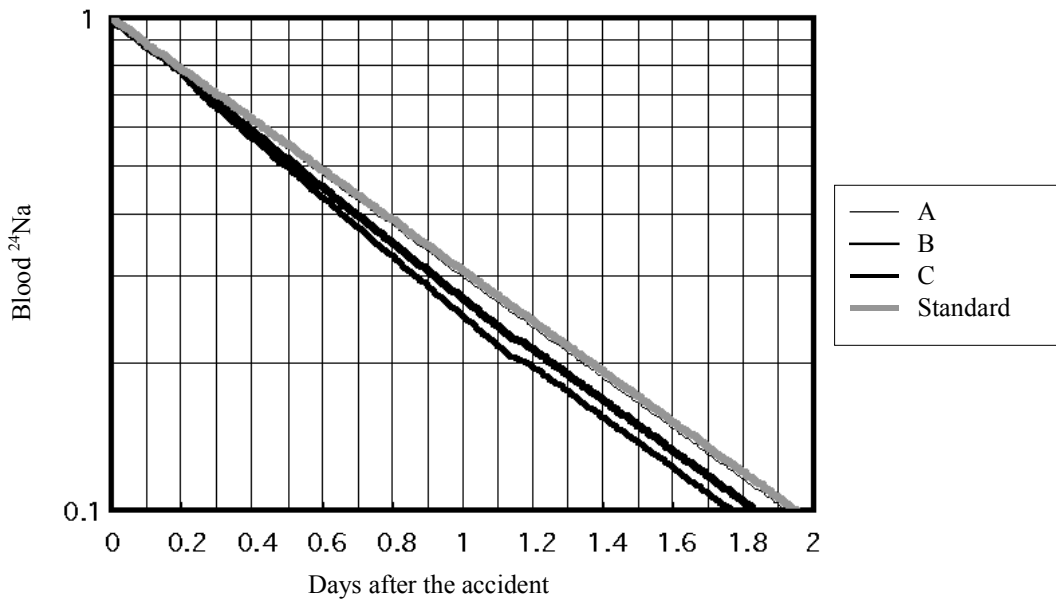

Fig. IV.B.2 Effect of intravenous administration on time course of stable Na in the blood

(2) Time course of ^{24}Na activity in blood

Next, time courses of ^{24}Na activity in blood are simulated in Fig. IV.B.3. As in Fig. IV.B.2, Fig. IV.B.3. shows results obtained when the rate of transfer from plasma to tissue λ_1 is assumed to be 33.3 d^{-1}. "Standard" in this Figure indicates the result assuming a biological half-life of 10 days according to the ICRP model.
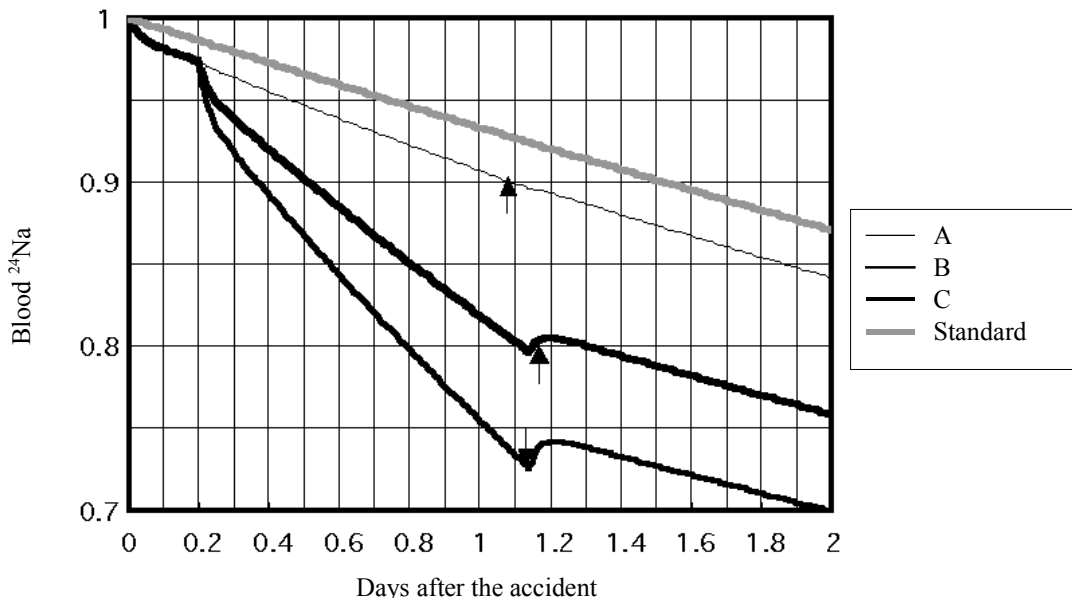
Fig. IV.B.3 Effect of intravenous administration on time course of blood ^{24}Na

To show explicitly the time course of ^{24}Na in the blood, a simulation was performed on the assumption that ^{24}Na shows no radioactive decay. The result is shown in Fig. IV.B.4.

As in Fig. IV.B.2, arrows indicate the time of blood collection. Especially for Mr. B and Mr. C ^{24}Na increases a little after the time of 1.14 days because of the calculation assuming that the transfer rate into the bladder λ_3 returns to the value before the intravenous administration, resulting in the ^{24}Na being transferred from tissue to blood temporarily exceeding that from the blood to the bladder. This figure shows the possibility of accelerated ^{24}Na excretion due to the intravenous administration.

Fig. IV.B.4 Effect of intravenous administration on ^{24}Na in blood (assuming there is no radioactive decay of ^{24}Na)

Table IV.B.4 Ratios of specific activities of ^{24}Na in blood on its collection versus estimate based on the ICRP model

Worker	$\lambda_1 = 99.8$ d^{-1}	$\lambda_1 = 33.3$ d^{-1}	$\lambda_1 = 11.1$ d^{-1}
A	0.851	0.834	0.786
B	0.775	0.758	0.708
C	0.839	0.829	0.786

(3) Time course of specific activities of ^{24}Na in blood

The time course of specific activity of ^{24}Na in blood is shown in Fig. IV.B.5. These results are obtained when

the transfer rate from plasma to tissue λ_1 is assumed to be 33.3 d^{-1}, and also on the assumption that there is no radioactive decay in ^{24}Na. The specific activities at the time of blood collection show lower than the predicted values assuming a biological half-life of 10 days in all three workers.

The ratio of specific activity for each worker versus the "standard" was obtained and summarized in Table

IV.B.4 and Fig. IV.B.6. This calculation suggests that the specific activities at the time of blood collection are smaller by about 20% than the "standard", i.e., the specific activity at the time of exposure estimated based on the ICRP model might be underestimated by about 20%.
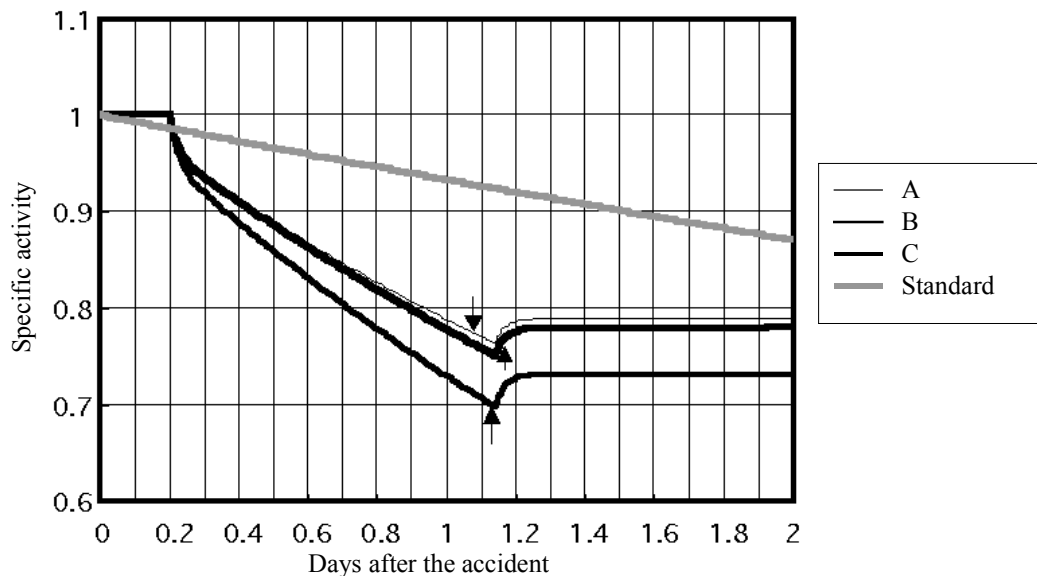

Fig. IV.B.5 Time course of specific activities of ^{24}Na in blood (assuming no radioactive decay of ^{24}Na)
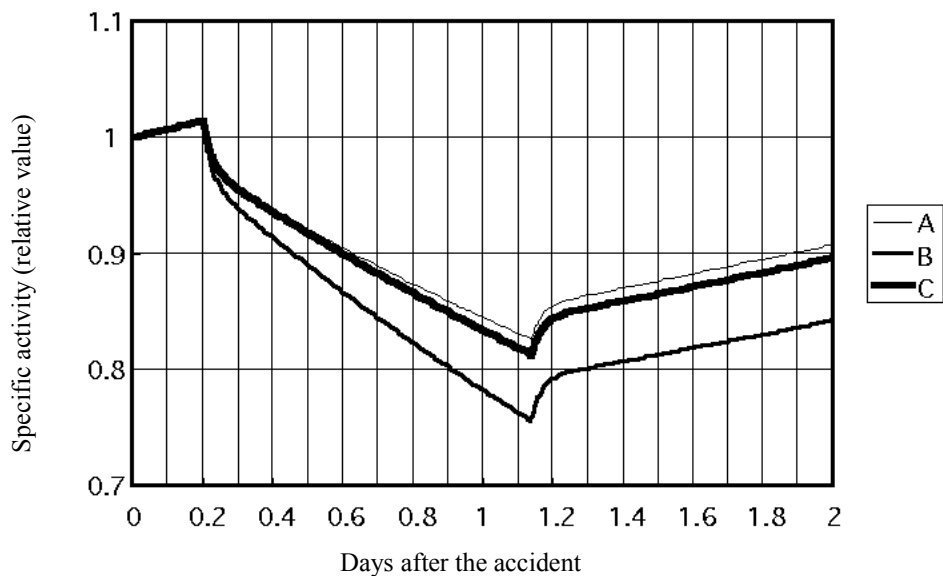

Fig. IV.B.6 Time course of specific activities of ^{24}Na in blood (relative value to estimate based on the ICRP model)

b.5. Summary

In this report, we discussed the acceleration of ^{24}Na excretion or dilution effects of specific activity associated with intravenous administration using a numerical simulation procedure and a compartment model. The

medical staff involved in treatment provided the data regarding intravenous administration and urinary excretion used for calculation. These results showed the possibility that specific activity at the time of exposure estimated based on the ICRP model might be underestimated by about 20%.

IV.B.c. Comparison of specific activities in several biological samples

Blood collection was performed for the purpose of clinical examination at about 3:40 p.m. on September 30, immediately after the exposed workers arrived at NIRS. Concentration of radionuclides was also measured in these blood samples. From the fact that 5 hours had passed since the accident, it is inferred that specific activity of exchangeable Na in the body might become uniform. Since blood left in a cylinder was used for measurement, its uniformity is presumably high. For these samples, the problem was that stable Na could not be measured, since a solubilizer that included Na had been added to the samples. In addition, error resulting from efficiency correction of measurements might be large, since the volume of samples collected on September 30 (e.g. 6.4 ml for Mr. A) was smaller than those collected on October 1.

The following are ratios of estimated blood ^{24}Na concentration at the time of exposure based on measurement of these samples versus that based on measurement of samples collected and measured by the same group on October 1.

Mr. A: 167 Bq ml^{-1} (Sep. 30) / 176 Bq ml^{-1} (Oct. 1)
= 0.949

Mr. B: 110 Bq ml^{-1} (Sep. 30) / 92.0 Bq ml^{-1} (Oct. 1)
= 1.20

Mr. C: 25.7 Bq ml^{-1} (Sep. 30) / 23.0 Bq ml^{-1} (Oct. 1)
= 1.12

These results suggest that blood ^{24}Na concentration at the time of exposure estimated in Section D.a.4 of Chapter II might have been underestimated by 10-20%.

There may be a similar dilution effect in urine, but the effect would be observed after a time interval. Since the urine samples were collected consecutively from September 30, the day of the accident, to 6 a.m. on October 1, there may be less effect of Na in the intravenous administration solution on the urine sample than the blood sample (collected on the afternoon of October 1). In short, the dilution effect in urine was presumed to be smaller than that in blood. For example, two composite urine samples were collected from Mr. B:

that taken until the evening of the day of the accident (September 30) showed about 5% higher specific activity than another collected after the evening (the "September 30 evening to October 1 morning" sample). The percentage of change with the elapse of time cannot be calculated because both samples were consecutively collected and mixed in the same container; however, it could be noted that the specific activity of ^{24}Na was declining.

A comparison of the specific activity in blood (collected in the afternoon of October 1) with urine (collected from September 30 to the morning of October 1), showed the value in urine to be higher by 9% for Mr. A, 20% for Mr. B, and 13% for Mr. C than that in blood, respectively. The dilution effect of stable Na in intravenous administration solution on ^{24}Na (decreased specific activity) may have appeared earlier in the blood, into which the intravenous administration fluid was injected directly, than in the urine.

A comparison of the specific activities of ^{24}Na in vomit samples (collected during transport to NIRS or immediately after arrival) with blood samples (collected on October 1) showed the value of vomit samples to be higher by 11% for Mr. A and 25% for Mr. B than their respective blood samples (Table IV.A.1). No solid matter was observed in the vomit of Mr. A and B, who had vomited several times since their exposure; it appeared to be a gastric juice-like liquid, with apparently uniform content. Vomit, which was not affected by the intravenous administration due to its being collected earlier than the other measured samples, appeared to show plausible specific activity due to exposure.

In the case of specific activities of ^{82}Br and ^{42}K it was observed that there were no marked difference among blood, urine, and vomit, since the intravenous administration would have contributed negligibly to decreased specific activities due to the low concentration of stable Br and K in the intravenous administration fluid.

In conclusion, we cannot exclude the likelihood of decrease in specific activity of ^{24}Na in blood collected on October 1 due to the dilution effect by stable Na in intravenous administration fluid. The decrease was estimated to be about 10-25%.

IV.C. Non-uniform dose distribution

The non-uniform dose distribution that occurred in this accident resulted from the close proximity of the source (the precipitation tank) and exposure to neutrons, which are sharply attenuated in the body. As described in Section E of Chapter II, non-uniform exposure to the surface of the skin and dose distribution deeper into the body was estimated by computational simulation using a mathematical model imitating the precipitation tank and its environment. Concerning non-uniform distribution, we can summarize as follows.

As explained in Section E of Chapter II, dose will differ markedly depending on the distance from the precipitation tank. This was especially the case for Mr. A, who was closest to the tank, the right side of his body was closer to the tank, leading to a difference in distance from the tank to parts of the body surface and different skin exposure. Also, there is a difference in bone concentrations of ^{32}P and ^{45}Ca. As discussed in Section E of Chapter II, the head, hands, and knees of Mr. B were highly exposed due to his posture at the time of the accident. On the other hand, Mr. C, who was outside the room containing the tank, would have received relatively uniform radiation.

In the depths of the body, neutron doses decrease exponentially with an apparent linear absorption coefficient of 0.17 cm^{-1}, i.e. showing a 50% decrease at depth of 4 cm. Therefore, neutron dose at the dorsal part would decrease to about 4% of the dose at the abdominal part. Gamma dose does not decrease as sharply as neutrons in the depths of the body; the dorsal dose would be about 30% of the abdominal dose. Therefore, the contribution of neutrons to the total absorbed dose decreases deeper inside the body, with the rate decreasing from 45% on the surface of the skin to 30% at a depth of 6 cm, to 25% at 10 cm, and to 10% on the surface of the back, leading to dominance of gamma dose with increasing depth.

Marked non-uniformity on the skin of the trunk was observed, especially in Mr. A. In the trunk, the highest dose was observed on the right side of the abdomen. The values, 27 Gy as neutrons and 35 Gy as gamma rays, were about 5 times and about 3 times higher than the average whole-body dose, respectively. In Mr. B, the dose on the skin of the chest and abdomen was relatively uniform. The highest dose, which was observed around the boundary between chest and abdomen, indicates 8.2 Gy for both neutrons and gamma rays, evaluated to be 1/3-1/4 of the maximum skin dose of Mr. A.

IV.D. Dose ratio between neutrons and gamma rays

As described in Section D.a. of Chapter II, the gamma dose was estimated based on (i) monitoring data of air dose and (ii) a graph given in IAEA Technical Report Series No. 211 (IA82) for use in emergencies. The results showed that the absorbed gamma ray dose was 1.6- (monitoring data) or 2.4-fold (IA82) higher than that of neutrons. However, the neutron dose in these calculations includes secondary gamma rays generated in the body.

On the other hand, as described in Section E of Chapter II, the gamma dose was estimated by computational simulation using a mathematical model reproducing the precipitation tank and its circumference. In this simulation, the dose caused by incident neutrons was evaluated separately for the charged particle component and the secondary gamma ray component generated in the human body. The percentage of each component was 82% for the charged particle and 18% for the secondary gamma ray. When the dose of secondary gamma rays was included in the neutron dose, the absorbed dose of gamma rays reaches 1.83-fold (Mr. A)

or 1.43-fold (Mr. B) of that of neutrons. On the other hand, when secondary gamma rays are included in the gamma dose, the absorbed dose of gamma rays reaches 2.43-fold (Mr. A) or 1.97-fold (Mr. B) of that of neutrons.

In the procedure described in Section D.a of Chapter II, the limited information available immediately after the accident had to be used for dose evaluation, on the basis of the need for rapid action in an emergency. Therefore, it should be noted that its accuracy is limited. In this report, the result of a computational simulation, using a mathematical model imitating the precipitation tank and its circumference, was chosen to be adopted as the dose ratio of neutrons and gamma rays for Mr. A and B. For Mr. C, for whom a computational simulation was not performed, the result of the simulation for Mr. A was chosen to be applied, due to the importance of not underestimating the risk. As a result, we adopted a method in which the gamma doses to Mr. A, Mr. B, and Mr. C were estimated by multiplying the neutron doses calculated from the specific activity of ^{24}Na in the blood by 1.83, 1.43, and 1.83, respectively.

IV.E. Relative biological effectiveness of fast neutrons in murine tissues

Abstract

The Relative biological effectiveness (RBE) of 13 MeV fast neutrons was investigated for acute toxicity to murine bone marrow and gut. Mice that received whole body irradiation with either fast neutrons or control gamma rays were checked daily for their survival. Mortality by Day 7 was used as an endpoint for gut toxicity, while that by Day 30 was for bone marrow toxicity. The LD_{50} was calculated from the dose-response curve, and used to obtain the RBE of fast neutrons relatives to gamma rays. The RBE of neutrons depended on organs concerned, and was 1.2 and 1.7 for bone marrow and gut, respectively. As gut toxicity emerges earlier than bone marrow toxicity, an RBE of 1.7 was use to calculate the minimal value of biological doses (Gy Equivalent, GyEq) for the workers of the Tokai-mura criticality accident.

Materials and methods

Mice

C3H/HeMsNrsf female mice aged 12-18 weeks old were used for this study. The animals were produced and maintained in specific pathogen-free (SPF) facilities at NIRS. Mice irradiated with gamma rays were kept in the specific pathogen-free facilities; while, mice receiving fast neutrons were transported to the accelerator facility shortly before the irradiation. Experiments were repeated at least twice and all data were combined. A total of 407 mice were used in these experiments with at least 5 mice for each irradiation dose.

Irradiation

Fast neutrons were generated by bombarding a beryllium target with 30 MeV deuterons from a cyclotron at NIRS. Doses were measured with an ER & G tissue-equivalent ionization chamber. The gamma-ray contribution was less than 5% and the mean energy of neutrons was 13 MeV (HI77). The dose rate was 65 ± 5 cGy min^{-1} at a target-tissue distance of 170 cm. Cs-137 gamma rays with a dose rate of 50 cGy min^{-1} at a target-tissue distance of 35 cm were used as the reference radiation. The beam buildup was obtained by placing mice in a Lucite jig with 5-mm wall thickness. Mice were irradiated over the whole body without anesthesia.

LD_{50} and RBE

Irradiated mice were kept alive in animal facilities after irradiation. Mortality was determined by checking mice every day for 7 days and every other day till day 30. The Dose-mortality relation was fitted to the Probit analysis. LD_{50}, a dose required to kill 50% of irradiated mice, was calculated along with a 95% confidence limit. The RBE was calculated by comparing LD_{50} values between gamma rays and neutrons, i.e., LD_{50} (g) / LD_{50} (n).

## Results

Dose-mortality relation

The dose-mortality relation for bone marrow and gut are shown in Fig. IV.E.1. Thirty days after gamma ray irradiation no mice died below 7 Gy while all mice at 8.5 Gy or over were dead. When the dose increased, 100% of the mice died within 7 days after receiving 16 Gy. The dose response for gut toxicity prominently shifted toward the right of that for bone marrow toxicity. The whole-body neutron irradiation was not lethal below 6.2 Gy
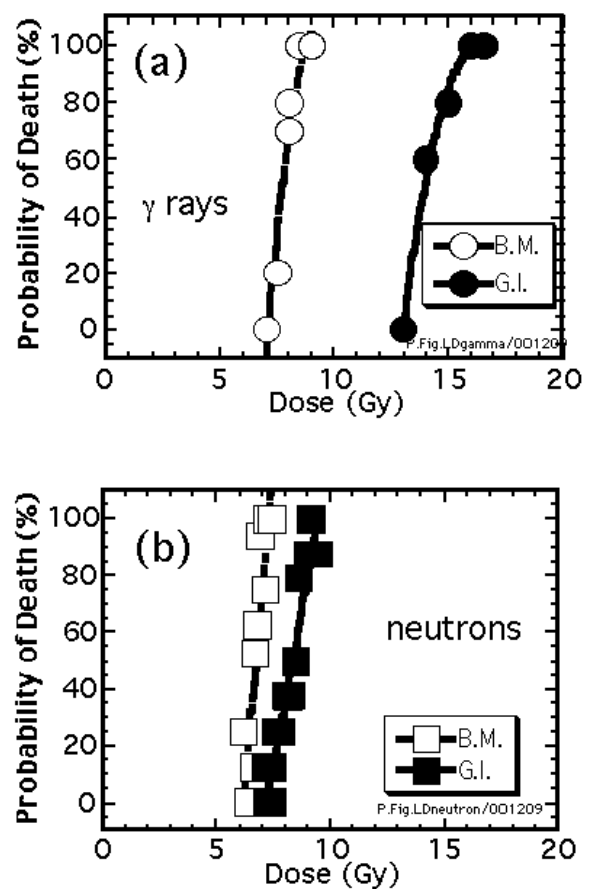
Fig. IV.E.1 Dose mortality relation after irradiation with _amma rays and neutrons

Mice received whole body irradiation with either (a) _amma rays or (b) fast neutrons.
Symbols: bone marrow; ($\bigcirc$, $\square$) and gut; ($\bullet$, $\blacksquare$).

Day 30, but caused 100% mortality at 7.2 Gy. The gut toxicity of neutrons required more doses than the bone marrow toxicity, even though the requirement was smaller than that for gamma rays. Fig. IV.E.2 compares gamma rays to neutrons for individual organs. Neutrons remarkably shifted the dose response toward the left for gut toxicity, while the shift was marginal for bone marrow toxicity.
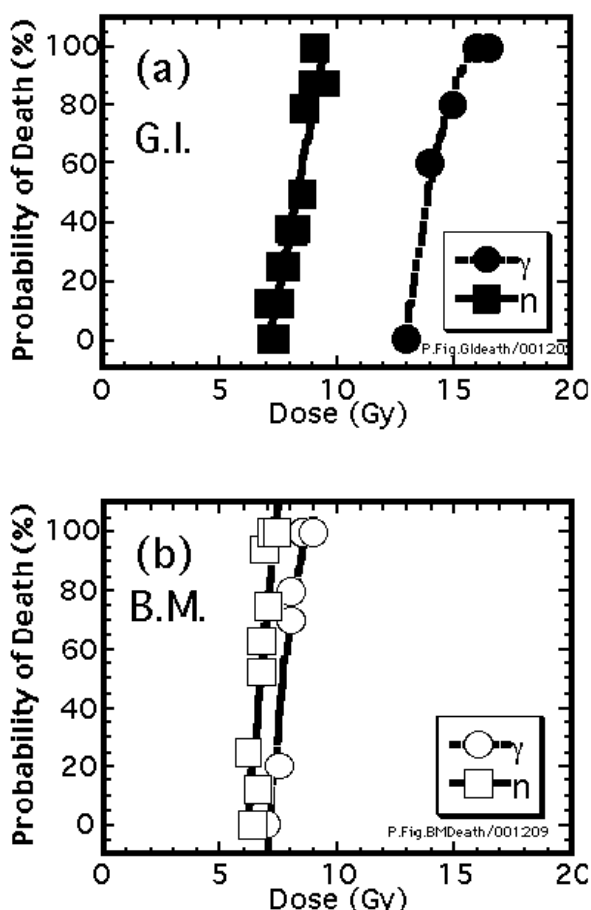
Fig. IV.E.2 Comparison of mortality between _amma rays and neutrons

Dose mortality relation for (a) gut toxicity and (b) bone marrow toxicity are compared between _amma rays (●, ○) and fast neutrons (■, □).

LD$_{50}$ and RBE

The LD$_{50/30}$ for neutrons was 6.7 Gy, and similar to that for _amma rays (Table IV.E.1). The RBE of neutrons for bone marrow toxicity was 1.16. The LD$_{50/7}$ for neutrons was 8.3 Gy, and much smaller than that for gamma rays. The RBE of neutrons for bone gut toxicity was 1.70.

Table IV.E.1 LD$_{50}$ and RBE

	Bone marrow toxicity		Gut toxicity	
	LD$_{50/30}$ (Gy)	RBE	LD$_{50/7}$ (Gy)	RBE
Gamma rays	7.8[a] (7.7-7.8)[b]		14.1[a] (13.8-14.4)[b]	
Neutrons	6.7[a] (6.6-6.8)[b]	16[a] (1.14-1.18)[b]	8.3[a] (8.2-8.4)[b]	70[a] (1.66-1.74)[b]

a: mean
b: 95% confidence limit

Discussion

We reported here the RBE values of 13 MeV neutrons accelerated by a cyclotron at NIRS. Employed reference beams were Cs-137 gamma rays. The RBE of neutrons generally depends on several factors, including neutron energy, dose and biological system. In radiotherapy, a RBE value of 3.0 is used for fast neutrons (GR78, TH89). The present results show that the RBE values of 13 MeV neutrons were 1.2 and 1.7 for bone marrow and gut toxicity, respectively. These values coincided with other reports using 22 MeV neutrons (GE75) and 25 MeV neutrons, but were smaller than those using fission neutrons (HA84). Dependence of RBE on neutron energy is clearly observed for oncogenic transformation, using monoenergetic neutrons from 0.23 MeV to 13.7 MeV (MI89).

The RBE of neutrons depends on dose, and increases with a decrease of dose. The RBE of 15 MeV neutrons for mouse bone marrow increases from 1.0 to 1.2 when the dose decreases form 5 to 1 Gy, while that for mouse intestinal crypt cells decreases from 2.2 to 1.6 when the dose increases from 8 to 2 Gy (BR81). When the dose decreases to near zero, maximal RBE for in vitro carcinogenic transformation is as large as 35 for 0.35 MeV neutrons (MI89). The dose dependence of RBE is due to the difference between photons and neutrons in the shape of cell survival curves at low doses, and can be related to the repair capacity of cells and tissues. Recent studies using HIMAC heavy particle beams suggest that the DNA repair genes for both homologous recombination and non-homologous end joining significantly contribute to determine the RBE of high LET radiation (AN01).

In conclusions, we propose a RBE value of 1.7 to calculate the biological doses (Gy Equivalent, GyEq) for the worker of the Tokai-mura criticality accident, as the gut toxicity emerges earlier than the bone marrow toxicity. This RBE value would, however, provide a minimal level of dose estimation for the workers, who were exposed to fission neutrons possessing lower energy than cyclotron fast neutrons.

Acknowledgements

IV.F. Characterization of RBE

It is very difficult to determine the relative biological effectiveness (RBE) of neutrons. In addition, the determination of RBE values for deterministic effects is more difficult than those for stochastic effects since several factors are taken into account for the selection of the right RBE value. ICRP Publ. 58 suggests that RBE defined to evaluate deterministic effects varies 5, 3, and 3 times depending on dose or dose rate, neutron energy, and targeted tissue, respectively (IC89b). RBE also depends on the biological effects of interest. These problems related to neutron irradiation are reviewed and the procedures adopted in the present dose assessment are discussed in this Section F.

IV.F.a. Radiation weighting factor

The radiation weighting factor defined by ICRP is one representation of RBE, which was defined taking into account radiation types and their energy for the purpose of radiation protection. Furthermore, it was originally defined for low dose or low dose rate exposures usually encountered by normal radiation workers, and only stochastic effects were considered as an index of effects on the human body. Therefore, it is inappropriate to use the radiation weighting factor defined by ICRP for the present dose estimation for the three workers exposed to high doses, since it falls within the dose range in which deterministic effects are concerned. In Paragraph 57 of ICRP Publ. 60, it is recorded that "the equivalent dose is not always the appropriate quantity for use in relation to deterministic effects, because the values of radiation weighting factors have been chosen to reflect the relative biological effectiveness (RBE) of the different types and energies of radiation in producing stochastic effects. For radiation with a radiation weighting factor greater than 1, the values of RBE for deterministic effects are smaller than those for stochastic effects. The use of the equivalent dose to predict deterministic effects for high LET radiation, e.g. neutrons, will thus lead to overestimates." (IC91). RBE applied to deterministic effect is described in ICRP Publ. 58 (IC89b). In the present report, the unit of Sievert (Sv) was decided not to use especially because use of Sv would lead to confusion as to which type of RBE was used. There should be a rule that the Sv unit should be used only for radiation protection purposes and should not be used if deterministic effects are expected.

IV.F.b. Difference depending on dose

It cannot be easily determined what kind of value should be used as RBE for deterministic effects of neutrons, which varies under the influence of various factors. One major factor is dose. A summary of previous studies on relationship between neutron dose and RBE where various radiation effects including cataract, chromosomal aberration, and skin injury were used as indexes for the effect of radiation confirms that RBE values are proportional to the reciprocal of the square root of dose and decrease with increase in dose (EN98). It also shows that RBE is about 2 around 1 Gy, and about 1.5 at 10 Gy. This indicates that greater biological effects of low LET control radiation found at high doses or high dose rates will decrease the relative biological effectiveness of high LET radiation. According to the experiences of radiotherapy, it is reported that the RBE for deterministic effects due to a single irradiation ranges between 1 and 5 (IC89b).

At ICRP, RBEm has been used as an RBE for deterministic effects. This value, determined by extrapolation to low dose or low dose rate irradiation conditions, is greater than those determined for high doses or high dose rates. The RBEm value for neutrons with energy between 1 and 3 MeV has been estimated to fall within 4 and 10 (IC89b). Therefore, if the RBEm were applied, their doses would be overestimated since the three workers were exposed to high radiation.

IV.F.c. Difference depending on energy

As required for radiation weighting factors of neutrons in ICRP Publ. 60, it was confirmed that neutron RBE for deterministic effects also depends on its energy spectrum. RBE is related to LET and, as seen in y distribution defined for neutron energy, LET reaches a maximum at slightly under 1 MeV of neutron energy. In other words, neutron RBE also reaches a maximum at around 1 MeV. The neutron energy spectrum of the present accident shows relatively high flux in the energy region where RBE has a large value since the present neutron was generated by fission and thermalized to some extent by water in the precipitation tank.

IV.F.d. Difference depending on dose rates

RBE is also affected by dose rate. It was found that there were differences of a few times among the effects of low LET radiation depending on dose rate; this difference of low LET radiation would affect the RBE of high LET radiation. In other words, the RBE of neutrons depends on the character of control radiation, high or low dose rate of X-rays or gamma rays. To confirm this effect, it is necessary to know the character of the low LET radiations that were used in the previous experiences. Exposure conditions in previous cases, in which deterministic effects were concerned as in this report, were mainly based on high dose rate conditions, such as radiotherapy. Therefore, the difference depending on dose rate may not have to be considered, since previous experiences

represent exposures to high dose rates.

In previous animal experiments, in the case of single exposure to neutrons with a mean energy of 1 – 5 MeV, RBE was determined to be 2.8 – 3.7 for the skin, 2.0 – 3.0 for the gastrointestinal tract, and 2.6 for the hematopoietic tissue. These results lead the conclusion that the RBE of 1 – 5 MeV neutrons are estimated to range between 2 and 4 in the case of single exposure to high dose rate (IC89b).

IV.F.e. Differences depending on the organs and tissues of the body

As shown by the above-mentioned results of the computational simulation and the reconstruction experiment employing TRACY, neutrons are rapidly attenuated in the body. Therefore, the dose received by each organ is markedly different to that received by the skin depending on the depth of the organ inside the body. If the incident direction of neutrons is not frontal but inclines to the right, as in the case of Mr. A, the depth of the organ in the body is different and the dose to the organ would be significantly different from that received by normal incident radiation.

Also, the RBE in an organ in the body depends on the neutron energy reached the organ since relative biological effectiveness depends on neutron energy. As described in Paragraph 233 of ICRP Publ. 74, it was revealed that the RBE of initial neutron energy between 10 keV and about 1 MeV becomes higher as it goes into the deeper sites in the body. RBE was estimated to be 8.8 for the testis and 2.8 for the lung in the case of exposure to 100 keV neutron from the front, and to be 4.8 for the lung and 1.3 for the testis in the case of exposure from the back (ED99). These differences reflect the decrease in neutron energy with increasing depth into the body as well as the mode of energy transfer from neutrons, i.e. the change in the dose contribution rate of charged particles and gamma rays.

In ICRP and other literature (KE72), it is reported that the RBE of neutrons differs depending on the organ. For example, maximal RBE of fission neutrons in low dose range was reported to be very high at 50 for chromosomal aberration of lymphocyte. On the other hand, RBE of 14 MeV and 6 MeV neutrons was reported to be below 2 for inactivation of the intestinal wall and about 2 for skin injury, respectively.

IV.F.f. Calculation of biological gamma ray dose equivalent (GyEq)

In the dose estimations based on the present lymphocyte counting and chromosome analysis, biological gamma ray dose equivalent (GyEq) is derived using the degree of decrease in lymphocyte count or frequency of chromosomal aberration as an index. To compare with these values and contribute to the estimation of RBE, the biological gamma ray dose equivalent was estimated based on the results from specific activity on ^{24}Na in blood (see Table II.G.1 line ④) for various RBE values and are shown in Table IV.F.1.

Table IV.F.1 Calculation of biological gamma ray dose equivalent (GyEq)

Worker	RBE									
	1.0	1.2	1.4	1.6	1.8	2.0	2.5	3.0	3.5	4.0
A	15.3	16.4	17.5	18.5	19.6	20.7	23.4	26.1	28.8	31.5
B	7.0	7.6	8.2	8.7	9.3	9.9	11.4	12.8	14.3	15.7

ICRP Publ. 58 (IC89b) summarized RBE values for deterministic effects based on the results of animal experiments. The results show that an RBE of 1 – 5 MeV neutrons is equivalent to 2.8 – 3.7 for the skin, 2.0 – 3.0 for the gastrointestinal tract, and 2.6 for hematopoietic tissue, respectively.

IV.F.g. RBE applied in the present report

The various facts mentioned above demonstrate that the RBE for neutrons in the present accident could not simply be obtained as a single number. For accurate dose assessment using appropriate RBEs, the dose and energy spectrum for each organ needs to be obtained through a precise study of the spectrum of incident neutrons and computational simulations of reactions in the body. Therefore, the respective doses of neutrons and gamma rays were finally chosen to be expressed using units of Gy in the dose assessment based on blood ^{24}Na concentration. However, it is necessary to obtain a combined dose of neutrons and gamma rays for the evaluation of total biological effects due to the exposure. A value of RBE for neutrons had to be assumed for this purpose. In the full knowledge of the degree of ambiguousness involved, an RBE of 1.7 for neutrons was provisionally applied to enable comparison of the dose assessment of ^{24}Na in blood with the dose assessment of prodromes, lymphocyte count, and chromosomal aberrations that were based on systemic effects due to total dose derived from neutrons and gamma rays. This RBE value was obtained from the results of the study, conducted at NIRS on LD$_{50/7}$ of intestinal death in mice using 13 MeV neutrons (KO01). Since the introduction of unit of Sv could create confusion, GyEq, already in use in the medical field, was selected for expressing integrated dose of neutron components and gamma ray components in the three workers. This value represents here a form of systemic mean dose. In this report, the range of the dose does not reflect non-uniform distribution in the body, but indicates the extent of the estimate resulting from various methods

of dose assessment. The estimated dose provided important information for estimating and evaluating the overall prognosis of the exposed workers.

However, in the case of non-uniform exposure, such as experienced by the two workers exposed to high doses in this accident, the estimation of the dose in each organ might be more useful to predict the onset time and severity of injury of each organ. Also, it is preferable that the dose of each radiation component, i.e. neutrons and gamma rays for example, should be determined in Gy separately for each organ.

IV.G. Consistency of symptoms with dose estimation

IV.G.a. Whole-body dose estimate

In this accident, three workers were estimated to have been exposed to 19, 9.0, and 2.9 GyEq, respectively. Mr. A died on Day 82 and Mr. B on Day 210. There are no other recorded cases of such long-term survival after the exposure to such high doses. Maximal survival time was 9 days so far in the case of total body exposure in criticality accidents. In the criticality accident at Sarov, the Russian Republic in 1997, the victim died approximately 60 hours after exposure. Regarding exposures other than in criticality accidents, one case survived as long as 113 days after exposure of 10 Gy due to ^{60}Co radiation. On October 18, 1999, when we visited IAEA and reported the dose estimates for the three workers (estimated values at that time 18, 10, and 2.5 GyEq, respectively), it was pointed out that our dose assessment was likely to be wrong (NA02b). However, the estimated doses using three dose assessment methods based on blood components, chromosomal aberrations, and ^{24}Na specific activity showed good agreement, indicating that the proposed dose estimate was reasonable. It was not contradicted by the clinical courses of the three exposed workers. Although the fact of long survival in spite of exposure to high dose would appear to go against previous experience, it reflects the quality of intensive care they received.

IV.G.b. Onset time of gastrointestinal symptom

Gastrointestinal symptom following abdominal exposure to high dose is well known as a typical result of radiation injury. According to previous experience, the gastrointestinal symptom develop between several days and 2 weeks after exposure to 6 – 10 Gy or more, leading to diarrhea and gastrointestinal bleeding. These symptoms generally develop on and after Day 4 following exposure to 10 Gy or more, and on about Day 7 after exposure to 6 – 10 Gy. In this accident, it was expected that the two workers exposed to high doses would exhibit diarrhea early on. However, in the case of Mr. A, exposed to the highest dose, serious diarrhea (500 – 1,000 ml) developed on Day 26, and melena and upper gastrointestinal hemorrhage developed on Days 47 and 50, respectively. Regenerated-like mucosa were observed during endoscopy of the upper and lower gastrointestinal tracts on Day 14, and mucosa were found in clinical laboratory tests in the 7th week (FU01). In the case of Mr. B, gastrointestinal bleeding developed on Day 145 after exposure (NA01). Dose calculation for each part of the body using the computational simulation shows that the abdominal dose exceeded 10 Gy from gamma rays alone. Therefore, early onset of gastrointestinal symptom would have been expected regardless of the dose contribution of neutrons. There might be therapeutic effects from gastrointestinal sterilization, amino acid administration, and peripheral vascular cell transplantation. However, in the case of Mr. A, a total of 410 ml, produced during 10 attacks of diarrhea and a total of 1,350 ml in 6 attacks of diarrhea were observed on October 1 (Day 2) and October 2 (Day 3), respectively. There was no diarrhea for two weeks from October 3 (Day 4) (FU01). This diarrhea may correspond to the symptoms observed in previous experiences.

IV.G.c. Local dose assessment

Since blood circulating in the whole body was used for measurement of blood lymphocytes, chromosomal aberrations, and ^{24}Na concentrations, the estimated dose represents an averaged one in the whole body. Non-uniform exposure of the body could thus only be recorded by measuring activated product concentration in hair and bone. However, measurement of ^{32}P and other nuclides in the hair of Mr. A could provide only the rough qualitative information that the dose to the lower abdomen was higher than that to the head, due to the small hair sample size and limited sampling points (see Section B of Chapter III). In the case of Mr. B, there was no difference in dose between the head and lower abdomen. This rough information indicates the difference in the orientation of the body of Mr. A and Mr. B with respect to the precipitation tank at the time of the accident. On the other hand, measurement of ^{32}P and ^{45}Ca in bone samples from 14 sites of Mr. A, which were provided after death, revealed that a significantly high concentration was present in the 7th rib and right anterior superior iliac spine (see Section E of Chapter III). A slightly higher concentration was also observed in the femoral bone, indicating that Mr. A was probably exposed with his abdomen closest to the tank and with his body leaning to the right. This finding corresponds to the early development of erythema on the skin of the trunk (YA01), and the difference in intestinal symptoms endoscopically observed between right and left (FU01). However, there is no evidence of severe radiation burns to Mr. A's right upper arm in either bone measurements or the computational simulation. On the other hand, for Mr. B, no significant difference was observed in the measured dose in the bone. This result does not agree closely with the expression of erythema, i.e. the characteristic that erythema appeared initially on the distal hands and feet as well as face and then spread to the whole body over a period of two months (YA01).

Inconsistencies between clinical findings in skin injury on the right upper arm and radioactivity concentration in the bone of the right forefinger could be understood by the following explanation: as pointed out in the computational simulation (Fig. II.E.5), the dose around the precipitation tank depends to a high degree on location. For example, neutron dose and gamma ray dose at the surface of the precipitation tank were 1.6 and 1.4 times higher than those at a point 15 cm distant from the

surface, respectively at the height of 165 cm from the floor. In addition, neutrons are significantly attenuated in the body. Therefore, these differences might be expected, taking into account the difference in distance to upper arm and middle finger, combined with the possibility of additional shielding effect of other fingers and the funnel.

Although dose distribution on the body surface obtained from the computational simulation indicates that the abdomen, especially the right side, of Mr. A was exposed to the highest dose, which was closely consistent with clinical findings, it was pointed out that there was no result in the simulation corresponding to the above-mentioned severe radiation burn on the right upper arm. In the computational simulation, the distances of Mr. A and B from the precipitation tank at the time of the accident was estimated by the interviews of Mr. B and Mr. C, measurement results of radioactivity concentration in their hair and bone, and a replica of their working positions using a mockup tank. However, it is not known whether the actual situation was reproduced accurately. In the computational simulation, the dose to both hands of Mr. A, which were assumed to have been positioned above the tank to support the funnel, was calculated. According to measurements of the bone of the forefinger and observed skin symptoms, there might be a need to assume the situation upper arm was closer to the tank without much change in the distance between the precipitation tank and the right hand.

IV.H. Dose estimation chronology

The three workers who encountered the sever accident were not wearing personal dosimeters at the time of the accident, and NIRS did not receive any precise information about the accident itself when they arrived at our institute. As soon as the three workers were received at our institute the measurements of their belongings, nose smear samples and vomit samples were carried out by Germanium detectors in order to determine the dose as well as the exposure patterns. It was soon found that the three workers received high doses due to neutrons and gamma rays produced by the criticality accident and all the radiation emitted from their bodies came from the neutron induced radionuclides in their bodies. Based on a series of measurements, it was also estimated that there was very limited or no inhalation of uranium and fission products in the solid state, and that internal exposure was about three orders of magnitude smaller than external exposure. In addition, ^{91}Sr, ^{140}Ba, ^{140}La, etc., whose presence was found through measurement of their underwear and hair, were identified as isotopes derived from ^{91}Kr and ^{140}Xe gases generated as fission products.

On the second day (October 1) after the three workers were admitted into NIRS, the dose could not be estimated by the measurements of samples collected from the workers, a rough estimation was obtained based on the extent of decrease in lymphocyte counts. Mr. C was estimated to have been exposed to 3-5 Sv, and the other two workers (Mr. A and Mr. B) were more than 8 Sv. In the early stages after the accident, the neutron spectrum, positional relations between workers and the precipitation tank, and the percentages of neutrons and gamma rays were unclear; therefore, accurate dose estimation could not be performed. However, the absorbed dose (Gy) was estimated using the provisional value of ^{24}Na concentration in blood and the dose conversion factor (275 Bq ml^{-1} corresponds to about 14 Gy) shown in the IAEA report for the criticality accident at Sarov, the Russian Republic on June 17, 1997 (IA01) since the doses needed to be determined as soon as possible for medical treatment. Then the absorbed doses were converted to GyEq, the biological gamma ray dose equivalents for the three workers to be 18, 10, and 2.5 GyEq (reported at the time in units of Sv in press), respectively, on October 2 under the assumption that RBE was 1.7 based on the observation of intestinal death in mice due to neutrons irradiation with an average energy of 13 MeV (Be (d, n) reaction). Later, the doses in the three workers were re-evaluated to be 10 – 20 and higher, 6 – 10, and 1 – 4.5 GyEq on October 12, taking into account the measurements of ^{24}Na activity, chromosome aberration, lymphocyte count, the whole body counter, and other data. Those estimates were quoted in the Report of the Criticality Accident Investigation Committee (GE99a) and the Interim Report on Dose Estimation for Three Victims of JCO Accident (NA00).

In the present report, a more reliable dose was estimated based on the additional measurements and further investigation. Neutron fluence and number of nuclear fissions were also calculated. The dose to each worker at present is estimated to be 16-23, 6-8, and 3 GyEq respectively, using the evaluation based on blood component (especially lymphocyte count), and 24.5, 8.3, and 3.0 GyEq using chromosome analyses. Neutron and gamma ray dose was estimated to be 5.4 and 9.9, 2.9 and 4.1, and 0.81 and 1.5 Gy, respectively, using the specific activity of ^{24}Na in blood and computational simulation. Also, the biological gamma ray dose equivalent was estimated to be 19, 9.0, and 2.9 GyEq based on measurements of ^{24}Na in blood, with RBE assumed to be 1.7 for neutrons. The dose only for Mr. C was estimated using a human counter to be 2.2 GyEq for total dose due to neutrons and gamma rays using the same RBE value.

As a whole, the present doses are derived to be 16-25, 6-9, and 2-3 GyEq for three workers based on the entire dose estimation methods. These values show a good agreement with the initial estimation (18, 10, 2.5 GyEq) and the values in the interim report (16 – 20 and higher, 6 – 10, and 1 – 4.5 GyEq) taking into account the variability inherent in dose estimation procedures, individual non-uniform dose distribution, and tissue sensitivity.

V. CONCLUSION

It has been more than two years since the criticality accident occurred at JCO. After providing initial dose estimation, the Dose Estimation Working Group for Three Victims has carried out a detailed investigation of the exposure to the three workers involved in this accident using additional samples including the bone and teeth of the two workers, for whom the accident was regrettably fatal, as well as the computational simulation and the reconstruction experiment employing a transient experiment criticality facility. This report summarized these studies for utilization in the future although the Working Group sincerely hopes that no such accident will ever happen again.

As a result of the efforts and dedicated work of researchers and technologists in various fields at NIRS, dose assessment as well as exposure condition of the three exposed workers were provided rapidly, and appropriate steps could be taken for the planning of the medical treatment required immediately after the accident. The dose assessment was not an easy task since there are various ways for the dose assessment and for the expression of doses. Exposure in a criticality accident, including exposure to neutrons, made this job difficult. In particular, it was impossible to give one firm estimate, since two workers, working near the precipitation tank where the accident happened, were non-uniformly exposed over their whole body, and a variety of factors needed to be taken into account to be able to gain insight into the clinical symptoms. However, since the doses needed to be reported promptly for medical reasons, estimated doses in the three workers were released as biological gamma ray dose equivalent (GyEq), hedged around with various assumptions. Generally, the unit of the doses is very difficult to understand, but may be appropriate for use by clinicians. The estimated doses based on the rate of lymphocyte count decrease and the chromosome analysis were suitable to be expressed in GyEq since the exposure was a mixture of neutrons and gamma rays. This unit was effective in evaluating acute radiation symptoms in the workers exposed to a high dose.

The dose assessment conducted at NIRS functioned very effectively in various expertise from the beginning and enabled emergency radiation medical treatment in a timely manner. NIRS is proud of itself that various dose assessment methods were available and could provide dose estimates within an appropriate range. Fortunately, government funding for NIRS enabled these aims be accomplished.

REFERENCES

AK01   Akashi, M: Dose Estimation of Victims Severely Exposed Based on Initial Symptoms in The Criticality Accident in Tokaimura. International Symposium on The Criticality Accident in Tokaimura, Medical Aspects of Radiation Emergency. Edited by H. Tsujii and M. Akashi, NIRS-M-146, 72-80 (2001).

AN01   Ando, K.: High LET Radiobiology at NIRS-Current Status and Future Plan-. *Physica Medica* **17**, Suppl. 292-295 (2001).

BA95   Baranov, A. E., Guskova, A. K., Nadejina, N. M. and Nugis, Vyu: Chernobyl Experience: Biological Indicators of Exposure to Ionizing Radiation. *Stem Cells* **13** (Suppl. 1) 69-77 (1995).

BR81   Broerse, J. J. and Battermann, J. J.: Fast Neutron Radiotherapy: For Equal or for Better? *Medical Physics* **8** (6), 751-60 (1981).

BR97   Briesmeister, J. F.: Los Alamos National Laboratory Report LA-12625-M (1997).

CO78   Corbridge, D. E. C.: Phosphorous; an Outline of Its Chemistry, Biochemistry and Technology (Elsevier, Amsterdam) (1978).

CR81   Cross, W. G.: Neutron Activation of Sodium in Phantoms and the Human Body. *Health Physics*. **41**, 105-121 (1981).

ED99   Edwards, A. A.: Neutron RBE Values and Their Relationship to Judgments in Radiological Protection. J. Radiol. Prot. **19**, 93-105 (1999).

EN98   Engels, H. and Wambersie, A.: Relative Biological Effectiveness of Neutrons for Cancer Induction and Other Late Effects: A Review of Radiobiological Data. *Recent Results in Cancer Research*, **150**, 54-87 (1998).

EN01   Endo, A., Yamaguchi, Y. and Ishigure, N.: Analysis of Dose Distributions for the Heavily Exposed Patients in the Criticality Accident at Tokai-mura. JAERI-Research 2001-035 (2001).

FE93   Feng, Y., Brown, K. S., Casson, W. H., Mei, G. T., Miller, L. F. and Thine, M.: Determination of Neutron Doses from Criticality Accidents with Bioassays for Sodium-24 in Blood and Phosphorus-32 in Hair. ORNL/TM-12028, Oak Ridge National Laboratory, pp. 91 (1993).

FI96   Firestone, R. B.: Table of Isotopes Eighth Edition (1996).

FU93a   BAS Technical Information No.3. Fuji Film (1993).

FU93b   BAS Technical Information No.4. Fuji Film (1993).

FU99   Fujimoto, K.: Nuclear Accident in Tokai, Japan. *J. Radiol. Prot.,* **19**, No 4, 377-380 (1999).

FU00a   Fujimoto, K.: Criticality Accident at Tokai-mura. Proceedings of 10th International Congress of the International Radiation Protection Association, S-1, Hiroshima, May 14-19 (2000).

FU00b   Fujimoto, K., Noda, Y., Yamaguchi, Y. and Endo, A.: Nuclear Accident in Tokai, Japan. *Radiation Protection in Australasia,* **17**, 67-70 (2000).

FU00c   Fujimoto, K.: Nuclear Accident in Tokai, Japan. *SSI News*, **18**, No 3, 15-17 (2000).

FU01   Futami, S., Nishida, M., Ishii, T., Yamaguchi, I., Suzuki, S., Sakamoto, T. and Maekawa, K.: Case Presentation of Worker A. International Symposium on The Criticality Accident in Tokaimura, Medical Aspects of Radiation Emergency. Edited by H. Tsujii and M. Akashi, NIRS-M-146, 142-153 (2001).

GE75   Geraci, J. P., Jackson. K. L., Christensen, G. M., Thower, P. D. and Fox, M. S.: Cyclotron Fast Neutron RBE For Various Normal Tissues. *Radiology* **115**: 459-63 (1975).

GE99a   The Nuclear Safety Commission: The Report of the Criticality Accident Investigation Committee, in Japanese (1999).

GE99b   The Nuclear Safety Commission: the Criticality Accident Investigation Committee, the Ninth Meeting Materials, in Japanese (1999).

GE00   Japan Atomic Energy Research Institute: JAERI-Tech 2000-074 (2000).

GR78   Griffin, T. W., Laramore, G. E., Parker, R. G., Gerdes, A. J., Hebard, D. W., Blasko, J. C. and Groudine, M.: An Evaluation of Fast Neutron Beam Teletherapy of Metastatic Cervical Adenopathy from Squamous Cell Carcinomas of the Head and Neck Region. *Cancer* **42**: 2517-20 (1978).

HA92   Hayata, I., H. Tabuchi, A. Furukawa, N. Okabe, M. Yamamoto and K. Sato: Robot System for Preparing Lymphocyte Chromosome. *J. Radiat. Res.*, **33,** Supple. 231-241 (1992).

HA94   Hanson, W. R., Crouse, D. A., Fry, R. J., Ainsworth, E. J.: Relative Biological Effectiveness Measurements Using Murine Lethality and Survival of Intestinal and Hematopoietic Stem Cells after Fermilab Neutrons Compared to JANUS Reactor Neutrons and ^{60}Co Gamma Rays. *Radiation Research* **100** (2), 290-297 (1994).

HA01a   Hayata, I., Kanda, R., Minamihisamatsu, M., Furukawa, A. and Sasaki, M. S.: Chromosome Analysis in Three Patients. International Symposium on The Criticality Accident in Tokaimura, Medical Aspects of Radiation Emergency. Edited by H. Tsujii and M. Akashi, NIRS-M-146, 82-89 (2001).

HA01b   Hayata, I., Kanda, R., Minamihisamatsu, M., Furukawa, A. and Sasaki, M. S.: Cytogenetical Dose Estimation for 3 Severly Exposed Patients in the JCO Criticality Accident in Tokai-mura. *J. Radiation Research*, **42**, Supplement 149-155 (2001).

HI77   Hiraoka, T., Kawashima, K., Hoshino, K and Matsuzawa, H.: Dosimetry of Fast Neutron Beams at the NIRS Cyclotron. *Nippon Acta Radiologica* **37**, 369-76 (1977).

HO48   Hoffman, J. G.: Radiation Doses in the Pajarito

Accident of May 21, 1946. *LA-687* (1948).

HU59 Hurst, G. S., Ritchie, R. H. and Emerson, L. C.: Accidental Radiation Excursion at the Oak Ridge Y-12 Plant-III, Determination of Radiation Doses, *Health Phys.,* **2**, 121-133 (1959).

HU96 Hughes, H. G.: LANL memorandum X-6: HGH-93-77 (1996).

IA82 IAEA: Dosimetry for Criticality Accidents – A Manual. Technical Reports Series No.211 (1982).

IA86 IAEA: Technical Reports Series 260. Biodosimetry: Chromosomal Aberration Analysis for Dose Assessment (1986).

IA98 IAEA / WHO: Safety Reports Series No.2, Diagnosis and Treatment of Radiation Injuries (1998).

IA01 IAEA: The Criticality Accident in Sarov, International Atomic Energy Agency, Vienna, STI/PUB/1106, ISBN 92-0-100101-0 (2001).

IC75 ICRP Publication 23. Reference Man: Anatomical, Physiological and Metabolic Characteristics, Pergamon Press, Oxford (1975).

IC80 ICRP Publication 30. Part 2. Limits for Intakes of Radionuclides by Workers. *Annals of the ICRP,* **4** (3/4) (1980).

IC87 ICRP Publication 51. Data for Use in Protection Against External Radiation, *Annals of the ICRP*, **17** (2/3) (1987).

IC89a ICRU Report 44. Tissue Substitutes in Radiation Dosimetry and Measurement (1989).

IC89b ICRP Publication 58. RBE for Deterministic Effects. *Annals of the ICRP*, **20** (4) (1989).

IC91 ICRP Publication 60. 1990 Recommendations of the International Commission on Radiological Protection. *Annals of the ICRP,* **21** (1-3) (1991).

IC92 ICRU Report 46. Photon, Electron, Proton and Neutron Interaction Data for Body Tissues (1992).

IC96 ICRP Publication 74. Conversion Coefficients for Use in Radiological Protection against External Radiation *Annals of the ICRP*, **26** (3/4) (1996).

IS01a Ishigure, N., Endo, A., Yamaguchi, Y., and Kawachi, K.: Dose Reconstruction for Heavily Exposed Patients of the Criticality Accident in Tokai-mura - Joint Research Program between the NIRS and JAERI. International Symposium on The Criticality Accident in Tokaimura, Medical Aspects of Radiation Emergency. Edited by H. Tsujii and M. Akashi, NIRS-M-146, 110-119 (2001).

IS01b Ishigure, N., Endo, A., Yamaguchi, Y. and Kawachi, K.: Calculation of the Absorbed Dose for Overexposed Patients at the JCO Criticality Accident in Tokai-mura. *J. Radiation Research*, **42**, Supplement 137-148 (2001).

IW93 Iwasaki, M., Miyazawa, C., Uesawa, T. and Niwa. K.: Effect of Sample Grain Size on the CO_3^{3-} Signal Intensity in ESR Dosimetry of Human Tooth Enamel. *Radioisotopes* **42**, 470-473 (1993).

IW95 Iwasaki, M., Miyazawa, C., Uesawa, T., Itoh, I. and Niwa, K.: Differences in the Radiation Sensitivity of Human Tooth Enamel in an Individual and among the Individuals in Dental ESR Dosimetry. *Radioisotopes*

44, 785-788 (1995).

IW98 Iwasaki, M., Miyazawa, C., Uesawa T., and Itoh, I.: ESR Dosimetry of Human Teeth Enamel from a Subject Undergoing Radiation Treatment for Cancer of the Epipharynx. *Radioisotopes* **47**, 138-142 (1998).

JA66 Jackson, S. and Dolphin, G. W.: The Estimation of Internal Radiation Dose from Metabolic and Urinary Excretion Data for a Number of Important Radionuclides. *Health Phys.*, **12**, 481-500 (1966).

KA99 Kanda, R., Hayata, I. and Lloyd, D.: Easy Biodosimetry for High-dose Radiation Exposures Using Drug-induced, Prematurely Condensed Chromosomes. *Int. J. Radiat. Biol*. **75**, 441-446 (1999).

KE72 Kellerer, A. M. and Rossi, H. H.: The Theory of Dual Radiation Action. *Curr. Top. Radiat. Res*. Q. **8**: 85 (1972).

KE83 Kennedy, N. S. et al.: Normal Levels of Total Body Sodium and Chlorine by Neutron Activation Analysis. *Phys. Med. Bio.*, **28,** 215-221 (1983).

KO94 Kosako, K., Maekawa, F., Oyama, Y., Uno, Y. And Maekawa, H.: FSXLIB-J3R2: A Continuous Energy Cross Section Library for MCNP based on JENDEL-3.2. JAERI-Data/Code (1994).

KO00 Komura, K.,Yamamoto, M., Muroyama, T. et al.: The JCO Criticality Accident at Tokai-mura, Japan: an Overview of the Sampling Campaign and Preliminary Results. *J. Environmental Radioactivity* **50**, 3-14 (2000).

KO01 Koike, S. and Ando, K: Relative Biological Effectiveness of Fast Neutrons in Murine Tissues. International Symposium on The Criticality Accident in Tokaimura, Medical Aspects of Radiation Emergency. Edited by H. Tsujii and M. Akashi, NIRS-M-146, 66-71 (2001).

MA68 Maruyama, T: Radiation dose estimation in criticality accident 2. Neutron capture probability of phantoms. *Nippon Acta Radiologica*, **27**, 1347-1353 (1968).

MI89 Miller, R. C., Geard, C. R., Brenner, D. J., Komatsu, K., Marino, S.A., Hall, E. J.: Neutron-Energy-Dependent Oncogenic Transformation of C3H 10T1/2 Mouse Cells. *Radiation Research* **117** (1), 114-27 (1989).

MI98 Miyahara, R: Autoradiography and Radiography Imaging Plate and its Application. *Radioisotope* **47**, 143-154 in Japanese (1998).

MI01 Miyahara, R: JAERI, Nuclear technology and Education Center, Autoradiography, Textbook in Japanese (2001).

MI02 Miyamoto, K., Watanabe, Y., Yukawa, M., Takeda, H., Nishimura, Y., Ishigure, N., Hirama ,T. and Akashi, M.: Reconstruction of Two Victims' Posturing Based on the Induced Radioactivities in Their Bones in the Criticality Accident in Tokai-Mura, Japan. *Health Physics*, **83**, No. 1 (2002).

MU99 Muramatsu, Y. and Yoshida, S.: Effects of Microorganisms on the Fate of Iodine in the Soil Environment. *Geomicrobiology J.,* **16**, 85-93 (1999).

MU01a Muramatsu, Y., Ishigure, N., Noda, Y., Yonehara, H.,

Yoshida, S., Yukawa, M., Tagami, K., Ban-nai, T., Uchida, S., Akashi, M., Hirama, T. and Nakamura, Y.: Estimation of Radiation Doses for Three Exposed Patients in the Tokai0mura Accident Based on [24]Na in Their Biological Materials. International Symposium on The Criticality Accident in Tokaimura, Medical Aspects of Radiation Emergency. Edited by H. Tsujii and M. Akashi, NIRS-M-146, 90-100 (2001).

MU01b Muramatsu, Y., Noda, Y., Yonehara, H., Ishigure, N., Yoshida, S., Yukawa, M., Tagami, K., Ban-nai, T., Uchida, S., Akashi, M., Hirama, T. and Nakamura, Y.: Determination of Radionuclides in Biological Materials from Three Heavily Exposed Workers for Estimating an Individual's Neutron Fluence in the Tokai-mura Criticality Accident. *J. Radiation Research*, **42**, Supplement 117-128 (2001).

NA82 Nakajima,T. The Use of Organic Substances as Emergency Dosimeters. *Int. J. Appl. Radiat. Isot.* **33**, 1077-1084 (1982).

NA94 Nakajima, T. Estimation of Absorbed Dose to Evacuees at Pripyat-City Using ESR Measurements of Sugar and Exposure Rate Calculations. *Appl. Radiat. Iso.,* **45**, 113-120 (1994).

NA95 Nakagawa, T., et al.: *J. Nucl. Sci. Technol.,* **32**, 1259-1271 (1995).

NA96 Nakajima, T.: Biodosimetry. V. Biodosimetry with ESR Equipment. *Radioisotopes* **45**, 113-124 (1996).

NA98 Nakamura, N. et al.: A Close Correlation between ESR Dosimetry from Tooth Enamel and Cytogenetic Dosimetry from Lymphocytes of Hiroshima Atomic-bomb Survivors. *Int. J. Radiat. Biol*, **73**, 619-627 (1998).

NA00 National Institute of Radiological Sciences: Interim Report on Dose Estimation for Three Victims of JCO Accident. Edited by K. Kawachi and K. Fujimoto NIRS-M-138, in Japanese (2000).

NA01 Nagayama, H., Takahashi, T.A., Misawa, K., Ooi, J., Iseki. T., Yamada, Y., Yamashita, N. And Asano, S.: Case Presentation of Worker B. International Symposium on The Criticality Accident in Tokaimura, Medical Aspects of Radiation Emergency. Edited by H. Tsujii and M. Akashi, NIRS-M-146, 154-158 (2001).

NA02a National Institute of Radiological Sciences: Final Report on Dose Estimation for Three Victims of JCO Accident. Edited by K. Fujimoto, NIRS-M-153 in Japanese (2002).

NA02b National Institute of Radiological Sciences: The report of the criticality accident in a uranium conversion test plant in Toaki-mura. Edited by H. Murata and M Akashi, NIRS-M-154 (2002).

NI02 Nishimura, Y., Takeda, H., Miyamoto, K., Watanabe, Y., Kouno, F., Kuroda, N., Kim, H. S. and Yukawa, M.: Determination of ^{32}P in Urine for Early Estimation of Neutron Exposure Level for Three Victims in the JCO Criticality Accident. *J. Radiol. Prot.* **22**, 25-29 (2002).

NO66 Norman, A. and Sasaki, M. S.: Chromosome-exchange Aberrations in Human Lymphocytes. *Int. J. Radiat. Biol*. **66**, 321-328 (1966).

NO80 M. Noguchi: Gamma ray spectrometry. Nikkan-Kougyo-Shinbunsya (1980).

OK85 Okajima, S.: Reassessment of A-bomb Dosimetry, in Ikeya, M and Miki, T eds, 1st Int. Symp on ESR Dation, Tokyo, p.381. IONICS, Tokyo (1985).

RA99 Rannou, A. (IPSN): Private communication (1999).

SC96 Schnetger, B. and Muramatsu, Y.: Determination of Halogens, with a Special Reference to I, in Geological and Biological Samples using Pyrohydrolis for Preparation and ICP-MS and IC for Measurement. *Analyst*, **121**, 1627-1631 (1996).

SE90 Sekiguchi, M.: Vital elements for living organism. *Rinshou-kensa*, **34**, 1384-1393 (1990).

SH97 Shiraishi, K.: Sensitivity Comparison for Electron Spin Resonance (ESR) on Carbohydrates as Dosimeter Materials*. Adv. ESR Appl.*, **13**, 4-10 (1997).

SH00 Shiraishi, K., Kimura, S., Yonehara, H., Takada, J., Ishikawa, M., Igarashi, Y., Aoyoama, M., Komura, K., and Nakajima, T.: Survey of External Dose around the JCO Facility Using Sugar Samples and ESR Methods*. Adv. ESR Appl.*, **16**, 9-14 (2000).

SN69 Snyder, W. S., Ford, M. R., Warner, G. G. and Fisher, H. L. Jr.: Estimates of Specific Absorbed Fractions for Photon Sources Uniformly Distributed in Various Organs of a Heterogeneous Phantom. *J. Nucl. Med.*, **10**, Supplement No.3 (1969).

TA99 Tanaka, K., Gajendiran, N., Endo, S., Komatsu, K., Hoshi, M. and Kamada, K.: Neutron Energy-Dependent Initial DNA Damage and Chromosomal exchange. *J.Radiation Research* **40**, Supplment.53-59 (1999).

TA01 Takeda, H., Miyamoto, K., Yukawa, M., Nishimura, Y., Watanabe, Y., Kim, H. S., Fuma, S., Kuroda, N., Kouno, F., Joshima, H., Hirama, T. and Akashi, M.: Bioassay for Neutron-dose Estimations of Three Patients in the JCO Criticality Accident in Tokai-mura. *J. Radiation Research*, **42**, Supplement 129-135 (2001).

TH89 Thomas, F. J., Krall, J., Hendrickson, F., Griffin, T. W., Saxton, J. P., Parker, R. G. and Davis, L. W.: Evaluation of Neutron Irradiation of Pancreatic Cancer - Results of a Randomized Radiation Therapy Oncology Group Clinical Trial - *American Journal of Clinical Oncology* **12** (4): 283-9 (1989).

UN88 UNSCEAR: Sources, Effects And Risks of Ionizing Radiation. UNSCEAR 1988 Report (1988).

WA99 Waters, L. S.: TPO-E83_G-UG-X-00001 (1999).

WA01 Watanabe, Y., Yukawa, M., Miyamoto, K., Takeda, H., Nishimura, Y., Akashi, M., Fujimoto, K., Fuma, S., Hirama, T., Ishigure, N., Joshima, H. and Kouno, F.: Neutron Fluence Sistribution by Bone and Hair. International Symposium on The Criticality Accident in Tokaimura, Medical Aspects of Radiation Emergency. Edited by H. Tsujii and M. Akashi, NIRS-M-146, 102-108 (2001).

YA92 Yamaguchi, Y: FANTOME-90: A Computer Code to Calculate Photon External Doses for a Phantom with Movable Arms and Legs. *Hoken Butsuri* **27**, 143-148 (1992).

YA01   Yamaguchi, Y.: Initial Reaction of the Skin after Radiation Exposure. International Symposium on The Criticality Accident in Tokaimura, Medical Aspects of Radiation Emergency. Edited by H. Tsujii and M. Akashi, NIRS-M-146, 190-192 (2001).

YO96   Yoshida, S., Muramatsu, Y., Tagami, K. and Uchida, S.: Determination of Major and Trace Elements in Japanese Rock Reference Samples by ICP-MS. *Int. J. Environ. Anal. Chem.* **63**, 195-206 (1996).

YO97   Yoshida, S. and Muramatsu, Y.: Determination of Major and Trace Elements in Mushroom, Plant and Soil Samples Collected from Japanese Forests. *Intern. J. Environ. Anal. Chem.* **67**, 49-58 (1997).

APPENDICES

A. Initial Action

A.a. Preparation for admittance of the workers by to the Radiation Safety Section

1. Around 11:20 AM on September 30, 1999, NIRS was informed of the radiation accident at Tokaimura. The Radiation Safety Section staff was assembled for the preparation in case of the arrival of the workers.

2. Around 11:30 AM on the same day, the floor of the whole path from the entrance to Radiation Emergency Handling Suite in the Third Research Building was covered with vinyl sheets and polyethylene-coated paper for the possibility of contamination due to the accident. The facilities (air conditioning, ventilation, water works, off-gas monitors, etc.) were tested and confirmed to be functioning, and radiation measurement devices (alpha, beta and gamma ray survey meters, pocket dosimeters, etc.) and related devices (half face masks, air samplers, etc.) were readied.

3. Around 11:40 AM, it was announced that the three workers would be moved to NIRS.

4. Around 1:00 PM, it was announced that the three workers were brought to the heliport in Chiba city by an Ibaraki Prefectural helicopter and then transferred by ambulance from the heliport to NIRS. Three members of the Radiation Safety Section were assigned to welcome them at the heliport. They were appointed to detect any radioactive contamination and carry out decontamination, if necessary, of the workers, crew and helicopter.

5. Around 1:30 PM, relevant NIRS staff, except individuals involved in the decontamination process, were planned to wear light radiation protection suits. However, further information arrived later that the accident occurred at the uranium hexafluoride (UF_6) handling facility, number of exposed workers is three and they might have suffered internal exposure. The Radiation Emergency Handling Suite staff changed their strategy to that of saving life. The protection level of each staff was raised to medium (half facemask, cotton gloves, rubber gloves, radiation protection suits and overshoes).

6. Around 2:00 PM, three assigned staff from the Radiation Safety Section were dispatched to the heliport in an ambulance provided by Chiba Fire Station, carrying radiation measurement devices and wearing protective suits. More news of possible serious external exposure arrived.

7. Around 2:30 PM, the ambulance arrived at the heliport. This was reported to NIRS and a briefing was held by the rescue staff in charge of transportation from the heliport to NIRS. The rescue team decided to wear their protective suits for infectious protection (disposable white robe, medical mask, rubber gloves, etc.).

8. Around 2:40 PM, the three workers arrived at the heliport in Chiba. Two of them were suffering diarrhea and vomiting. Three Radiation Safety staff began a direct radiation emergency survey of the workers. The survey of the three workers in the helicopter had revealed extremely high counts, especially around the chest (max. 12 kcpm by GM, while alpha rays were not detected). Since one of the workers was in a very serious condition, they were immediately moved into the ambulance placing the first priority on saving life. Rescue staff, equipped with pocket dosimeters, also rode in the ambulance.

9. Around 3:00 PM, the three workers left the heliport in the ambulance, accompanied by one doctor and one Radiation Safety staff member, after informing NIRS headquarters of their departure. Two Radiation Safety Section staff remained at the heliport to continue measurements of radioactive contamination and carry out decontamination, if necessary, of the helicopter and the pilot.

10. On the way to NIRS, worker Mr. A said that he felt hot (he was fully wrapped with a blanket and vinyl sheet in addition to being fully clothed). A Radiation Safety staff removed the blanket and sheet with the permission of the doctor present. Mr. A felt very sick and vomited onto the vinyl sheet. (The vomit was kept in a plastic bag).

11. Around 3:30 PM, the ambulance arrived at NIRS. After the workers were carried into the Radiation Emergency Handling Suite, measurements of the accompanying doctor, rescue staff and the ambulance, etc. were carried out to detect any radioactive contamination. No surface contamination was found. As for the workers, the survey meters indicated high levels of count (max. 26 kcpm on the GM survey meter, no alpha particles detected). The measurement results for the rescue staff were reported in writing to the Head Office of Chiba Fire Station.

12. Although no contamination was found on the overalls of the accompanying doctor, NIRS kept them for further measurements. The doctor, provided with replacement overalls by NIRS, returned to the heliport by car dispatched by Chiba Fire Station and flew back to Ibaraki Prefecture.

13. The Radiation Safety Section kept the clothes and personal possessions of two workers who were in somewhat better condition, as well as their excrement and

vomit, for the measurement to identify radionuclides.

14. A survey meter for surface contamination and a whole body counter revealed the accompanying JCO employee not to be contaminated.

A.b. Preparations to admit the workers to the Radiation Emergency Handling Suite

1. At 11:45 AM, on 30 September 1999, the Radiation Emergency Handling Suite initiated the operating test of their whole body counter and thyroid radiation monitor in response to an emergency call from the Radiation Safety Section.

2. Around 1:00 PM on the same day, the operating tests were complete. The Radiation Safety staff began to cover the floor of the facilities, without any precise information regarding how the accident had occurred, where the workers come from, how they were injured, whether they had suffered internal or external exposure, or what was the source of the radiation.

3. Around 2:00 PM, when further information was brought that seriously exposed workers would be transferred, an accident had occurred in a uranium processing facility and they were going to be brought by helicopter, it was clear that the accident had been serious. Judging from all the information received, including the additional information that one worker was seriously exposed and that life saving would be the top priority, the decision was made to use the Ge detector for the contamination measurement and monitoring, instead of a bed-type thyroid monitor. Arrangements were made judging from the accident at an uranium fabrication facility to ready the alpha ray survey meter, GM survey meter, NaI (Tl) scintillation survey meter, exhaled air sampler and alpha/beta monitor for wound, in addition, other necessary devices were also gathered mainly from Division of radiotoxicology and Protection and Division of Education and Science Services. Operation tests on all pieces of equipment were performed.

4. Around 3:00 PM, when the helicopter landed at Toke heliport in Chiba, the Radiation Emergency Handling Team re-confirmed the full preparedness for the estimated arrival at 3:30.

A.c. Contamination measurement of the exposed workers

1. At 3:25 PM, the three exposed workers were measured for surface contamination levels using an alpha ray survey meter and GM survey meter. Three staff teams comprising one for alpha ray survey meter, one for GM survey meter and a recorder for each worker performed these measurements. A series of extremely high count rates were reported and recorded.
  GM Survey results (BG: 100 cpm included)
    Mr. A: approx. 13 kcpm at the head and approx. 26 kcpm at the upper half of the body.
    Mr. B: approx. 15 kcpm at the upper half of the body.
    Mr. C: approx. 6 kcpm at the head, approx. 4 kcpm at the upper half of the body.

2. In the entrance hall, from the fact that the indicator of the GM survey meter jumped out of its range, it was recognized that they had been exposed to an unusually high dose. Surface contamination by alpha particles of the workers and the blanket in which Mr. A was wrapped was within the background range. Director of radiation Health Division decided that measurement by whole body counter and thyroid monitor in the Radiation Emergency Handling Suite should be canceled and the workers should be transferred to the Hospital for Charged Particle Therapy in NIRS, since life saving was the top priority.

3. The three workers were transported to the Hospital of Charged Particle Therapy at NIRS.

Measurement results by TLD ($CaSO_4$(TM)) for three workers that were carried out on October 1 are shown in Data-1, area survey results in Data-2.

TLD Measurement Record

Date of measurement：Friday, October　1, 1999

Note:
　TLD settled over the bed clothes because it was not possible to set on directly to their body.
　It does not mean that they put on the bed clothes all through the duration TLD settled.

Mr. A　　**Mr. B**　　**Mr. C**
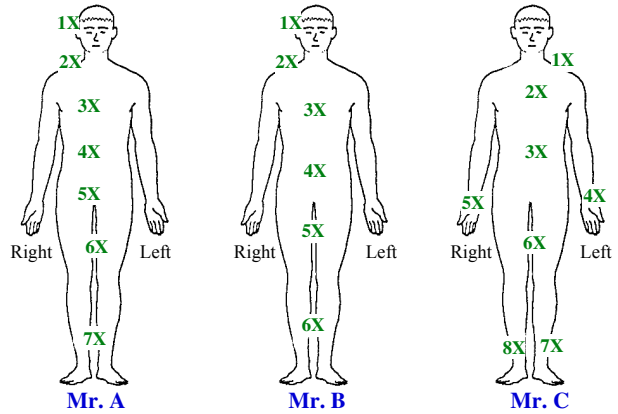
	TLD No.	Region	Time of installation	Time of uninstallation	Results (μSv/hr)
	1	Head	16:53	17:23	7.7
	2	Right shoulder	16:53	17:23	10.1
	3	Breast	16:53	17:23	7.7
Mr. A	4	Abdomen	16:53	17:23	8.0
	5	Lower abdomen	16:53	17:23	9.3
	6	Thigh	16:53	17:23	7.6
	7	Legs	16:53	17:23	7.1
	1	Head	16:51	17:21	7.1
	2	Right shoulder	16:51	17:21	7.2
	3	Breast	16:51	17:21	7.0
Mr. B	4	Abdomen	16:51	17:21	6.2
	5	Thigh	16:51	17:21	7.1
	6	Legs	16:51	17:21	8.4
	1	Left shoulder	17:05	18:35	7.3
	2	Breast	17:05	18:35	6.0
	3	Left hand	17:05	18:35	5.8
Mr. C	5	Right hand	17:05	18:35	5.7
	6	Thigh	17:05	18:35	5.8
	7	Left leg	17:05	18:35	7.3
	8	Right leg	17:05	18:35	5.4

Data-1
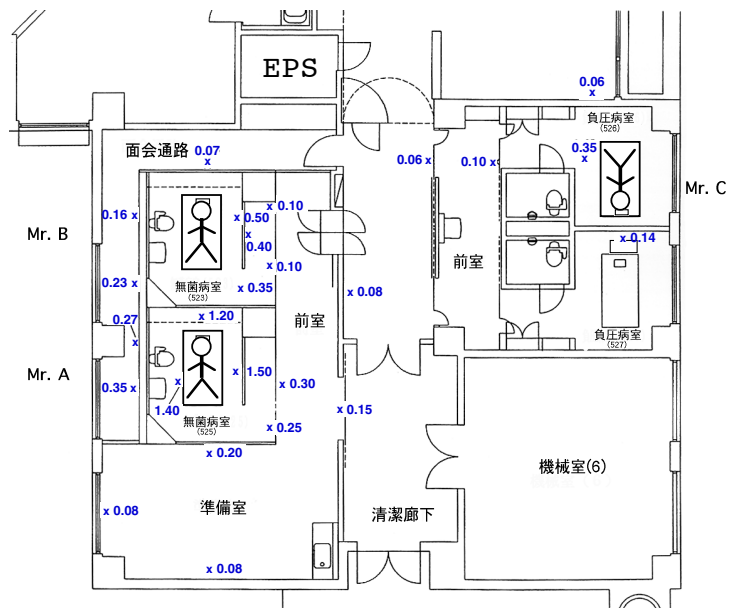
Area survey data

Measurement:　9:40 Friday Oct. 10, 1999
Instrument:　Scintillation surveymeter
　　　　　　（Aloka TCS-161）
Unit:　μSv/hr

Source of radiation:
　^{24}Na due to the activation of ^{23}Na in the body

Data-2

87

A.d. Radiation measurement of biological samples and their possessions obtained from three workers

1. From vomit sample, which was measured at the earliest stage, a peak indicating ^{24}Na appeared on the Ge detector installed in the Radiotoxicology Research Building. It was then passed to the Radiation Emergency Handling Suite for more precise measurement.

2. At the same time (3:55 on September 30,1999), using the Ge detector in the Radiation Emergency Handling Suite, the first measurement by gamma ray spectrometry was made of the mobile phone carried by the most heavily exposed worker. The first sharp peaks in the spectra were for ^{24}Na (2,754.0, 1,368.6 keV), ^{56}Mn (2,113.1, 1,810.7, 846.8 keV) and ^{198}Au (411.8 keV) which formed rapidly with a dead time of almost 10%. At that moment, the radioactivity was understood to have been induced by the activation due to neutron irradiation. At 4:40 PM, measurement of Mr. A's vomit started. When photo peaks for ^{24}Na and ^{42}K (1,524.7 keV) appeared, it was reported to Countermeasures Headquarters that the accident had involved exposure due to neutron.

3. After reporting this to the Countermeasures Headquarters, it was concluded that multiple measurements would be necessary to perform precise dose estimation. The Environmental Radiation Measurement Laboratory in the third Research Building was requested to help with these measurements since their Ge detector was calibrated and ready for use.

4. Later on, the filter of an exhaled gas sampler, a 100 yen coin, 500 yen coin, wristwatch, underwear, outerwear, belt, absorbent cotton used for the smear of the nostrils and other items were measured. From 7:00 PM, samples (coin, vomit) were measured for dose estimation using the Environmental Radiation Measurement Laboratory's Ge detector. In order to obtain an accurate result as possible, measurement was performed with several Ge detectors on the same samples, as well as repeated measurement taking into account the decay of ^{24}Na. On October 1, 1999, the qualitative results of almost all the samples were reported at the meeting of the Network Council for Radiation Emergency Medicine.

5. At the Countermeasures Headquarters meeting in the early morning of October 1, 1999, it was decided that the blood and hair would be the next targets for the measurement to estimate dose from ^{24}Na. Dose estimation of the three workers was conducted by measuring the concentration of ^{24}Na in the blood, using three Ge detectors including one installed in the First Research Building.

A.d.1. Gamma spectroscopy of the workers' samples

While the contamination levels of the three workers were examined using survey meters, gamma spectra of the samples described below were collected using Ge detectors. Smear samples from the nostrils and hair samples were selected to check surface contamination, and vomit and filters of exhaled air samplers were selected to check internal contamination. In addition, underwear, outerwear (changed after the accident) and belts were also measured. Underwear was treated as samples for determining the radionuclides derived from rare gases produced as fission products at the time of the accident, since they had not been changed until they arrived NIRS. The measurements of their blood samples are described in detail in Chapter II. The bed linen (towels and sheets, etc.) at the Hospital for Charged Particle Therapy was also examined. Result of the measurements on these samples and detected nuclides are shown in the tables below.

A.d.2. Gamma spectroscopy of the workers' possessions

While the workers were being transferred, the personal possessions in the pockets of their jackets were measured. They stated in the initial interview that they kept all personal items in a locker near the entrance of No. 1 Uranium Test Building, next to the Conversion Building. Later, it became clear that they kept their wristwatches on and took their mobile phones into the Conversion Building. The coins were not certain whether they were brought into the Conversion Building. Radionuclides detected from these samples showed evidence of having been irradiated by neutrons. The measurement results are shown below.

Table -1

Samples	Radionuclides detected	Starting time (m.d hh:mm)	Elapsed time (hr)*	Duration of measurement (sec)	Spectrum No.
vomit (A)	Na-24, K-42, Br-82, Br-80	09.30 18:25	7.83	6002	MCA-01
smear	Na-24	10.01 05:13	18.63	8000	MCA-02
filter of air sampler	BG g-rays (Uranium & Thorium Series)	09.30 16:40	6.08	5198	MCA-03
blood 20 ml (A-1)	Na-24, K-42	10.01 14:49	28.23	3000	MCA-04
blood 20 ml (A-2)	Na-24, K-42	10.02 08:48	46.22	6000	
blood 20 ml (B-1)	Na-24, K-42	10.01 16:47	30.20	4000	MCA-05
blood 20 ml (B-2)	Na-24, K-42	10.02 12:20	49.75	2004	
blood 20 ml (B-3)	Na-24, K-42	10.02 16:46	54.18	6000	
blood 20 ml (C-1)	Na-24, K-42	10.02 10:31	47.93	6000	MCA-06
hair~100 mg (C-1)	Ba-140, La-140,	10.15 12:15	361.67	3000	
whole hair (C-2)	Ba-140, La-140, Sr-91, Y-91, Na-24	10.01 20:41	34.10	43000	MCA-07
hair 6.24gr (C-3)	Ba-140, La-140	10.15 17:00	366.42	75000	MCA-08
all towels, 1st day	Na-24, Sr-91, Y-91, Ba-140, La-140	10.02 13:10	50.58	5000	MCA-09
towels, 2nd day (A)	Na-24	10.02 14:50	52.25	3000	MCA-10
bed sheets	Na-24	10.02 15:40	53.08	2000	MCA-11
underwear-1	Na-24, Br-80, Br-82, Sr-91, Ba-139, K-42	09.30 23:22	12.78	2000	MCA-12
underwear-2	Na-24, Br-82, Sr-91, Ba-140, La-140	10.02 23:50	61.25	36000	
underwear-3	Br-82, Ba-140, La-140, Sb-122, Sb-124, Na-24	10.05 17:50	127.25	55000	
underwear-4	Br-82, Ba-140, La-140, Sb-122, Sb-124, Na-24, I-131	10.10 15:30	244.9 2	66000	
underwear-5	Ba-140, La-140, Sb-122, Sb-124, I-131	10.22 09:50	527.25	111000	MCA-13
outer clothing (B)	Na-24, Cu-64, Zn-69, Sr-91, Y-91, Sb-122	10.01 00:21	13.77	2000	MCA-14
belt (C)	Mn-56, Sr-91, Y-91, Na-24	10.01 01:00	14.42	5000	MCA-15

* Elapsed time: Elapsed time from the accident (10:35 Sept. 30, 1999) until the measurement started.

A.d.2. Gamma spectroscopy of the samples related to the workers

While the parents were being transferred, personal possessions in the pockets of their jackets were measured. According to the hearing investigation in the beginning, they kept them in the locker near the entrance of No.1 Uranium Test Building next to Conversion Building.

Later on it became clear that a wrist watch and a mobile telephone carried with them in to the Conversion Building. As for coins, not cleared out. Radionuclides detected from those samples were activated component parts materials by neutron. Only for parts easier to handle in shape and structure, quantitative measurement performed. The results are shown below.

Table-2

| Samples	Radionuclides detected	Started time (m.d hh:mm)	Elapsed time (hr)*	Duration of measurement (sec)	Spectrum No.
G-Shock (A carried)	Na-24, Mn-56, Au-198, Pr-138, As-76, Cr-51	09.30 22:42	12.12	2000	MCA-16
G-Shock	Mn-54, Au-198, Ta-182, Cr-51, Co-60, Fe-59, Zn-65, Ag-110m, Sc-46, Sb-124, La-140	10.26 18:12	631.62	64000	MCA-17
G-Shock titanium lid	Sc-46, Ag-110m, Hf-181, Cr-51, Co-60	11.02 16:09	797.57	241002	MCA-18
G-Shock battery CR2016	Cr-51, Ta-182, Au-198, Sb-124, Ag-110m, Mn-56,	10.06 09:34	142.98	28921	
G-Shock battery	Co-58, Sc-46, Co-60, Fe-59, Zn-65	10.04 18:33	103.97	51002	
G-Shock battery	Cr-51, Co-58, Mn-54, Fe-59, Co-60	11.13 10:01	1055.43	466002	MCA-19
G-Shock circuit board	Ta-182, Co-58, Co-60, Cr-51, Zn-65, Ag-110m, Sb-124, Au-198	11.05 12:00	865.42	250000	MCA-20
nickel 100yen coin(1980)	Mn-56, Cu-64, Ni-65, Co-58	09.30 21:11	10.60	2000	MCA-21
nickel 500yen coin(1996)	Mn-56, Cu-64, Ni-65, Co-58	09.30 22:03	11.47	2000	MCA-22
Rolex (C carried)	Zn-65, Cr-51, Au-198, La-140, Ba-140, Br-82, Ag-110m, Co-58, Co-60, Fe-59	10.08 22:06	203.52	72000	MCA-23
Rolex stainless lid	Cr-51, Co-58, Co-60, Fe-59, La-140, Mn-54	10.18 18:00	439.42	165000	MCA-24
Rolex stainless lid	Cr-51, Co-60, Co-58, Fe-59, La-140, Mn-54	10.30 16:49	726.23	150036	
Rolex battery SR-626SW	Ag-110m, Zn-65, Cr-51	11.01 10:35	768.00	100002	MCA-25
mobile phone(whole)	Mn-56, Na-24, Br-82, W-187, Sb-122, Cu-64, Ni-65, Au-198, La-140	09.30 15:55	5.33	1502	MCA-26
mobile phone (battery)	Co-60, Sb-124, Br-82, Au-198, Sb-122	10.03 18:01	79.43	52602	MCA-27
mobile phone (battery)	Co-60, Sb-124, Au-198	10.17 11:00	408.42	78000	MCA-28

* Elapsed time: Elapsed time after the accident (10:35 Sept. 30, 1999) until the measurement started.

89

Spectra of the measured samples are shown in Data-3 through Data-13. The background spectra of the detector are shown in Data-14 for reference. In background spectra, gamma rays from a component part of the Ge detector, especially peak at 185.72 keV of ^{235}U are marked._Half-life, gamma energy and emission rate of radionuclides which were clearly fission products of uranium are shown in Data-15-1 and Data-15-2. Reference: "Richard B. Firestone: Table of Isotopes. Eighth Edition, John Wiley & Sons, Inc., New York (1998)"

B.d.3. Gamma ray spectrometer (Ge detector)

An Ortec N-type HpGe model BMX-20190, spectroscopy amplifier model 572 and MCA model 7700 were used with ADC 2192ch (0.34 keV/ch) for measurement. As calibration sources, a 20 mm^2-area ^{152}Eu source (16.6 kBq 1989.11.10 of JRIA 8901) and a standard gamma source package (Amersham MIX-SD QCD.1 Source No. 2696QB (37 kBq 1999.05.01)) were used. A structural diagram of the Ge detector and shielding materials are shown in Data-16, and the efficiency curve of the Ge detector is illustrated in Data-17.
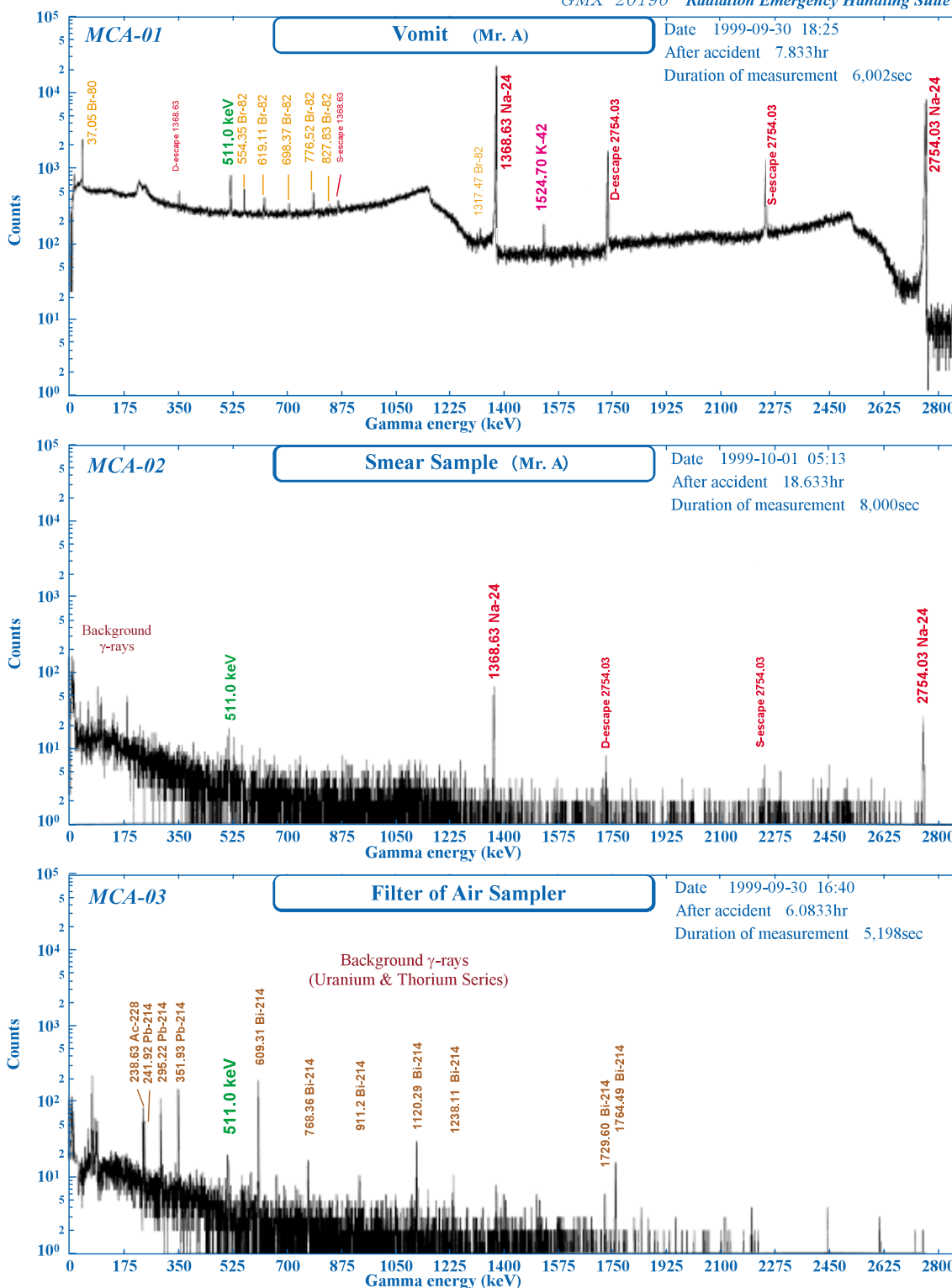
MCA-01 (vomit):   Vomit absorbed by tissue paper in a polyethylene bag was measured inside a styrene container, inside diameter 85 mm x 120 mm. The neutron-activated radionuclides ^{24}Na, ^{82}Br and ^{80}Br were found.

MCA-02 :   Smear sample (Bent cotton stick) measured in a polyethylene bag. Distance between sample and detector: 12 mm. Only ^{24}Na was detected as a radionuclide and no internal exposure was found.

MCA-03 (filter of air sampler) :
   Filter of air sampler used near the mouth was measured. The detected radionuclides were all background nuclides. It was decided that internal exposure by fission products in criticality could be disregarded.

Data-3
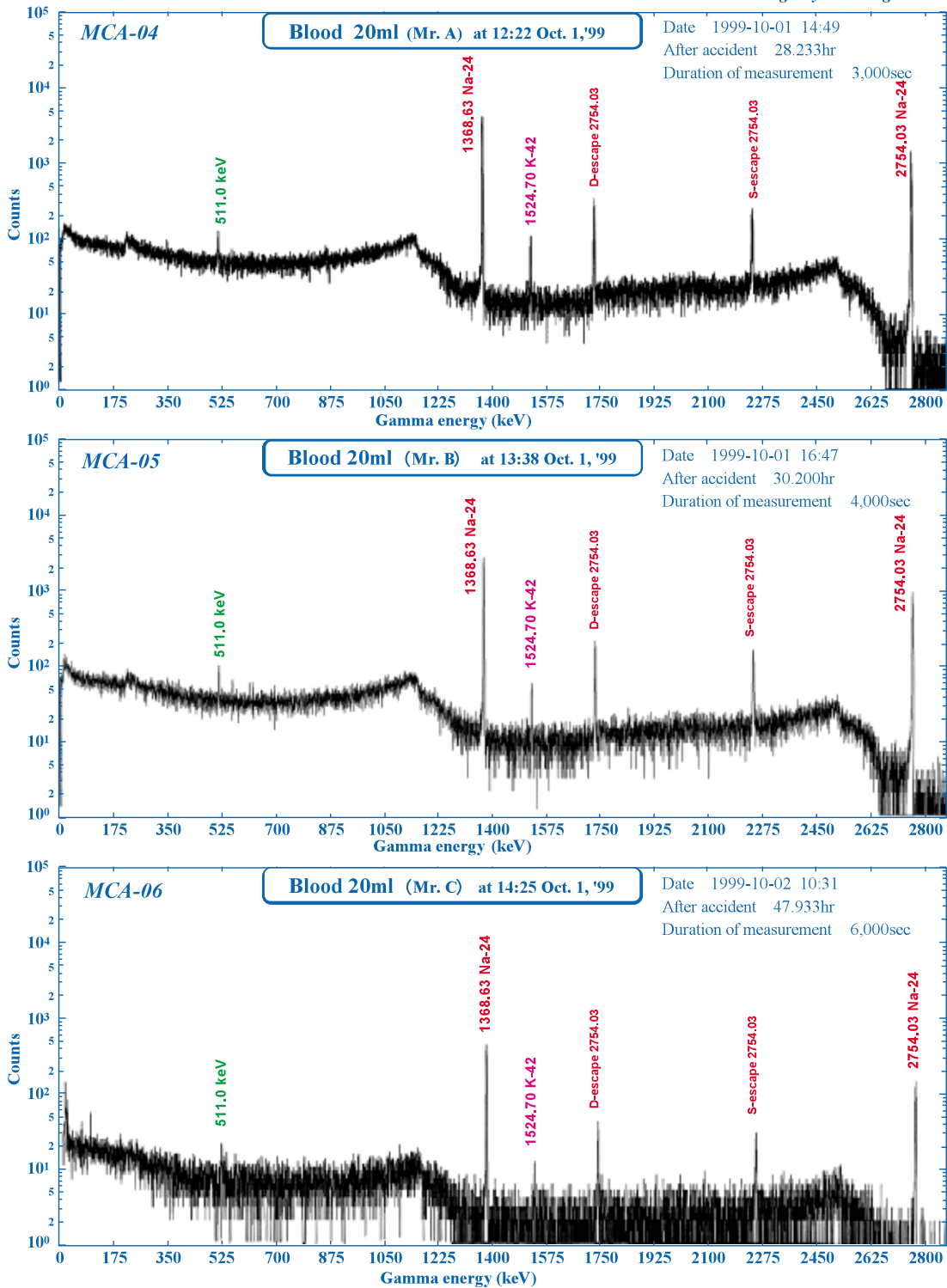
MCA-04 (blood of Mr. A), MCA-05 (blood of Mr. B), MCA-06 (blood of Mr. C):
>   20 ml of blood measured in styrene plastic container (U-8), inside diameter 45 mm x 60 mm. ^{24}Na and ^{42}K were detected as neutron-activated radionuclides

Conditions:
S-D: 10 mm Measurement efficiency: 2,754.0 keV: 0.00463, 1,368.6 keV: 0.00923, 1,524.7 keV: 0.00830
(NIST NG2 Standard Solution was used.)

Details are described in Chapter II, Section D.a of this report.

Data-4

GMX-20190 **Radiation Emergency Handling Suite**
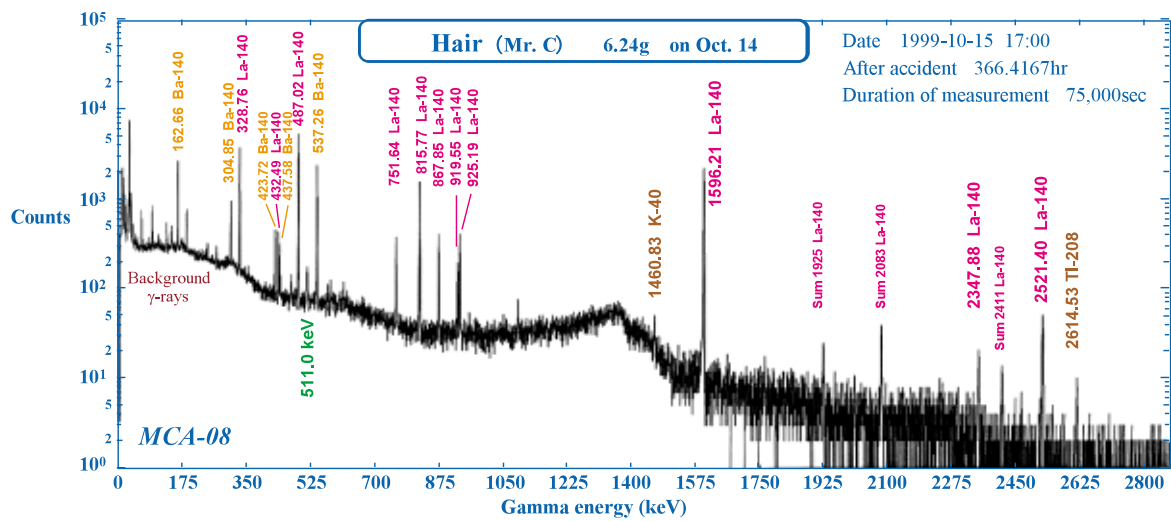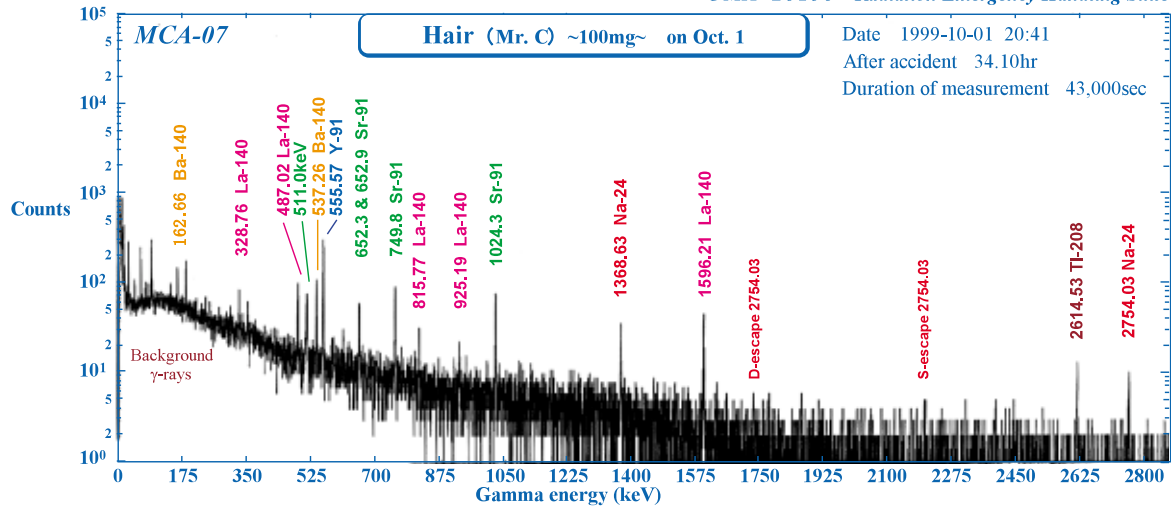
MCA-07 (Hair sample from Mr. C):

    Small amount of hair measured in a polyethylene bag. Distance between sample and detector is 10 mm. The radionuclides; ^{24}Na, ^{140}Ba, ^{140}La, ^{91}Sr and ^{91}Y were found. ^{24}Na was neutron-activated, and the rest were fission products. ^{24}Na was detected from other workers as well.

MCA-08 (Hair sample from Mr. C):

    Fourteen days after the accident, hair (6.24g) was measured in a 4 mm-square container (5 mm x 5 mm) at 15 mm from detector. The radionuclides ^{140}Ba and ^{140}La were found: they appeared to be fission products attached to the hair.

The contamination levels in the hair samples of the other two workers working in the Conversion Building show relatively low readings, since they were wearing helmets.

Data-5
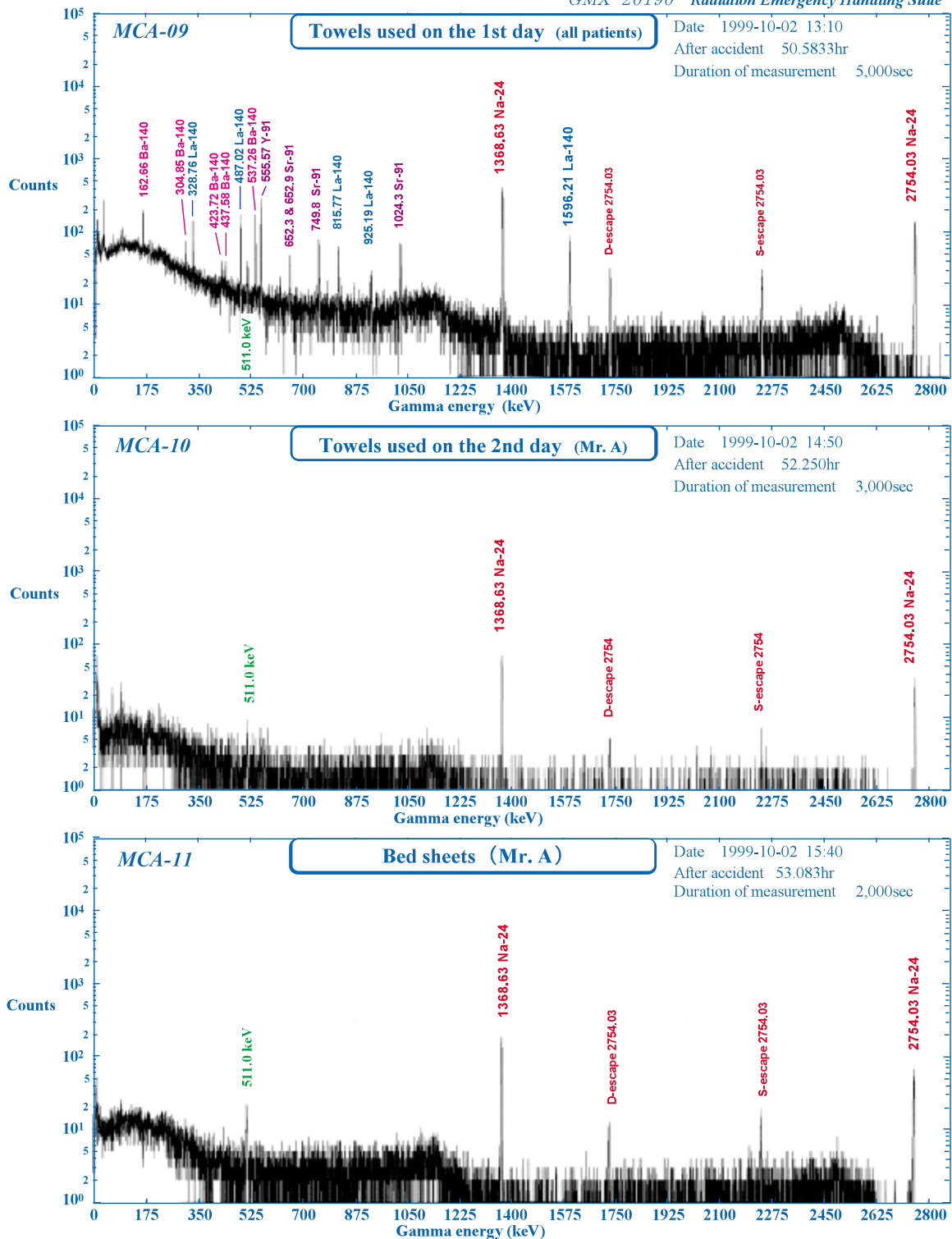
MCA-09 (towels):

    The towels (about 20 pieces) used by three workers on their arrival at the Hospital for Charged Particle Therapy were measured in polyethylene bags (approx. 8 liter in size). The radionuclides ^{24}Na, ^{140}Ba, ^{140}La, ^{91}Sr, ^{91}Y were found. ^{24}Na was the neutron activation product of sweat. The rest were fission products, indicating surface contamination of the bodies.
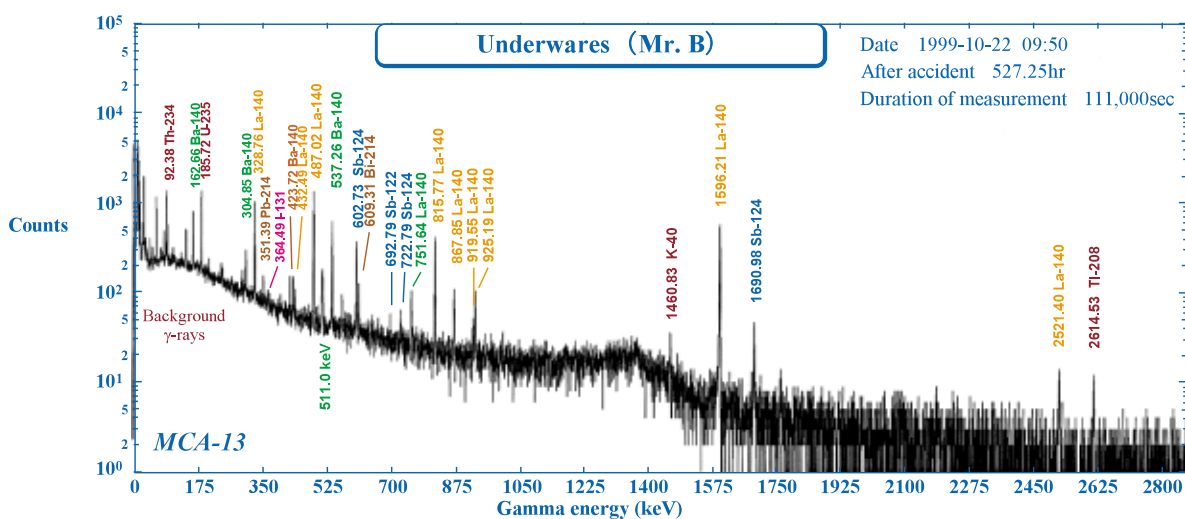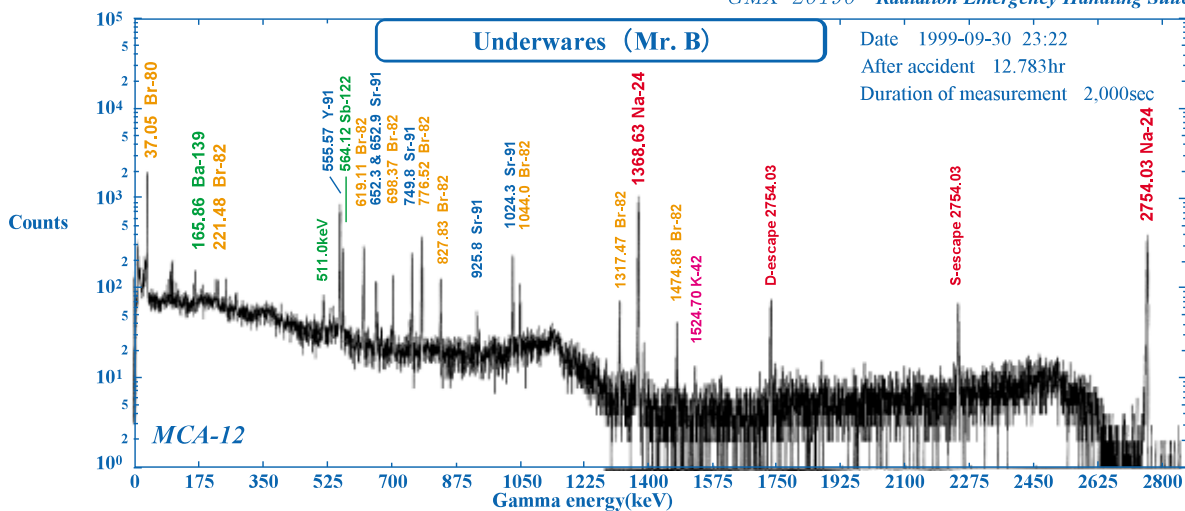
MCA-10 (towels used by Mr. A):

    Towels used by Mr. A on Oct. 2 were measured in polyethylene bags (approx. 3 liters in size). Only the radionuclide ^{24}Na was found, indicating that all surface contamination by fission products had been wiped off by towels on the first day.

MCA-11 (Mr. A's bed sheets):

    The only neutron activation product of ^{24}Na was detected as ^{24}NaCl in sweat.

Data-6

MCA-12 (Mr. B's underwear):

    Underwear worn at the time of the accident and during transportation to the Hospital for Charged Particle Therapy was measured in a styrene container with inside diameter 85 mm x 120 mm.

    The radionuclides ^{24}Na, ^{42}K, ^{80}Br, ^{82}Br, ^{91}Sr, ^{122}Sb and ^{139}Ba were detected.

    The only neutron activation product of ^{24}Na was detected as ^{24}NaCl in sweat; the remainders were fission products.

MCA-13 (Mr. B's underwear): Measured taking into account the time elapsed after the accident.

    The radionuclides ^{140}La, ^{140}Ba, ^{122}Sb, ^{140}Sb and ^{131}I were found as major fission products.
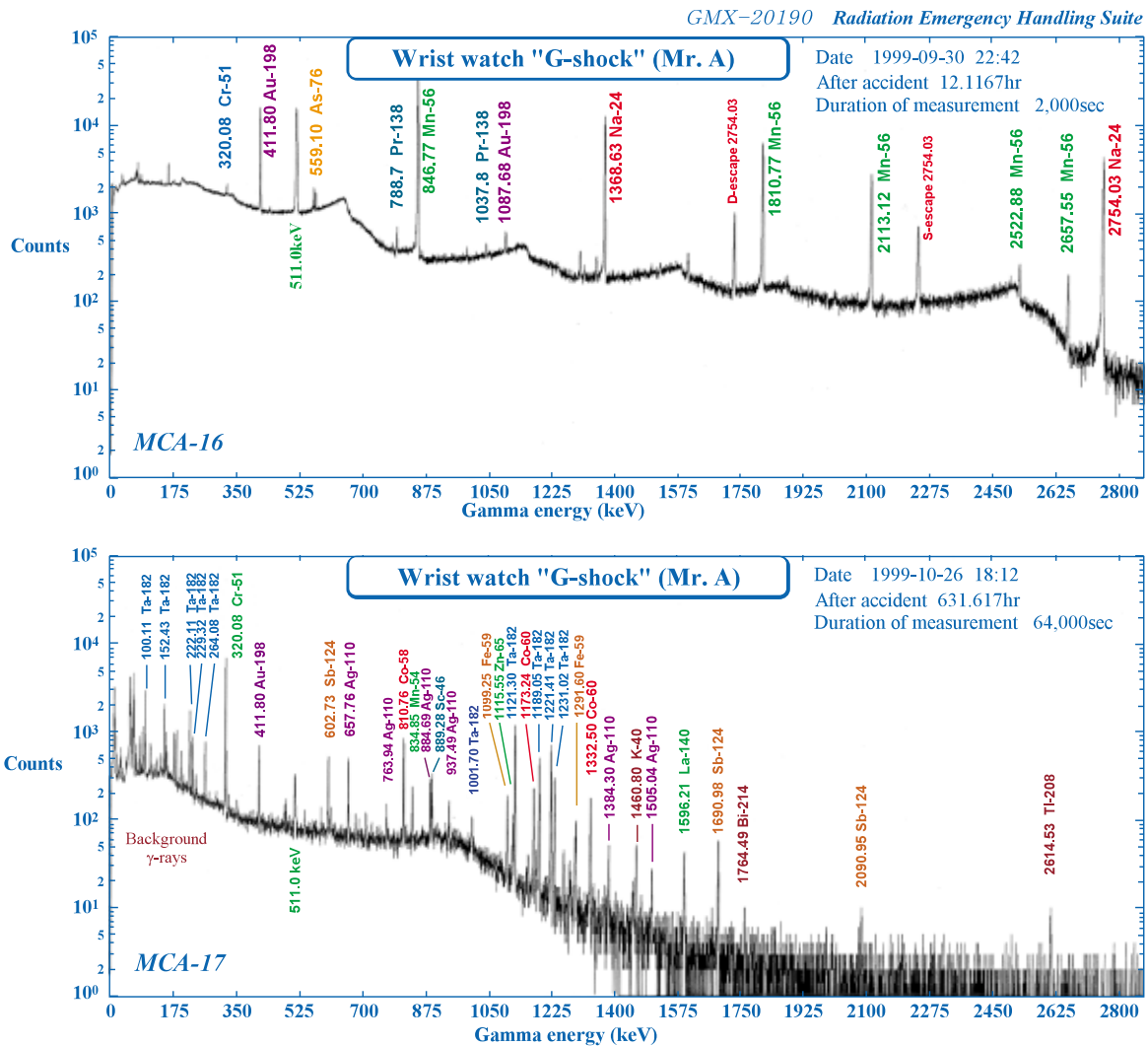
Data-7

95
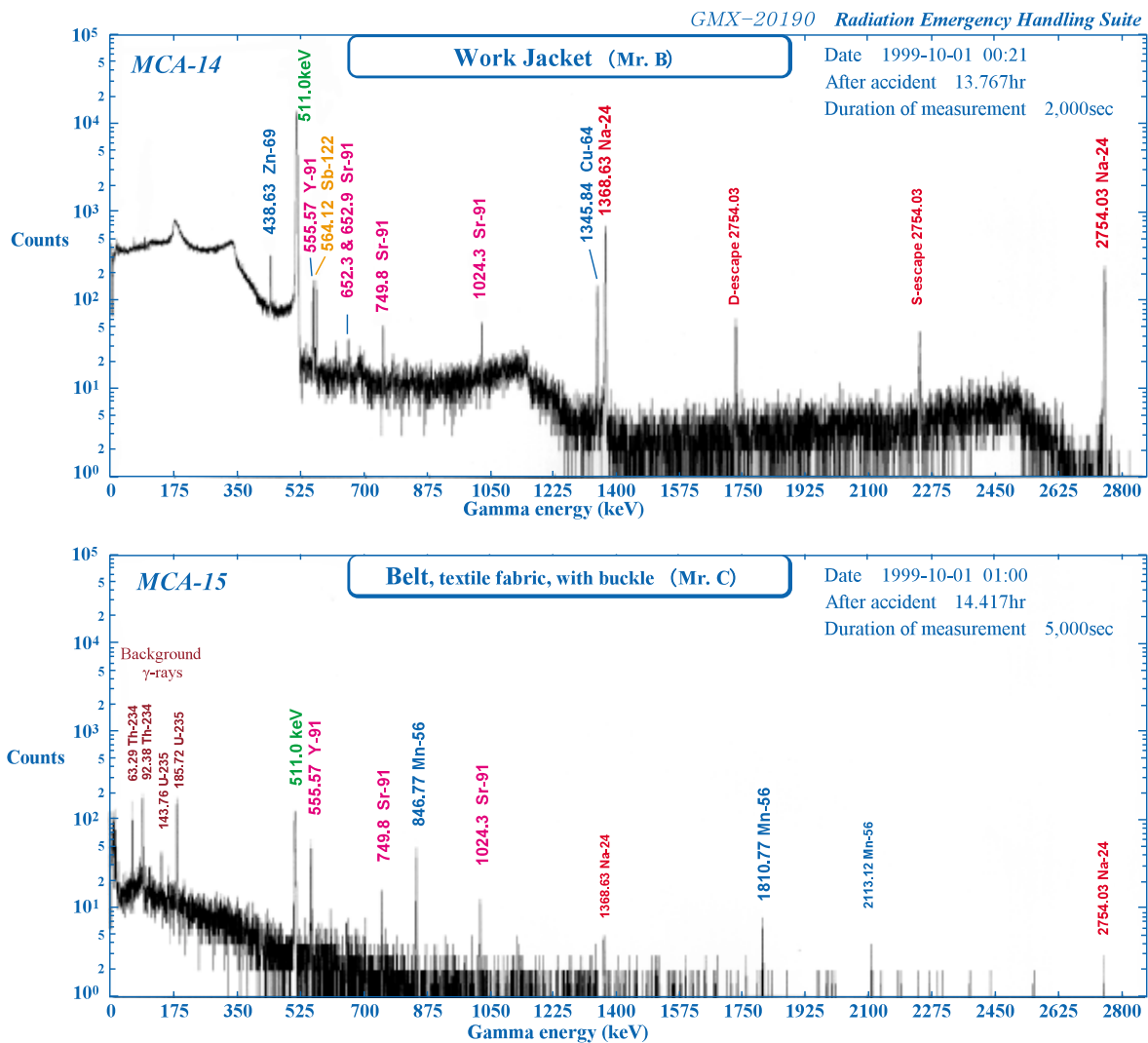
MCA-14 (Mr. B's jacket):

    The jacket was changed after the accident. A jacket kept in a locker at the entrance to the Conversion Building (according to his statement) was measured in a polyethylene bag.

    Radionuclides ^{24}Na, ^{64}Cu, ^{69}Zn, ^{91}Y, ^{91}Sr and ^{122}Sb were found. The radionuclide ^{24}Na, activated by neutron, appeared as ^{24}NaCl in sweat; ^{64}Cu and ^{69}Zn were metallic elements activated by neutrons. The rest were fission products.

MCA-15 (Mr. C's belt):

    A fabric belt with a buckle worn by Mr. C during transportation was measured in a polyethylene bag.

    The radionuclides ^{56}Mn, ^{91}Sr and ^{91}Y were found and ^{56}Mn was neutron activation product of the metal in the buckle. The rest were fission products.

Data-8

GMX–20190 *Radiation Emergency Handling Suite*

Wrist watch "G-shock" (Mr. A)

Date   1999-09-30 22:42
After accident 12.1167hr
Duration of measurement   2,000sec

MCA-16

Wrist watch "G-shock" (Mr. A)

Date   1999-10-26 18:12
After accident 631.617hr
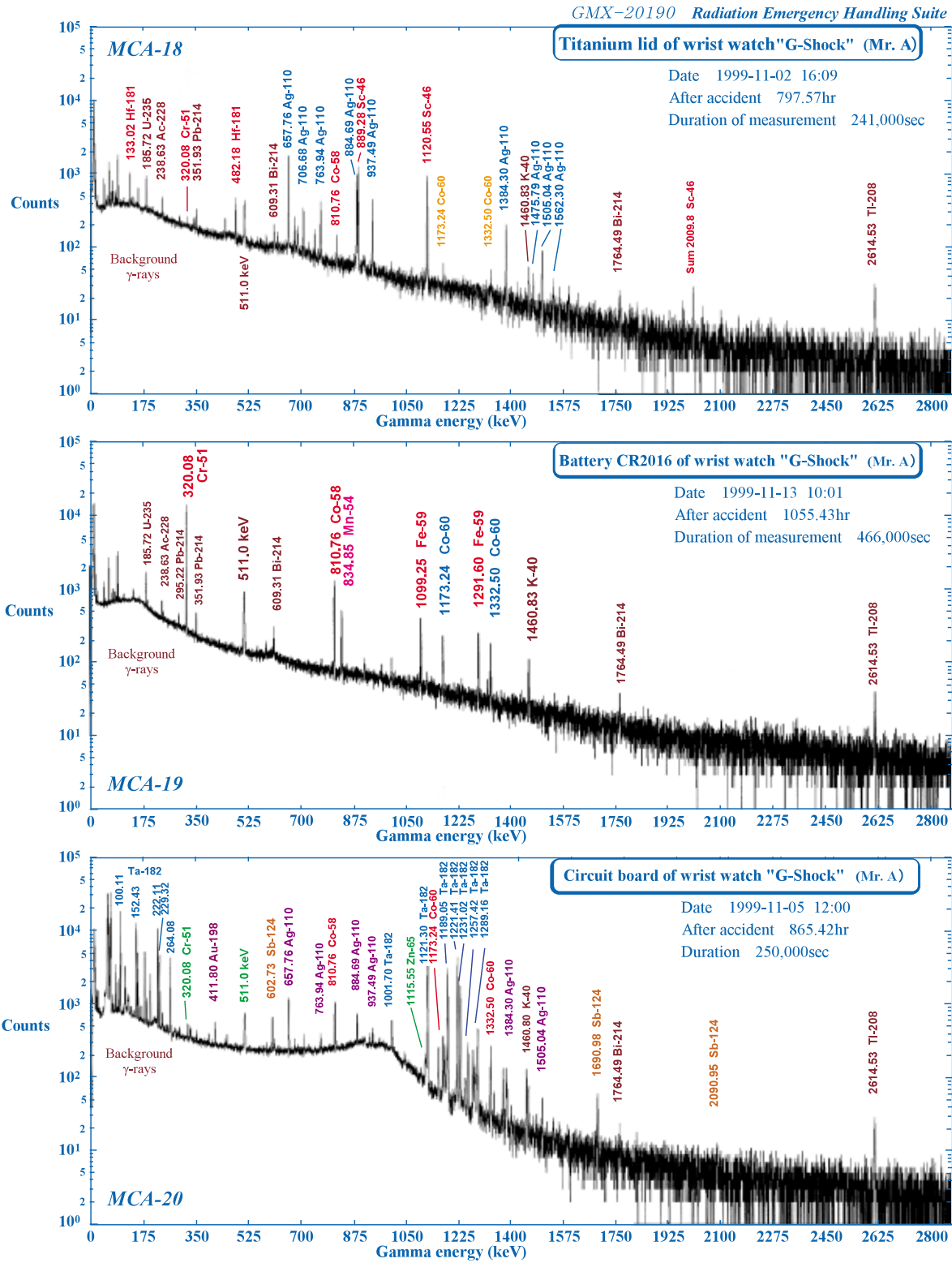Duration of measurement   64,000sec

MCA-17

MCA-16 (Mr. A's wristwatch):

    A wristwatch that Mr. A was confirmed to have been wearing on his wrist at the time of accident) was measured in a polyethylene bag. The watch was a Casio digital quartz G-Shock Fisherman.

    The radionuclides ^{24}Na, ^{56}Mn, ^{198}Au, ^{138}Pr, ^{76}As and ^{51}Cr were found. Metallic elements of component parts activated by neutrons were detected.

    The origin of ^{24}Na might be NaCl in the belt contaminated from the hand.

MCA-17 (Mr. A's wristwatch):

    After the decay of short-lived radionuclides, further measurements revealed radionuclides ^{182}Ta, ^{110}Ag, ^{60}Co, ^{59}Fe, ^{58}Co, ^{54}Mn, ^{51}Cr, ^{65}Zn, ^{198}Au, ^{124}Sb, etc. Those nuclides were neutron activation products of metallic parts in the watch.

    Neither the watch nor its LED was functioning on its arrival.

Data-9

GMX-20190   Radiation Emergency Handling Suite

MCA-18

Titanium lid of wrist watch "G-Shock" (Mr. A)

Date   1999-11-02 16:09
After accident   797.57hr
Duration of measurement   241,000sec

Counts — Gamma energy (keV)

Background γ-rays

Peak labels: 133.02 Hf-181; 185.72 U-235; 238.63 Ac-228; 320.08 Cr-51; 351.93 Pb-214; 482.18 Hf-181; 511.0 keV; 609.31 Bi-214; 657.76 Ag-110; 706.68 Ag-110; 763.94 Ag-110; 810.76 Co-58; 884.69 Ag-110; 889.28 Sc-46; 937.49 Ag-110; 1120.55 Sc-46; 1173.24 Co-60; 1332.50 Co-60; 1384.30 Ag-110; 1460.83 K-40; 1475.79 Ag-110; 1505.04 Ag-110; 1562.30 Ag-110; 1764.49 Bi-214; Sum 2009.8 Sc-46; 2614.53 Tl-208

Battery CR2016 of wrist watch "G-Shock" (Mr. A)

Date   1999-11-13 10:01
After accident   1055.43hr
Duration of measurement   466,000sec

MCA-19

Background γ-rays

Peak labels: 185.72 U-235; 238.63 Ac-228; 295.22 Pb-214; 320.08 Cr-51; 351.93 Pb-214; 511.0 keV; 609.31 Bi-214; 810.76 Co-58; 834.85 Mn-54; 1099.25 Fe-59; 1173.24 Co-60; 1291.60 Fe-59; 1332.50 Co-60; 1460.83 K-40; 1764.49 Bi-214; 2614.53 Tl-208

Circuit board of wrist watch "G-Shock" (Mr. A)

Date   1999-11-05 12:00
After accident   865.42hr
Duration   250,000sec

MCA-20

Background γ-rays

Peak labels: 100.11; 152.43; 222.11; 229.32; 264.08; Ta-182; 320.08 Cr-51; 411.80 Au-198; 511.0 keV; 602.73 Sb-124; 657.76 Ag-110; 763.94 Ag-110; 810.76 Co-58; 884.69 Ag-110; 937.49 Ag-110; 1001.70 Ta-182; 1115.55 Zn-65; 1121.30 Ta-182; 1173.24 Co-60; 1189.05 Ta-182; 1221.41 Ta-182; 1231.02 Ta-182; 1257.42 Ta-182; 1289.16 Ta-182; 1332.50 Co-60; 1384.30 Ag-110; 1460.80 K-40; 1505.04 Ag-110; 1690.98 Sb-124; 1764.49 Bi-214; 2090.95 Sb-124; 2614.53 Tl-208

MCA-18 (backside lid of watch):
 The removed backside lid (made of mainly titanium; approx. 38 mm φ x 1.5 mm, 8.14 g) was measured in a polyethylene bag. The neutron-activated radionuclides ^{46}Sc, ^{110}Ag, ^{181}Hf, ^{51}Cr and ^{60}Co were found.

MCA-19 (watch battery):
 The removed lithium battery (CR2016; 20 mm φ x 1.5 mm) was measured from a distance of 10 mm. The radionuclides ^{51}Cr, ^{58}Co, ^{60}Co, ^{59}Fe and ^{54}Mn were found, and those were neutron activation products of metallic parts of the battery.

MCA-20 (IC board of watch):
 Circuit board (approx. 24 mm φ) was measured from a distance of 10 mm.
 The radionuclides ^{182}Ta, ^{110}Ag, ^{60}Co, ^{198}Au, ^{58}Co and ^{124}Sb were found. Electronic components activated by neutrons were detected. (Ta from tantalum condenser, Ag from residence unit and Au from connecting materials)

Data-10
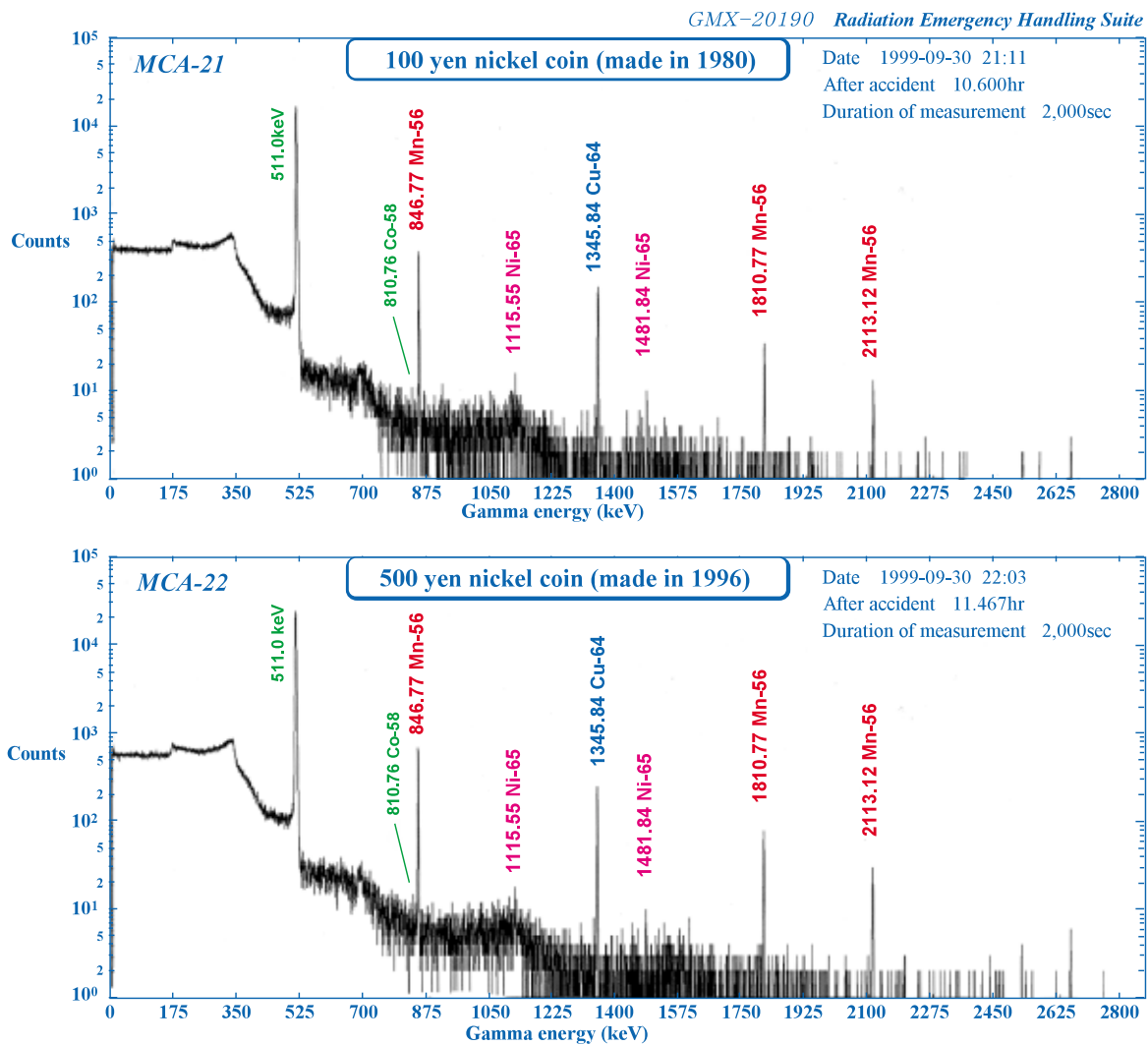
MCA-21 (100 yen coin):

100 yen nickel coin (1980, 22.6 mm φ, 4.72 g) was measured from a distance of 10 mm.
The neutron-activated radionuclides ^{56}Mn, ^{64}Cu, ^{65}Ni and ^{58}Co were found.

MCA-22 (500 yen coin):

500 yen nickel coin (1996; 26.5 mm φ, 7.15 g) was measured from a distance of 10 mm.
The neutron-activated radionuclides ^{56}Mn, ^{64}Cu, ^{65}Ni and ^{58}Co were found.

According to the Mint Bureau, both 100 yen and 500 yen coins consist of Cu: 75.0 wt% and Ni: 25.0 wt%. Other details are kept confidential to prevent forgery. Fluorescent X-ray analysis showed that the 100 yen coin also contained approximately Mn: 0.1 wt%, Si: 0.4 wt%, and the 500 yen coin contained Mn: 0.2 wt%, Si: 1.0 wt%.

Coins like these can be helpful samples for dose estimation if their precise composition and position at the time of accident were known. As for ^{58}Co, another later measurement confirmed its presence.

Estimated activity at the time of the accident:
100 yen nickel coin: ^{56}Mn 850 Bq (± 10%), ^{64}Cu 14.6 kBq (± 5%), ^{65}Ni 180 Bq (± 30%) and ^{58}Co ----.
500 yen nickel coin: ^{56}Mn 1.8 kBq (± 10%), ^{64}Cu 10.4 kBq (± 8%), ^{65}Ni ---- and ^{58}Co 0.18 Bq.

Data-11

GMX−20190 **Radiation Emergency Handling Suite**

Main unit of wrist watch (Rolex) (Mr. C)

Date 1999-10-08 22:06
After accident 203.52hr
Duration of measurement 72,000sec

MCA-23

Stainless lid of wrist watch (Rolex)

Date 1999-10-18 18:00
After accident 439.42hr
Duration of measurement 165,000sec

MCA-24

Battery SR-626SW **of wrist watch** (Rolex)

Date 1999-11-01 10:35
After accident 768.00hr
Duration of measurement 100,002sec

MCA-25

MCA-23 (Mr. C's wristwatch):
  The wristwatch of Mr. C was confirmed to have been wearing on his wrist at the time of the accident was measured in a polyethylene bag. The watch was a Rolex analog quartz.
  The radionuclides ^{51}Cr, ^{198}Au, ^{65}Zn, ^{140}La, ^{110}Ag, ^{140}Ba, ^{60}Co, ^{59}Fe, ^{82}Br and ^{58}Co were found. Neutron-activated metallic elements in component parts were also detected.

MCA-24 (Stainless steel back lid from Mr. C's wristwatch) :
  (approx. 30 mm φ, 2.84 g) was measured from a distance of 10 mm. The radionuclides ^{51}Cr, ^{60}Co, ^{59}Fe, ^{58}Co, ^{140}La, ^{140}Ba, ^{54}Mn, ^{124}Sb, etc. were found. Neutron-activated metallic elements of component parts were detected.

MCA-25 (Wristwatch battery):
  This alkaline button battery (SR-626SW) was measured from a distance of 10 mm. The neutron-activated radionuclides ^{110}Ag, ^{51}Cr, ^{65}Zn, ^{140}La, etc. were found, and neutron-activated component parts of the battery were detected.

Data-12

100

GMX−20190 *Radiation Emergency Handling Suite*

Data-13
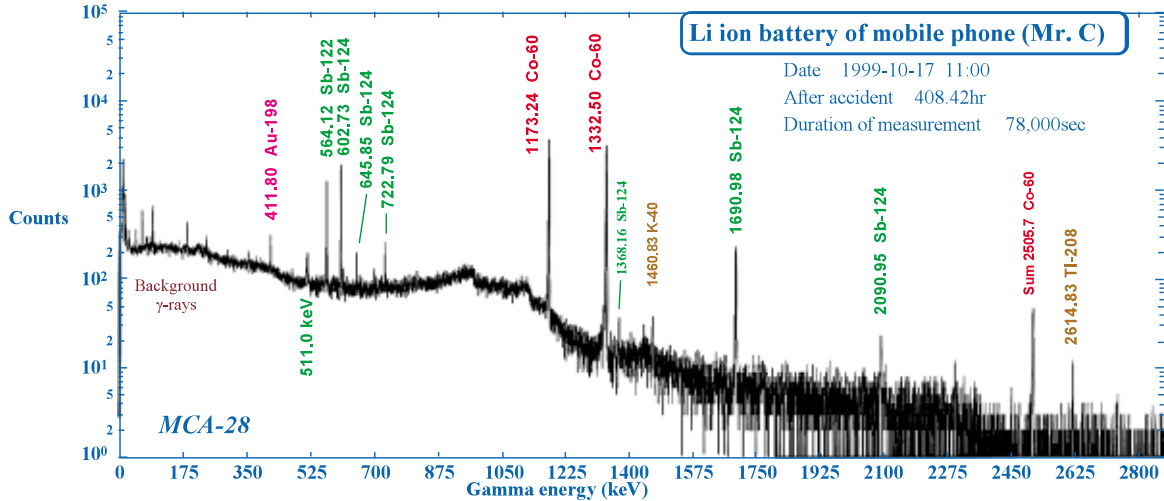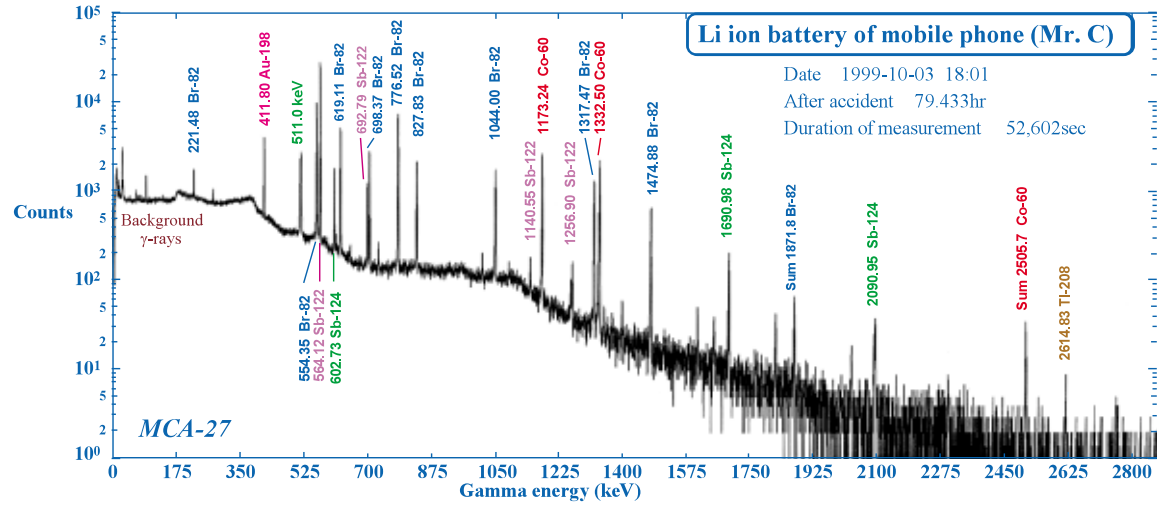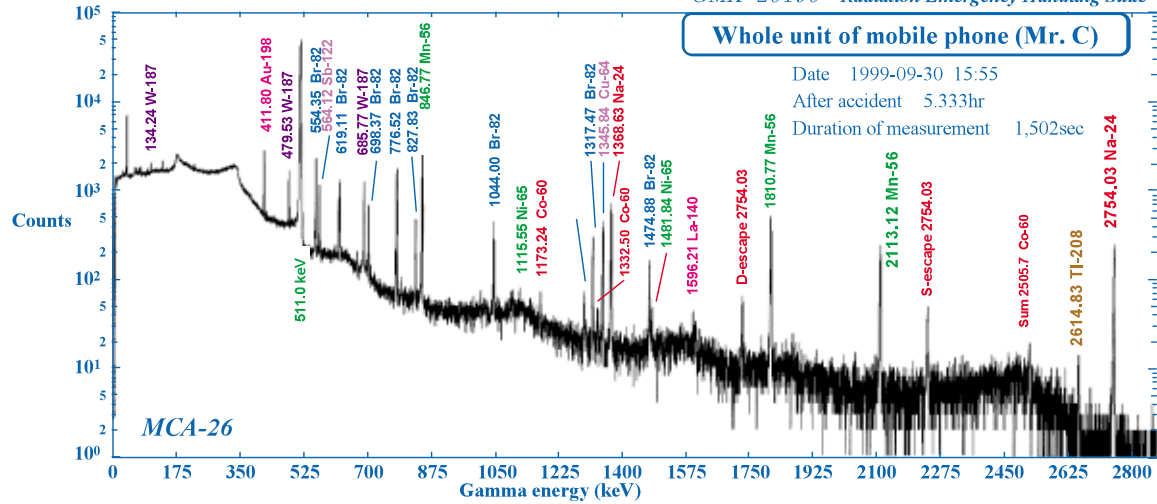
MCA-26 (mobile phone):

The mobile phone present at the Conversion Test Facility at the time of the accident was measured in a polyethylene bag.

The radionuclides ^{24}Na, ^{56}Mn, ^{64}Cu, 187W, ^{198}Au, ^{60}Co, ^{65}Ni and ^{82}Br were found. Neutron-activated metallic elements of component parts were detected.

MCA-27 (Rechargeable battery):

The phone's lithium-ion rechargeable battery (approx. 22 x 45 x 7 mm, 22 g) was measured from a distance of 10 mm. The radionuclides ^{124}Sb, ^{60}Co, ^{82}Br, ^{122}Sb, ^{198}Au, etc. were found. Neutron-activated IC component materials were detected.

MCA-28 (rechargeable battery):

Later measurements using the same method as for MCA-27 revealed the radionuclides ^{60}Co, ^{124}Sb, ^{122}Sb and ^{198}Au. ^{60}Co (with a longer half-life) was detected as neutron-activated LiCoO$_2$ (anode material).

GMX-20190   Radiation Emergency Handling Suite

Background（With shielding materials）

Duration of measurement：
1,105,700sec 1999-12-03

L1:12.95keV Th Lα
L2:16.05keV Th Lβ
L3:19.10keV Th Lγ

K1:74.815keV Bi Kα2
K2:77.107keV Bi Kα1
K3:79.290keV Po Kα1
K4:81.069keV Rn Kα2
K5:83.787keV Rn Kα1
K6:87.349keV Bi Kβ1
K7:89.807keV Po Kβ1

Counts

Gamma energy（keV）

Background（With shielding materials）

Duration of measurement
1,105,700sec 1999-12-03
Total count rate: 4.00cps

Counts

Gamma energy（keV）

Background γ-rays measured by a Ge Detector   [Energies & Intensities]

Uranium Series				Thorium Series				Actinium Series			
Source	Half-life	γ energy (keV)	Intensity (%)	Source	Half-life	γ energy (keV)	Intensity (%)	Source	Half-life	γ energy (keV)	Intensity (%)
234Th	24.10d	63.29	4.84	228Ac	6.13h	129.06	2.42	235U	7.04x10⁸y	109.16	1.54
		92.38	2.81			209.25	3.89			143.76	10.96
		92.8	2.77			270.25	3.46			163.33	5.08
226Ra	1.62x10³y	186.21	3.28			328.07	2.95			185.72	57.2
214Pb	26.8m	241.92	7.46			338.32	11.27			205.31	5.01
		295.22	19.2			463.10	4.4	227Th	18.74d	113.16	0.655
		351.93	37.1			794.95	4.25			235.97	12.13
214Bi	19.9m	609.31	46.1			911.16	25.8			256.25	6.91
		768.35	4.88			964.77	4.99	223Ra	11.435d	269.46	13.7
		934.06	3.16			968.97	15.8	219Rn	3.96s	271.23	10.8
		1120.29	15.0			1588.23	3.22	211Pb	36.1m	427.09	1.76
		1238.11	5.92	212Pb	10.64h	238.63	43.60			832.01	3.52
		1377.67	4.02			300.09	3.34				
		1407.98	2.48	212Bi	1.0092h	727.33	6.65				
		1509.23	2.19			1620.56	1.51	Source	Half-life	γ energy (keV)	Intensity (%)
		1729.58	3.05	208Tl	3.053m	277.36	2.27	40K	1.277x10⁹y	1460.83	10.67
		1764.49	15.9			510.77	8.13	(Annihilation radiation)		511.0	
		2204.21	4.99			583.19	30.36				
		2447.86	1.55			860.56	4.47				
210Pb	22.3y	46.54	4.25			2614.53	35.64				

Background gamma radiation
1. 511 keV: Annihilation radiation produced in the process of extinction of positrons originating in cosmic rays or high-energy gamma rays.
2. 1,460.8 keV ± 40 keV: From concrete used as construction material.
3. Component parts of Ge detector contain aluminum, stainless steel, copper, lead, etc. Naturally radioactive isotopes (232Th, 238U, 235U and their progenies) were detected in the aluminum and lead. Gamma rays from 235U, 234Th, etc. near the detector are found after shielding against indoor radon or gamma rays from construction materials. They cannot be clearly detected without shielding from ambient sources.
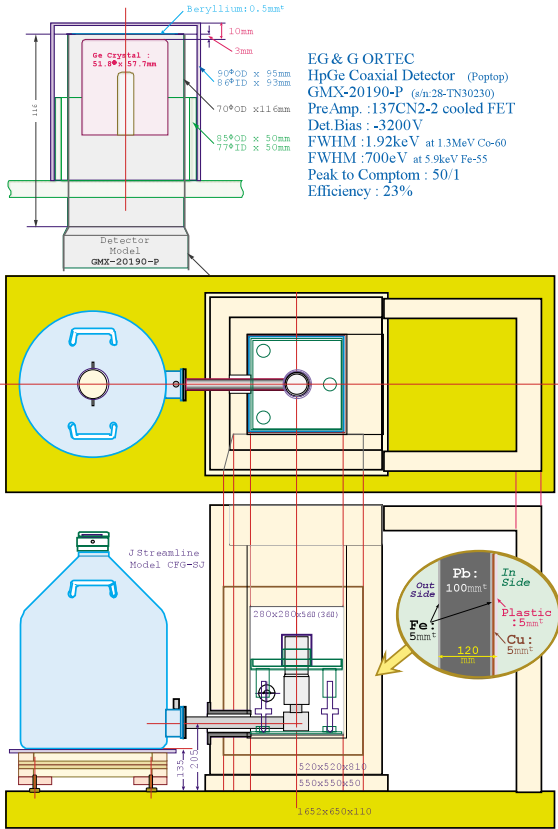
Data-14

Nuclides	Half life	Decay mode	Means of production
γ energy(keV)		Intensity(%)	

As-76 25.867hr β⁻ ⁷⁶As(n,γ)
559.10 (45.)
657.04 (6.2)
1216.10 (3.42)
Br-80 4.4205hr IT ⁷⁹Br(n,γ)
37.05 (39.1)
Br-82 35.30hr β⁻ ⁸¹Br(n,γ)
221.48 (   )
554.35 (70.8)
619.11 (43.4)
698.37 (28.49)
776.52 (83.5)
827.83 (   )
1044.00 (27.23)
1317.47 (   )
1474.88 (   )
Sr-91 9.63hr β⁻ U(n,f)
620.1 (   )
652.3 (2.97)
652.9 (8.0)
749.8 (23.61)
925.8 (3.84)
1024.3 (33.)
Y-91 58.51d β⁻ U(n,f)
555.57 (94.9) IT:49.7min
1204.77 (0.3)
Ag-110 249.79d β⁻ ¹⁰⁹Ag(n,γ)
446.81 (   )
620.36 (   )
657.76 (94.0)
677.62 (   )
687.02 (   )
706.68 (   )
744.28 (   )
763.94 (22.14)
818.03 (   )
884.69 (72.2)
937.49 (34.13)
1384.30 (24.12)
1475.79 (   )
1505.04 (   )
1562.30 (   )
Sb-122 2.7238d EC+β⁺ ¹²¹Sb(n,γ)
1140.55 (0.76)
Sb-122 2.7238d β⁻ ¹²¹Sb(n,γ)
564.12 (71.)
692.79 (3.85)
1256.90 (0.81)
Sb-124 60.20d β⁻ ¹²³Sb(n,γ)
602.73 (98.26)
645.85 (7.456)
713.78 (   )
722.79 (10.81)
1368.16 (   )
1690.98 (47.79)
2090.95 (5.51)
I-131 8.0207d β⁻ ¹³⁰Te(n,γ)¹³¹Te
80.19 (2.62) ¹³¹Te->¹³¹I
284.31 (6.14) U(n,f)
364.49 (81.7)
636.99 (7.17)
722.91 (1.773)
Pr-138 2.12hr EC+β⁺
302.7 (80.)
390.9 (6.1)
547.5 (5.23)
788.7 (100.)
1037.8 (101.)
Ba-139 83.06min β⁻ ¹³⁹La(n,p)
165.86 (23.7) U(n,f)
1420.5 (0.26)
Ba-140 12.752d β⁻ U(n,f)
29.96 (14.1)
162.66 (6.22)
304.85 (4.29)
423.72 (3.15)
437.58 (   )
537.26 (24.39)
La-140 1.6781d β⁻ ¹³⁹La(n,γ)
328.76 (20.3) U(n,f)
432.49 (   )
487.02 (45.5)
751.64 (   )
815.77 (23.28)
867.85 (   )
919.55 (   )
925.19 (6.90)
1596.21 (95.4)
2347.88 (   )
2521.40 (   )

Na-24 14.959hr β⁻ ²³Na(n,γ)
1368.63 (100.)
1732.03 (D-Escape 2754)
2243.03 (S-Escape 2754)
2754.03 (99.944)
K-42 12.360hr β⁻ ⁴¹K(n,γ)
312.6 (0.336)
1524.70 (18.)
Sc-46 83.79d β⁻ ⁴⁵Sc(n,γ)
889.28 (99.984) ⁴⁶Ti(n,p)
1120.55 (99.987)
Cr-51 27.702d EC ⁵⁰Cr(n,γ)
320.08 (10.)
Mn-54 312.3d β⁻ ⁵⁴Fe(n,p)
834.85 (99.976) ⁵⁵Mn(n,2n)
Mn-56 2.5785hr β⁻ ⁵⁵Mn(n,γ)
846.77 (98.9) ⁵⁶Fe(n,p)
1810.77 (27.2)
2113.12 (14.3)
2522.88 (0.99)
2657.55 (0.653)
Co-58 70.82d EC+β⁺ ⁵⁸Ni(n,p)
810.76 (99.) ⁵⁹Co(n,2n)
Fe-59 44.503d β⁻ ⁵⁸Fe(n,γ)
142.65 (1.02) ⁵⁹Co(n,p)
192.35 (3.08)
1099.25 (56.5)
1291.60 (43.2)
Co-60 5.2714y β⁻ ⁵⁹Co(n,γ)
1173.24 (99.974) ⁶⁰Ni(n,p)
1332.50 (99.986) ⁶³Cu(n,α)
Cu-64 12.70hr EC+β⁺ ⁶³Cu(n,γ)
1345.84 (0.473) ⁶⁵Cu(n,2n)
Ni-65 2.5172hr IT ⁶⁸Zn(n,γ)
366.27 (4.81)
1115.55 (15.43)
1481.84 (24.)
Zn-65 244.26d EC+β⁺ ⁶⁴Zn(n,γ)
1115.55 (50.60)
Zn-69 13.76hr EC ⁶⁸Zn(n,γ)
438.63 (94.77)
Hf-181 42.39d β⁻
133.02 (43.3)
345.92 (15.12)
482.18 (80.50)
Ta-182 114.43d β⁻ ¹⁸¹Ta(n,γ)
67.75 (41.2)
84.68 (   )
100.11 (14.10)
152.43 (   )
156.39 (   )
179.40 (   )
222.11 (   )
229.32 (   )
264.08 (   )
1001.70 (   )
1121.30 (34.9)
1189.05 (16.23)
1221.41 (26.98)
1231.02 (   )
1257.42 (   )
1289.16 (   )
W-187 23.72hr β⁻ ¹⁸⁶W(n,γ)
72.00 (11.14)
134.24 (8.85)
479.53 (21.8)
551.52 (   )
618.26 (   )
685.77 (27.3)
772.89 (   )
Au-198 2.69517d β⁻ ¹⁹⁷Au(n,γ)
411.80 (96.)
675.88 (0.804)
1087.68 (0.159)

Data-15

## A.d.3. Gamma ray spectrometer (Ge detector)

Ortec N-type HpGe model BMX-20190, spectroscopy amplifier model 572 and MCA model 7700 were used with ADC 2192ch (0.34 keV/ch) for measurement. As calibration sources, a ^{152}Eu 20 mm^2-area JRIA8901 source (16.6 kBq 1989.11.10) and standard Amersham MIX-SD QCD.1 gamma source package, Source No. 2696QB (37 kBq, 1999.05.01) were used. A structural diagram of the Ge detector and the shielding materials is shown in Data-16, and the efficiency curve of Ge detector is illustrated in Data-17.

Radiation Emergency Handling Suite
  Detecting structure of Ge gamma spectrometer

Data-16
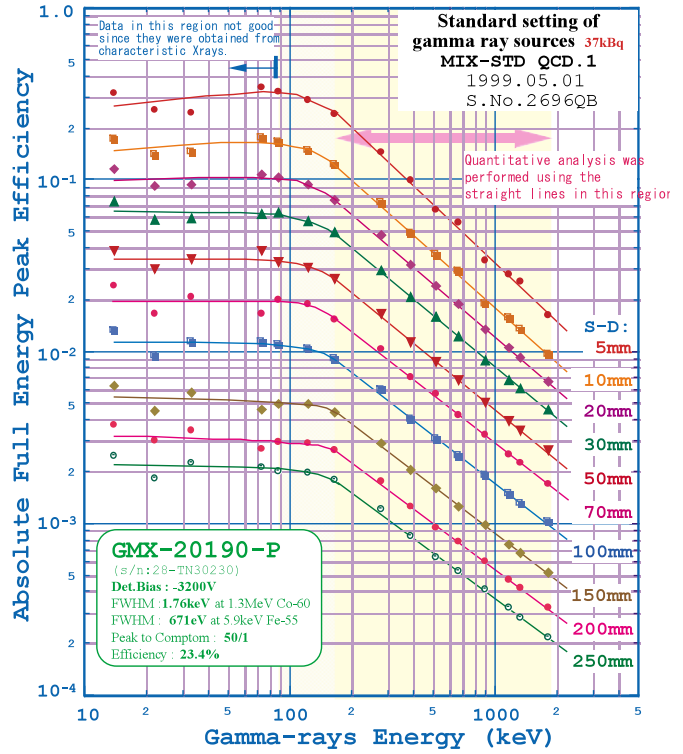
Calibration source : QCD.1 Source No.2696QB
           Reference   Date : 1 May 1999

Radionuclide	Gamma-ray Energy(keV)	Gamma-rays per second
Cd-109	88.03	861
Co-57	122.1	782
Ce-139	165.9	897
Hg-203	279.2	2650
Sn-113	391.7	2820
Sr-85	514.0	5217
Cs-137	661.7	3364
Y-88	898.0	8512
Co-60	1173	4512
Co-60	1333	4515
Y-88	1836	8998

Standard source (flat disk), 9 radionuclides were mixed in it, was settled on the center shaft of detector. Efficiency curve was given in above figure as a function of the distance between the detector and source placed on axis.
The regression lines of the efficiency obtained by least square fitting in the energy range of 150keV~2000keV are shown in the right bottom table.

Efficiency Calibration Equation
Gamma-ray Energy 150keV< γ(keV) < 2000keV

S-D: 5mm Eff. = 78.866 * γ(keV)^(-1.1264)   R^2= 0.99693
S-D: 10mm Eff. = 28.299 * γ(keV)^(-1.065)   R^2= 0.99901
S-D: 20mm Eff. = 14.234 * γ(keV)^(-1.0218)   R^2= 0.9987
S-D: 30mm Eff. = 8.1686 * γ(keV)^(-1.0005)   R^2= 0.99995
S-D: 50mm Eff. = 3.8367 * γ(keV)^(-0.97328)   R^2= 0.99936
S-D: 70mm Eff. = 1.9157 * γ(keV)^(-0.93698)   R^2= 0.99644
S-D:100mm Eff. = 1.0369 * γ(keV)^(-0.92681)   R^2= 0.99804
S-D:150mm Eff. = 0.46457 * γ(keV)^(-0.9077)   R^2= 0.99842
S-D:200mm Eff. = 0.25378 * γ(keV)^(-0.89025)   R^2= 0.99878
S-D:250mm Eff. = 0.17095 * γ(keV)^(-0.8896)   R^2= 0.99836

Data-17

B. Chemical analysis

Introduction

A part of the hair and urine samples obtained from the three workers who were exposed to high radiation were measured by the Japan Chemical Analysis Center (JCAC) to crosscheck the measurements by NIRS using a low background beta ray spectrometer and liquid scintillator. A box of matches in an ordinary house about 120 m from the precipitation tank where the accident occurred was also analyzed by JCAC to obtain information on fast neutron fluence. Tasks carried out in JCAC included chemical analysis to obtain the concentration of the stable isotopes of phosphorus, sulfur,

sodium, potassium, and calcium and measurement of ^{32}P radioactivity concentration. The following is the report submitted by JCAC for our request of the measurements.

B.a. Analysis

B.a.1. List of samples and analysis items

Table B.1 lists samples used by JCAC and items of analysis. Part of the workers' hair obtained by NIRS was used by JCAC as analysis samples. Urine samples were collected from Mr. A during the period from October 2 to 3, 1999.

Table B.1 Samples and analyzed isotopes

Sample	Date of sample received	Analyzed isotope
Mr. A Right head hair	Oct. 12, 1999	^{32}P, P, S
Mr. A Left head hair	Oct. 12, 1999	^{32}P, P, S
Mr. B head hair	Oct. 12, 1999	^{32}P, P, S
Mr. C head hair	Oct. 18, 1999	^{32}P, P, S
Mr. A Urine	Oct. 18, 1999	^{32}P, P, Na, K, Ca
Match head	Oct. 21, 1999	^{32}P, P, S
Matchbox striking surface	Oct. 25, 1999	^{32}P, P, S

^{32}P : radiochemical analysis of ^{32}P
P : elementary analysis of phosphorus
S : elementary analysis of sulfur
Na : elementary analysis of sodium
K : elementary analysis of potassium
Ca : elementary analysis of calcium

B.a.2 Analysis period

The samples listed above were analyzed by JCAC between October 16 and November 5, 1999.

B.b. Analytical method

B.b.1. Preparation of samples

1) Hair

Hair samples offered by NIRS were used as samples as they are for analysis.

2) Urine

Urine samples (freeze-dried) provided by NIRS were dissolved by adding water. Samples diluted with a fixed amount (100 ml) were then used for analysis.

3) Matches

The heads of the matches were removed from the sticks using a sharp knife and the heads used as analysis samples. The striking surfaces of the matchboxes were also cut off together with the underlying paper and then shredded for analysis.

B.b.2. Decomposition of samples

1) Hair and matches

Each sample in varying amounts of 0.5 to 3 g was placed in an airtight stainless steel container into which sodium hydrate, an absorbent had been previously placed. Oxygen was injected into the container and the sample burned. After cooling, the sodium hydrate was poured into a test tube and mixed with cleansing water of the container. Hydrochloric acid was added to this mixture to neutralize the sample and the volume adjusted to 250 ml. Of this solution, 200 ml was subjected to analysis for ^{32}P and the remaining to analysis for P and S.

2) Urine

A 30 ml portion of urine was mixed with sulfuric acid, nitric acid, and aqueous hydrogen peroxide solution. The mixture was then heated to decompose its organic content. Water was added to adjust the quantity to 50 ml for use as ^{32}P analysis sample solution. Another 30 ml portion was also mixed with nitric acid and aqueous hydrogen peroxide solution and heated to decompose its organic content. Water was then added to adjust the volume to 50 ml for use as samples for analysis of P, Na, K, and Ca.

B.b.3. Analysis of ^{32}P

1) ^{32}P sample solution (a 5 ml portion of urine sample) was mixed with a phosphorus carrier (PO_4^{3-}), iron and cobalt carrier. The mixture was heated and condensed into

a solution with a volume of about 40 ml.

2) After the insoluble contents in the solution had been filtered out, phosphorus was isolated as phosphorus ammonium molybdate precipitate. After precipitation, ammonia solution was added for dissolution to carry out re-precipitation of the phosphorus ammonium molybdate. Ammonium phosphate magnesium was then precipitated out. The precipitate was placed on filter paper for use as a sample for beta-ray measurement.

3) Beta-ray measurement samples were measured for 100 minutes using the low background beta ray spectrometer.

4) Measured samples were dissolved in hydraulic acid and diluted. The diluent was then measured for emission intensity using an ICP emission analyzer to determine the recovery percentage of phosphorus.

5) The net counting rates of measurement samples were then calculated. Radioactivities were calculated by making appropriate corrections, such as counting efficiency and chemical recovery, to the net counting rates. Analysis results were adjusted by decay correction at 10:30 am on September 30, 1999.

B.b.4. Analysis of phosphorus (P)

1) Urine and matches
    To determine the quantity of phosphorus present, phosphorus analysis sample solutions were placed in an ICP emission analyzer, as they were or diluted, to measure the emission intensity of phosphorus.

2) Hair
    A portion of phosphorus analysis sample solution was mixed with ammonium molybdate solution and tin chloride solution, and adjusted to a fixed volume. The solution was then measured for absorbency at 700 nm by spectrophotometer to determine the quantity of phosphorus (molybdenum blue absorption photometry).

B.b.5. Analysis of sulfur

    A dilution of the S analysis sample solution was measured using ion chromatography to determine the quantity of sulfate ions present. The concentration of sulfur was then calculated from the concentration of sulfate ions.

B.b.6. Analysis of sodium, potassium and calcium

    Dilutions of Na, K, and Ca sample solutions were measured by ICP emission analyzer for emission intensity of phosphorus to determine the quantity of sodium, potassium, and calcium.

B.b.7. Measuring equipment

1) ^{32}P
Low background beta ray spectrometer, Aloka LBC-471Q

2) Phosphorus
    ICP emission spectral analyzer, Perkin Elmer OPTIMA 3300XL
Spectrophotometer, Hitachi U-2000A

3) Sulfur
    Ion chromatograph. Yokokawa Analytical Systems IC7000

4) Sodium, potassium and calcium
    ICP emission spectral analyzer, Perkin Elmer Optima 3300XL

B.c. Analytical results

Table B.2.(a) Analytical results of contents and radioactivity

Sample	Sulfur (mg g^{-1})	Phosphorus (mg g^{-1})	^{32}P	
			Measurement date	Radioactivity (Bq g^{-1})
Mr. A Right head hair	29	0.12	Oct.25, 1999	1.8 $\pm$ 0.04
Mr. A Left head hair	28	0.11	Oct.25, 1999	1.0 $\pm$ 0.03
Mr. B Head hair	37	0.12	Oct.25, 1999	1.9 $\pm$ 0.08
Mr. C Head hair	32	0.11	Oct.26, 1999	0.34 $\pm$ 0.021
Mr. A Urine	--	1.2 mg ml^{-1}	Oct.30, 1999	2.0 $\pm$ 0.09 Bq ml^{-1}
Match head	52	<0.06	Oct.19, 1999	(-0.009 $\pm$ 0.012)*
Matchbox striking surface	2.3	16	Oct.19, 1999	(0.009 $\pm$ 0.019)*

Notes:
1. Errors in the ^{32}P analysis results are counting errors (1s). When the count is less than three times its counting error, a * mark is attached, with the count shown in parentheses.
2. The analysis results of ^{32}P are the values as of 10:30 a.m. on September 30, 1999.

Table B.2. (b) Analytical results of urine sample of Mr. A

Sample	Sodium (mg ml^{-1})	Potassium (mg ml^{-1})	Calcium(mg ml^{-1})
Urine of Mr. A	0.61	1.1	2.0

B.d. Discussion of the results

The Dose Estimation Working Group for Three Victims received the above analysis results from JCAC and compared them with the measurements made in NIRS. Fig. B.1 shows the activity reduction due to decay of ^{32}P in the measurement samples. The straight line drawn over the Figure is an estimation based on the half-life of ^{32}P. Since the measurement points vary along the line, it is clear that no other nuclides were present during the measurements and that ^{32}P alone was measured. Next, Fig. B.2 shows the counting efficiency of ^{32}P, while Fig. B.3 to Fig. B.5 show the analytical curve for determination of each element. Although no detailed description of dilution rate is available, it is assumed that sample solutions were diluted to a factor of 10 to 50 in order to place the measurements within the range of these curves. The results of determinations using these analytical curves are given in Table B.2. (a) and (b). When these results were compared with the data shown in Chapter III, which are discussed briefly in Chapter III Section B for hair samples, significant differences were found in general. One exception is the concentration of sulfur in the hair, as shown in Table III.B.4, which shows relatively good agreement. Another exception is the concentration of sodium and potassium in the urine samples, shown in Table III.D.2, which also show relatively good agreement, in spite of the sampling dates being different. For phosphorus concentration in hair shown in Table III.B.2, the difference between the two sets of data is a factor of two. The difference in

phosphorus concentration in the urine is greater, although the sampling dates are different (See Table III.D.2). On the other hand, in comparison with the ^{32}P concentrations shown in Table III.B.4, the values in Table B.2.(a) are all lower, with some showing an approximately four-fold difference. For ^{32}P in urine samples taken at different dates, the value of Table B.2. (a) is less than one third than the results obtained in NIRS. In NIRS the results for ^{32}P in urine samples provided by the low background beta ray spectrometer, shown in Table III.D.2, are in relatively good agreement with those from the liquid scintillation counter shown in Table III.D.4.

There is no knowing what exactly caused these differences, but NIRS also measured comparison standard materials using ICP-AES and found a good agreement between these and other data. In addition, the measurement values of ^{32}P as measured by the low background beta ray spectrometer and by the liquid scintillation counter by different measuring staff are in good agreement with each other. These facts suggest that the results of Table B.2. (a) are influenced by any serious bias.

We also examined whether it is possible to evaluate dose by using the concentration of ^{32}P in matchsticks, as shown in Table B.2. (a), but no ^{32}P could be detected. This is probably because, even though there is a relatively high phosphorus and sulfur content in match heads, the matches used for analysis were located too far away from the precipitation tank to be reached by the neutrons emitted during the accident.
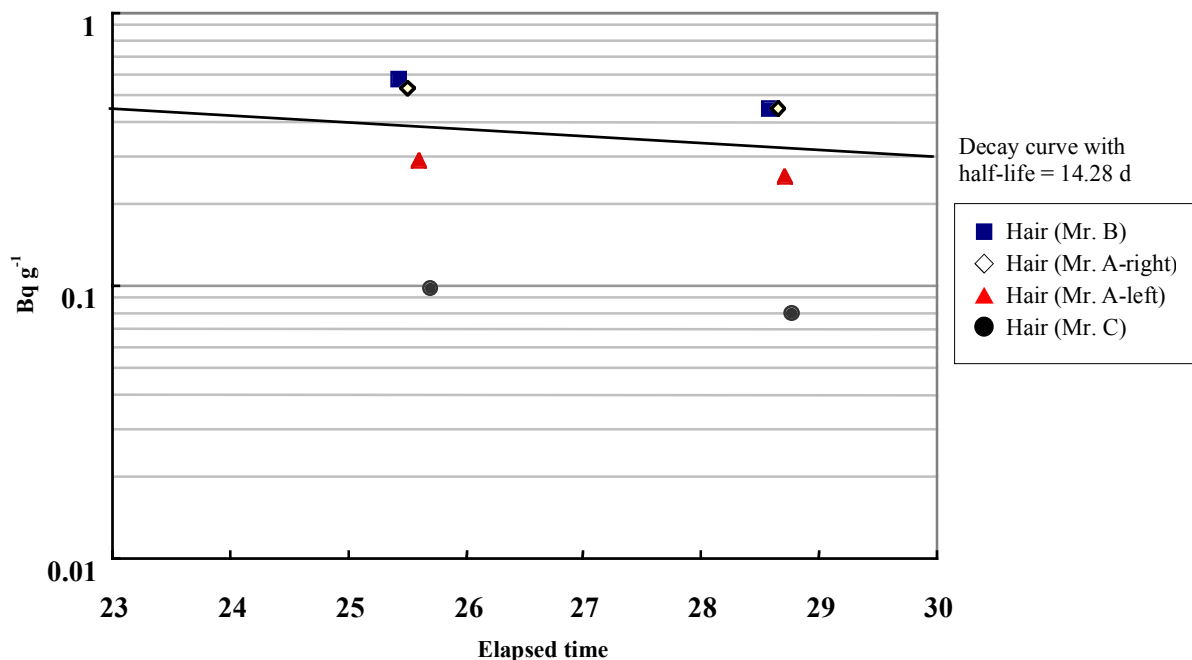

Fig. B.1 Decay of ^{32}P in measurement samples
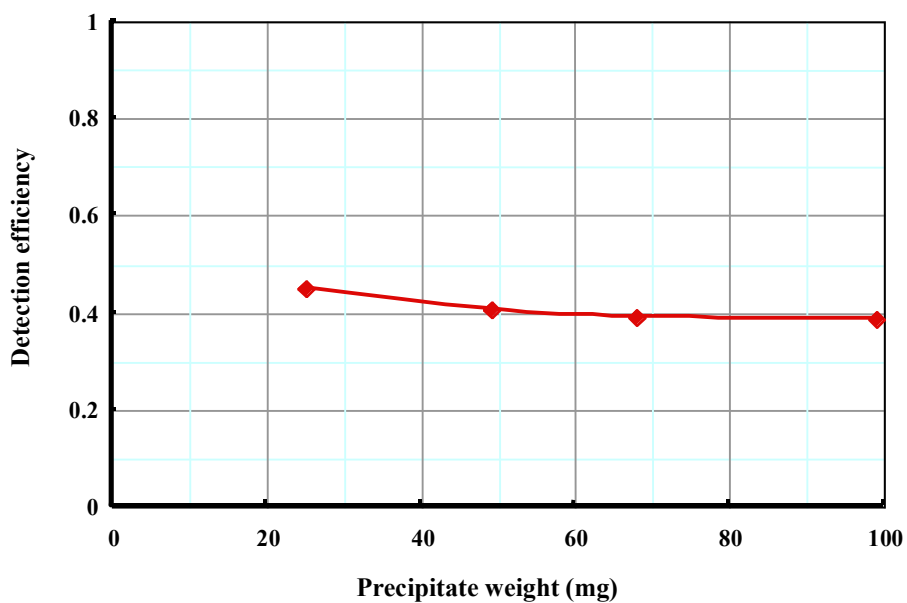
Fig. B.2 Detection efficiency of low background beta ray spectrometer for ^{32}P

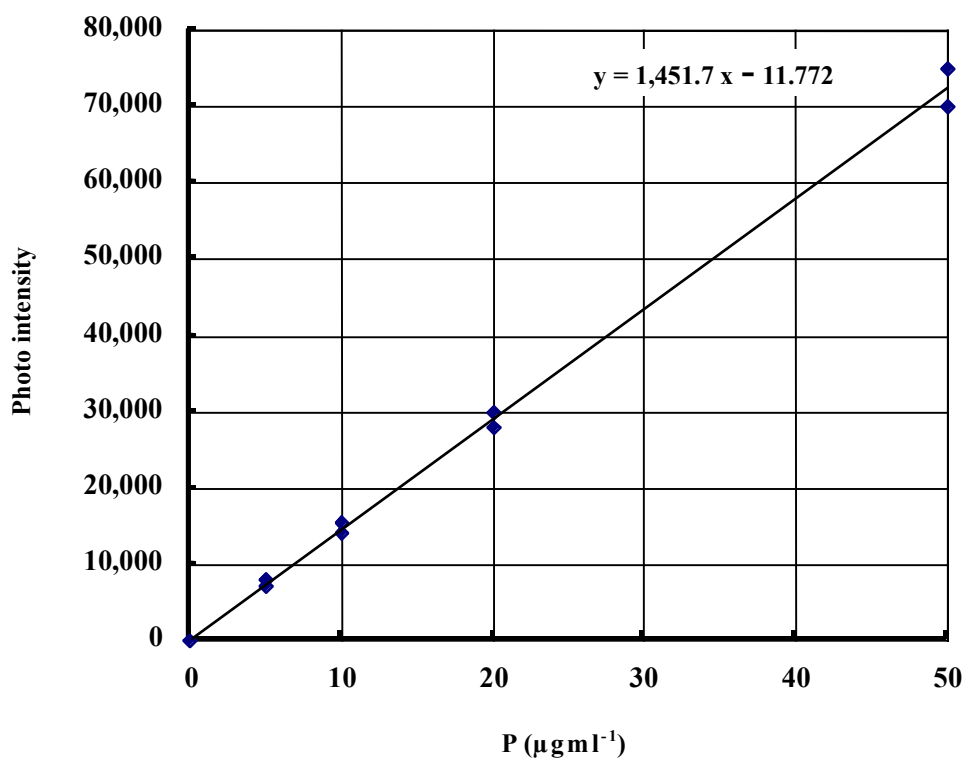$$y = 1{,}451.7\,x - 11.772$$

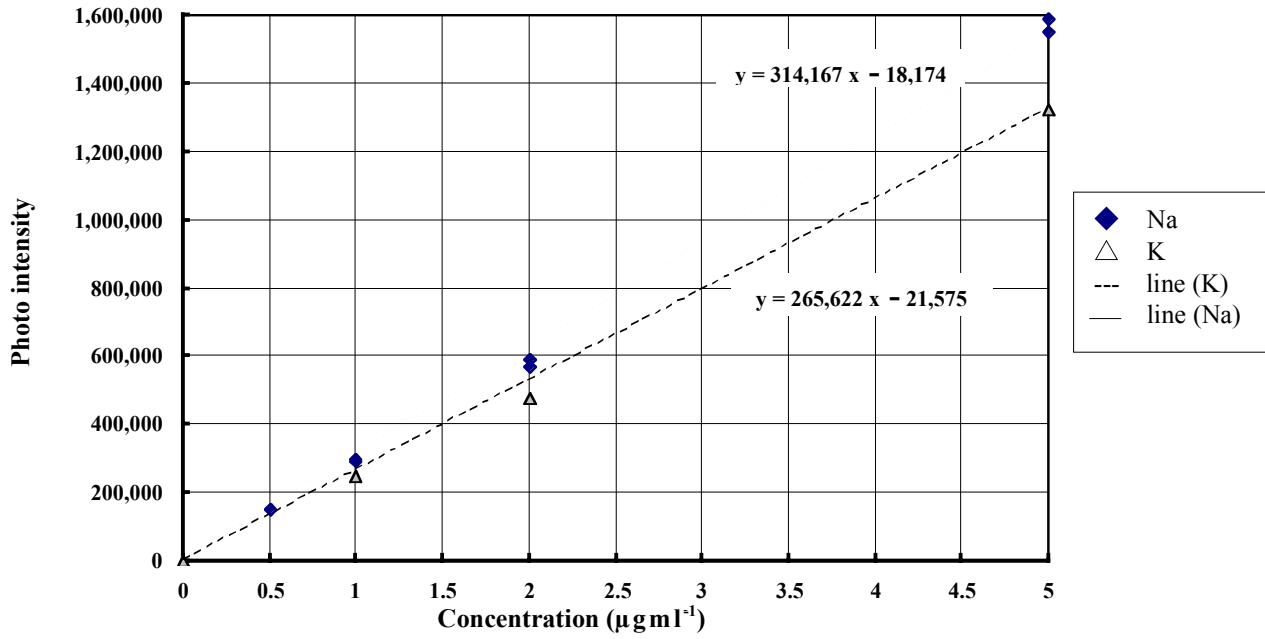**Fig. B.3 Analytical curve of phosphorus recorded by ICP emission analyzer**

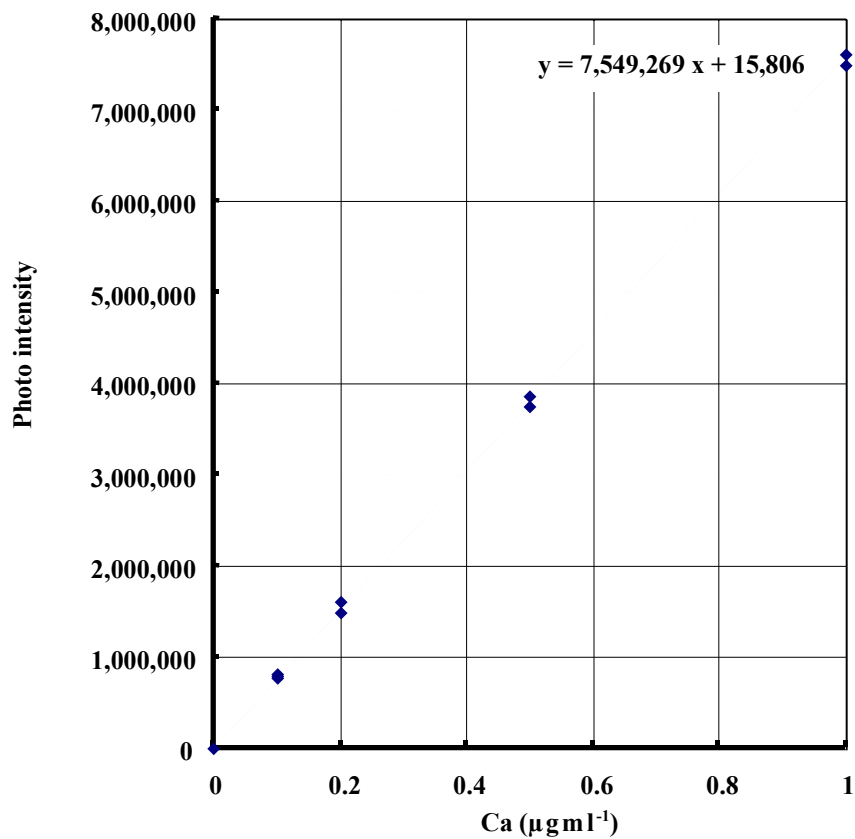**Fig. B.4 Analytical curves of sodium and potassium recorded by ICP emission analyzer**

Fig. B.5 Analytical curve of calcium recorded by ICP emission analyzer